APTD-0762

Contract EHSH 71-002
S/N 17220.00

PB 203 463

# ANALYSIS AND ADVANCED DESIGN STUDY OF AN ELECTROMECHANICAL TRANSMISSION

APRIL 1971

Details of illustrations in
this document may be better
studied on microfiche

Prepared for

OFFICE OF AIR PROGRAMS
ENVIRONMENTAL PROTECTION AGENCY
Ann Arbor, Michigan

Reproduced by
NATIONAL TECHNICAL
INFORMATION SERVICE
Springfield, Va. 22151

TRW
SYSTEMS GROUP

ONE SPACE PARK • REDONDO BEACH, CALIFORNIA 90278

**BIBLIOGRAPHIC DATA SHEET**

**1. Report No.** APTD- 0762

**2.**

**3. Recipient's Accession No.**

**4. Title and Subtitle**
Analysis and Advanced Design Study of an
Electromechanical Transmission

**5. Report Date** April 1971

**6.**

**7. Author(s)**

**8. Performing Organization Rept. No.**

**9. Performing Organization Name and Address**
TRW Systems Group
One Space Park
Redondo Beach, California 90278

**10. Project/Task/Work Unit No.**

**11. Contract/Grant No.** EHSH 71-002

**12. Sponsoring Organization Name and Address**
Office of Air Programs
Environmental Protection Agency
Ann Arbor, Michigan

**13. Type of Report & Period Covered**

**14.**

**15. Supplementary Notes** DISCLAIMER-This report was furnished to the Office of Air Programs by TRW Systems Group, One Space Park, Redondo Beach, California 90278 in fulfillment of Contract EHSH 71-002

**16. Abstracts**

The report deals with the design and data analysis of a heatengine-battery hybrid propulsion system for vehicles. The first portion of the work performed is devoted to the following tasks: Evaluation of the performance of the Electromechanical Transmission (EMT) operating on a dynamometer; Performance of engineering trade-off studies on the power conditioning units of the Speeder (generator) and Torquer (traction motor) subsystems and presentation of up-graded design criteria; Assessment of the performance of the Speeder(

**17. Key Words and Document Analysis. 17a. Descriptors**

Electric power transmission
Engines
Design criteria
Performance evaluation
Dynamometers
Generators
motors
Electric batteries
Internal combustion engines

**17b. Identifiers/Open-Ended Terms**

Electromechanical Transmission
Hybrid engines
Traction
Torquer
Speeder

**17c. COSATI Field/Group** 13B, 21C

**18. Availability Statement**
UNLIMITED

**19. Security Class (This Report)** UNCLASSIFIED

**20. Security Class (This Page)** UNCLASSIFIED

**21. No. of Pages** 155

**22. Price**

FORM NTIS-35 (10-70)

COPY FOR FIRL

USCOMM-DC

**BIBLIOGRAPHIC DATA SHEET**

1. Report No. APTD- 0762

2.

3. Recipient's Accession No.

4. Title and Subtitle
Analysis and Advanced Design Study of an Electromechanical Transmission

5. Report Date
April 1971

6.

7. Author(s)

8. Performing Organization Rept. No.

9. Performing Organization Name and Address
TRW Systems Group
One Space Park
Redondo Beach, California 90278

10. Project/Task/Work Unit No.

11. Contract/Grant No.
EHSH 71-002

12. Sponsoring Organization Name and Address
Office of Air Programs
Environmental Protection Agency
Ann Arbor, Michigan

13. Type of Report & Period Covered

14.

15. Supplementary Notes DISCLAIMER-This report was furnished to the Office of Air Programs by TRW Systems Group, One Space Park, Redondo Beach, California 90278 in fulfillment of Contract EHSH 71-002

16. Abstracts

The report deals with the design and data analysis of a heat engine-battery hybrid propulsion system for vehicles. The first portion of the work performed is devoted to the following tasks: Evaluation of the performance of the Electromechanical Transmission (EMT) operating on a dynamometer; Performance of engineering trade-off studies on the power conditioning units of the Speeder (generator) and Torquer (traction motor) subsystems and presentation of up-graded design criteria; Assessment of the performance of the Speeder and Torquer machines and the presentation of design criteria for advanced versions of both machines; Development of advanced operational concepts such as start-up techniques and means for up-grading the transfer of the Torquer system between the motor and generator operating states; Development of analytic models of Torquer system operation and use of these models to assess the effect of design parameters. The second portion of the study was intended to provide operational data on the performance of an internal combustion engine when used within the context of a hybrid power train.

17. Key Words and Document Analysis. 17a. Descriptors

Electric power transmission
Engines
Design criteria
Performance evaluation
Dynamometers
Generators
Motors
Electric batteries
Internal combustion engines

Details of Illustrations in this document may be better studied on microfiche

17b. Identifiers/Open-Ended Terms

Electromechanical Transmission
Hybrid engines
Traction
Torquer
Speeder

17c. COSATI Field/Group 13B, 21C

18. Availability Statement
Unlimited

19. Security Class (This Report)
UNCLASSIFIED

20. Security Class (This Page)
UNCLASSIFIED

21. No. of Pages
155

22. Price

Contract EHSH 71-002
S/N 17220.00

# ANALYSIS AND ADVANCED DESIGN STUDY OF AN ELECTROMECHANICAL TRANSMISSION

APRIL 1971

Prepared for

**OFFICE OF AIR PROGRAMS**
**ENVIRONMENTAL PROTECTION AGENCY**
**Ann Arbor, Michigan**

**TRW**
*SYSTEMS GROUP*

*ONE SPACE PARK • REDONDO BEACH, CALIFORNIA 90278*

BLANK PAGE

# ANALYSIS AND ADVANCED DESIGN STUDY
# OF AN
# ELECTROMECHANICAL TRANSMISSION

April 1971

Prepared for the
Office of Air Programs
Environmental Protection Agency

Under Contract No. EHSH 71-002

by

TRW Systems Group
One Space Park
Redondo Beach, California 90278

S/N 17220.000

# FOREWORD

This report contains a summary of work performed by TRW Systems for the Office of Air Programs, Environmental Protection Agency, under contract EHSH 71-002.

Dr. George H. Gelb was responsible for overall project direction and report editing. Mr. Baruch Berman was responsible for the design and development of the electrical systems. Dr. Elias Koutsoukos was instrumental in developing the emission testing procedures and instrumentation. Dr. T.C. Wang provided the computer analysis of the electrical system and played a role in overall system analysis. Other members of the technical staff who contributed to the work include: Messrs. H. Gehm and L. Inouye - electrical subsystem, Mr. W. Potter - engine control and instrumentation and Messrs. E. Hoover and R. Lewis - technical support.

## TABLE OF CONTENTS

Page

Summary and Recommendations . . . . . . . . . . . . . . . . . . . . . . . . 1

Introduction . . . . . . . . . . . . . . . . . . . . . . . . . . . . . . 6

1.0 The Electromechanical Transmission (EMT) . . . . . . . . . . . . . 8
  Description of Concept and Modes of Operation . . . . . . . . . . 8
  System Functional Requirements . . . . . . . . . . . . . . . . . . 13

2.0 Torquer System . . . . . . . . . . . . . . . . . . . . . . . . . . 14
  Review of Candidate Torquer Systems . . . . . . . . . . . . . . . 14
  Selection of Torquer System . . . . . . . . . . . . . . . . . . . 20
  Time Ratio Control (TRC) Systems . . . . . . . . . . . . . . . . . 20
  Selection of Power Pass Elements for TRC . . . . . . . . . . . . . 28
  Trade-off and Selection of a Power Control Unit (Torquer PCU). . 36
  Description of EMT Torquer System . . . . . . . . . . . . . . . . 60

3.0 Speeder System . . . . . . . . . . . . . . . . . . . . . . . . . . 65
  System Requirements and Selection Criteria . . . . . . . . . . . . 65
  Selection of the Speeder . . . . . . . . . . . . . . . . . . . . . 65
  Rational of Speeder Operating Mode and PCU Selection . . . . . . 65
  Speeder PCU . . . . . . . . . . . . . . . . . . . . . . . . . . . . 67

4.0 Rotating Machines . . . . . . . . . . . . . . . . . . . . . . . . 70
  Torquer Selection . . . . . . . . . . . . . . . . . . . . . . . . . 70
  Torquer Specifications . . . . . . . . . . . . . . . . . . . . . . 70
  Speeder Specifications . . . . . . . . . . . . . . . . . . . . . . 71

5.0 Dynamometer Testing of the EMT System . . . . . . . . . . . . . . 73
  EMT Dynamometer Equipment . . . . . . . . . . . . . . . . . . . . . 73
  Instrumentation and Data Processing . . . . . . . . . . . . . . . 73
  Computation Subroutines . . . . . . . . . . . . . . . . . . . . . . 81
  Computer Print-Out and Data Presentation . . . . . . . . . . . . . 94
  Data Logging . . . . . . . . . . . . . . . . . . . . . . . . . . . . 95
  EMT Dynamometer Performance on LA-4 Route . . . . . . . . . . . . 95
  Statistical Representation of EMT-Dynamometer Operation . . . . 104
  Summary of EMT-Dynamometer Testing . . . . . . . . . . . . . . . . 120

6.0 Advanced Design Study of Torquer System . . . . . . . . . . . . . 124
  Torquer Drive System Analysis . . . . . . . . . . . . . . . . . . . 124
  Torquer Design . . . . . . . . . . . . . . . . . . . . . . . . . . . 138
  Torquer Design Improvements . . . . . . . . . . . . . . . . . . . . 141
  Speed Charging of the Torquer . . . . . . . . . . . . . . . . . . . 145
  Chopper Frequency Selection and Power Control Improvements . . . 146
  Torquer System Failure Analysis . . . . . . . . . . . . . . . . . . 149

7.0 Advanced Design of the Speeder System . . . . . . . . . . . . . . 161
  Review of Speeder Performance on LA-4 Tests . . . . . . . . . . . 161
  Machine Losses . . . . . . . . . . . . . . . . . . . . . . . . . . . 161
  Speeder PCU Improvements . . . . . . . . . . . . . . . . . . . . . . 170
  Preliminary Design of an Advanced Speeder PCU Control Circuit. . 179
  Speeder System Failure Analysis and Protection . . . . . . . . . 182

Page

8.0 Advanced EMT Power Train Operational Concepts . . . . . . . . . . 190
Solid State Switching System . . . . . . . . . . . . . . . . . . 190
EMT Power Train Start-Up Concepts . . . . . . . . . . . . . . . . 202
Override Options to the EMT System . . . . . . . . . . . . . . . . 204

9.0 Effect of Selected Parameters on Exhaust Emissions from an Internal Combustion Engine . . . . . . . . . . . . . . . . . . . . 206
Introduction . . . . . . . . . . . . . . . . . . . . . . . . . . 206
Determination of Engine Emissions During Cold and Hot Operation 206
Effectiveness of a Three-Component Catalyst on Exhaust Emission 228
Prediction of Emission Signature of an EMT System with a Three-Component Catalytic Drive . . . . . . . . . . . . . . . . . . 228

References . . . . . . . . . . . . . . . . . . . . . . . . . . . 231

A-1 Comparison of Boost-Buck and Boost PCUs for Regeneration . . . 232

A-2 Mathematical Model of Torquer System . . . . . . . . . . . . . 236

# NOMENCLATURE

The following set of symbols and definitions are used in the report. In places where other symbols are used, they will be defined at that point and are to be used only for the section in which they appear.

V - instantaneous value of a voltage, volts
I - instantaneous value of a current, amperes
t - time (units either omitted or presented under particular usage)
T - period of chopper operation, seconds
f - frequency, 1/T, hz
L - inductance, henrys
C - capacitance, farads
R - resistance, ohms
E - generated voltage of a machine, volts
S - denotes a saturable reactor
D - denotes a diode
SW - denotes a switch
F - denotes a fuse
F,R - denotes forward or reverse direction

Subscripts

c - chopper; commutation
g - generator
T - Torquer
B - battery
S - Speeder
on - power pass element conducting
off - power pass element not conducting

Greek Letters

$\alpha$ - ratio of power pass element on time to total chopper period; $t_{on}/T$
$\beta$ - ratio of commutating SCR time on to total chopper period

Averaging: a bar (-) over any quantity g means

$$\bar{g} \equiv \int \frac{g(t)\,dt}{\text{defined time interval}}$$

BLANK PAGE

## Summary and Recommendations

TRW Systems Group has performed a study entitled "Analysis and Advanced Design Study of an Electromechanical Transmission" under contract EHSH-71-002 for the Air Pollution Control Office of the Environmental Protection Agency. This report presents the results of work done during the period of the contract from July 13, 1970 to April 26, 1971.

The work performed falls into two major divisions. The first portion is devoted toward eight tasks. These tasks were to:

- Evaluate the performance data of the Electromechanical Transmission (EMT) operating on a dynamometer
- Perform engineering trade-off studies on the power conditioning units of the Speeder (generator) and Torquer (traction motor) subsystems and to present up-graded design criteria
- Assess the performance of the Speeder and Torquer machines and to present design criteria for advanced versions of both machines
- Develop advanced operational concepts such as start-up techniques and means for up-grading the transfer of the Torquer system between the motor and generator operating states
- Develop analytic models of Torquer system operation and to use these models to assess the effect of design parameters.

The second portion of the study was intended to provide operational data on the performance of an internal combustion engine (ICE) when used within the context of a hybrid power train. Of particular significance is the determination of the role of the cold period of operation to total engine emissions. Preliminary data on the effectiveness of a catalyst on engine emissions was gathered.

All of the experimental work was gathered from a breadboard version of the EMT. The equipment was built to prove the EMT principle, and has performed satisfactorily as a basis for assessing the performance of a hybrid system designed for low engine emission operation. The units which comprised the breadboard EMT were assembled rapidly on the basis of their availability. None of the rotating machines or gearing was optimized to any degree. Therefore, it must be recognized that the breadboard EMT's performance is indicative of first effort equipment and major system improvements are possible.

The EMT was operated on the dynamometer and driven over the LA-4 route, a route typical of driving in the Los Angeles area (Section 5.1). Various operators, using strip chart driver's aids, drove the equipment under dynamometer settings representative of vehicles weighing 2000 to 4000 pounds. The dynamometer testing revealed the following:

- The overall transmission efficiency of the EMT for LA-4 operation is approximately 50%. Efficiency as defined as the demanded road load energy divided by the engine shaft output energy (Sections 5.6 through 5.8). Fuel consumption is about 18 miles per gallon.
- Major inefficiencies can be associated with each of the major subsystems which were purchased or built without time for detailed design trade-offs--
    - the Torquer subsystem is inefficient due to the impact of the chopper on the current flow through the Torquer
    - the Speeder is a lossy machine whose efficiency is further degraded by its operation into a rectified and chopped load
    - the gear box is a primary source of inefficiency--the breadboard gear box is greatly overdesigned, with excessive lubrication and unnecessary gear losses.
    - the component efficiencies should be improved greatly by redesign and selection of equipment for the specific type of EMT service.
- Battery impedance impacts heavily on the overall utilization of engine power. It limits the maximum charge and discharge powers and accounts for a major source of energy loss.
- The battery receives almost equal charging energy from the Speeder and Torquer and thus the generator efficiency of the latter must be improved.
- The effectiveness of regenerative braking in providing battery charge power is small with respect to the contribution coming from the engine. Means should be evolved for increasing its effect by improved Torquer generator operation and redesign of the braking controls and control limits (Section 5.8).
- All major subsystems with the exception of the Speeder functioned in ambient air without forced cooling during tests on the LA-4 cycle.

Computer studies of the Torquer drive system have verified the importance of the selection of chopper frequency and machine inductance on Torquer system efficiency. The filtering effect of the armature circuit inductance impacts the system performance in two ways. With increased inductance the resistive losses in all elements of the circuit decrease and magnetic losses in the machine are reduced. Increased chopper frequency decreases the ohmic losses of the system (Section 6.1).

Two methods are available for increasing the Torquer efficiency; the addition of armature circuit inductance by increased series windings or an external choke, and the lamination of the flux carrying elements of the machine. Experimental evidence shows that both approaches increase the machine efficiency significantly (Section 6.3). Further economic and engineering trade-offs are required to determine the best approach or combination of approaches.

Losses in the Speeder system can be reduced by improved aerodynamic design and a lower operating speed, the latter with some weight penalty. Major hysteresis and eddy current losses are introduced by operating the alternator into a rectifier and chopper. The resulting current waveforms contain 3rd, 5th and 7th harmonics which can be greater than 10%. An advanced Speeder design should incorporate a higher flux gap density and low electrical conductivity pole faces (Section 7.2).

The present Torquer system uses a variable chopper frequency to control the power flow at low speeds. Reduced frequency is required to lessen the effect of undesired commutation power. Analyses of the EMT system have revealed that a single frequency (1 KhZ) chopper mode of operation is desirable both from the standpoint of component efficiency and cost reduction. Various techniques are possible for using a constant frequency system such as auxiliary commutation or power pulse skipping coupled with synchronized commutation command. The latter is an attractive scheme since no additional power circuit elements are required. Fast turn-off SCRs can be used with the EMT circuitry, allowing further reductions in the size of commutation circuit components and affording increased system control range (Section 6.5).

The ramp and pedestal control technique utilized on the breadboard Torquer PCU*offers a means for an improved Speeder PCU. Other techniques are suggested for improving the Speeder control (Section 7.4).

---

*power control unit

Solid state switching of the Torquer PCU between the drive and regeneration configuration has been demonstrated. The development of this system proceeded in a series of steps from an all electromechanical relay contactor system, to one in which SCRs and diodes are employed for current direction control (Section 8.1).

Advanced Torquer PCU systems should employ several safety protection and detection features including overcurrent and oscillation failure circuits along with thermal overload protection (Section 6.6). The advanced Speeder system will provide primary protection by field sequencing. Faults will be detected by oscillation failure, overcurrent and low battery voltage detectors (Section 7.5).

The EMT hybrid relaxes the driveability requirements placed on the internal combustion engine and allows the engine to operate in a manner so as to reduce emissions while retaining fuel economy.* Emissions of hydrocarbons (HC) and carbon monoxide (CO) during the period immediately following engine start-up account for a majority of the total emissions which occur during the DHEW cycle test. A primary factor affecting ICE cold start emissions is the rate of choke removal. Experiments indicated that the hydrocarbon (HC) and carbon monoxide (CO) mass rates can be reduced 50% and 80-90%, respectively, from that of a conventional engine by increased choke relief rates (Section 9.2).

In a hot ICE, CO and HC mass rates are relatively insensitive to air-fuel ratios beyond stoichiometry (∿18-19) and are directly related to engine power level. Oxides of nitrogen ($NO_x$) are quite sensitive to air-fuel ratio and the $NO_x$ mass rates decrease rapidly with increased air-fuel ratios in excess of stoichiometry. $NO_x$ mass rates also show a non-linear increase with increased power level. Spark retard causes a slight decrease in HC and CO levels and a strong decrease in $NO_x$. As engine power level is increased, leaner mixtures can be burnt without adversely affecting HC and CO production (Section 9.2.3).

---

*"An Electromechanical Transmission for Hybrid Vehicle Power Trains - Design and Dynamometer Testing", G.H. Gelb, N.A. Richardson, T.C. Wang, and B. Berman, Society of Automotibe Engineers, Paper No. 710235, January 1971.

The 1975 standards for CO can be met with rapid choke removal and lean carburetion. While the HC levels are reduced by leaning, the standards are exceeded within a few minutes after engine start. A three-component catalyst system was tested which shows some promise for $NO_x$ and HC control during hot operation. The catalyst performs best near stoichiometry, suggesting a fuel economy advantage over lean engine operation (Section 9.3).

Several actions are recommended in order to more fully explore the potentialities of the EMT system:

- Design requirements for advanced Torquer and Speeder machines should be developed into specific designs integrated with the power conditioning equipment. Second generation hardware should be procured and the improvements experimentally verified.
- A second phase of power conditioning equipment development should be initiated. The new equipment should incorporate the circuit features determined in this study. Emphasis should be placed on utilizing lower cost power elements and developing packaging and vehicle integration concepts.
- Work should be directed toward improving the gearing of the EMT and incorporating the clutching and activation functions into the gear box.
- Methods of controlling the prime mover power level in the various operating modes should be investigated. Trade-offs and hardware development of the activators and Torquer interfaces should be conducted.
- Development of specialized ICE exhaust control approaches should be undertaken including further experimental evaluation of catalyst performance during the cold period. Fuel usage rates should be established for various mixture ratios. Exhaust recirculation coupled with a simple oxidizing catalyst should be evaluated in terms of the unique manner of EMT-ICE operation.
- Further dynamometer test work should evaluate the dynamics of the power train during drive-regenerate transfer, mode transition and acceleration from standstill. The smoothness of system operation should be defined and means explored, if necessary, to refine system stability.
- Definition of major components should be made for a variety of vehicle sizes ranging from urban vehicles through full-sized passenger cars.
- The economy of hybrid operation should be evaluated and combined with other system costs to establish the cost of EMT-hybrid ownership.

## INTRODUCTION

TRW Systems has performed a study entitled "Analysis and Advanced Design Study of an Electromechanical Transmission" under contract number EHSH-71-002 for the Air Pollution Control Office of the Environmental Protection Agency. This report presents the results of work performed during the period July 13, 1970 to February 13, 1971. It is concerned with the eight (8) tasks of the contract as originally negotiated. A ninth task associated with the study of the transient emission behavior of an internal combustion engine during its cold period of operation was added to the contract, extending the contract period to April 26, 1971.

This report deals with the design and data analysis of a heat engine-battery hybrid propulsion system for vehicles. In particular, the work focuses on the analysis and design of a transmission termed the Electromechanical Transmission (EMT). The report is divided into nine (9) sections structured in such a way that the reader is first acquainted with the basic features of the EMT. Later sections treat design tradeoffs developed during the construction of breadboard, proof-of-principle equipment and the testing of that equipment on a dynamometer. The remaining sections are addressed to design changes which have or should be undertaken to improve system performance.

Section 1 presents a short review of the basic operational modes of the transmission developed by TRW Systems, the Electromechanical Transmission, EMT. It describes and stresses the functional requirements placed on the equipment by the hybrid system.

Section 2 discusses the traction system of the EMT and in particular to various methods of controlling the Torquer (the traction device of the EMT). A short discussion of candidate systems is presented leading to the selection of a DC chopper using pulsewidth modulation. Various TRC* philosophies and circuits are reviewed and their salient points discussed. Finally, a specific TRC system and circuit are chosen and its operation and critical components are described.

---

*time ratio controlled

The generator system (Speeder system) is discussed in Section 3. A review is made of various AC and DC system concepts in view of the unique functional requirements of the Speeder system. A description of the breadboard Speeder PCU is presented.

Section 4 describes the rotating machines used in the present system. Manufacturers specifications and construction details are given.

The dynamometer testing of the EMT can be found in Section 5. Included are test descriptions, data reduction routines, and presentation of test data. Conclusions are drawn from the data useful for further design. Problems encountered during the test program are discussed.

Section 6 contains the results of advanced analytical and design work related to an improved Torquer and Torquer PCU. Included are recommended methods of improving machine performance along with suggested machine ratings in view of actual operating experiences. A computer-oriented analysis of the Torquer system is presented with trade-offs of major system parameters. The effects of frequency of chopper operation are indicated. Reference is made to advanced logic control systems and the critical problems of Torquer-EMT interfaces and system protection are discussed.

Section 7 discusses the results of an advanced design study of the Speeder and Speeder PCU. Included is an analysis of losses and stability limitations in the present system. Failure modes are identified and possible remedies are suggested.

Some advanced power train operational concepts are discussed in Section 8. In particular a unique solid state drive-to-regeneration switching system for the Torquer is described. Certain hybrid power train start-up concepts are suggested and related to possible emission control schemes. Transmission override options are discussed.

Section 9 describes work conducted to establish the emission characteristics of an internal combustion engine during start-up and hot operation. Preliminary data on a three-component catalyst system are presented. DHEW cycle emissions are projected.

# 1.0 THE ELECTROMECHANICAL TRANSMISSION (EMT)

## 1.1 Description of Concept and Modes of Operation

The EMT is a particular form of a parallel-connected hybrid power train which attempts to utilize heat engine energy as efficiently as possible while minimizing the excursions of prime mover power and speed.[1]*

The EMT configuration and its basic power and information flow paths are shown in Figures 1.1 and 1.2. Power produced by the engine is delivered to the input (sun gear) of a planetary gear system. The planetary gear system algebraically divides the input power between the planet carrier and the ring gear in direct proportion to the speeds of those elements. The speeds in turn are related through the system gear ratios to the input shaft speed. In the present implementation the planet carrier gear is connected to a generator--termed the Speeder--while the ring gear drives the propeller shaft of the vehicle. A traction motor--termed the Torquer--is coupled directly through a fixed gear ratio to the propeller shaft.

In Mode One, as shown in Figure 1.1, the engine is run at constant throttle, constant speed at a power setting consistent with the average power required of the vehicle in urban operation. The constant torque output of the engine is delivered to the Speeder and propeller shafts, thus these two shafts receive a constant torque input in direct relationship to the planetary gear ratios.

In order to maintain the engine speed constant it is necessary that the Speeder produce an electromagnetic shaft torque which when reflected through the gearing to the engine shaft is equal and opposite to that produced by the engine. If the engine departs from the desired reference speed, the differential information is used through the Speeder controller to increase or decrease the Speeder torque and thus bring the engine into control. The function of the Speeder as its name suggests is to control the engine speed while the power train is in Mode One.

Because the engine-produced torque on the propeller shaft is constant, the Torquer is used to augment or reduce the torque available to the wheels for tractive effort. The Torquer therefore must be capable of operating

---

*Numbers in brackets refer to references in bibliography.

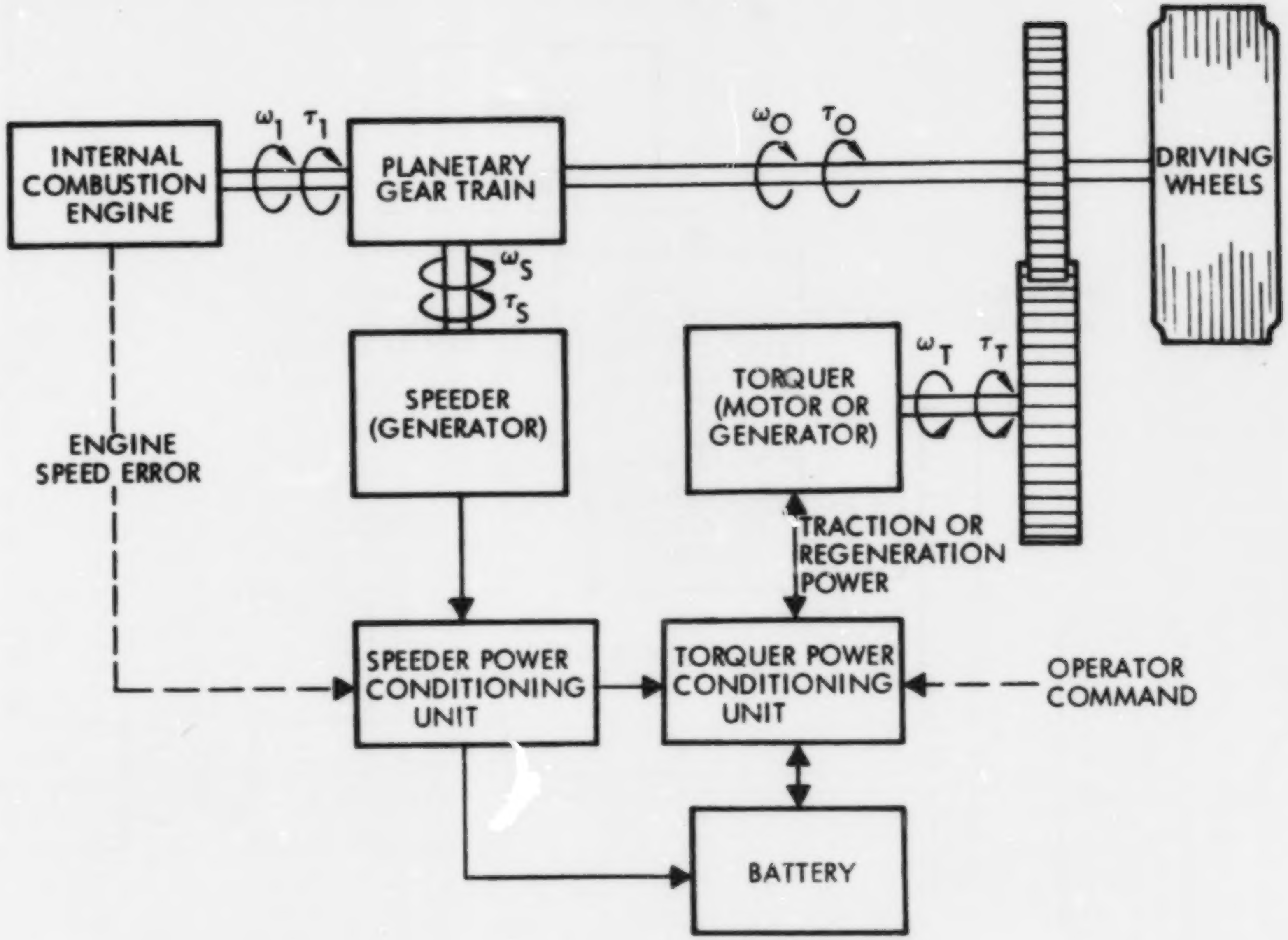
INTERNAL COMBUSTION ENGINE
$\omega_1$
$\tau_1$
PLANETARY GEAR TRAIN
$\omega_O$
$\tau_O$
DRIVING WHEELS
$\omega_S$
$\tau_S$
SPEEDER (GENERATOR)
TORQUER (MOTOR OR GENERATOR)
$\omega_T$
$\tau_T$
ENGINE SPEED ERROR
TRACTION OR REGENERATION POWER
SPEEDER POWER CONDITIONING UNIT
TORQUER POWER CONDITIONING UNIT
OPERATOR COMMAND
BATTERY

FIGURE 1.1
EMT MODE ONE OPERATION

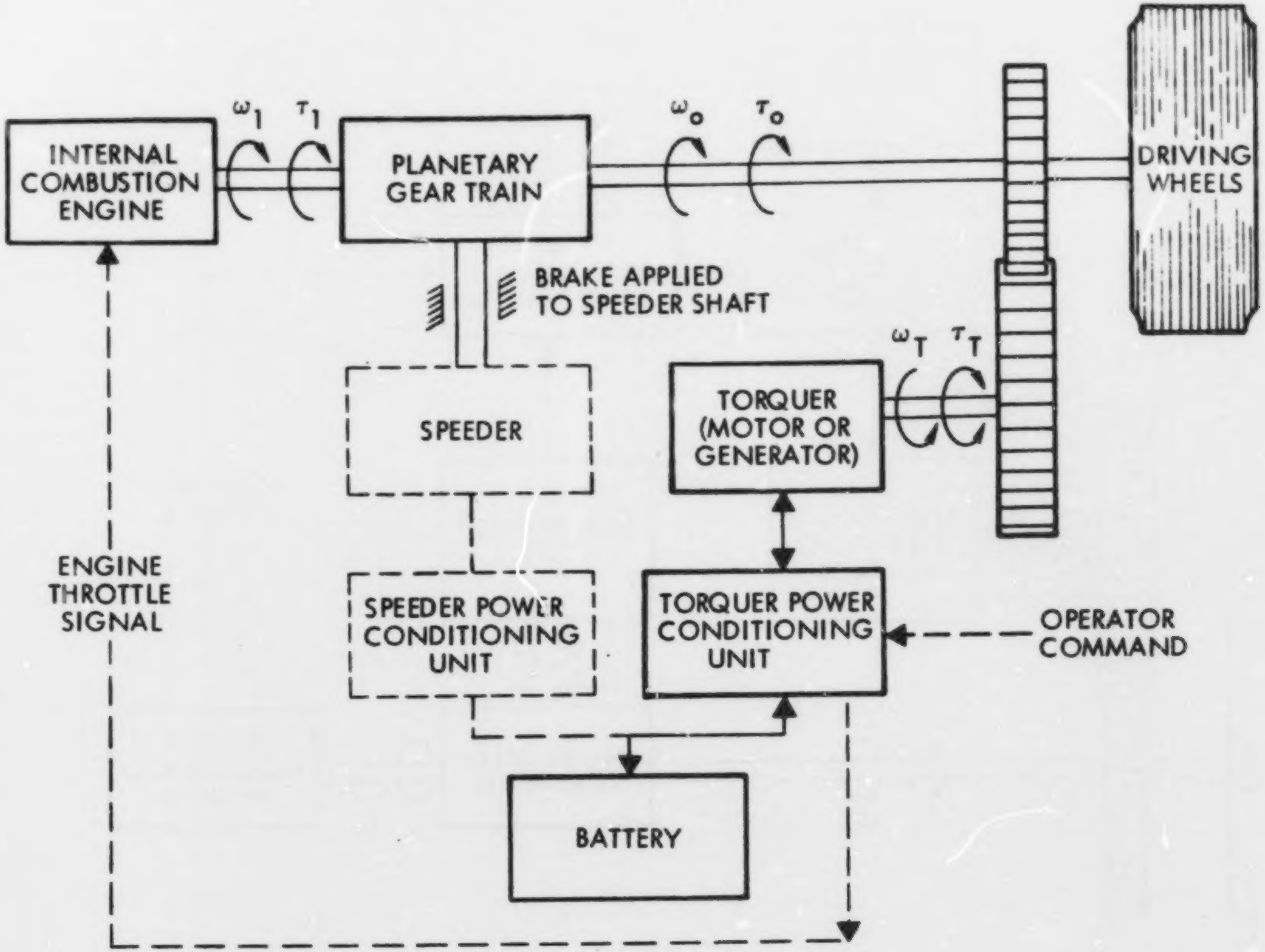
INTERNAL COMBUSTION ENGINE
$\omega_1$
$\tau_1$
PLANETARY GEAR TRAIN
$\omega_o$
$\tau_o$
DRIVING WHEELS
BRAKE APPLIED TO SPEEDER SHAFT
$\omega_T$
$\tau_T$
SPEEDER
TORQUER (MOTOR OR GENERATOR)
ENGINE THROTTLE SIGNAL
SPEEDER POWER CONDITIONING UNIT
TORQUER POWER CONDITIONING UNIT
OPERATOR COMMAND
BATTERY

FIGURE 1.2
EMT MODE TWO OPERATION

as both a motor and as a generator, and as its name suggests function to modulate the propeller shaft torque delivered to the wheels.

At a predetermined speed typical of the departure from urban operation, the transmission transfers into Mode Two as shown in Figure 1.2 and allows the engine to operate at higher power levels consistent with highway cruise. In this mode a small brake is applied to the Speeder shaft, stopping it and locking it out of the power flow. The engine is now directly coupled to the rear wheels and its speed must change directly with road speed. Throttle level of the engine is adjusted on the basis of electrical power flow in the Torquer in such a way that the throttle is always moved to a power setting where the engine takes over the total propulsion requirement. If the Torquer power demand increases, the engine throttle setting slowly increases until the engine output matches the new steady road demand. If the Torquer demand decreases or goes into a generator manner of operation, the engine slowly throttles back.

Figure 1.3 presents an operational map of the EMT power train. Assumed engine power levels, vehicle weight and transition speed from Mode One to Mode Two operation are indicated. The envelope of probable maximum road power demand during urban operation was developed from an analysis of driving missions in Los Angeles traffic.[2] Five regions of EMT operation are indicated in the figure.

The first region is associated with the low acceleration events in which the engine torque available directly to the road is equal or exceeds the road torque requirement. In this area the excess engine power is diverted to the battery with both Speeder and Torquer acting as generators.

In the second region engine power is equal or greater than the road power demand, but it is not available at the proper torque level. The Speeder accepts engine power, transfers it to the Torquer which delivers the power to the road at the required torque level. As indicated, the excess engine power is directed through the Speeder to the battery for charging.

The third region is that in which the road power and torque demands exceed the engine output. Here the battery is called upon to provide

FIGURE 1.3
OPERATIONAL MAP OF EMT POWER TRAIN

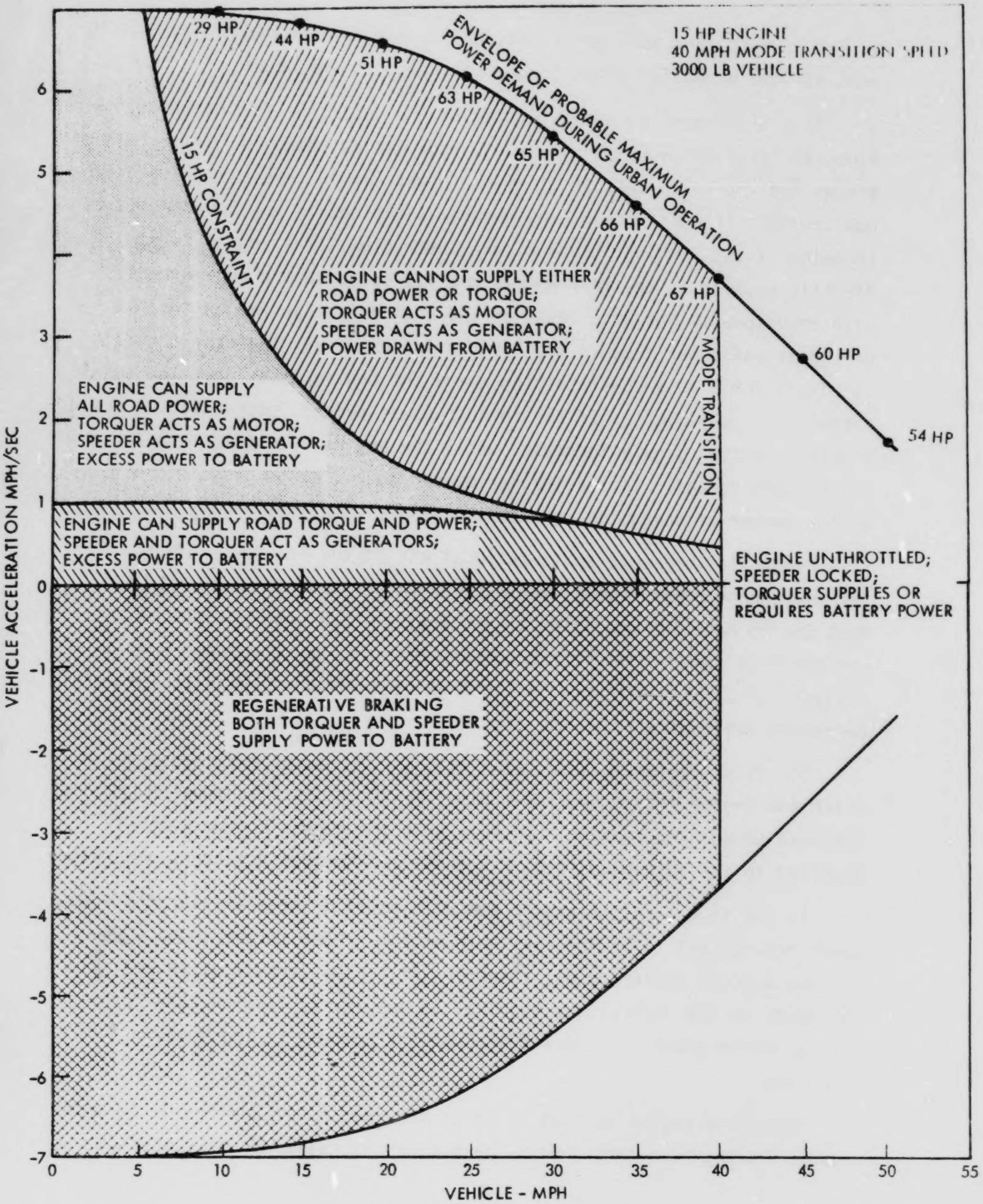

peaking power. The torque converter operation of the Speeder-Torquer combination continues.

Above the 40 mph mode transition speed the transmission transfers Mode Two and the Speeder is removed from the power loop. As previously indicated, the power train still acts as a hybrid but the engine must throttle up and adjust its speed to meet the higher average road power and speed demands.

The fifth region is associated with all deceleration events. Because of the dual manner of Torquer operation, regenerative (and/or dynamic) braking is built into the system. Regenerative braking in either Mode One or Mode Two can be used for battery charging.

## 1.2 System Functional Requirements

### 1.2.1 Speeder System

The Speeder System must perform two functions; to serve as a major mechanical-to-electrical energy converter, delivering engine output to the battery bus and as an engine load controller, varying its load so as to maintain the engine under speed control. It must be capable of operation as a variable speed, quasi-constant torque generator, while delivering electrical power to a battery bus whose voltage can rapidly vary under changing battery loads and charge states.

### 1.2.2 Torquer System

The Torquer System must serve as a mechanical-to-electrical (generator) and electrical-to-mechanical (motor) energy converter. It must be capable of responding in a controlled, stable fashion to operator input commands so as to modulate the torque at the driving wheels. It must operate over a wide range of shaft torque levels while taking or delivering electrical power from a battery bus whose voltage can rapidly vary under changing battery loads and charge states. In addition, the Torquer System must provide primary traction power flow information to the prime mover power control system so that the prime mover may be adjusted to reflect Mode Two (high speed) operation.

## 2.0 TORQUER SYSTEM

### 2.1 Review of Candidate Torquer Systems

The manner of torque and power control, cost and complexity of the machine and controller are all dependent on the machine selected.

The electromechanical torque of all electric motors is proportional to the integrated product of the radial magnetic field in the air gap and the axial current in the armature (in space phase with the magnetic field). The rating of an electric motor is limited by three factors:

- magnetic saturation of the iron circuit
- temperature rise due to internal losses
- mechanical stresses imposed on the rotating parts

Depending on its design, the horsepower/weight ratio, torque-current, and torque-speed characteristics of the various types of traction motors can be quite different. The method of speed control, regenerative or dynamic braking, and the complexity of power conditioning may also vary appreciably. In general, the series DC traction motor and the low frequency AC series commutator motor have dominated the field of variable speed electric drive systems because of their speed-torque characteristics and simplicity of control. However, some recent experimental vehicles have been constructed using induction motors which have used the simpler rotating machines at the expense of sophisticated inverter power circuits.

Table 2.1 presents a list of the machines which could be used for the Torquer. The table summarized important features of each machine as well as its control equipment. While the AC synchronous machines do not have a mechanical commutator as do most DC machines, they require additional rotor position information for torque and speed control, making their power conditioning systems somewhat complex and costly. Synchronous machine systems do not have the simplicity of control as DC machines nor the rugged, low cost construction of induction machines. In view of this and since they have not found any favor in electrically propelled vehicles to this time, they are not considered further.

### TABLE 2.1
### CANDIDATE TORQUER SYSTEMS

| Type of Machine | Starting Torque | Commutator or Slip Ring | Relative Rotor Speeds | Relative Power Density | Can be Used as Generator? | Relative Machine Cost | External Power Conditioning | Relative Complexity of PCU | Relative Reliability of PCU |
|---|---|---|---|---|---|---|---|---|---|
| I. DC Machine | | | | | | | | | |
| a. shunt | low-medium | commutator | lowest | low | yes | highest | DC chopper | simplest | highest |
| b. series | high | commutator | lowest | modest | yes | highest | DC chopper | simplest | highest |
| c. compound | high | commutator | lowest | modest | yes | highest | DC chopper | simplest | highest |
| d. brushless | low-medium | none | highest | high | yes, may be difficult | medium | DC-AC with position sensor | complex | fair |
| II. AC Synchronous | | | | | | | | | |
| a. conventional | medium | slip ring | medium | modest-high | yes | medium | DC-AC with frequency control & position sensor | most complex | lowest |
| b. permanent magnet | low | none | highest | high | may be difficult | un-known | | most complex | lowest |
| c. solid rotor | low-medium | none | highest | highest | yes | un-known | | most complex | lowest |
| III. Induction Machine | | | | | | | | | |
| a. wound rotor | medium | slip ring | medium | high | yes** | medium | DC-AC and frequency control, also require reactive power supply | complex | medium |
| b. squirrel cage | medium | none | high | high | yes* | lowest | | complex | medium |

---

*Need external power conditioning

**Need reactive power supply

It should be noted that the average machine losses in a parallel connected hybrid as the EMT are smaller than an equivalent weight vehicle employing electric traction only. The ratings normally applied to motors should be reduced in EMT application since the average propulsion power (road load) is supplied by the prime mover and not the electrical motor.

### 2.1.1 DC Machine Systems

The simplest system which might be used for the Torquer would be a reostat or contactor controlled DC motor. The literature contains a great deal of information relative to these systems dating back to the earliest days of vehicle traction. It is generally accepted that such systems have the following disadvantages:

- Reostat System
    - poor efficiency at part load
    - limited regenerative capability
- Contactors
    - jerkiness of operation
    - non-uniform utilization of the battery cells

At the present time the combination of power semiconductors with DC motors and sliding contact commutators offers one of the simplest and cheapest means of providing adequate starting torque, speed control, and regenerative or dynamic braking.

The relationship between the torque, $\tau$, and armature current, $I_a$, of a DC motor is:

$$\tau = 0.1174 \times 10^{-8} \, pZa \, \phi \, I_a \text{ lb-ft} = K_A \, \phi \, I_A$$

where:

p = number of poles
Za = number of turns per armature circuit
$\phi$ = flux per pole (lines)

For the armature materials to be fully utilized, the magnetic materials should be saturated and the armature conductors should carry a current density consistent with the cooling capability of the machine. At very low speeds the electric loading may have to be reduced because of poor ventilation. But, to a first approximation, the product of p and $Z_aI_a$ is constant for an armature of given dimensions. Therefore, the dimensions of a DC armature and hence also of the whole machine, may be regarded as being functions of its rated torque.

The power output/input weight of DC machines increases rapidly with the machine's rotational speed. However, the maximum speed of a conventional DC machine is limited by mechanical commutator contact requirements and centrifugal forces on the armature windings. In an electric vehicle traction machine power densities ranging from 0.06 to 0.2 hp/lb are typical. It is only by going to brushless configurations that high power densities are possible, approaching 1.0 hp/lb.

The brushes of DC machines are typically claimed as a major disadvantage of this type of machine. The brushes do wear in service and must be replaced. The additional weight and volume that the brushes, brush holders and commutator add could be used in an induction machine for the production of torque and power. In terms of wear, brush life has been cited in one case as a minor problem, with a useful life expectancy of 50,000 miles.[3] With proper care to avoid pitting of the commutator, long lifetimes can be expected. While the increased weight, volume and cost of brushes and commutators are disadvantages they must be traded off against the increased cost and complexity of induction machinery power control systems.

### 2.1.2 Induction Motors

A polyphase induction motor consists of stator (primary) and rotor (secondary) windings. When supplied from a voltage or current source, a "rotating" magnetic field is set up by the primary winding currents which induce currents on the secondary side. The secondary winding is closed either by a short circuit in a squirrel-cage motor, or by an external impedance in the wound-rotor motor. The interaction of the magnetic field and secondary current produces an electromagnetic torque which is maintained as long as there is relative motion between the structure of the primary and secondary windings. Since the secondary currents are created by induction alone, no commutation or brushes are needed, and higher speed operation is possible. Advantages of this machine are its rugged and simple construction and high horsepower/weight ratio. For these reasons it has received some interest in recent times for vehicle use.

The torque-speed characteristic of an induction motor can be expressed as

$$\Upsilon = \frac{r_2 V^2}{s n_s (r_1 + \frac{r_2}{s})^2 + x^2}$$

where:

$V$ = voltage input per phase

$r_1$ = primary resistance per phase

$r_2$ = secondary resistance per phase referred to the primary

$x$ = total equivalent leakage reactance per phase

$n$ = rotational speed of the rotor

$n_s = \frac{2f}{p}$ = synchronous speed (f is the source frequency, p is the number of poles)

$s = \frac{n_s - n}{n_s}$ = slip

In the typical torque-speed characteristics of the induction motor, there is a region where the motor is stable. This region is defined as $s_m < s < o$ where $s_m$ is the maximum or breakdown torque. In this region, $s < s_m$, a reduction in load causes the machine to speed-up. In practice the point $s = s_m$ is unstable and the maximum obtainable torque at rated current is considerably less than the maximum speed. Using typical values of machine parameters in the torque-slip equation it can be shown that for a low slip (high efficiency) induction motor:

- the breakdown torque is less than three times the rated torque
- the line current at maximum torque is approximately four times rated current
- the power factor at maximum torque is approximately 0.7.

These values compare unfavorably with a series DC motor. The series machine is capable of producing three to four times the torque per ampere as is the induction machine. Moreover, the DC motor does not exhibit the stability problem of the induction motor.

### 2.1.3 AC Motor Control Systems

The speed of an induction motor can be controlled by one or a combination of the following:

- varying the applied voltage, V
- changing the synchronous speed, $n_s$ by varying the applied frequency or changing the number of poles
- varying the resistance of the motor windings (wound rotor construction).

The most satisfactory means of speed control is to vary both V and f, yet maintain their ratio constant. When $V/f = B =$ constant, the machine will be able to operate with essentially constant flux density, yet will be capable of producing almost constant torque throughout most of the operating speed range. (At very low speeds the effect of stator resistance becomes extremely important and higher terminal voltages must be applied to develop constant torque.)

There are several control systems which have been developed for the control of AC machines (synchronous and induction); they can be broadly classified into:

- DC link inverters - those devices which accept DC power and invert it to a controlled voltage and frequency
- Cycloinverters - those devices which transform AC power to a controlled lower frequency and controlled voltage.

Since the latter devices are driven by an AC source they are not relevant to battery powered systems.

There are two types of DC link inverters for AC motor control. They are the pulse width modulating inverter and the variable voltage and frequency inverter.

In the variable voltage, variable frequency inverter, the DC source voltage is first chopped to the desired voltage level and then inverted to the correct frequency. The pulse width modulated inverter performs these two operations using a single set of components. While the former system contains more components, the waveform presented to the AC machine by the latter has a much lower harmonic content, offering better machine efficiency.

## 2.2 Selection of Torquer System

The selection of a system to use as the Torquer system involves an assessment of both ability to perform required functions and the cost to perform those functions. In terms of overall system cost, a judgment is difficult. To make a rational decision involves a projection of the unit costs of machines and solid state devices which are presently only manufactured in small quantities. However, in view of the present cost of semi-conductor devices, it is reasonable to assume that while their cost may fall significantly in the future, the large number required for AC systems will still result in a total system cost higher than that of a DC system using a more expensive machine. Coupled with the simpler control system, higher reliability (fewer solid state components) and better machine characteristics, a DC Torquer system was selected for the EMT.

## 2.3 Time Ratio Control (TRC) Systems

### 2.3.1 General Considerations of TRC

TRC is that method of control which employs a power switching device (designated the power pass element) between a power source and a load. The power pass element either allows full conduction of power or completely blocks the power flow. The pass element alternates between the conducting and blocking states on a cyclical basis according to a controlling signal. Power delivered to the load is controlled by adjusting the pass element duty cycle. A variety of devices may be used as power pass elements--contactors, SCR's (silicon controlled rectifiers) or transistors. A more complete description of switching elements and their limitations can be found in Section 2.4.

The basic elements of a TRC circuit are shown in Figure 2.1; they include a power (voltage source), a power pass element (switch), and a load.

The following general definitions apply to TRC control methods:

- chopping frequency, $f_c$, the cyclical frequency at which the power pass element changes from conduction to blocking state
- chopping period, $T = \frac{1}{f_c} = t_{on} + t_{off}$

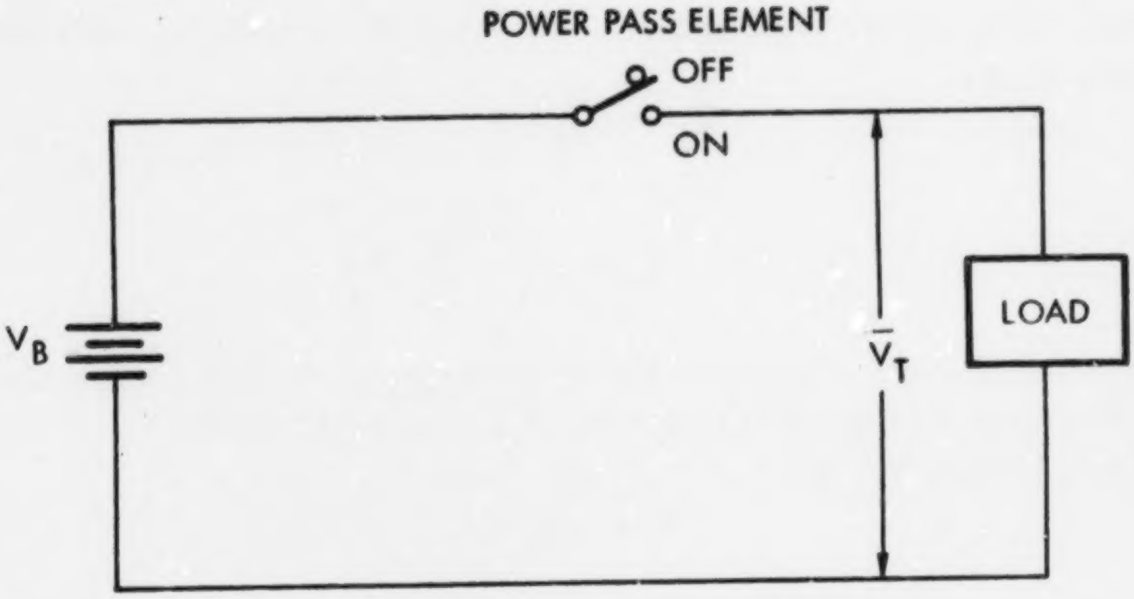
POWER PASS ELEMENT
OFF
ON
$V_B$
$\bar{V}_T$
LOAD

FIGURE 2.1
SIMPLIFIED TRC CIRCUIT

- on-time, $t_{on}$, the conduction time per cycle
- off-time, $t_{off}$, the blocking time per cycle
- duty cycle, $\alpha$, the ratio of on-time to chopping period; i.e., $\alpha = \frac{t_{on}}{T}$ .

Figure 2.2 shows a circuit technique for voltage step-down (buck control of a series wound machine). The switch, S, opens and closes in a controlled fashion, giving rise to the current waveforms in the motor and battery as shown in A . The diode is included to provide a path for the armature current when S is opened. For the limiting condition of very large series inductance, L, the armature current, $I_A$, will be as in case B, and

$$\overline{I_A} = \frac{\alpha V_B - E_g}{R_a}$$

$$\overline{I_B} = \alpha \overline{I_A} = \alpha \left( \frac{\alpha V_B - E_g}{R_a} \right)$$

Neglecting the resistance losses it can be shown that the average (DC) terminal voltage of the machine, $\overline{V_T}$, is related to the battery voltage, $V_B$, as:

$$\overline{V_T} = \alpha V_B$$

The circuitry included within the dashed lines of Figure 2.2 is termed the power control unit, PCU, and may be regarded as providing DC voltage transformer action as described by the above equation.

There are other power control functions to which TRC can be applied. The Speeder system of the EMT utilizes a boost; that is, voltage step-up technique for transforming (boosting) the rectified voltage output of the Speeder to battery bus voltage. The concept of intermittent power source to load connection is again used, although in a different configuration. The boost technique will be more fully described in Section 2.5.8.2.

FIGURE 2.2

CIRCUIT TECHNIQUE FOR VOLTAGE STEP-DOWN (BUCK) POWER CONDITIONING

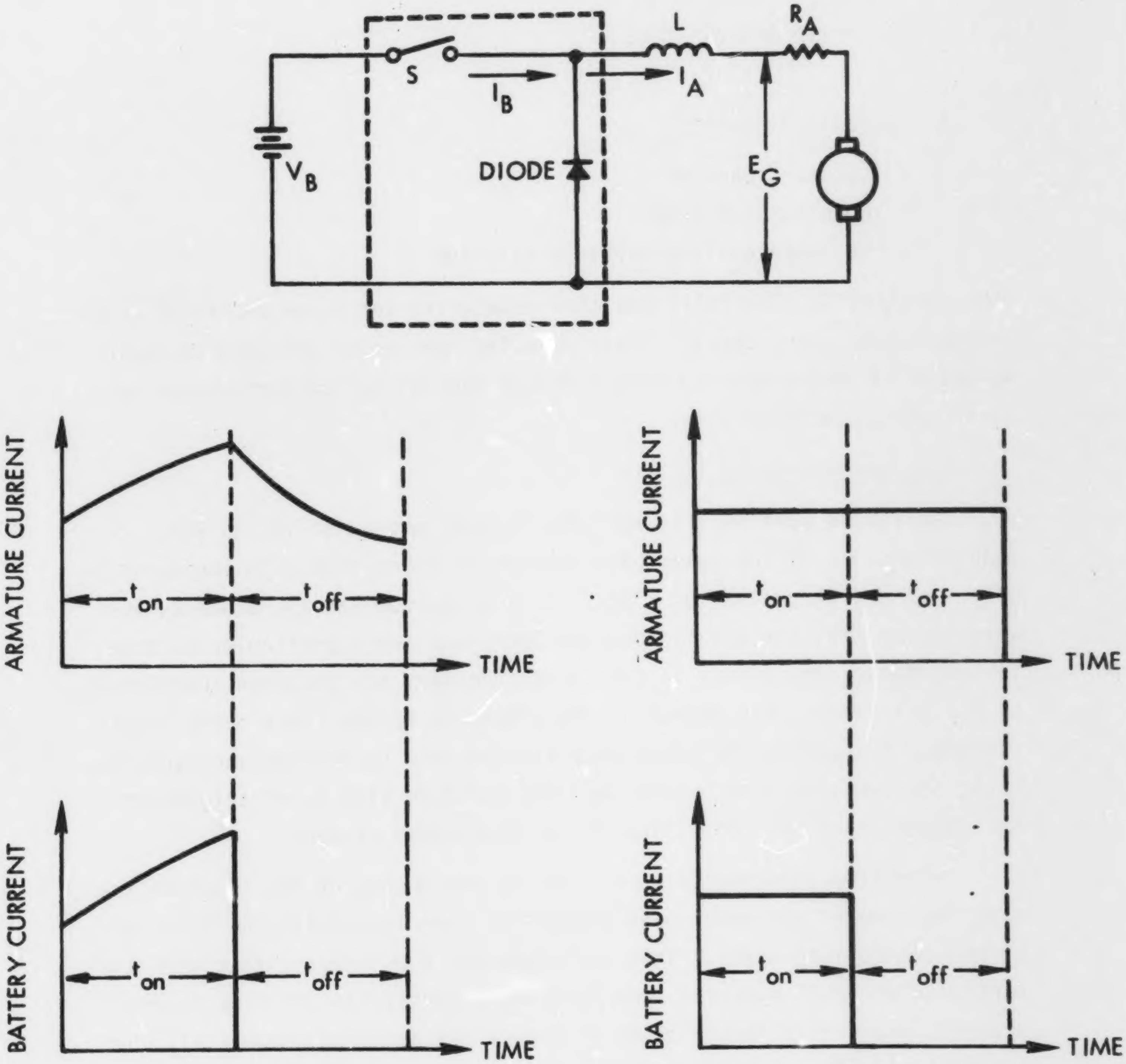
L
$R_A$
S
$I_B$
$I_A$
$V_B$
DIODE
$E_G$
ARMATURE CURRENT
$t_{on}$
$t_{off}$
TIME
BATTERY CURRENT

A. GENERAL CASE

B. LIMITING CASE ($L_A$ VERY LARGE)

### 2.3.2 TRC Techniques

#### 2.3.2.1 Description of TRC Techniques

There are several control schedules which can be used to modulate the TRC duty cycle, $\alpha$. The methods include:

- constant frequency
  - controlled on-time
  - controlled off-time

- variable frequency
  - constant on-time
  - constant off-time
  - variable on-time/variable off-time

Other methods such as pulse position modulation and pulse amplitude modulation are not considered. Their relative complexity and cost of implementation do not appear to result in substantial system performance gains over those enumerated above.

Constant Frequency TRC

Controlled on-time (Figure 2.3A) is that method of TRC in which the conduction time of the power pass element is coincident with the duration of the controlling timer or clock. This technique has the property that when the control circuit is operated open loop and a particular on-time is programmed, any errors in the clock frequency are absorbed, completely, by the off-time. This method is characterized by the clock pulse simultaneously triggering the power pass element into conduction and synchronizing the variable time pulser, and the variable time pulse triggering the cessation of the conduction of the power pass element.

Controlled off-time (Figure 2.3B) is the method of TRC in which the blocking time of the power pass element is coincident with the duration of the controlling timer. This technique has the property that when the control circuit is operated open loop and a particular off-time is programmed, any errors in the clock frequency are absorbed, completely, by the on-time. This method is characterized by the clock pulse simultaneously triggering the power pass element into the blocking state and synchronizing

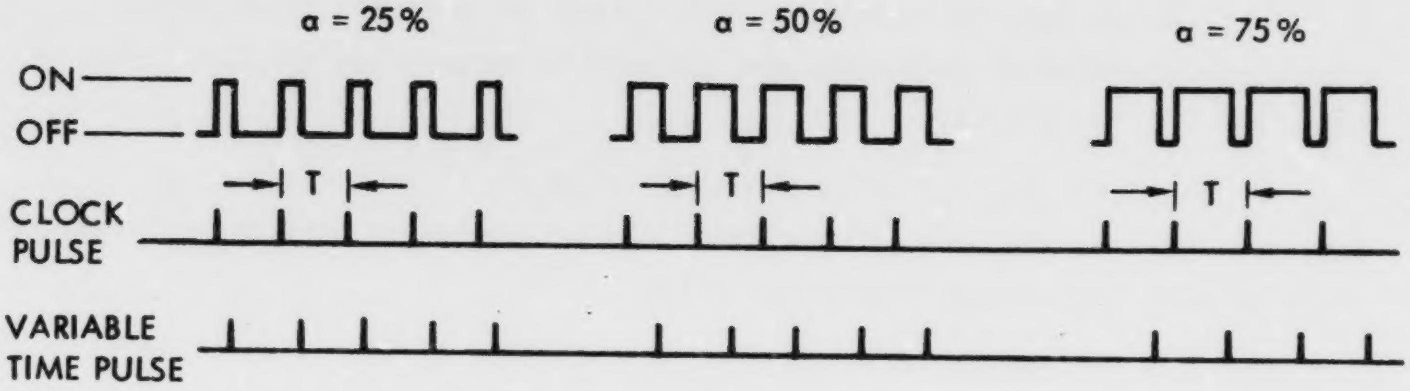
α = 25%
α = 50%
α = 75%
ON
OFF
T
T
T
CLOCK PULSE
VARIABLE TIME PULSE

FIGURE 2.3A

CONSTANT FREQUENCY-CONTROLLED ON-TIME

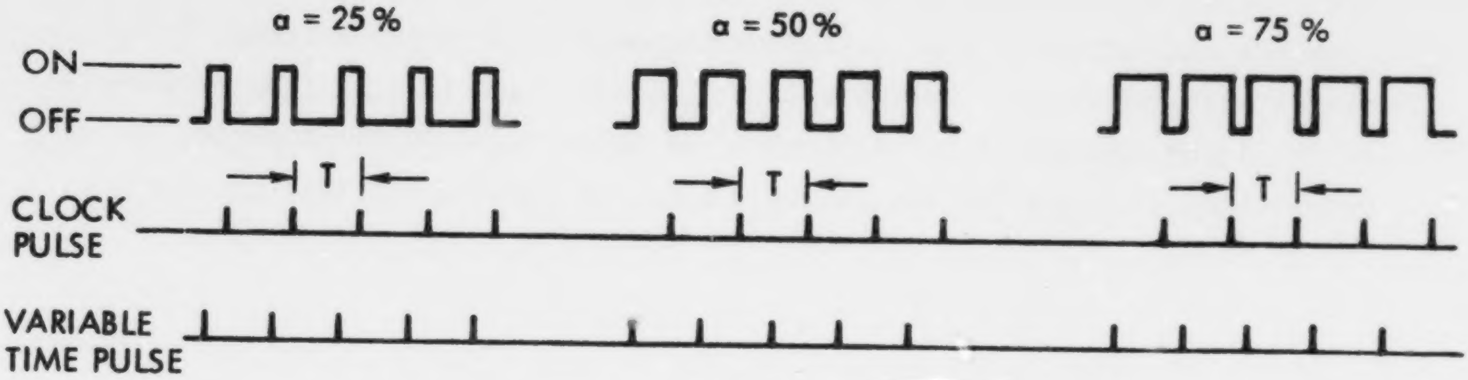
α = 25%
α = 50%
α = 75%
ON
OFF
T
T
T
CLOCK PULSE
VARIABLE TIME PULSE

FIGURE 2.3B

CONSTANT FREQUENCY-CONTROLLED OFF-TIME

the variable time pulser, and the variable time pulse triggering the power pass element into conduction.

In a system where a single timer is used for establishing the chopping frequency and the commanded period (such as a ramp and pedestal system as described in Section 7.3.1), the "on" time and "off" time are interdependent and should be self-compensating in such a manner as to maintain the desired duty cycle.

Variable Frequency TRC

Constant on-time TRC refers to that scheme in which the conduction time per cycle remains unchanged over the entire range of duty cycles and frequencies (Figure 2.4A).

Constant off-time TRC refers to that scheme in which the blocking time per cycle of the power pass element remains unchanged over the entire range of duty cycles and frequencies (Figure 2.4B).

Variable on-time/variable off-time is that type of TRC in which both the conduction time per cycle and the blocking time per cycle of the power pass element are adjusted simultaneously in order to vary the duty cycle. Constant frequency operation is a special form of this control method.

### 2.3.2.2 Trade-off of TRC Methods

An analysis of the above control methods was carried out to determine their relative merits in terms of: (1) the linearity between input commands and output levels, i.e., how the machine terminal voltage, $\overline{V_T}$, varies with the control variable ($f_c$, $t_{on}$, etc.) and (2) the time required for an input command to be realized as an output $\overline{V_T}$. In the analyses it was assumed that the TRC system would obey the idealized situation, i.e.,

$$\overline{V_T} = \frac{t_{on}}{T} V_B$$

$$\alpha = \frac{t_{on}}{t_{on} + t_{off}}$$

$$\overline{V_T} = \alpha V_B$$

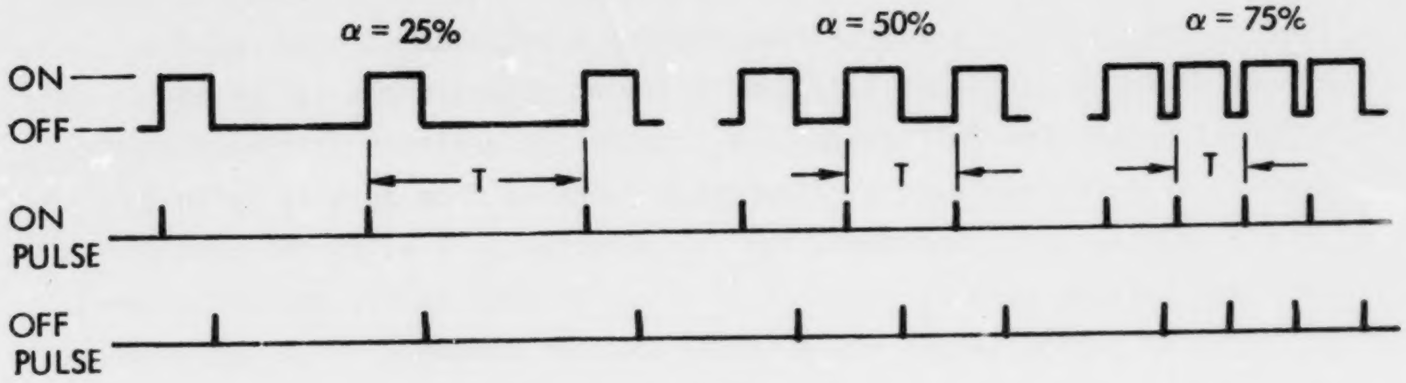
α = 25%
α = 50%
α = 75%
ON
OFF
T
ON PULSE
OFF PULSE

FIGURE 2.4A
VARIABLE FREQUENCY - CONSTANT ON-TIME

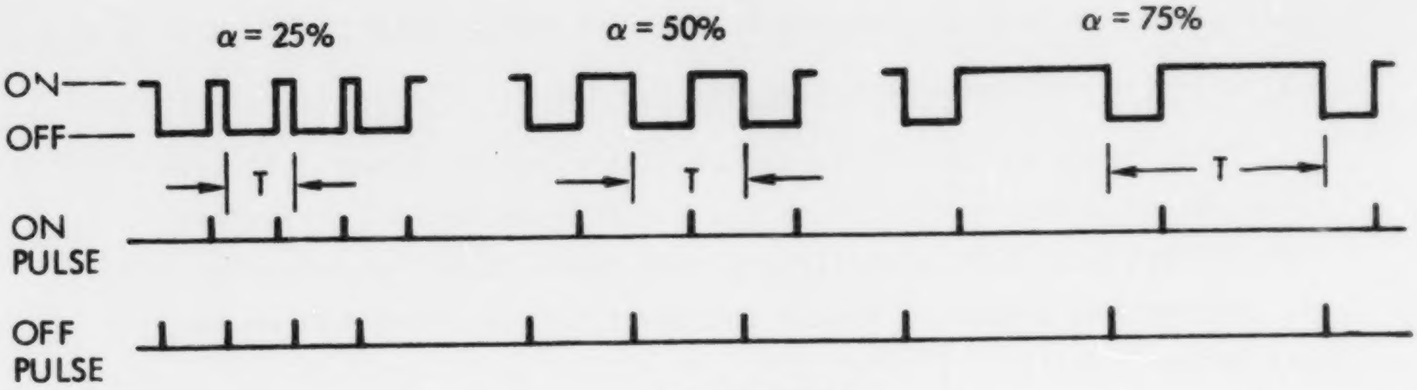
α = 25%
α = 50%
α = 75%
ON
OFF
T
ON PULSE
OFF PULSE

FIGURE 2.4B
VARIABLE FREQUENCY - CONSTANT OFF-TIME

In each case the range of $\overline{V}_T$ desired is between zero and $V_B$ as the duty cycle varies between zero and one.

Figure 2.5 and 2.6 indicate the variation of $\overline{V}_T$ with the respective control variables. In all cases, there is a linear relationship of output to input and on this basis there is no reason for the selection of one system over another. However, when one examines variable frequency operation in the light of the time required for a response to occur with a change in command (Figure 2.7) the following observations can be made. In order to obtain the full range of $\overline{V}_T$ control in variable frequency operation it is necessary that the frequency range be from zero to infinity. In the constant off-time mode, full $\overline{V}_T$ requires $\frac{1}{f_c} \to \infty$; in the case of constant on-time zero $\overline{V}_T$ requires $\frac{1}{f_c} \to \infty$. In both cases, the requirement of infinite period length would impose extreme slowness of system response to variations in input commands. At the other end, the requirement of $\frac{1}{f_c} \to 0$ entails extremely high frequency operation. In view of the frequency limitations of all candidate power pass elements, full range operation of the TRC would be limited.

There are secondary reasons for the selection of a constant frequency system which will be described further in Section 6. However, in passing it is important to note the simplification of magnetic and semiconductor design with constant frequency operation. In turn, the ability to design about one operating frequency will minimize filtering requirements, reduce power peaks, losses, and component sizes and reduce potential stability problems.

## 2.4 Selection of Power Pass Elements for TRC

Three types of components are available for the power switching functions of a TRC system; these are: electromechanical contactors, transistors, and silicon controlled rectifiers, SCRs. A selection of the appropriate device to use as the power pass element must be based on consideration of:

- maximum current capability
- maximum voltage capability
- speed (switching time)
- maximum power capability

$$V_T = t_{on} f_c V_B$$

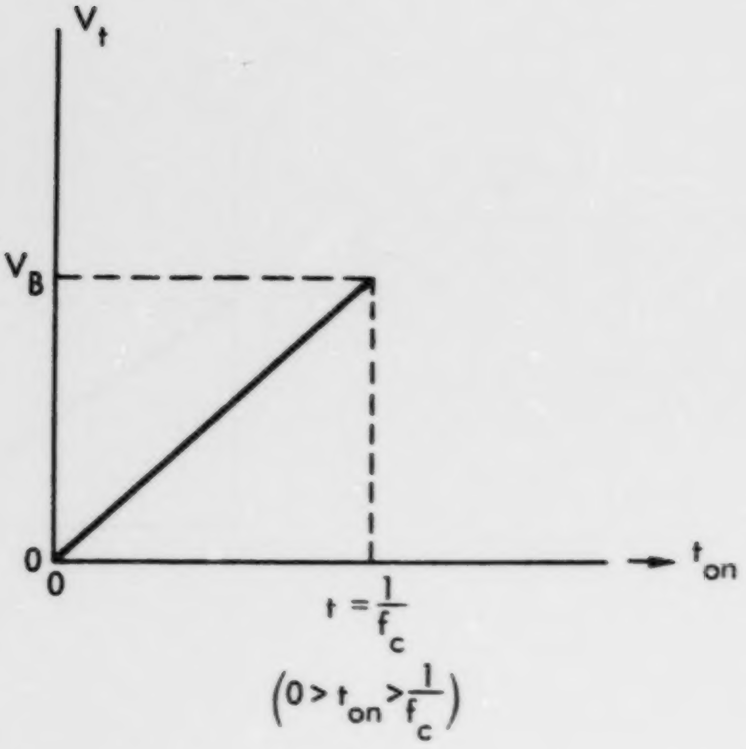

CONSTANT FREQUENCY - VARIABLE $t_{on}$

$$V_T = \left(T - t_{off}\right) f_c V_B$$

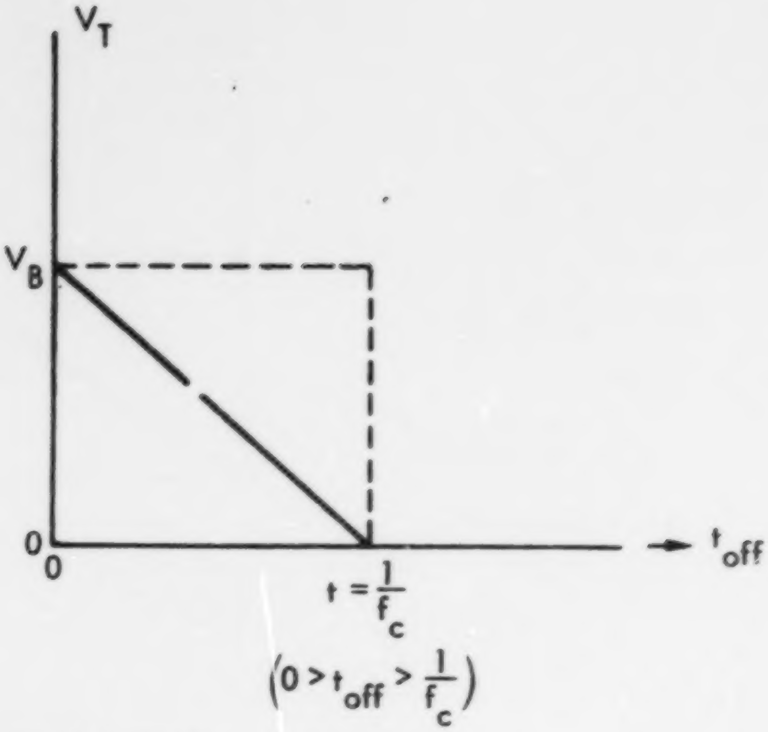

CONSTANT FREQUENCY - VARIABLE $t_{off}$

FIGURE 2.5

$$V_T = \frac{\frac{1}{f_c} - t_{off}}{\left(\frac{1}{f_c} - t_{on}\right) + t_{on}} V_B$$

$$V_T = \left(1 - t_{off} f_c\right) V_B$$

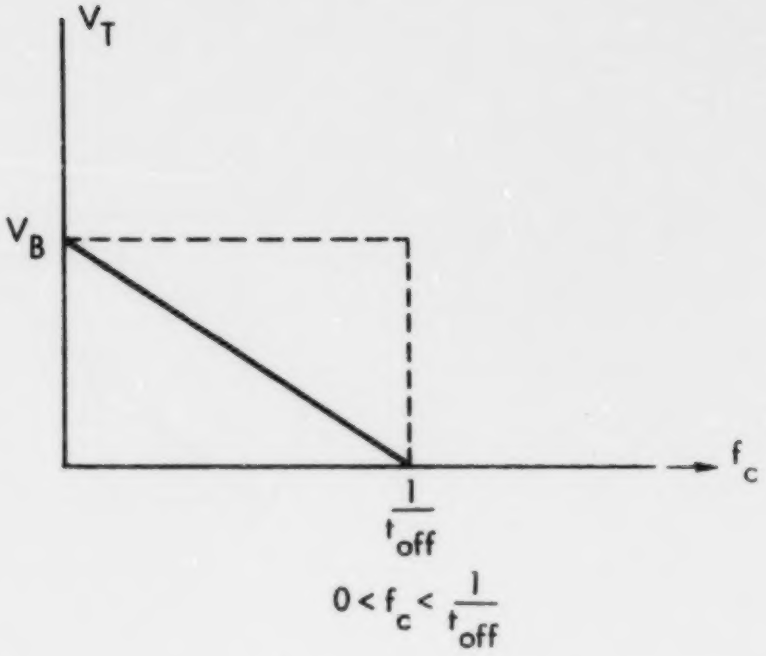

VARIABLE FREQUENCY - CONSTANT $t_{off}$

$$V_T = \frac{t_{on}}{\frac{1}{f_c}} V_B$$

$$V_T = t_{on} f_c V_B$$

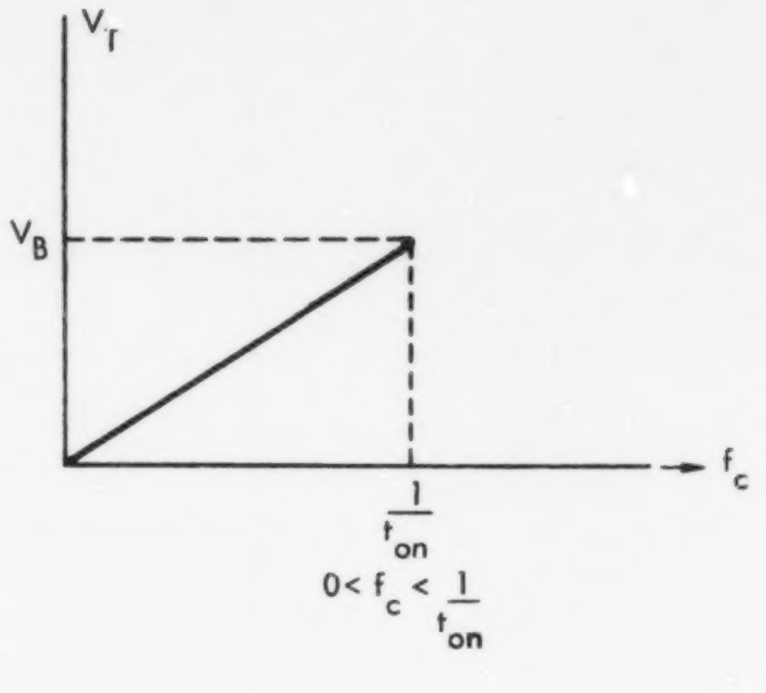

VARIABLE FREQUENCY - CONSTANT $t_{on}$

FIGURE 2.6

## VARIABLE FREQUENCY - CONSTANT ON-TIME

$t_{on} = K_2$

$$V_T = \frac{t_{on}}{t_{off} + t_{on}} V_B$$

$$V_T = \frac{K_2}{t_{off} + K_2} V_B$$

$0 > t_{off} > \infty$

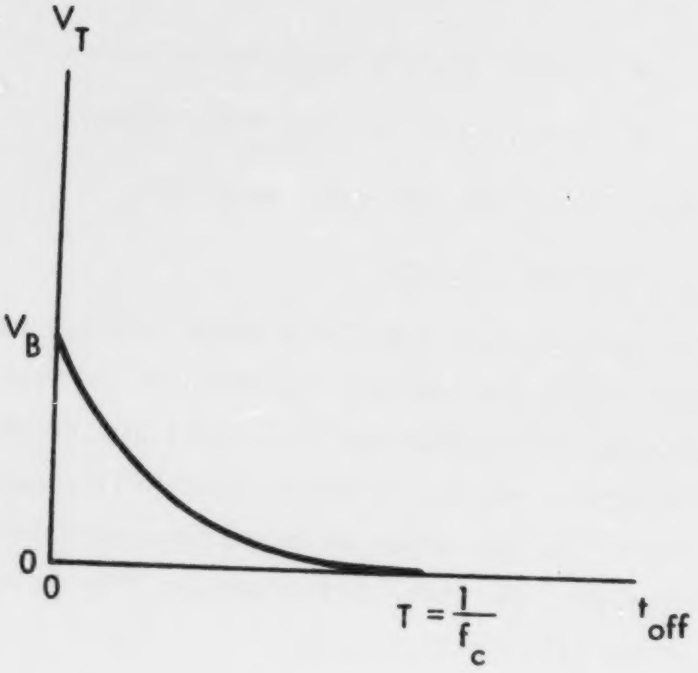

## VARIABLE FREQUENCY - CONSTANT OFF-TIME

$t_{off} = K_3$

$$V_T = \frac{t_{on}}{K_3 + t_{on}} V_B$$

$0 > t_{on} > \infty$

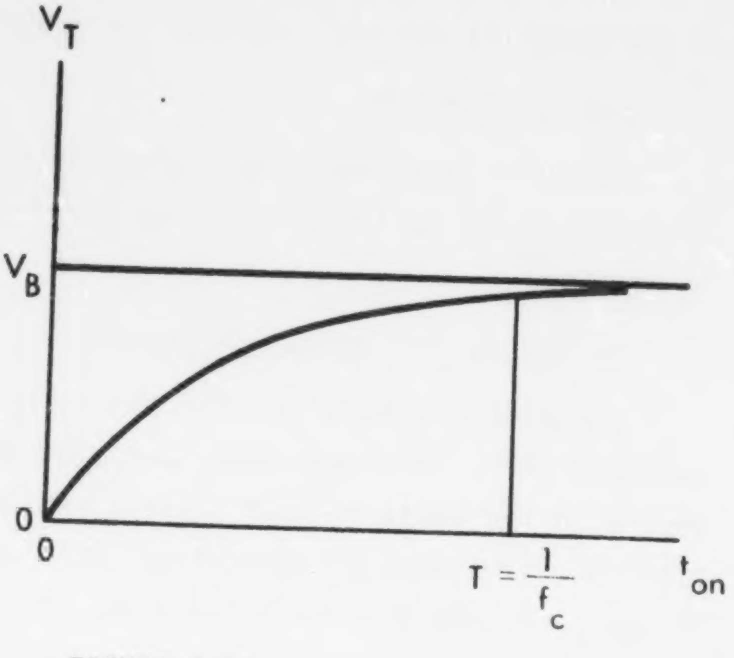

FIGURE 2.7

- ease of turn-off
- switching and conduction losses
- gain, gate or coil requirements

### 2.4.1 Electromechanical Contactors

Maximum Current

Devices are available with current ratings so high that there is essentially no current restriction in the present application. However in service, the contactor must make and break high current levels repeatedly. Contactors can be valuable switching elements if provisions are made to insure the contactor is not operated while current in flowing through its contacts. In this latter sense, they have been employed within the EMT system (see Section 8.1).

Maximum Voltage

Devices are available with voltage ratings so high that there is essentially no voltage restrictions in TRC systems.

Switching Time

Speed varies with the particular device selected but is typically of the order of 100 milliseconds for heavy duty devices.

Ease of Turn-Off

Turn-off is accomplished by either energizing or deenergizing the solenoid coil. An independent low level power source is required for energizing.

Switching and Conduction Losses

Losses are associated with the resistance of the contact and the solenoid coil. Although most losses occur in the solenoid coil, the losses in the contacts must be reckoned with and depend on load conditions and frequency of switching. Coil requirements depend on the size of the contactor and its KVA rating, the larger the rating, the more coil energizing power. For example, the contactor of the present Torquer system uses a 25 W, 24 V coil to make or break contacts rated at 300 amperes.

### 2.4.2 Transistors

#### Maximum Current

Currents up to 60 amperes can be handled in devices capable of blocking 300 volts in the forward direction.

#### Maximum Voltage

Transistors capable of blocking up to 1000 volts are available; however, their current capacity is limited to approximately 15 amperes.

#### Switching Time

The blocking-to-conduction time for transistors can be less than two microseconds.

#### Ease of Turn-Off

Transistors are conventionally turned-off by removal of the base drive. Turn-off time may be further reduced by application of a reverse bias of one-to-three volts to the base-emitter junction.

#### Switching and Conduction Losses

There are three sources of losses in transistors:

- Losses during the rise and fall time of current flow. These losses are due to the product of current flow times the forward voltage drop in the drive during the switching period.
- Collector saturation losses equivalent to the steady state (conduction) voltage drop through the device.
- Base drive losses related to voltage drops in the base (control) portion of the transistor.

The sum of the rise and fall time losses and the base drive losses are frequently of the order of the collector saturation losses. In the 60 ampere transistor noted above, approximately 60 watts are dissipated during the switching on and shutting off of the device. A similar power loss is associated with its steady state operation.

#### Gain

Transistors typically exhibit a current gain of 25 in analog control usage; however, when applied to saturated switching service as in a TRC system, the gain is derated to 10. The lower gain is used to insure the transistor remains saturated (over-apply the base signal to insure "a closure" of the switch) and to insure that the transistor traverses its analog region as rapidly as possible to approximate a switch more closely and to reduce dissipation.

It is important to note that transistors cannot resist voltages in a reverse direction and in circuits where a reverse bias is anticipated blocking diodes must be provided in series. This requirement adds not only additional complexity and sources of dissipation, but elevates the base-to-ground voltage with increased susceptability to noise.

### 2.4.3 SCRs

#### Maximum Current and Voltage

SCRs are presently available which can carry 470 amperes, block voltages up to 1200 volts, and retain a turn-off time of 15 microseconds. While units are available which can block up to 1700 volts and carry 850 amperes, their turn-off time is greatly increased. For example, a device with a 1200 volt, 1000 ampere rating will require approximately 150 microseconds to turn-off. As will be demonstrated later, turn-off time impacts heavily on the design and performance of a TRC system.

#### Switching Time

SCRs turn-on (reduce from an open-circuit state to a 5 volt forward drop) virtually instantaneously. They turn-off (regain blocking capability) in relatively longer periods. Turn-off times increase rapidly with current capacity and temperature. The best units available today in power levels appropriate for vehicle traction use have turn-off times in the neighborhood of 10 to 20 microseconds.

#### Ease of Turn-Off

SCRs cannot be turned off solely by the removal of the gate signal as in the case of a transistor; rather special commutation circuits or AC techniques must be used in conjunction with the removal of the gate. In any system the SCR is turned off by bringing the current flow through the device to zero. This is done by removing the voltage source or reverse biasing the voltage across the device. If provided by circuitry (such as clamping a capacitor across it) it is called forced commutation.

If provided by the power source such as the normal voltage reversal of an AC supply it is called natural or line commutation.

Switching and Conduction Losses

SCR losses can be separated into five basic components as follows:

- gate trigger losses
- turn-on losses
- forward conduction losses
- commutation losses
- turn-off losses

Gate losses are low typically 300 mw due to the very high switching gain. The effects of gate losses may be reduced even further by applying low duty cycle pulse commands as opposed to steady state commands.

Turn-on losses are significant during approximately the first 40μs following application of the trigger pulse. During this time the device passes through a highly dissipative analog region, where its forward voltage drop remains high. The steady state conduction losses are equal to the product of the SCR saturation (steady state) voltage-approximately 2.5V and the load current.

Commutation losses and turn-off losses are similar to turn-on losses. While commutation losses in the SCR itself are of the same order of magnitude as the turn-on losses, the circuitry which provides the energy for turn-off has losses associated within itself and must be included as a part of a total SCR-based TRC system.

### 2.4.4 Summary of Candidate TRC Power Pass Elements

It is apparent from the above considerations that electromechanical devices are too slow for use in an advanced TRC system. In view of the total number of switching cycles anticipated for vehicle use and the limited service capability of such devices for high power switching they are rejected.

Transistors, while providing the necessary switching speed and "arcless" circuit breaking, are not currently available in a power handling capacity sufficient for vehicle application with paralleling. Paralleling techniques introduce additional problems of base drive synchronization and current balancing.

It appears that SCRs are the only power pass element which can be used in a TRC system. Thus, evaluation of TRC power control circuitry is restricted to those systems employing SCR power pass elements.

### 2.5 Trade-off and Selection of a Torquer Power Control Unit (Torquer PCU)

This section describes several circuits considered as candidate power control units for the Torquer system. Attention is focused on drive systems employing a series wound traction motor. While the circuits investigated are by no means exhaustive of the total circuits which can be conceived, it is felt they are representative of the various classes of circuits which could be employed. A reference list is provided on additional circuits which could be or are presently employed in electric vehicle traction use.

Each of the circuits described has (or is meant to have) the following features in common:

- A fuse and a key operated master contactor is placed in series with the input to the controller. These are required for starting sequencing and operator and/or machinery protection.
- A flyback diode is provided across the motor to maintain a continuous motor current during the power SCR off time. Dynamic braking is possible in all cases.
- All circuits utilize forced commutation to turn the power SCR off.
- Switches ($SW_2$ and $SW_3$) are provided for selection of field polarity for drive or dynamic braking.
- A current sense transducer is included in the armature circuit which can be used for providing control signal for current limiting, switch and logic control and other protective and/or performance functions.
- The motor is represented by a series resistance (armature, field and brushes) and an inductance (series field, interpoles and armature).

Advantages and disadvantages are cited for each circuit and thus a note of explanation is required so that some ranking may be established. Circuits which require charging the commutation capacitor through the motor have two drawbacks. First, the rate of voltage build-up and the final voltage level of the capacitor will depend to some degree on the state of the motor back-EMF. In these situations, lockout protection (circuits which detect the potential inability of the commutation capacitor to provide enough energy to turn the power SCR off and thus inhibit the gating on of that SCR) may have to be included. Second, if charging power flows through the motor, there is a certain minimum amount of energy delivered per cycle to the motor through the commutation circuit even if the power SCR is not turned on. Low speed traction control may be difficult.

Circuits which discharge the commutation capacitor through the motor have an advantage and a disadvantage. The advantage lies in the more complete utilization of commutation power in that not only does it turn off the power SCR, it also provides tractive effort. On the other hand, the commutation discharge energy per cycle presents a low speed control problem as suggested above.

### 2.5.1 Circuit I (Figure 2.8)

#### Operation

Initially capacitor $C_1$ is discharged. SCRs 3, 1 and 2 are fired in that sequence. When SCR 3 is turned on $L_1$ and $C_1$ form an oscillating circuit. The voltage across $C_1$ oscillates for $180^0$ reverse biasing $SCR_3$ and turning it off. $C_1$ is left charged to approximately twice-battery voltage in a direction opposite that indicated in the figure. $SCR_1$ is then fired, delivering a power pulse to the motor load. $SCR_1$ is commutated off by turning $SCR_2$ on thus clamping a reversed voltage across $SCR_1$. $C_1$ discharges into $SCR_1$ and the load. As $C_1$ discharges, the current through $SCR_2$ goes to zero, commutating that device off. The PCU is then ready for the next cycle.

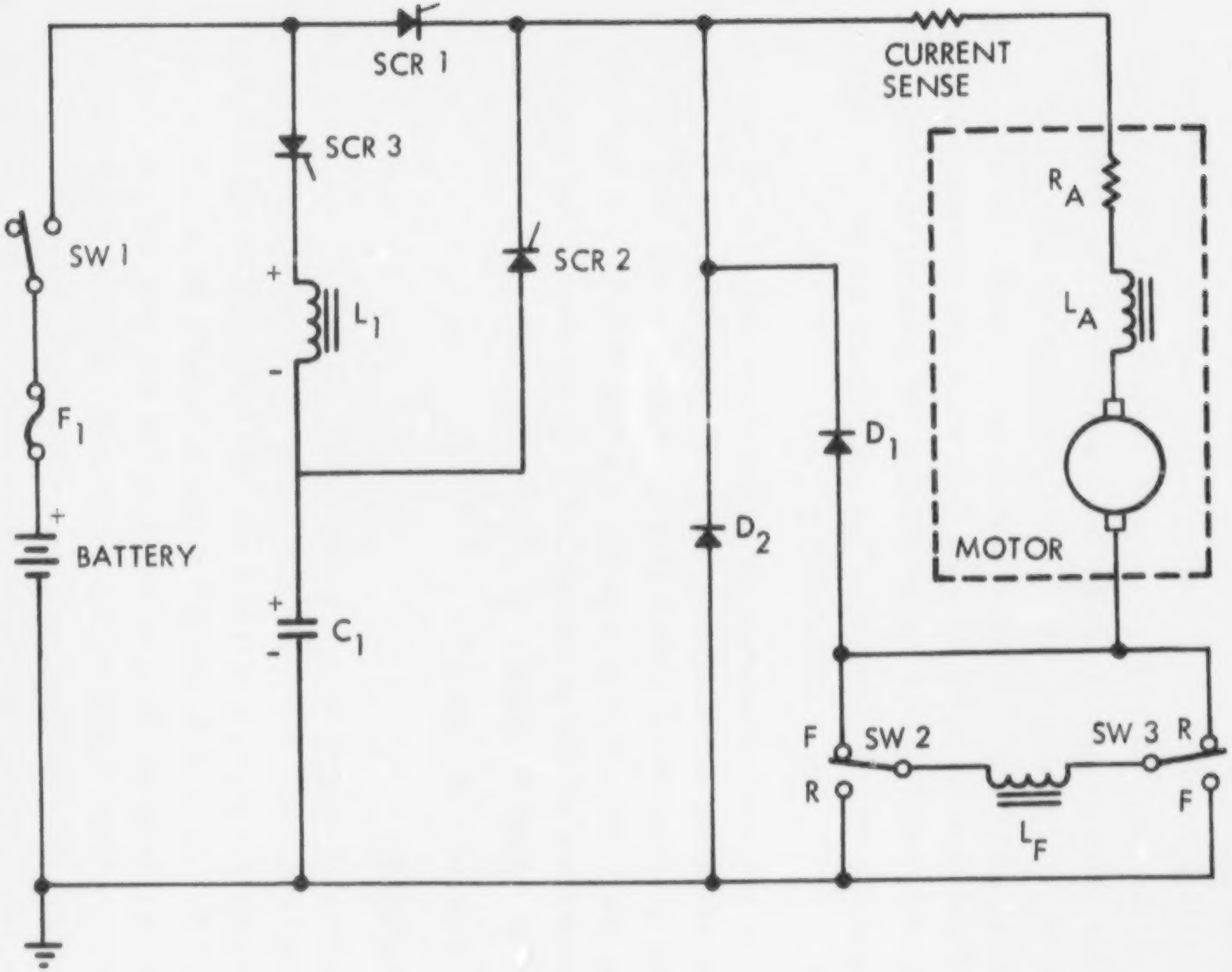
SCR 1
CURRENT SENSE
SCR 3
SW 1
$R_A$
SCR 2
+
$L_1$
$L_A$
-
$F_1$
$D_1$
+
BATTERY
$D_2$
MOTOR
+
$C_1$
-
F
SW 2
SW 3
R
R
F
$L_F$

FIGURE 2.8
CIRCUIT I

Advantages

- The charging current for the commutating capacitor does not flow through the motor load.
- Commutating energy discharges through the load.
- The commutation capacitor charges independently of the state or duty cycle ($\alpha$) of the power SCR, $SCR_1$, provided $SCR_2$ is not turned on before the charging oscillation is completed.

Disadvantages

- A specific SCR firing sequence is required, as well as synchronization of all gating signals.
- Three SCRs are needed.
- In the event $SCR_2$ fails to turn on, $SCR_1$ cannot be commutated off and the circuit is endangered.
- If $SCR_2$ is triggered before the charging oscillation is completed $SCR_1$ cannot be turned off.

### 2.5.2 Circuit II (Figure 2.9)

Operation

Initially the commutating capacitor, $C_1$, is discharged. When the power contactor, $SW_1$ is closed $L_1$ and $C_1$ form an oscillating circuit and oscillate for $180^o$, leaving $C_1$ charged approximately to twice battery voltage in the polarity indicated in the figure. The power SCR, $SCR_1$ is then fired, delivering a power pulse to the motor. In order to turn $SCR_1$ off, $SCR_2$ is turned on, discharging $C_1$ into $L_2$ and turning $SCR_1$ off. $L_2$ and $C_1$ oscillate $180^o$, charging $C_1$ to an opposite polarity and commutating $SCR_2$ off. ($L_1$ must be much larger than $L_2$ to insure $L_2$ and $C_1$ form the major oscillatory circuit.) After $SCR_2$ turns off, $L_1$ and $C_1$ again form an oscillatory loop, charging $C_1$ for the next cycle.

Advantages

- The charging and discharging current for $C_1$ does not flow through the motor
- The charging of $C_1$ is independent of the state or duty cycle of the power SCR, $SCR_1$
- $SCR_1$ and $SCR_2$ need no starting sequence relative to each other but must be synchronized.

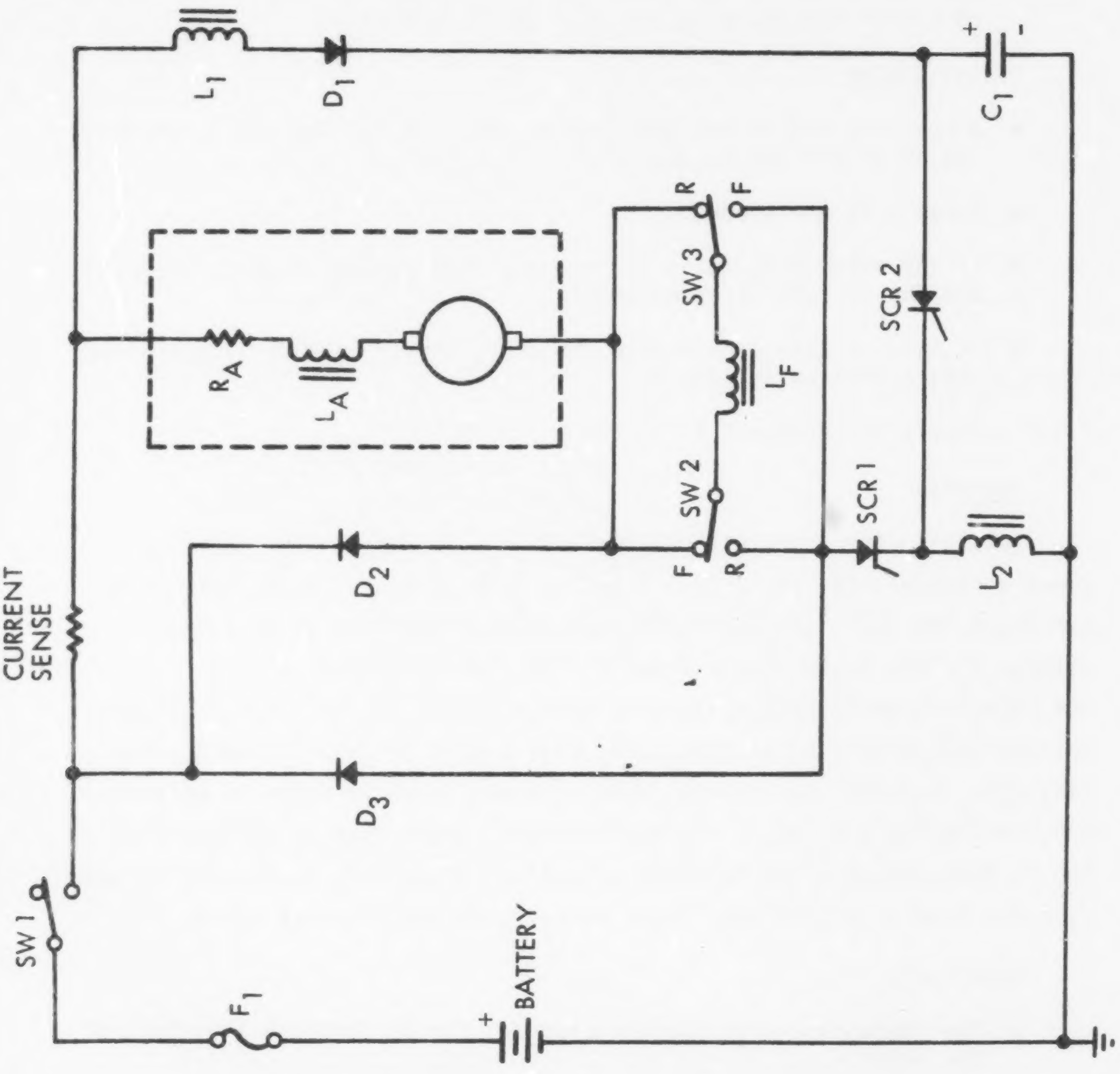
CURRENT SENSE
SW 1
$F_1$
+
BATTERY
$D_3$
$D_2$
F
R
SW 2
SCR 1
$L_2$
$L_F$
SW 3
R
F
SCR 2
$R_A$
$L_A$
$L_1$
$D_1$
$C_1$
+
-

FIGURE 2.9
CIRCUIT II

Disadvantages

- If the oscillation of $L_2$ and $C_1$ does not commutate $SCR_2$ off, or if $SCR_2$ assumes a permanent conduction state, the system is locked in an unsafe mode with the battery connected across $L_1$ and $L_2$, and unlimited current in $SCR_2$.
- Commutating capacitor energy does not flow through the motor.
- $L_2$ is an additional loss member placed in series with the load during the power pulse period when $SCR_1$ is on.

### 2.5.3 Circuit III (Figure 2.10)

Operation

When $SW_1$ is closed, the commutating capacitor, $C_1$, is charged in the polarity indicated via the saturable reactor $SR_1$, diode $DR_2$ and the motor. The path through $L_2$ and $DR_4$ is provided in the event the effective impedance of the load is too large to allow effective capacitor charging. $SCR_1$ is fired to deliver the power pulse to the motor load. To turn $SCR_1$ off, commutating $SCR_2$ is fired causing $L_1$ and $C_1$ to oscillate through $180^{o}$, charging $C_1$ to a polarity opposite to that indicated in the figure. $C_1$ is charged to a voltage equal to the battery. The saturable reactor is driven into a saturated state at the negative peak of the $180^{o}$ oscillation allowing $C_1$ to discharge through $SR_1$, $DR_2$ and the load. $SCR_1$ and $SCR_2$ are commutated off and $C_1$ goes to its initial condition ready for the next cycle.

Advantages

- The commutating capacitor charges completely, independent of the state or duty cycle of $SCR_1$.
- $C_1$ discharge energy flows through the load.
- No starting sequence is required for $SCR_2$ relative to $SCR_1$.

Disadvantage

- Capacitor charging current flows through the load.

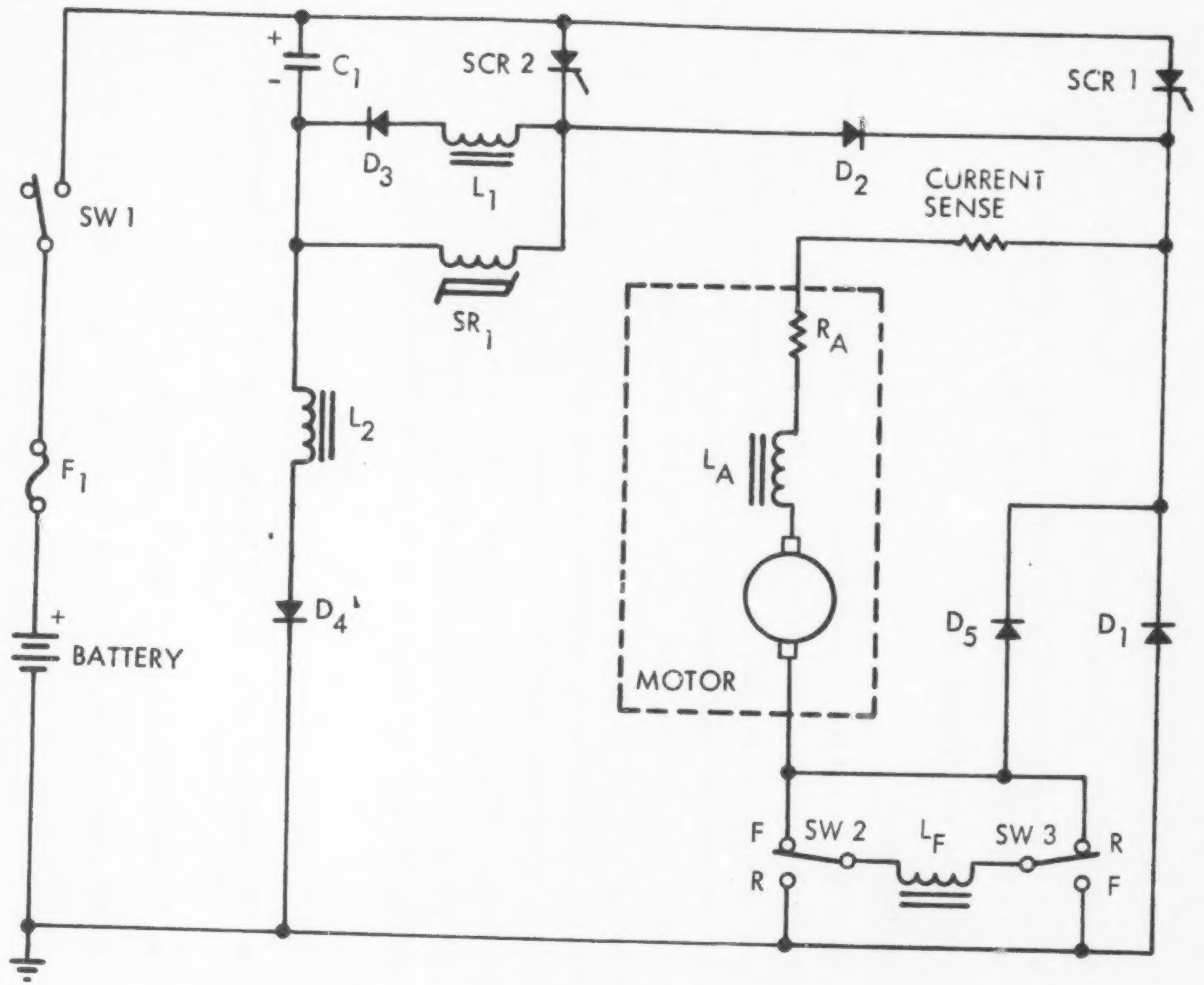
SCR 2
SCR 1
+
-
C1
D3
L1
D2
CURRENT SENSE
SW 1
SR1
RA
L2
F1
LA
+
BATTERY
D4
D5
D1
MOTOR
F
SW 2
LF
SW 3
R
R
F

FIGURE 2.10
CIRCUIT III

### 2.5.4 Circuit IV (Figure 2.11)

Operation

After $SW_1$ is closed, $SCR_1$ is fired, delivering a power pulse to the motor and inducing a voltage in the secondary of saturable transformer $T_1$ with terminals 1 and 3 positive, thereby charging $C_1$ in the polarity indicated. $SCR_2$ then fires discharging $C_1$ into the load and commutating $SCR_1$ and itself off. The cycle is then ready to be repeated.

Advantages

- Commutating capacitor discharges through the load.
- No firing sequence is required with respect to $SCR_1$ and $SCR_2$.

Disadvantages

- The commutating capacitor charging current does flow through the load.
- The voltage to which $C_1$ will charge is a function of the duty cycle, the state of conduction of $SCR_1$ and the load. However, depending on the minimum duty cycle and minimum load anticipated, it may be possible to consider the charging of $C_1$ independent of the load and duty cycle of $SCR_1$.
- If $T_1$ does not charge $C_1$ sufficiently, or if for some other reason $SCR_1$ fails to commutate off, the system is locked in an unsafe condition and the battery, motor and $SCR_1$ may be damaged.
- This circuit must operate with a variable frequency control system.

### 2.5.5 Circuit V (Figure 2.12)

Operation

$SCR_1$ is turned on delivering a power pulse to the load and charging the commutation capacitor $C_1$ to battery voltage at a polarity opposite to that indicated in the figure. $SCR_1$ is turned off by turning on $SCR_2$, clamping $C_1$ across $SCR_1$. $SCR_2$ remains in the conducting state allowing $C_1$ to charge through both the load and $R_1$ to the polarity indicated. When $SCR_1$ is subsequently fired, $SCR_2$ is commutated off by having $C_1$ clamped across it.

Advantages

- There are no important advantages to this circuit

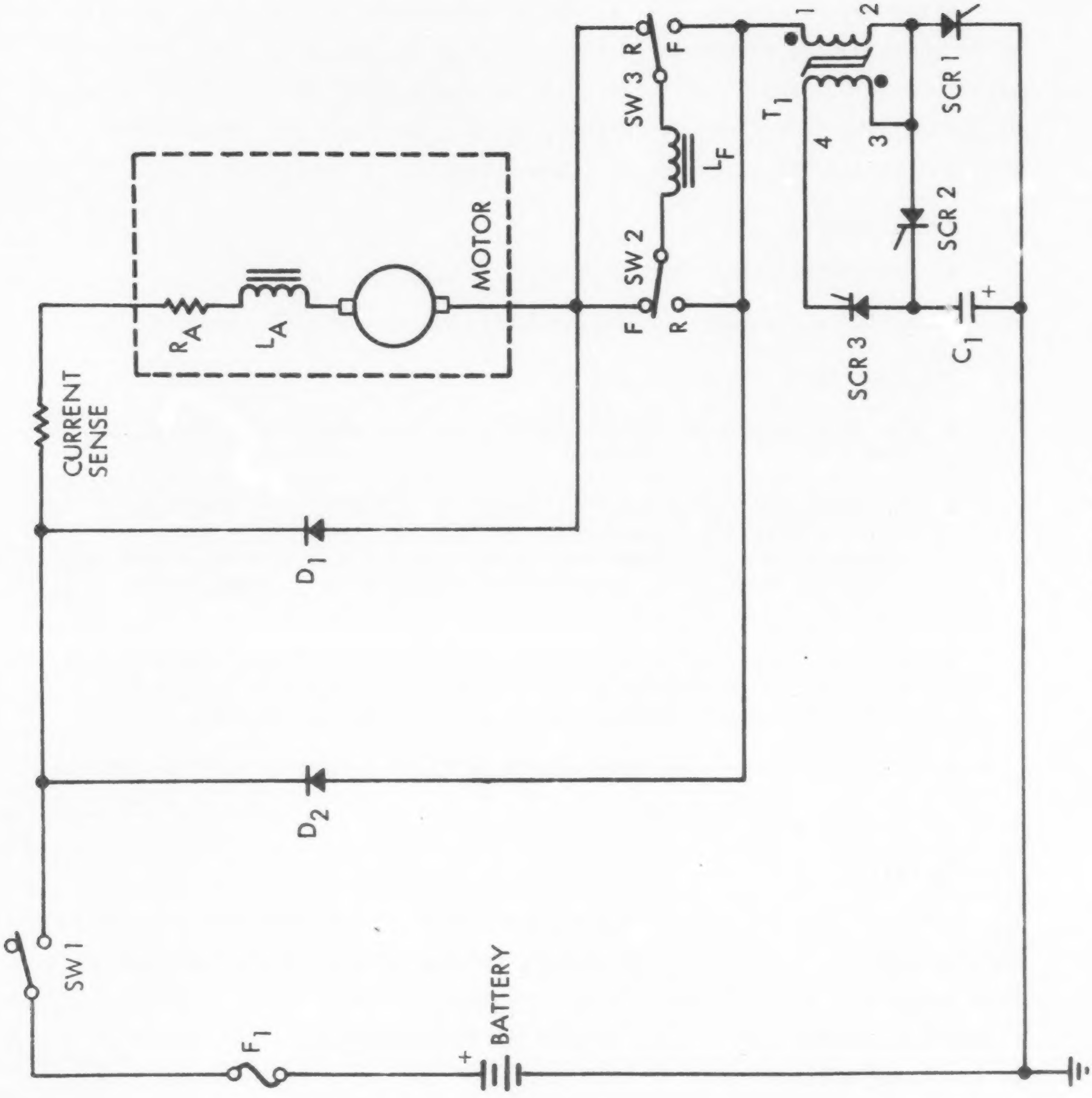
SW 1
F1
+
BATTERY
CURRENT SENSE
RA
LA
MOTOR
D1
D2
F
R
SW 2
SW 3
R
F
LF
T1
1
2
3
4
SCR 1
SCR 2
SCR 3
C1
+

FIGURE 2.11
CIRCUIT IV

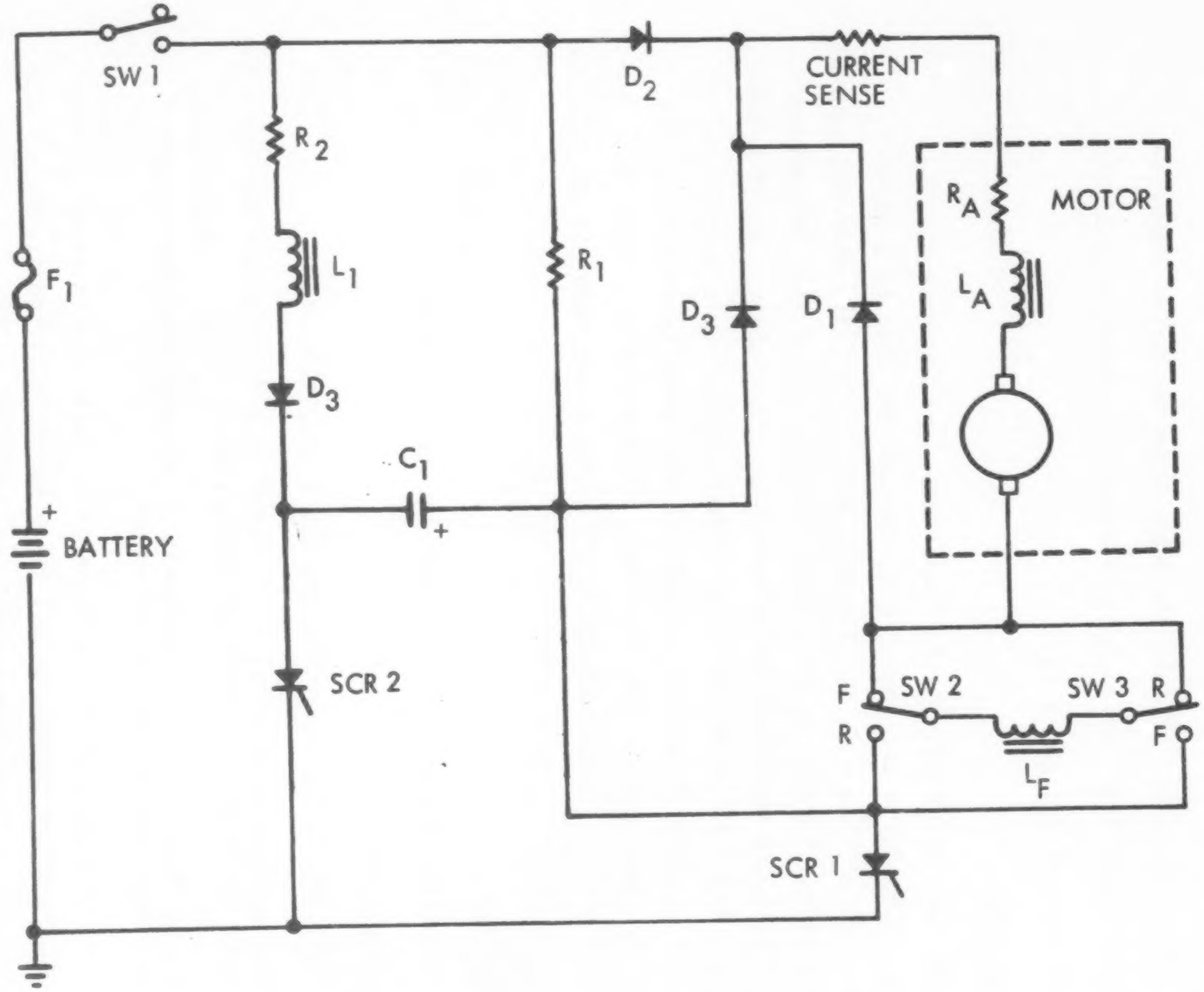
SW 1
F1
BATTERY
+
R2
L1
D3
C1
+
SCR 2
R1
D2
D3
CURRENT SENSE
D1
RA
MOTOR
LA
F
R
SW 2
SW 3
R
F
LF
SCR 1

FIGURE 2.12
CIRCUIT V

Disadvantages

- The voltage to which $C_1$ will charge is a function of the duty cycle and the state of conduction of $SCR_1$ and $SCR_2$. Although $L_1$ is included to provide resonant charging of $C_1$, commutation may still be a problem at very short duty cycles.
- Capacitor charging current flows through the load.
- The commutation circuit includes major resistive components.
- The upper limit of chopping frequency is limited by $R_2$ and $C_1$.

### 2.5.6 Circuit VI (Figure 2.13)

Operation

After $SW_1$ is closed, the following starting sequence must be followed. $SCR_2$ turns on, charging $C_1$ through the load to a polarity opposite that indicated in the figure. When $C_1$ is fully charged, current in $SCR_2$ ceases, turning $SCR_2$ off. $SCR_1$ is then fired, delivering a power pulse to the motor and establishing an oscillatory circuit between $C_1$ and $L_1$. After the current in the commutation circuit oscillates for $180^0$, $C_1$ is charged to battery voltage in the polarity indicated. To conclude the power pulse, $SCR_2$ is fired, discharging $C_1$ across $SCR_1$ commutating it off. $C_1$ continues to charge through the motor to an opposite polarity.

Advantage

- Capacitor energy is discharged through the motor.

Disadvantages

- The commutating capacitor charges through the motor.
- The voltage to which $C_1$ will charge is a function of the load, the duty cycle and the state of conduction of $SCR_1$.
- A starting circuit is required; if a proper sequence is not observed $SCR_1$ cannot be turned off.

2.5.7 Circuits I through VI are compared in Table 2.2 in terms of the major power handling components and their operational requirements. The total number of critical power components includes all SCRs, diodes, chokes, reactors and transformers which handle load or commutation power.

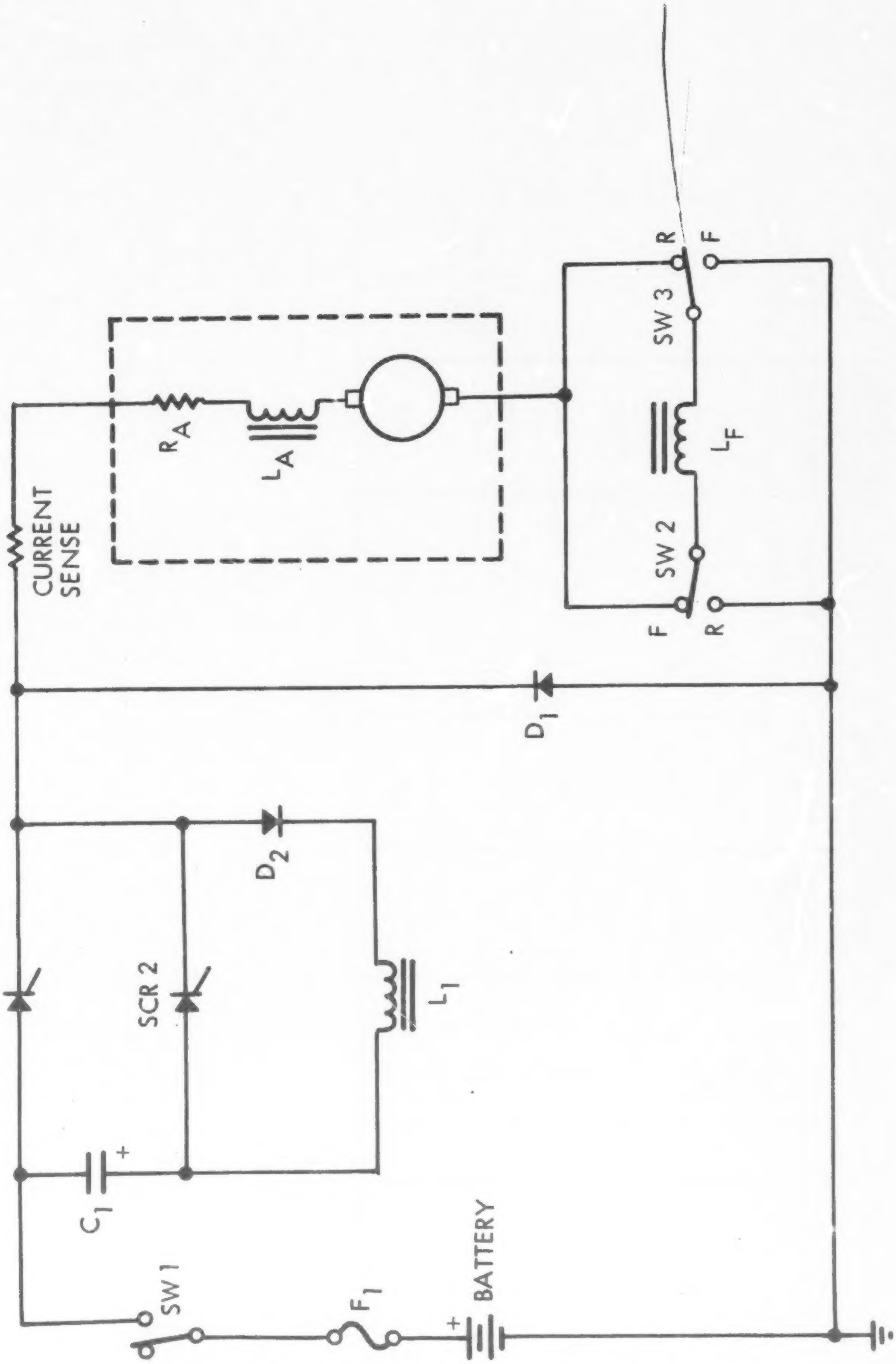
SW 1
F1
+
BATTERY
C1
+
SCR 1
SCR 2
D2
L1
D1
CURRENT SENSE
RA
LA
F
SW 2
R
LF
SW 3
R
F

FIGURE 2.13
CIRCUIT VI

## TABLE 2.2
## COMPARISON OF CANDIDATE DRIVE CIRCUITS

| Circuit | No. of SCRs | No. of Commut SCRs | No. of Power Diodes | No. of Chokes | No. of Saturable Reactors | Starting Sequence Required | No. of Semiconductors in Series with Load | Auxiliary Capacitor Charging | No. of Critical Power Components |
|---|---|---|---|---|---|---|---|---|---|
| I | 3 | 2 | 2 | 1 | 0 | yes | 1 | yes | 7 |
| II | 2 | 1 | 2 | 2 | 0 | no | 1 | yes | 8 |
| III | 2 | 1 | 3 | 2 | 1 | no | 1 | yes | 11 |
| IV | 3 | 2 | 2 | 0 | 1 | no | 1 | no | 7 |
| V | 2 | 1 | 3 | 1 | 0 | no | 2 | no | 10 (counting resistors) |
| VI | 2 | 1 | 2 | 1 | 0 | yes | 1 | no | 6 |

### 2.5.8 Selection of Torquer PCU Circuits

The circuits described in the previous sections have been used for traction drive systems where only motor operation and in some cases dynamic braking has been desired. The functional requirement of the Torquer system requires that the Torquer be equally capable of providing efficient and controllable regenerative operation. The following section describes considerations given to this requirement and circuitry to perform those functions.

#### 2.5.8.1 Single vs. Dual Controllers

Two techniques are available for providing drive and regeneration control. One method is to utilize two independent power controllers as shown in Figure 2.14. The second method is to employ a single controller which can be reconfigured by appropriate switching to perform in both modes.

The two controller system offers an advantage in that the transfer from drive to regeneration and vice versa can be made smoothly and with vanishingly small dead time for the transfer. However, it is obvious that such a system will contain nearly twice the major power processing elements as a single controller. On the basis of a greatly lowered part count and lower cost, methods of utilizing a single controller concept were explored.

#### 2.5.8.2 Consideration of Step-Down and Boost vs. Boost Power Processing Systems for Regenerative

While functioning as a generator, the Torquer must be capable of delivering power to the battery over a wide range of machine speeds and battery voltages. Two concepts for power processing and control are possible; step-down and boost and straight boost. While the discussion presented here is within the context of Torquer PCU trade-offs, it will also serve as a basis for trade-off decisions concerning the choice of a Speeder PCU system (see Section 3.3). The basic elements of both circuits are shown in Figure 2.15.

In the step-down and boost system, switch $S_1$ is opened and closed according to the TRC principles previously outlined. When the switch is closed, the generator EMF, $V_g$, is impressed across inductor L. When $S_1$

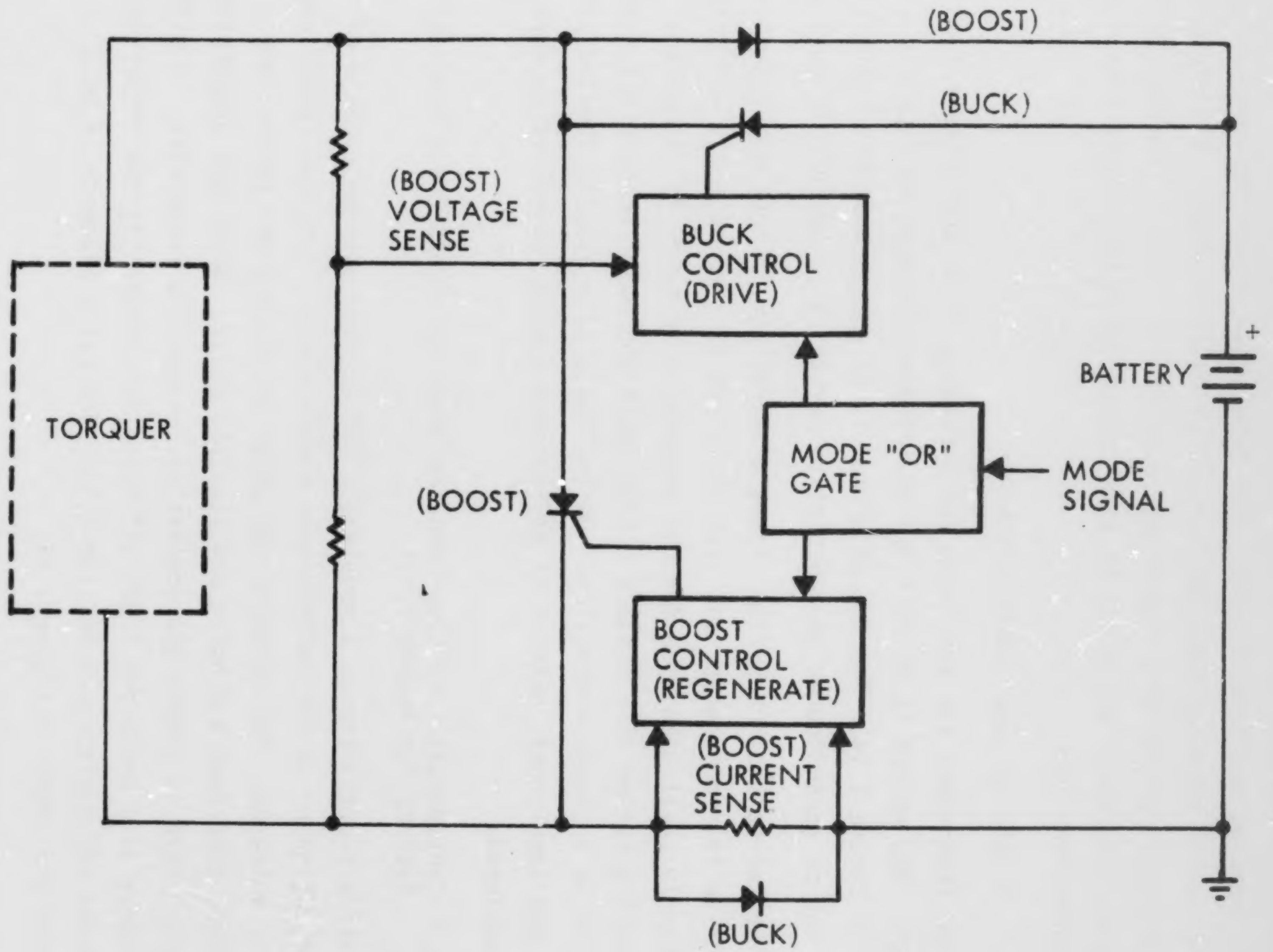
(BOOST)
(BUCK)
(BOOST)
VOLTAGE
SENSE
BUCK
CONTROL
(DRIVE)
+
BATTERY
TORQUER
MODE "OR"
GATE
MODE
SIGNAL
(BOOST)
BOOST
CONTROL
(REGENERATE)
(BOOST)
CURRENT
SENSF
(BUCK)

FIGURE 2.14
BUCK-BOOST TORQUER PCU WITH DUAL CONTROLLERS

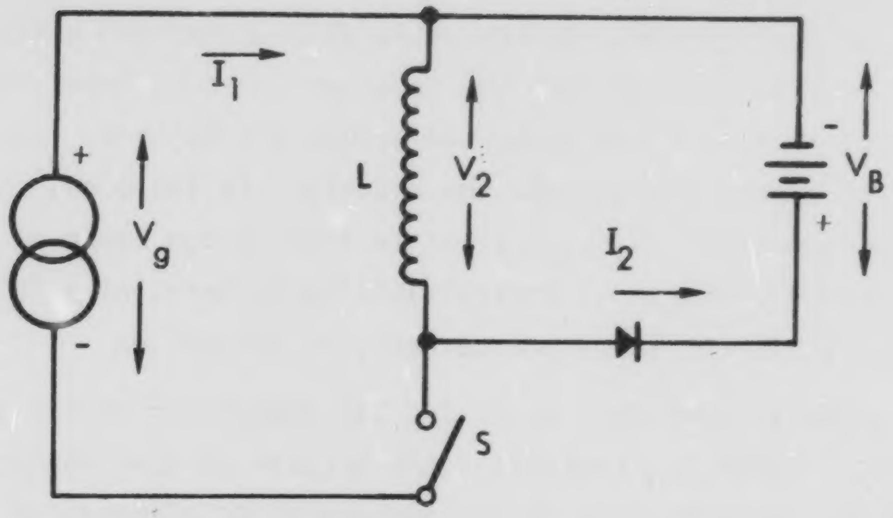
$I_1$
L
$V_2$
+
$V_g$
-
$I_2$
-
$V_B$
+
S

STEP-DOWN AND BOOST PCU

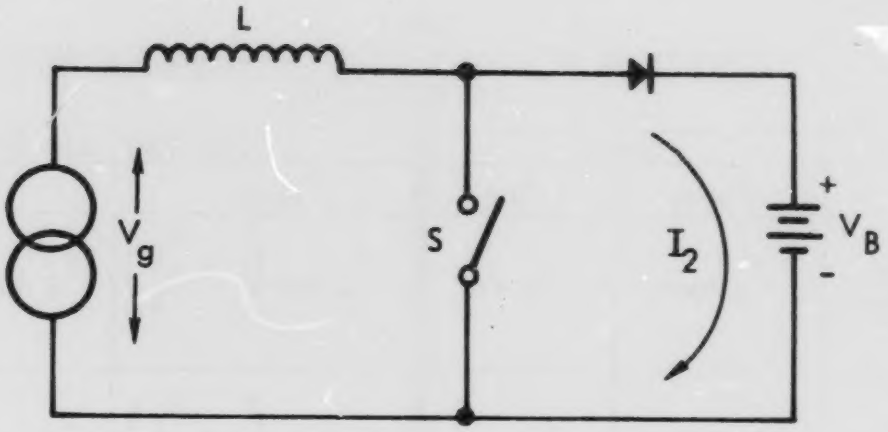

BOOST PCU

FIGURE 2.15
COMPARISON OF TRC GENERATOR CONTROL TECHNIQUES

is opened, the inductor voltage, $L \frac{di}{dt}$ must equal $V_B$, and the inductor discharges through the diode into the battery. Note that the voltage of the generator is unconstrained relative to the battery voltage, that is $V_g$ can be greater or less than $V_B$. On the other hand, the current through the generator is discontinuous.

In the boost system, switch $S_1$ is also opened and closed. When it is closed, the generator charges the inductor; when it opens, the sum of $L \frac{di}{dt}$ and generator voltage are impressed across the battery. The inductor discharges its stored energy into the battery. In the boost system the voltage of the generator is constrained in that it can never exceed $V_B$ and still retain any degree of controllability in terms of a TRC system in which machine torque (armature current) is controlled.

Appendix A-1 presents an analytical comparison of the two methods of processing. Table 2.3 summarizes the results of that analysis in terms of peak and rms current flows in the various major elements of the two systems. The comparison is based on the two systems reflecting the same average machine armature current $I_{g\ ave}$ in the rotating machine while delivering equal power to the battery.

TABLE 2.3

COMPARISON OF CURRENTS IN STEP-DOWN AND BOOST
AND BOOST PCUs

| | Boost | | Step-Down and Boost | |
|---|---|---|---|---|
| | $I_{peak}$ | $I_{RMS}$ | $I_{peak}$ | $I_{RMS}$ |
| Armature (generator) | $I_{g\ ave}$ | $I_{g\ ave}$ | $I_{g\ ave}\left(1 + \frac{V_g}{V_B}\right)$ | $I_{g\ ave}\sqrt{1 + \frac{V_g}{V_B}}$ |
| Reactor (or field) | $I_{g\ ave}$ | $I_{g\ ave}$ | $I_{g\ ave}\left(1 + \frac{V_g}{V_B}\right)$ | $I_{g\ ave}\left(1 + \frac{V_g}{V_B}\right)$ |
| Battery | $I_{g\ ave}\left(\frac{V_B}{V_g}\right)$ | $I_g \sqrt{\frac{V_B}{V_g}}$ | $I_{g\ ave}\left(1 + \frac{V_g}{V_B}\right)$ | $I_{g\ ave}\sqrt{\frac{V_g}{V_B} \quad 1 + \frac{V_g}{V_B}}$ |

While consideration of the two systems on the basis of design flexibility might favor the step-down and boost in that it allows use of a low voltage battery (small numbers of cells) and a modest to high voltage generator; the table shows that such a design attempt results in a greater difference in the peak and rms current. As shown in the numerical examples in the appendix the effects are:

- For equal torque capabilities, the losses in machine and chopper of the step-down and boost system are higher.
- The inductor (either an external or series winding) will have to be rated for higher currents to prevent saturation.
- The battery will operate at higher peak currents, increasing overvoltage and gassing problems.
- All conductors, contactors and solid state devices will have to be rated to carry higher peak and rms currents and dissipate more losses.

### 2.5.8.3 Adaption of Candidate Circuits to Torquer PCU Use

Circuits I through VI are shown only in the drive condition and thus must be modified for regenerative operation along guidelines stated in 2.5.8.1 and 2.5.8.2. Circuits I and II contain commutating capacitor circuits which are in parallel with the load circuit. Rearrangement of these circuits to fulfill the boost configuration would require additional circuit elements to intermittently break the commutation circuit path to ground. The additional circuitry would introduce additional cost and complexity factors.

Circuit IV contains a commutation circuit in series with the load and there does not raise the same objections of circuits I and II with regard to the complexity of rearrangement for regeneration. However, the additional SCR required (Table 2.2), added to the disadvantages listed for the circuit suggest that it is not a suitable circuit when compared to the remaining circuits III and VI. Circuit V has no advantage in this application.

Circuits III and VI are redrawn in Figures 2.16 and 2.17 with additional switches ($SW_4$) so as to be capable of both drive and regeneration. A more detailed qualitative and analytical comparison has been made of the two circuits in order to arrive at a final decision.

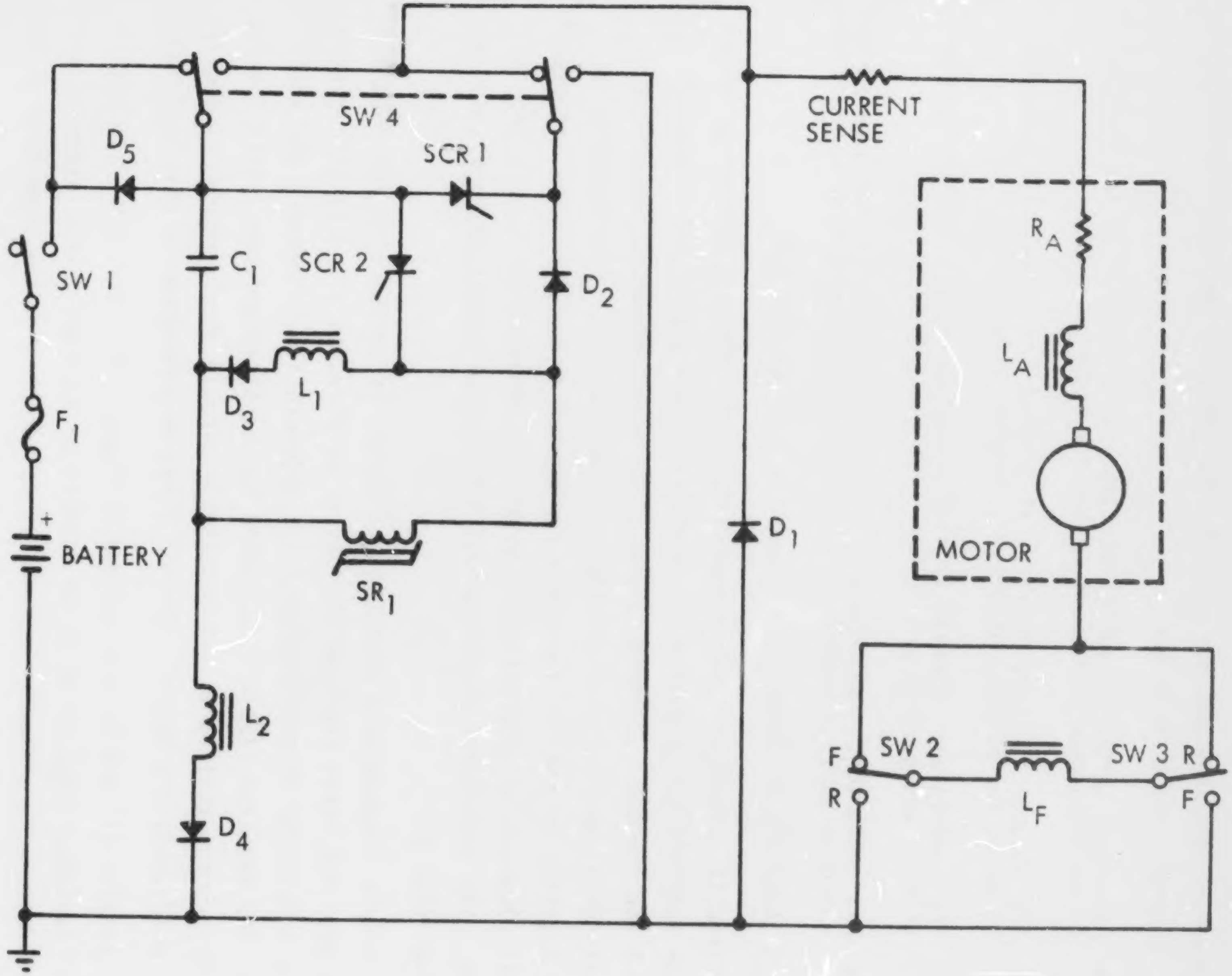
SW 4
$D_5$
SCR 1
SW 1
$C_1$
SCR 2
$D_2$
$D_3$
$L_1$
$F_1$
+
BATTERY
$SR_1$
$L_2$
$D_4$
CURRENT SENSE
$R_A$
$L_A$
$D_1$
MOTOR
F
SW 2
R
$L_F$
SW 3
R
F

FIGURE 2.16
CIRCUIT III MODIFIED FOR REGENERATION

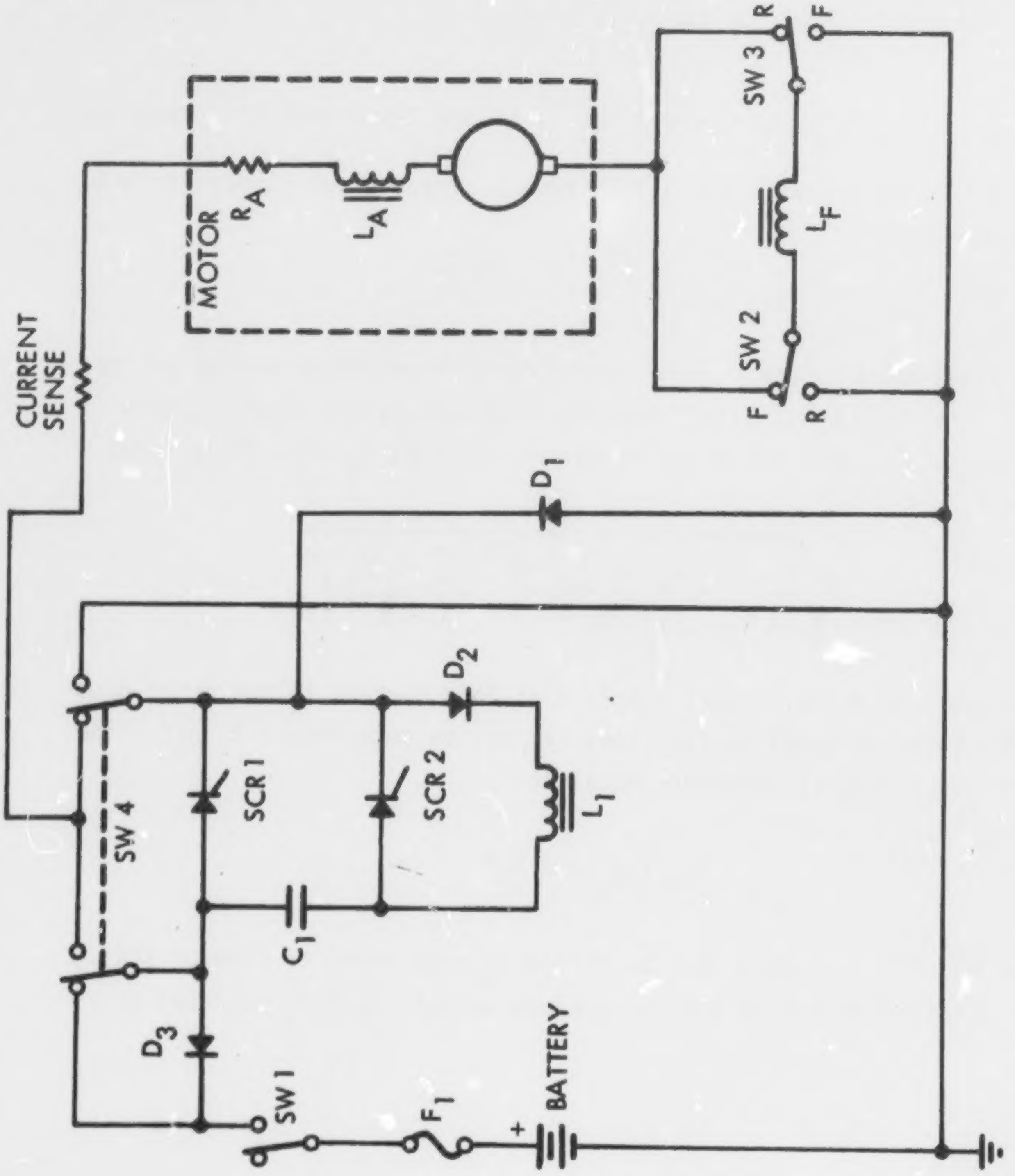
CURRENT SENSE
MOTOR
$R_A$
$L_A$
$L_F$
SW 2
SW 3
F
R
R
F
$D_1$
$D_2$
$D_3$
SCR 1
SCR 2
$L_1$
$C_1$
SW 4
SW 1
$F_1$
+
BATTERY

FIGURE 2.17
CIRCUIT VI MODIFIED FOR REGENERATION

Figure 2.18 shows the idealized current and voltage waveforms impressed on critical components of circuit VI. $SCR_1$ serves a dual function in the circuit; as well as conducting the power pulses to and from the motor, it also serves to complete the oscillation path for $C_1$ and $L_1$. The current in $SCR_1$ is therefore comprised of two components--the motor current, $I_M$, and the commutation capacitor charging current. The idealized peak current in $SCR_1$ can be shown to be:

$$I_{PK\ SCR_1} = I_M + \frac{V_B}{\sqrt{L_1/C_1}}$$ where $\sqrt{L_1/C_1}$ is the characteristic impedance of the oscillating circuit. In a like manner, the average current in $SCR_1$ can be shown to be:

$$I_{AVE\ SCR_1} = \frac{2V_B\ C_1}{T} + \frac{I_M\ t_N}{T}$$

The first term is the current contribution from the discharge of the capacitor. Since the capacitor charging component exists approximately for the period $\pi\sqrt{LC}$ and the motor component for time $t_N$, the RMS current in $SCR_1$ is:

$$I_{RMS\ SCR_1} \cong \sqrt{\left[\left(I_M + \frac{V_B}{\sqrt{L/C}}\right)\sqrt{\frac{\pi\sqrt{LC}}{2T}}\right]^2 + \left[I_M\sqrt{\frac{t_N}{T}}\right]^2}$$

When $SCR_2$ conducts it must supply full load current to the motor plus a current component equal to full load current to commutate $SCR_1$ off. The peak current in $SCR_2$ is therefore equal to:

$$I_{PK\ SCR_2} = 2\ I_M{}^*$$

$SCR_2$ current must flow for the period $t_c$, the turn-off time of $SCR_1$. Allowing a safety factor of 1.5 the average current in $SCR_2$ is equal to

---

*It must be noted that this peak exists for less than 10% of the turn-off time $t_c$. Thus, for practical purposes, $I_{PK\ SCR_2}$ is equal to $I_M$.

FIGURE 2.18
WAVEFORMS OF MODIFIED CIRCUIT VI

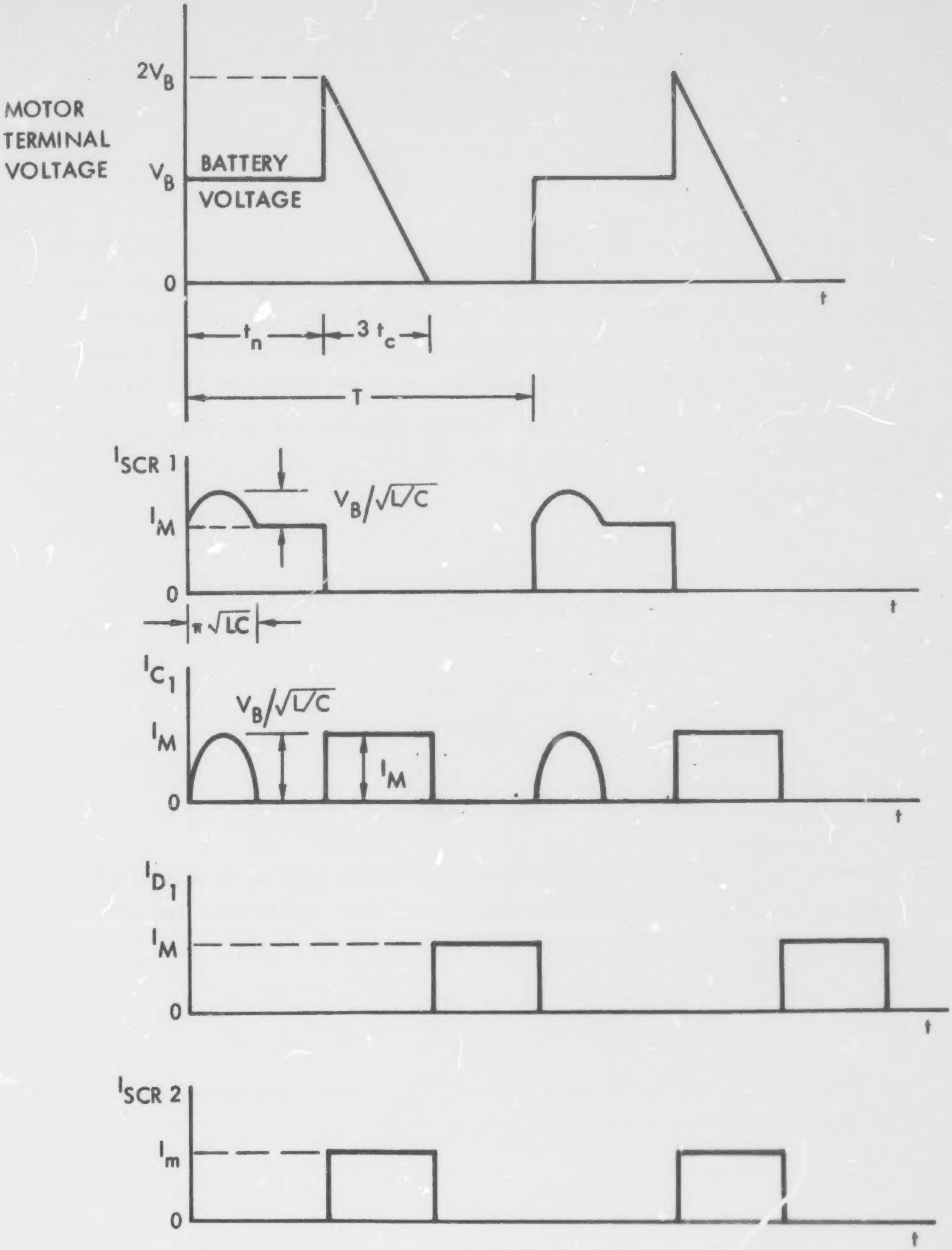
MOTOR
TERMINAL
VOLTAGE
$2V_B$
$V_B$
BATTERY
VOLTAGE
0
t
$t_n$
$3t_c$
T
$I_{SCR\,1}$
$I_M$
$V_B/\sqrt{L/C}$
0
t
$\pi\sqrt{LC}$
$I_{C_1}$
$V_B/\sqrt{L/C}$
$I_M$
$I_M$
0
t
$I_{D_1}$
$I_M$
0
t
$I_{SCR\,2}$
$I_m$
0
t

$$I_{AVE\ SCR_2} = \frac{1.5 \times I_M \times 2t_c}{T} = 3\,\frac{I_M\,t_c}{T}$$

Also:

$$I_{RMS\ SCR_2} = I_M\sqrt{\frac{3t_c}{T}}$$

(The transfer of load current from $SCR_1$ to $SCR_2$ is done very rapidly and $SCR_2$ is subjected to a high rate of current increase $(\frac{dI}{dt})$. In those uses where $\frac{dI}{dt}$ is large, local "hot spots" may occur in the SCR semiconductor junction due to a lack of current uniformity. Turn-on switching dissipation may lead to an excessive temperature rise and premature SCR failure.)

The waveforms associated with the modified circuit of Figure 2.16 are shown in Figure 2.19. When $SCR_1$ conducts, its current is the same as the motor current, $I_M$. Hence,

$$I_{PK\ SCR_1} = I_M$$

Since $SCR_1$ conducts for the period $t_N$;

$$I_{AVE\ SCR_1} = I_M\,\frac{t_N}{T}$$

and

$$I_{RMS\ SCR_1} = I_M\sqrt{\frac{t_N}{T}}$$

When $SCR_2$ conducts, it permits $C_1$ to resonate with $L_1$ through $180^0$. Since $C_1$ is charged to $V_B$ at the beginning of this oscillation and the circuit presents a characteristic impedance equal to $\sqrt{L_1/C_1}$

$$I_{PK\ SCR_2} = \frac{V_B}{\sqrt{L_1/C_1}}$$

The time of this $180^0$ oscillation is $\pi\sqrt{L_1/C_1}$. Since this occurs once each power cycle, the RMS current in $SCR_2$ is:

FIGURE 2.19
WAVEFORMS OF MODIFIED CIRCUIT III

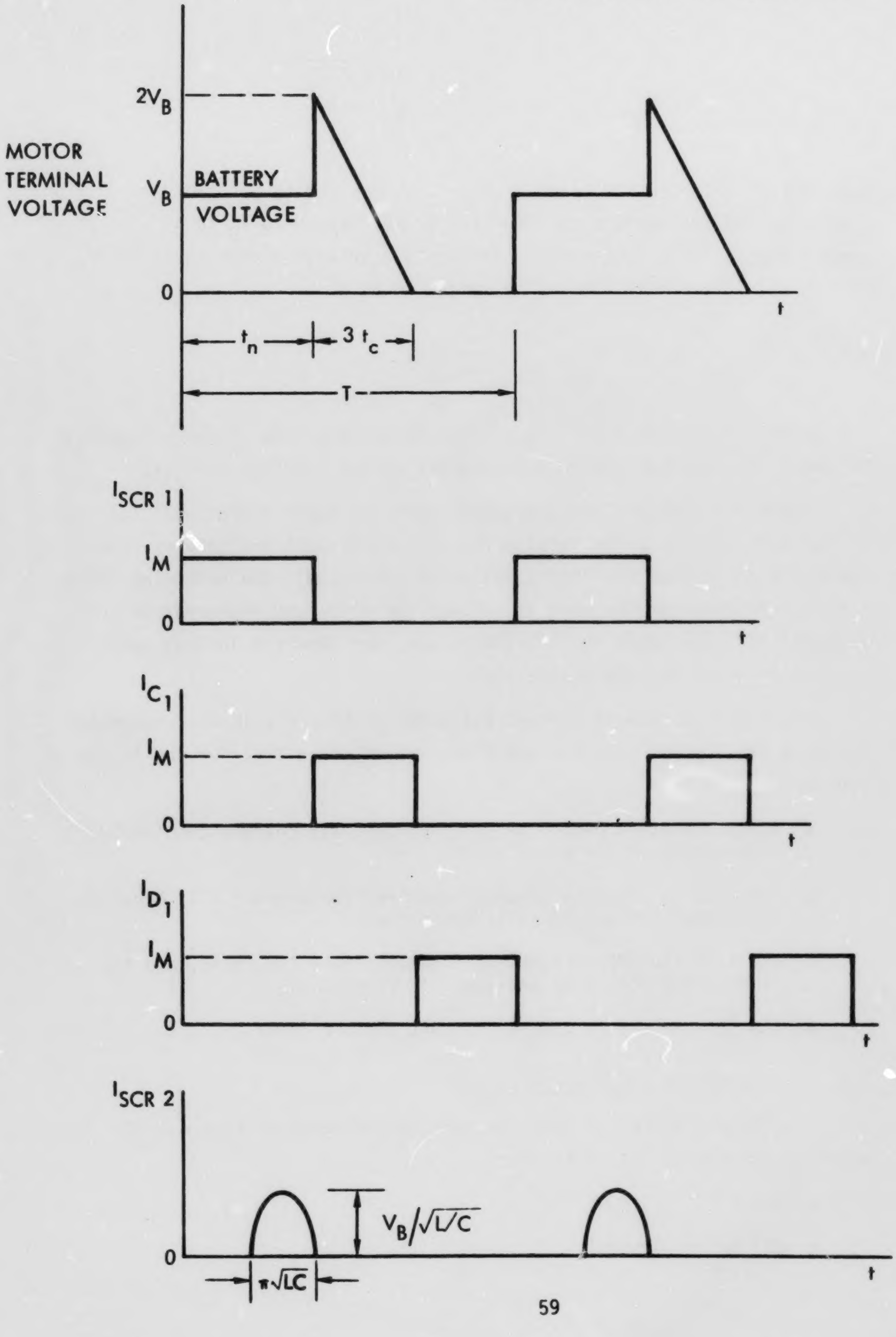
MOTOR TERMINAL VOLTAGE
$2V_B$
$V_B$
BATTERY VOLTAGE
0
t
$t_n$
$3\ t_c$
T
$I_{SCR\ 1}$
$I_M$
0
t
$I_{C_1}$
$I_M$
0
t
$I_{D_1}$
$I_M$
0
t
$I_{SCR\ 2}$
$V_B/\sqrt{L/C}$
0
t
$\pi\sqrt{LC}$

$$I_{RMS\ SCR_2} = \frac{V_B}{\sqrt{L_1/C_1}} \sqrt{\frac{\pi\sqrt{L_1C_1}}{2T}}$$

Immediately prior to $SCR_2$ conducting, $C_1$ is charged to $V_B$. At the conclusion of the commutation function $C_1$ is charged to $V_B$ in an opposite polarity. $C_1$ therefore traverses a voltage change equal to $2V_B$. The average current in $SCR_2$ is therefore equal to

$$I_{AVE\ SCR_2} = \frac{2V_B\ C_1}{T}$$

The current waveform in $SCR_2$ is sinosoidal and thus the $\frac{dI}{dt}$ impressed on it is lower than that on the commutating SCR of the previous circuit.

Table 2.4 compares the component count and major operational features of the two circuits. The total parts of each circuit are greater than Table 2.2 to include the incorporation of switch $SW_4$, the switching element required to transfer the circuit between the drive and regenerative configurations. The count for circuit VI does not show the lockout logic circuit required to insure safe start-up.

The modified form of circuit III shown in Figure 2.16 was chosen for hardware development over the modified form of circuit VI for the following reasons:

- The commutating capacitor $C_1$ of circuit III charges completely independent of the state of the load.
- There is no starting sequence required for circuit III, hence no additional lockout circuits are needed.
- The peak and RMS currents of the power pass SCR, $SCR_1$, and the commutating SCR, $SCR_2$ are lower in circuit III.
- The $\frac{dI}{dt}$ stresses in $SCR_2$ of circuit III are lower.

## 2.6 Description of EMT Torquer System

The Torquer system is shown in the block diagram of Figure 2.20. The major components of the system are:

- Battery
- EMT Master Control

## TABLE 2.4 CANDIDATE TORQUER PCU CIRCUITS

| Circuit | No. of SCR's | No. of Com. $SCR_1$ | No. of Power Diodes | No. of Chokes | No. of Saturable Reactors | Starting Sequence Required | No. of Semicond. in series with load | Auxiliary Capacitor Charging | No. of Critical Components |
|---|---|---|---|---|---|---|---|---|---|
| III Modified | 2 | 1 | 4 | 2 | 1 | No | 1 | Yes | 12 |
| VI Modified | 2 | 1 | 3 | 1 | 0 | Yes | 1 | No | 8 |

FIGURE 2.20
EMT BLOCK DIAGRAM OF TORQUER ELECTRICAL SUBSYSTEM

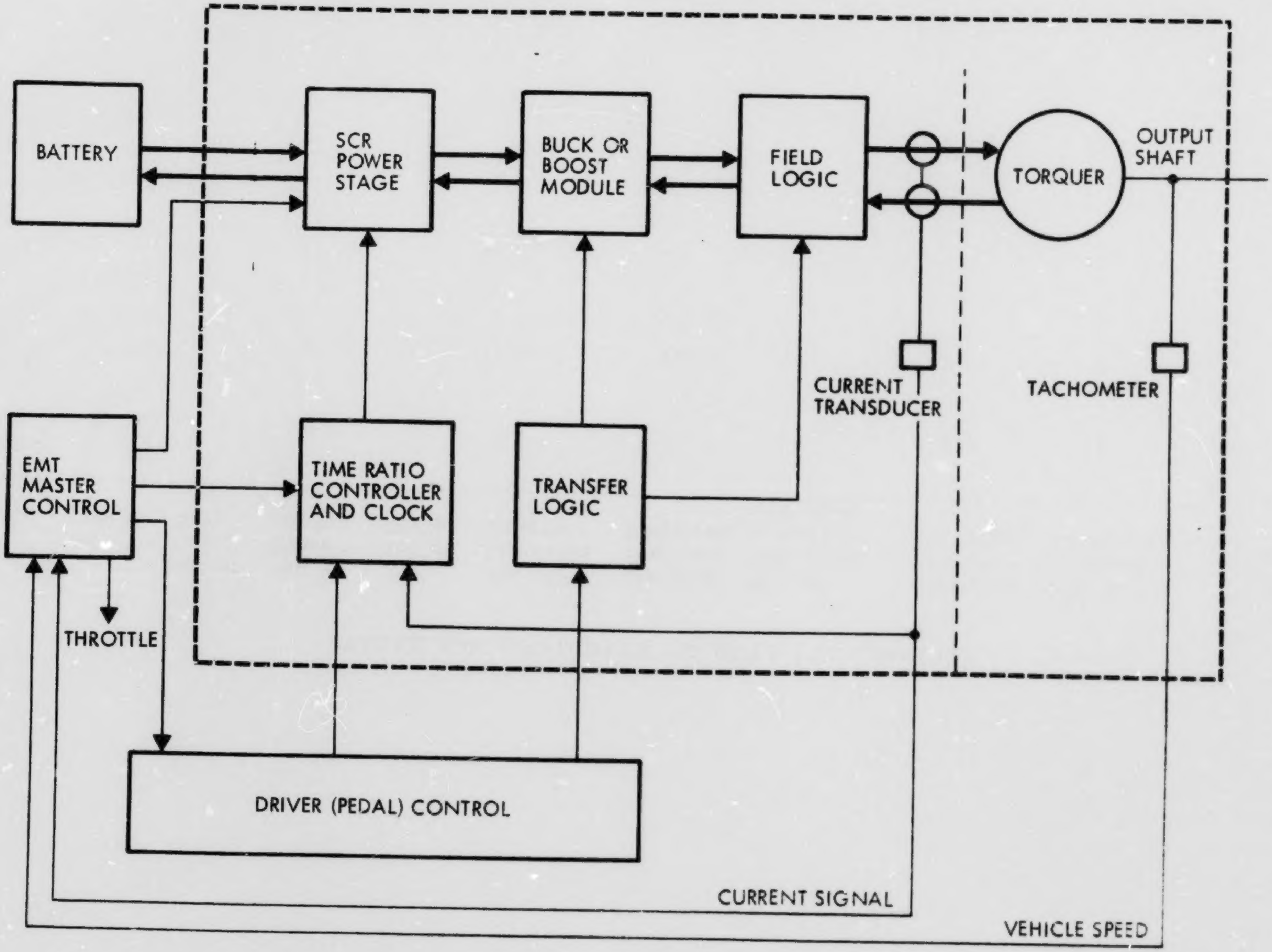
BATTERY
SCR POWER STAGE
BUCK OR BOOST MODULE
FIELD LOGIC
TORQUER
OUTPUT SHAFT
CURRENT TRANSDUCER
TACHOMETER
EMT MASTER CONTROL
TIME RATIO CONTROLLER AND CLOCK
TRANSFER LOGIC
THROTTLE
DRIVER (PEDAL) CONTROL
CURRENT SIGNAL
VEHICLE SPEED

- Pedal Control
- SCR Power Stage
- Buck/Boost Module
- Field Logic
- Time Ratio Control and Clock
- Transfer Logic
- Torquer

Torquer PCU

### 2.6.1 Battery

The battery chosen for the EMT system is a 200-volt, lead-acid, secondary battery. This voltage was chosen for the following reasons:

- A lower voltage would require larger current carrying capabilities in all major circuits.
- A higher voltage, while lessening the current carrying capability requirements would mean--
  - more cells in series with increased reliability and maintenance problems
  - higher voltage rated semiconductors
  - costlier insulation and manufacturing procedures.

### 2.6.2 EMT Master Control

The master control serves as a focal point for EMT operation in that it provides the link between engine and electric subsystems as well as the mechanism for Mode One-Mode Two transfer. The control receives vehicle speed information and transfers control of the engine throttle from the fixed value of Mode One operation to the variable level of Mode Two. In Mode Two, it processes Torquer current signals into position signals for the engine throttle servo system allowing the engine to slowly increase or decrease power as a slave to the electrical traction system. It also provides the control and actuation signals for applying the brake to the Speeder shaft during mode transfer.

### 2.6.3 Pedal Control

The pedal control is the means for operator torque input into the EMT-Torquer system. It consists of a pedal-driven potentiometer and switch system. Pedal full-off generates a control signal which results in maximum Torquer regeneration. Increased pedal deflection reduces the regeneration torque command. At approximately 50% of the full pedal travel, a switch on the pedal is activated, signaling the transfer logic to establish the buck module configuration and the drive polarity of the Torquer. Increasing pedal deflection commands increasing Torquer drive torque.

### 2.6.4 SCR Power Stage

The power stage consists of the power pass SCR and associated commutation circuitry of the modified version of circuit III. This stage processes the power flow between the Torquer and battery according to a duty factor and chopper frequency determined by the time ratio controller and clock circuit.

### 2.6.5 Buck/Boost Module

The buck/boost module establishes the functional state of the PCU and the wiring of the power stage. One position of a switch connects the module for buck operation and the other position connects it for boost operation.

### 2.6.6 Field Logic

The field logic controls the polarity of the motor field according to the "buck" or "boost" requirements.

### 2.6.7 Time Ratio Controller and Clock

The time ratio controller compares the value of the pedal torque command with the actual Torquer torque (measured by the Torquer armature current) and generates an error signal which causes the duty cycle ($\alpha$) of the power stage to change. The clock establishes the operating frequency of the chopper system.

### 2.6.8 Transfer Logic

The transfer logic receives direction from the pedal control and directs the Torquer PCU into the buck (drive) or boost (regeneration) configuration.

## 3.0 SPEEDER SYSTEM

### 3.1 System Requirements and Selection Criteria

The functional requirements of the Speeder system were described in Section 1. They are summarized below:

- To regulate the engine speed during Mode One operation by providing a controlled modulation of the electromagnetic torque reflected to the engine shaft.
- To deliver power to the battery bus over a wide variety of Speeder speeds and battery voltages.

These requirements must be satisfied by a system which offers low cost, weight and size, with high reliability and efficiency.

### 3.2 Selection of the Speeder

There are various candidate generators which differ in construction and control method details. Table 3.1 presents a qualitative assessment of various generators which could be used as the Speeder. Only two specific types of electric generators are considered suitable for Speeder use: conventional DC generators and conventional synchronous generators. The conventional DC machine is attractive because the electrical load is DC.

Conventional synchronous generators are also considered suitable for this application. The synchronous generator (alternator) has been completely accepted by the automobile industry over the DC generator. Even though additional rectifiers are required for the DC load, AC synchronous machines offer the advantages of lower cost, lighter weight and freedom of commutation problems. In the case of the Torquer, the use of an AC machine was complicated by the need for positional and/or frequency information to be supplied to the PCU for torque control. If an AC machine is used solely as a generator, these requirements are not present. In view of these considerations, the conventional synchronous generator was adopted as the Speeder.

### 3.3 Rational of Speeder Operating Mode and PCU Selection

In order to control the torque of a simple alternator one can control the field,armature current or both. It can be shown that for constant torque and voltage output, the field current must vary inversely with the

TABLE 3.1 CANDIDATE SPEEDER MACHINES

| Type of Generator | Electromagnetic Torque controlled key | Mechanical Commutator | Slip Ring | Windings on Rotor | Relative Rotor Speed | Relative Power Density | Relative Cost | Generator Stability Problems |
|---|---|---|---|---|---|---|---|---|
| I. D. C. Generator | | | | | | | | |
| a. Conventional | field flux and armature current | Yes | No | Yes | lowest | low to medium | high | No |
| b. Brushless D. C. | field flux and armature current | No | No | Yes | high | medium | very high at present | Unknown |
| II. A. C. Synchronous | | | | | | | | |
| a. Conventional | field flux & armature current | No | Yes | Yes | medium | high | medium | Yes |
| b. Permanent Magnet | armature current | No | No | No | high | medium | high | Yes |
| c. Solid Rotor | field flux and armature current | No | No | No | highest | highest | very high | Yes |
| III. Induction Generator | | | | | | | | |
| a. Wound Rotor | stator current and rotor resistance | No | Yes | Yes | medium | high | medium | Yes |
| b. Squirrel cage | stator current | No | No | Yes | high | high | low | Yes |

machine speed. Under these conditions the field current becomes very large at low speed and to avoid driving the field into deep saturation, the machine must be over-designed with excessively large pole areas. At high speeds, the armature current becomes large compared with the field current and the machine must be designed to withstand armature reaction. Electric rotating machinery is most completely utilized when it is operated with its magnetic elements just saturated and its copper conductors continually carrying their design current. Therefore, the machine control concept which promises lightest weight and lowest cost is the one which utilizes the machine at high speed, with a saturated field excitation and constant armature current. Such a concept will produce a constant torque machine having a voltage output approximately proportional to the machine's speed. It is evident that a simple power conditioning and control system is needed so that the variable output voltage of the machine can be transformed to battery voltage in order to deliver machine power to the battery.

A simple method of power conditioning is to tap change at the battery, i.e., connecting the output of the generator to various voltage points of the battery as the generator voltage varies. This method is slow acting and leads to unbalanced battery charging.

### 3.4 Speeder PCU

The more attractive way of controlling the Speeder power is through the use of a boost type controller utilizing the TRC techniques of Section 2.5.8.2. The type of PCU which was developed is designated as a voltage boost type power processor with constant current capability. A schematic of the Speeder PCU is shown in Figure 3.1. It is very similar to the Torquer PCU in that it utilizes the same commutation techniques. However, the PCU does not require mode transfer modules or logic. It does contain additional elements; a full wave rectifier and energy storage inductor. The latter is necessary since the armature of the alternator cannot be used for energy storage as was the series field winding of the Torquer.

The commands for turning on the power SCR, $SCR_1$, and the commutating SCR, $SCR_c$, arise from a logic control system which compares the actual engine speed to a reference speed and adjusts the duration of power SCR

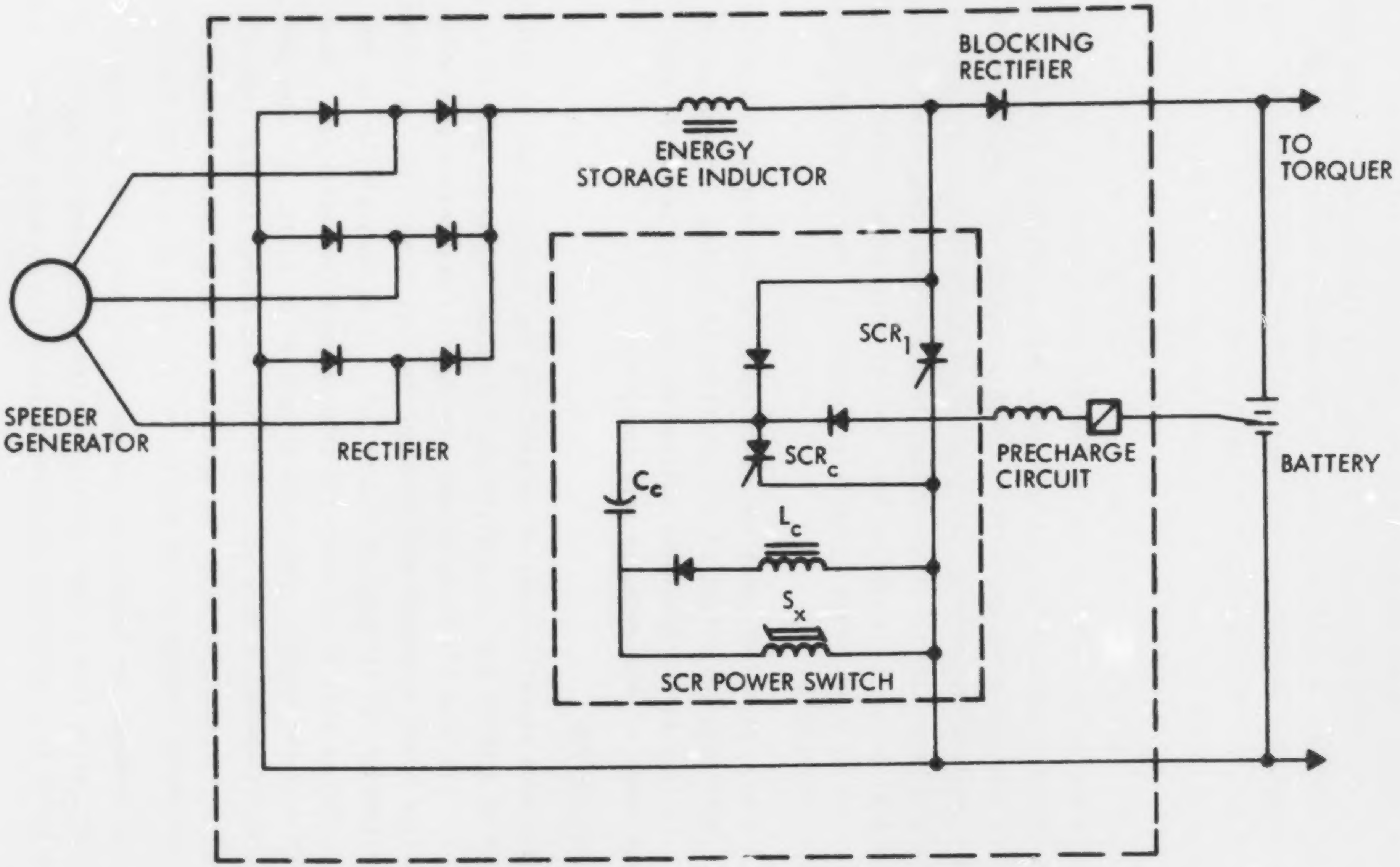
BLOCKING RECTIFIER
ENERGY STORAGE INDUCTOR
TO TORQUER
SPEEDER GENERATOR
RECTIFIER
$SCR_1$
$SCR_c$
PRECHARGE CIRCUIT
BATTERY
$C_c$
$L_c$
$S_x$
SCR POWER SWITCH

FIGURE 3.1

conduction time. This in turn, determines the energy stored in the inductor and the load reflected back to the engine.

Two additional control features are presently in use within the Speeder PCU. The first is a torque lockout feature which turns the Speeder field off when the engine speed is below 1300 rpm. This allows the engine to be cranked and come up to power during system start-ups. The second circuit feature is field control circuit which adjusts the Speeder field to insure the Speeder output voltage does not exceed battery bus voltage. In such a situation the Speeder PCU would lose control because the source current would flow into the battery unimpeded. This method of voltage control is at odds with previous arguments in favor of constant excitation operation. This area is further discussed in Section 8.

## 4.0 ROTATING MACHINES

### 4.1 Torquer Selection

In Section 2.1.4 a DC machine was selected for the Torquer system. The circuit trade-offs of Section 2.4 assumed the use of a series wound motor. While there was no reason given in that section, a comparison of shunt and series motors shows that series motors are better suited to the conditions of the Torquer because of the following factors:

- The series motor develops a large torque at low speeds, ideal for traction purposes.
- The series motor possesses a high free-running (or light load) speed.
- The field of the series machine is only utilized when the machine is producing torque; parasitic losses are avoided.

The Torquer must be able to operate as a generator. For a shunt machine, the field current is undirectional, therefore, the machine changes from motor to generator mode of operation naturally if the back emf is higher than the source voltage. A series motor will not do so unless its series field is reversed through mechanical switching. In view of the need for Torquer PCU switching and sequencing in any case, field reversal can be coupled to changes in PCU operational modes.

### 4.2 Torquer Specification

The Torquer used in the EMT breadboard demonstration is a series wound DC motor built by the General Electric Company. The rating of the machine is as follows:

27 shaft horsepower @ 7200 rpm; 180 VDC, 130 amperes

Measured resistances (25°C)

Armature -------------- .0174 ohm
Commutating field ----- .0075 ohm
Series field ---------- .0087 ohm

Calculated inductances (unsaturated)

Armature -------------- 0.3 mh
Commutating field ----- 0.14 mh
Series field ---------- 2.58 mh

Temperature rise and cooling (at rated conditions): 90°C with 150 CFM at 2" $H_2O$ forced ambient air

Mechanical over-speed capability: 10,000 rpm

The machine has a shunt tickler field rated at 10% of the series field ampere-turns. This was built into the machine in the event there was difficulty in establishing flux for voltage build-up during regeneration. The field was not used since the Torquer PCU inherently provides this function through its precharge and commutation process.

Weight ------------------------ 153 pounds

Armature inertia -------------- .031 lb/ft/sec$^2$

Dimensions -------------------- 9 3/4" diameter x 20 1/4" overall length

A characteristic map of the machine operating at rated DC voltage is shown in Figure 4.1.

## 4.3 Speeder Specifications

The machine was purchased from available equipment and consequently not optimized for the EMT service.

| | | |
|---|---|---|
| Speed (rpm) | 1,000 | 10,000 |
| Output (kw) | 1.0 | 10.0 |
| Stator current (amps RMS) | 52.0 | 42.0 |
| Full load voltage (volts RMS) | 11.0 | 138.0 |
| Phase | 3 | 3 |
| Input torque (lb-ft)-input | 10 | 10 |
| No-load voltage | 14.4 | 144.0 |
| Frequency ($H_z$) | 66 | 660 |
| Field excitation (rated) | 3.3 amps at 14 volts | |
| Overspeed capability | 15,000 rpm | |
| Weight | 37 pounds | |
| Size | 9 3/4" diameter x 8 1/2" overall length | |

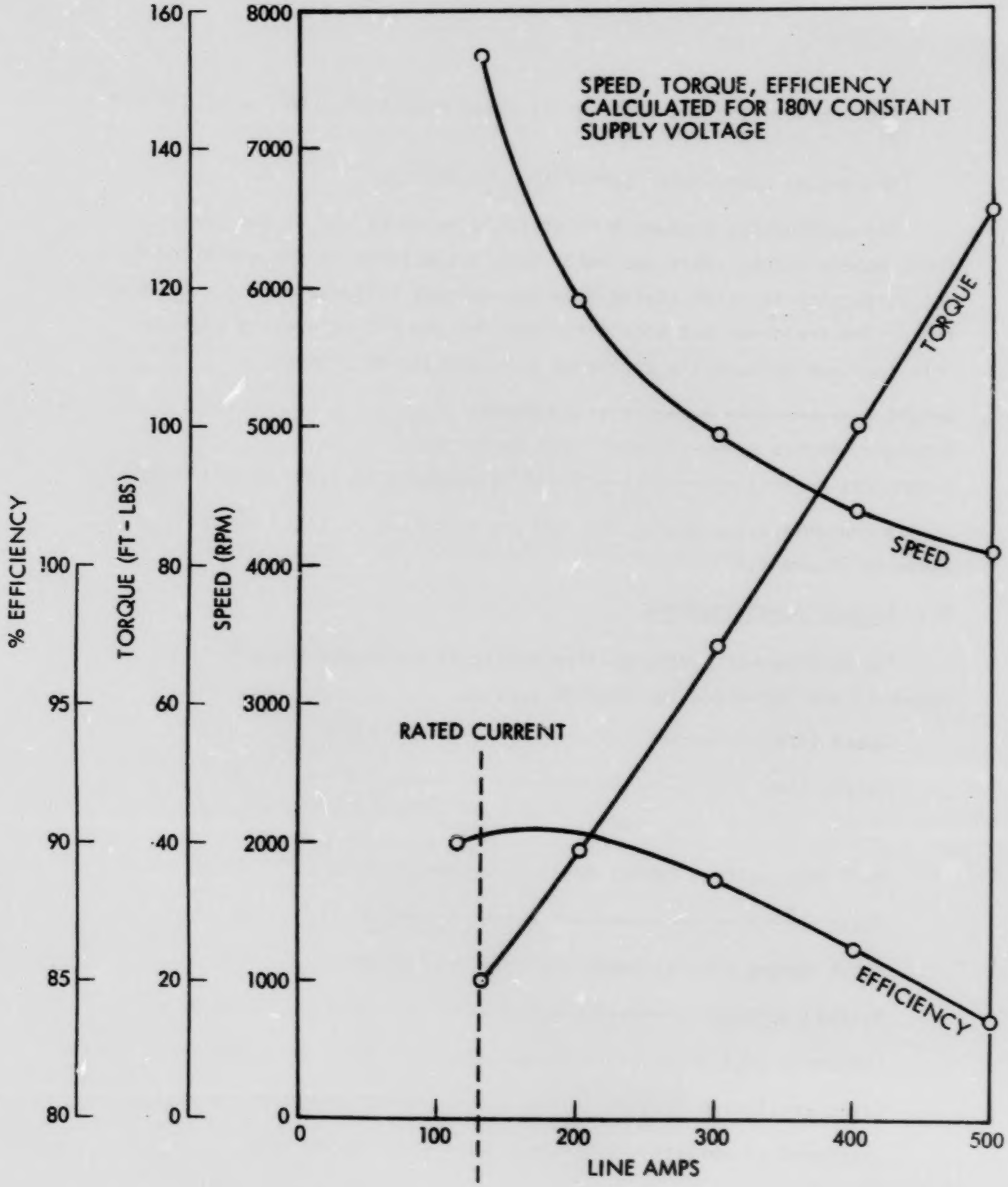

FIGURE 4.1
DC PERFORMANCE OF THE TORQUER

# 5.0 DYNAMOMETER TESTING OF THE EMT SYSTEM

The EMT breadboard equipment was tested on a dynamometer during the spring of 1970. A series of tests were conducted to evaluate overall system and individual component efficiencies and to establish the magnitude of power flow through each of the paths to and from the propeller shaft. The data was hoped to be useful in; understanding the major sources of system inefficiencies, characterizing the nominal and peak levels of component operation and exploring the impact of vehicle weight, battery size and engine power on system performance.

## 5.1 EMT Dynamometer Equipment

The EMT dynamometer equipment is indicated in the block diagram of Figure 5.1. Figure 5.2 shows a picture of the test stand. The engine, a 1968 VW 1600 cc ICE equipped with intake port fuel injection, drives through a planetary gear set adapted from a conventional automatic transmission. The Speeder and Torquer are connected through the gear box as indicated in the photograph of Figure 5.3. The dynamometer load consisted of a Clayton Manufacturing Co. power absorber to simulate aerodynamic and road drag and a Clayton Variable Inertia Flywheel assembly to represent the inertia of the vehicle.

The equipment was operated from an adjacent control area with the operator controlling the power train through the pedal controller and a brake pedal actuating a disc brake on the propeller driving the dynamometer. The operator used a driver's aid consisting of a strip chart recorder with an actual velocity-time trace taken from the LA-4 driving pattern. A copy of the trace is to be found in Figure 5.4

## 5.2 Instrumentation and Data Processing

A block diagram of the instrumentation points is shown in Figure 5.5. Signals from the various transducers were conditioned (attenuated or amplified and filtered) and then recorded on analog magnetic tape. The data was processed off-line as follows. The analog tapes were converted to digital tapes. These tapes were then used as data inputs to a complete data processing, computation and print-out program.

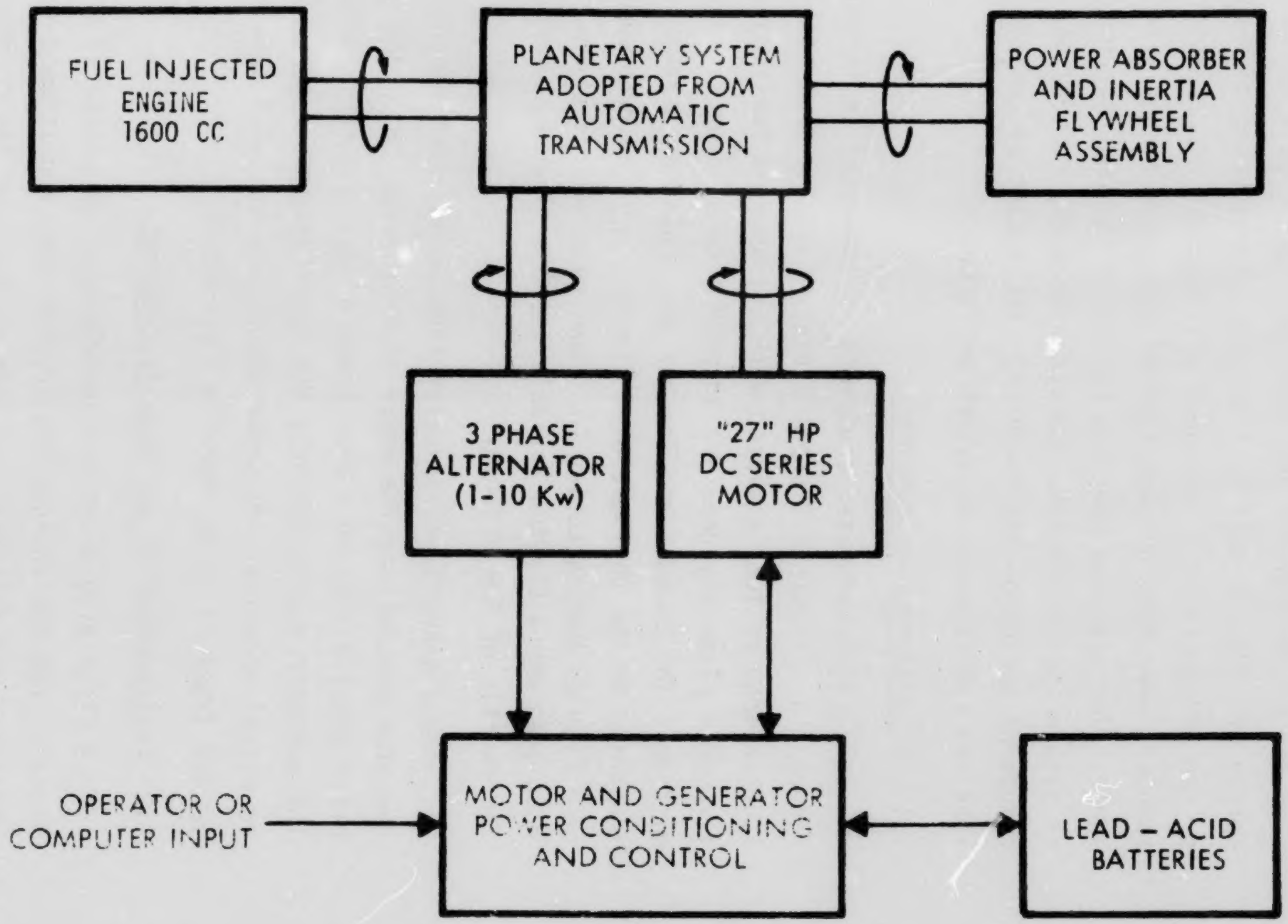
FUEL INJECTED ENGINE 1600 CC
PLANETARY SYSTEM ADOPTED FROM AUTOMATIC TRANSMISSION
POWER ABSORBER AND INERTIA FLYWHEEL ASSEMBLY
3 PHASE ALTERNATOR (1-10 Kw)
"27" HP DC SERIES MOTOR
OPERATOR OR COMPUTER INPUT
MOTOR AND GENERATOR POWER CONDITIONING AND CONTROL
LEAD – ACID BATTERIES

FIGURE 5.1
EMT DYNAMOMETER DEMONSTRATION

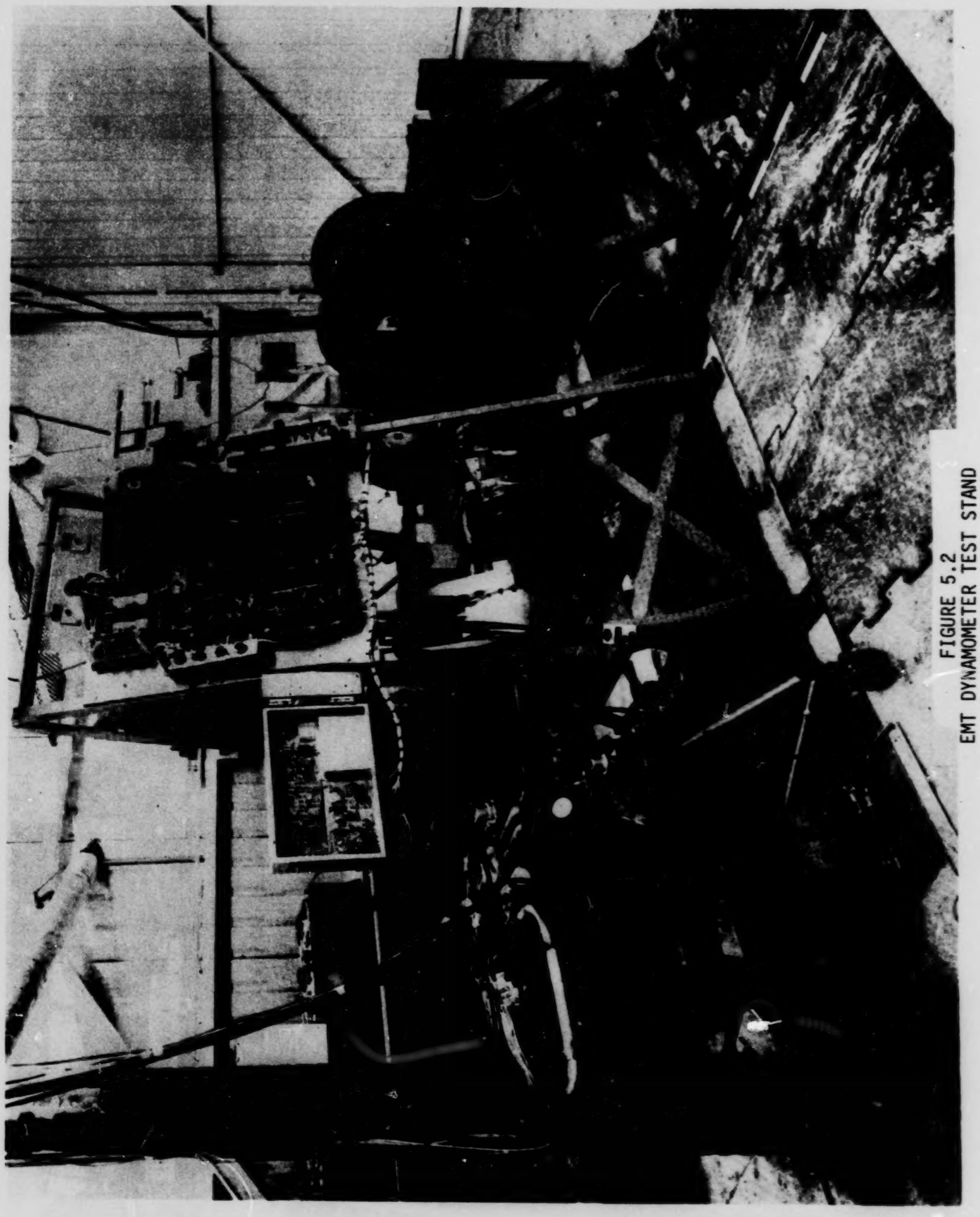

FIGURE 5.2
EMT DYNAMOMETER TEST STAND

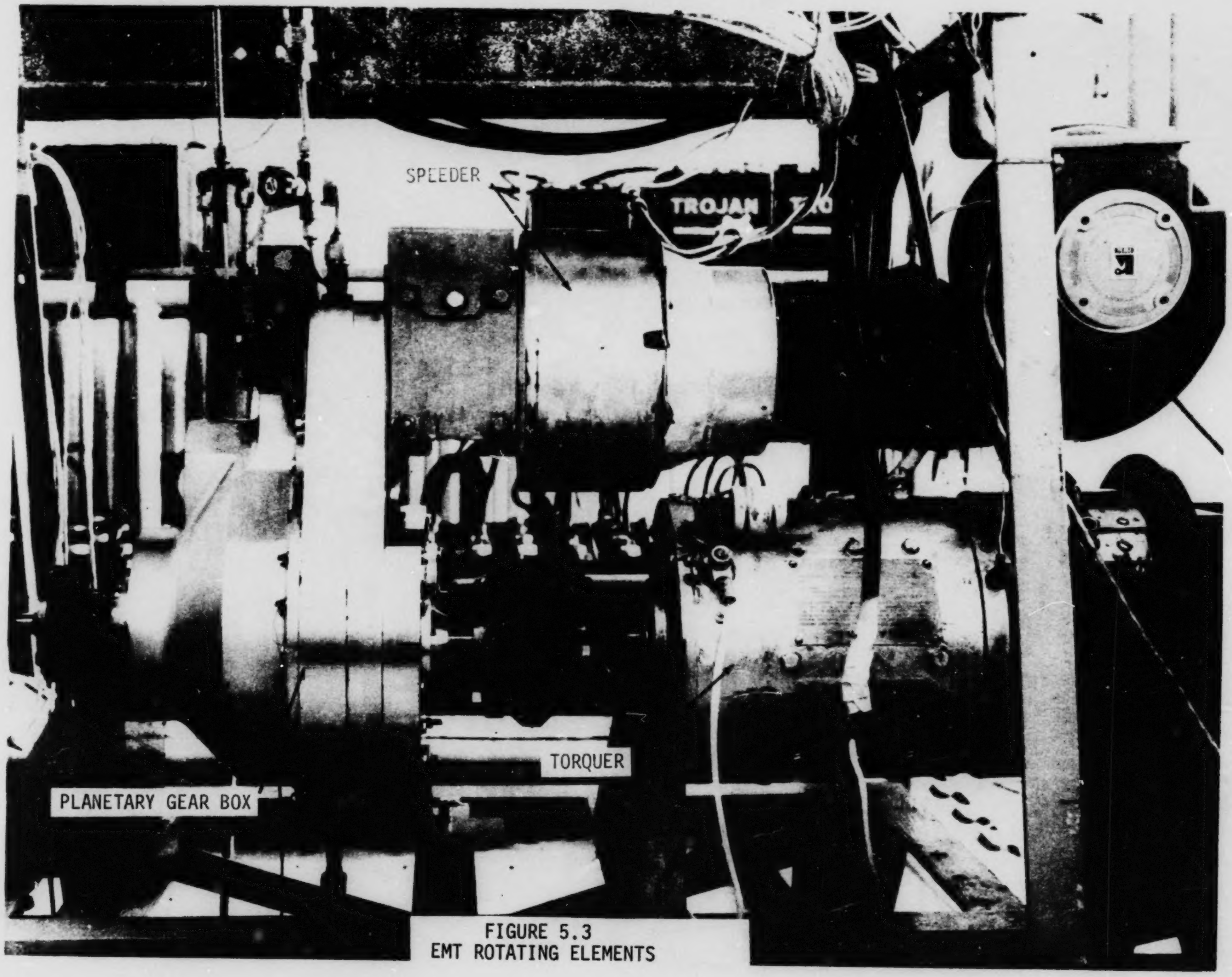
SPEEDER
TROJAN
TORQUER
PLANETARY GEAR BOX

FIGURE 5.3
EMT ROTATING ELEMENTS

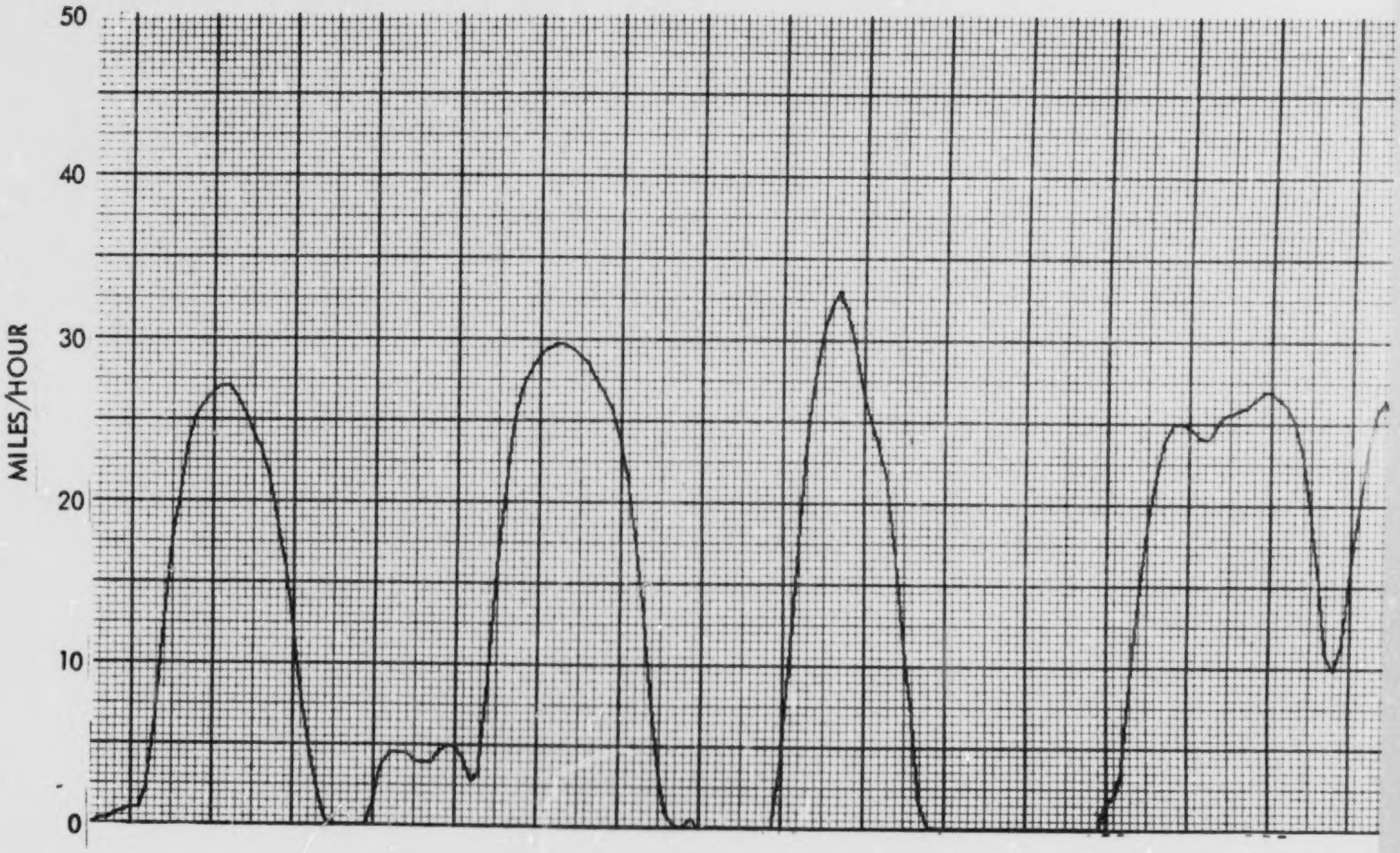

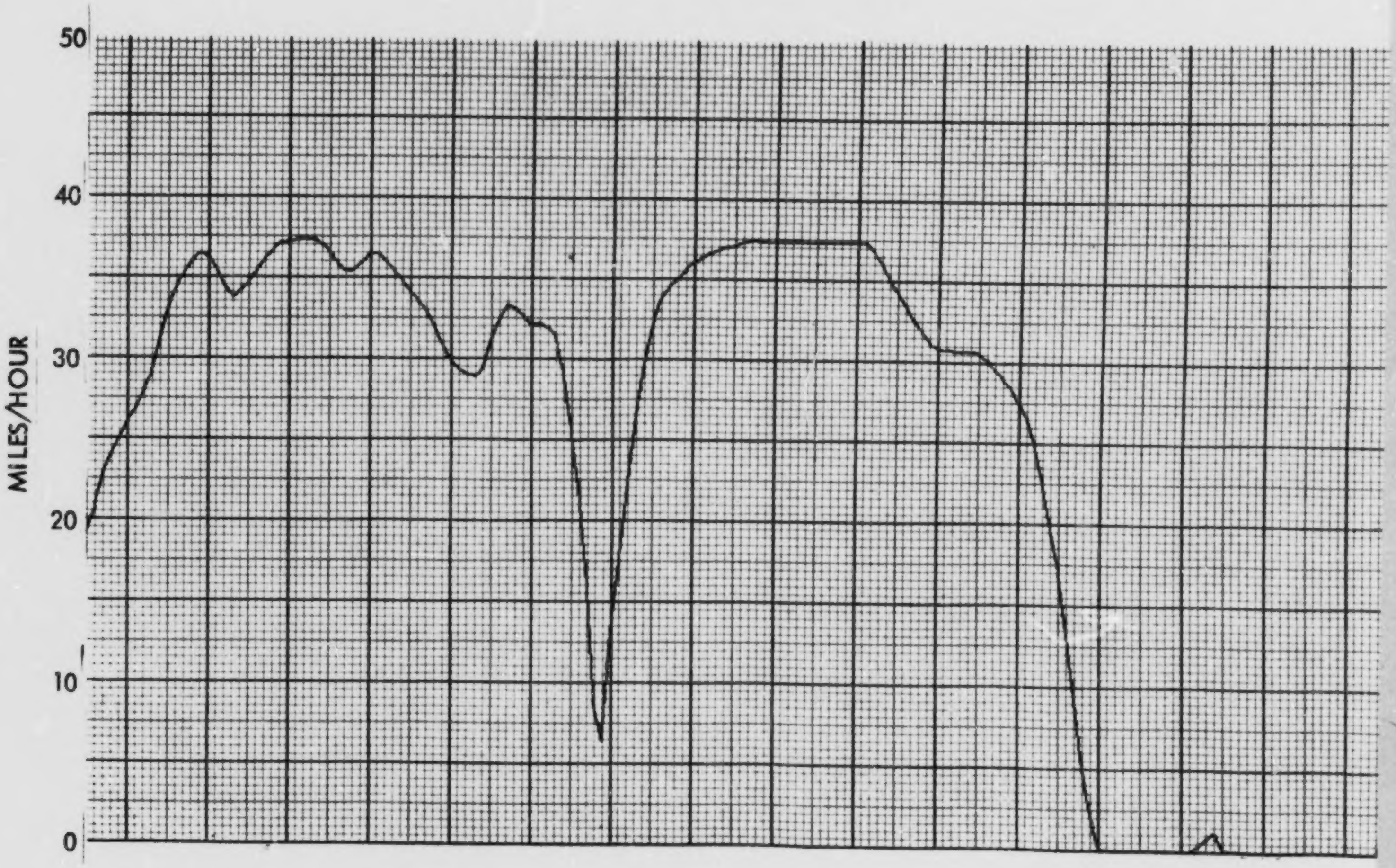

a

SAMPL

FIGURE 5.4 (Cont'd)

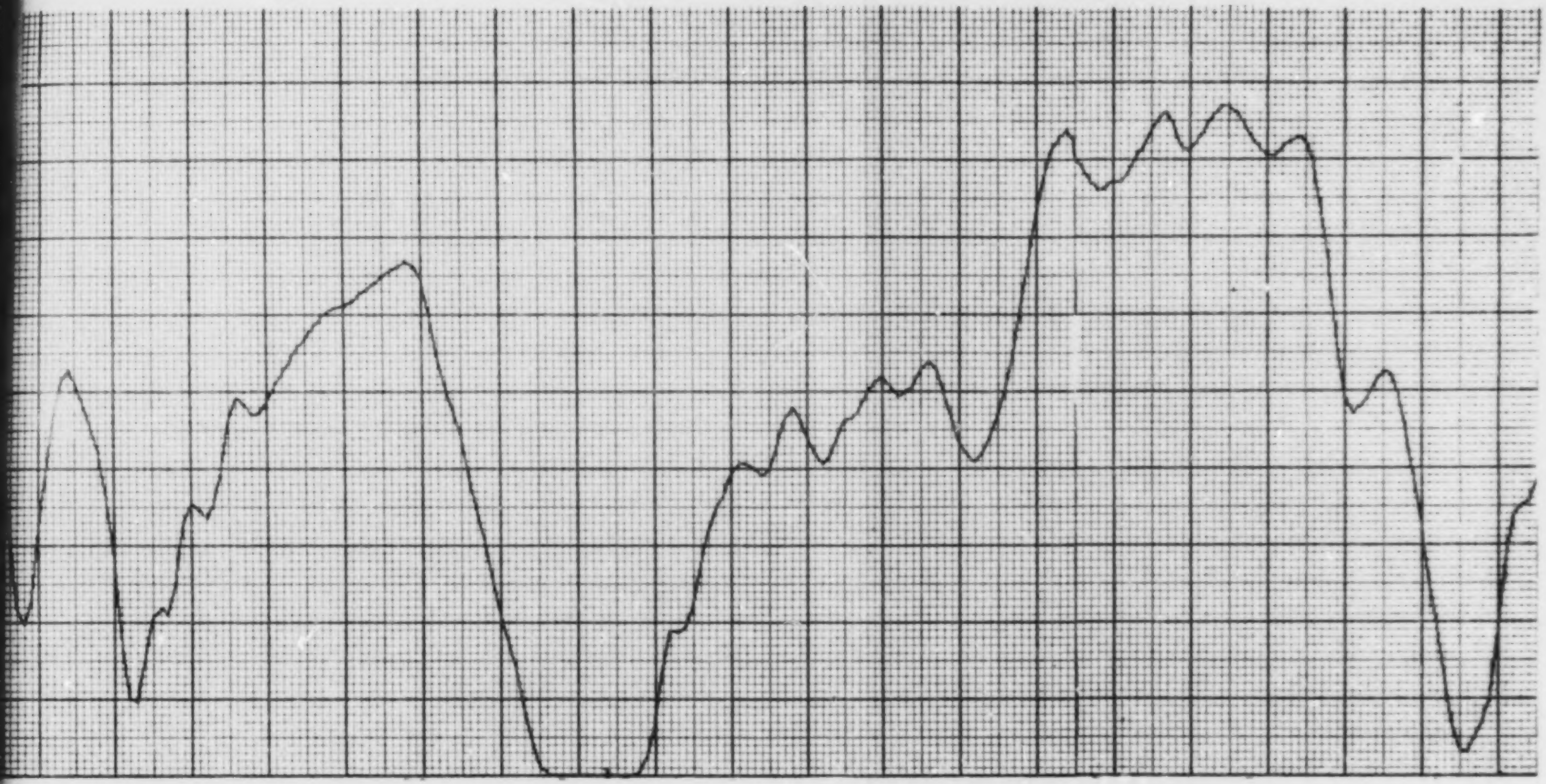

0 TO 350 SECONDS

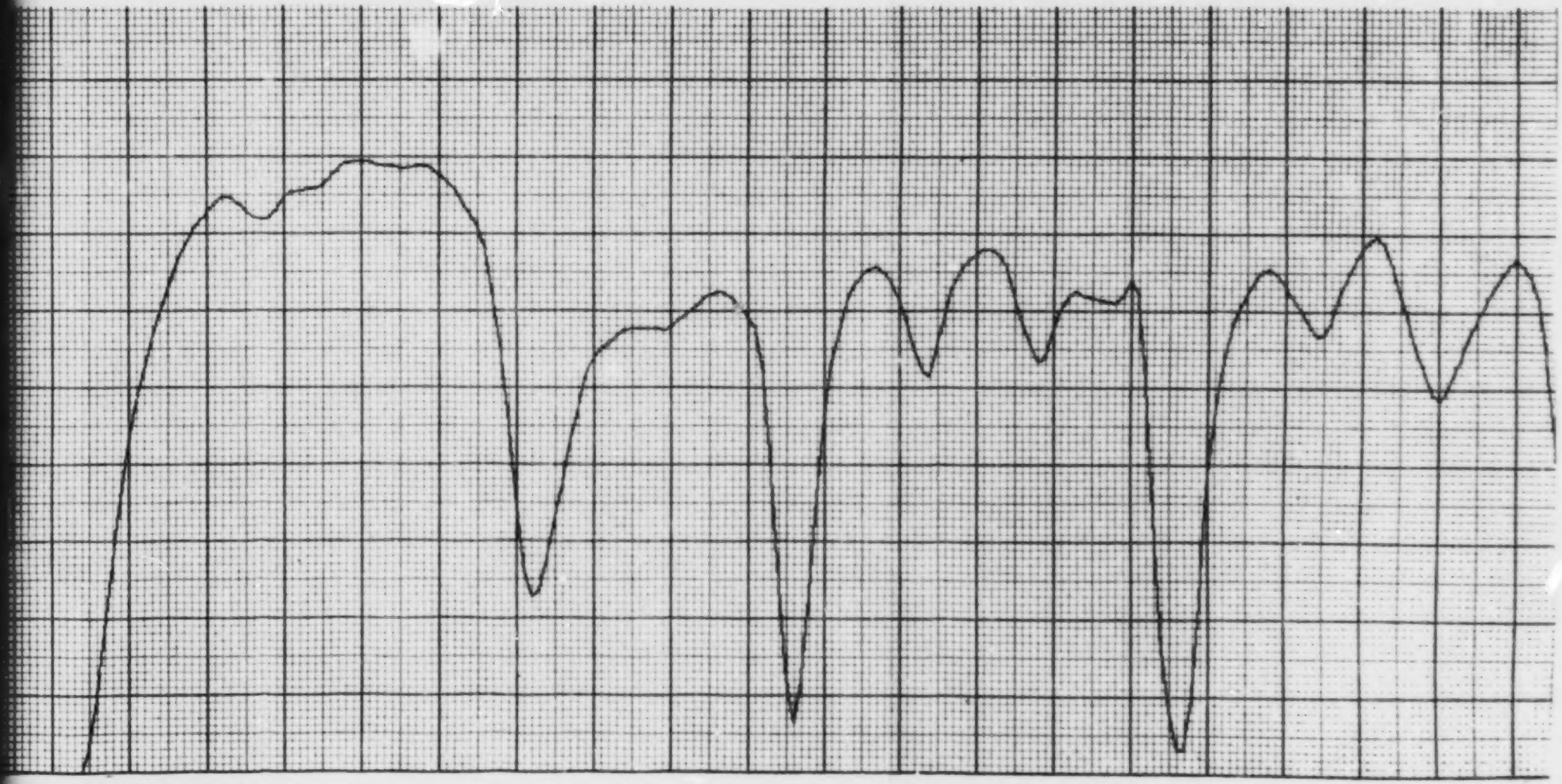

350 TO 700 SECONDS

FIGURE 5.4

SAMPLE LA-4 SPEED TIME CHARACTERISTICS

BLANK PAGE

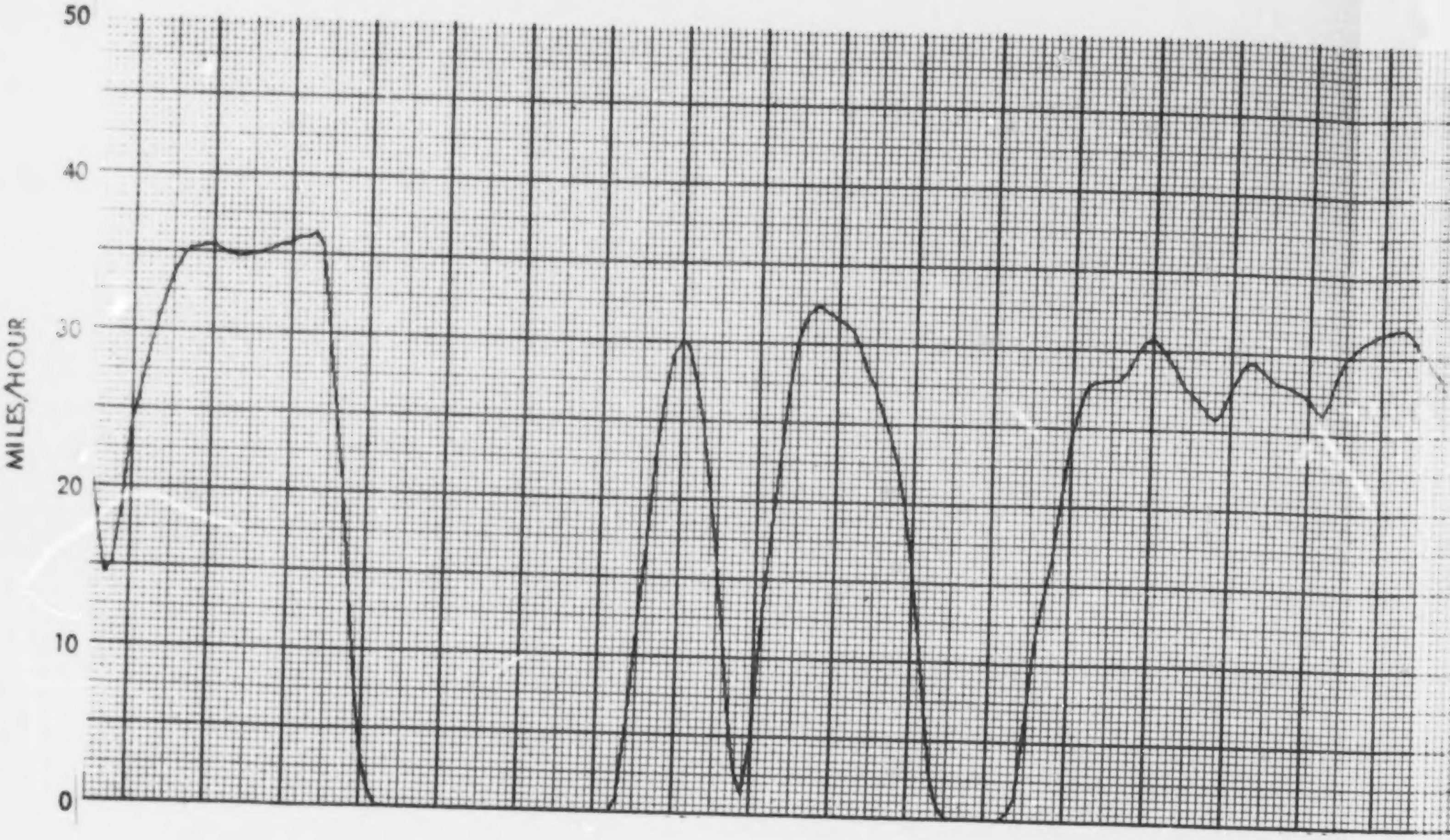

700 TO 105

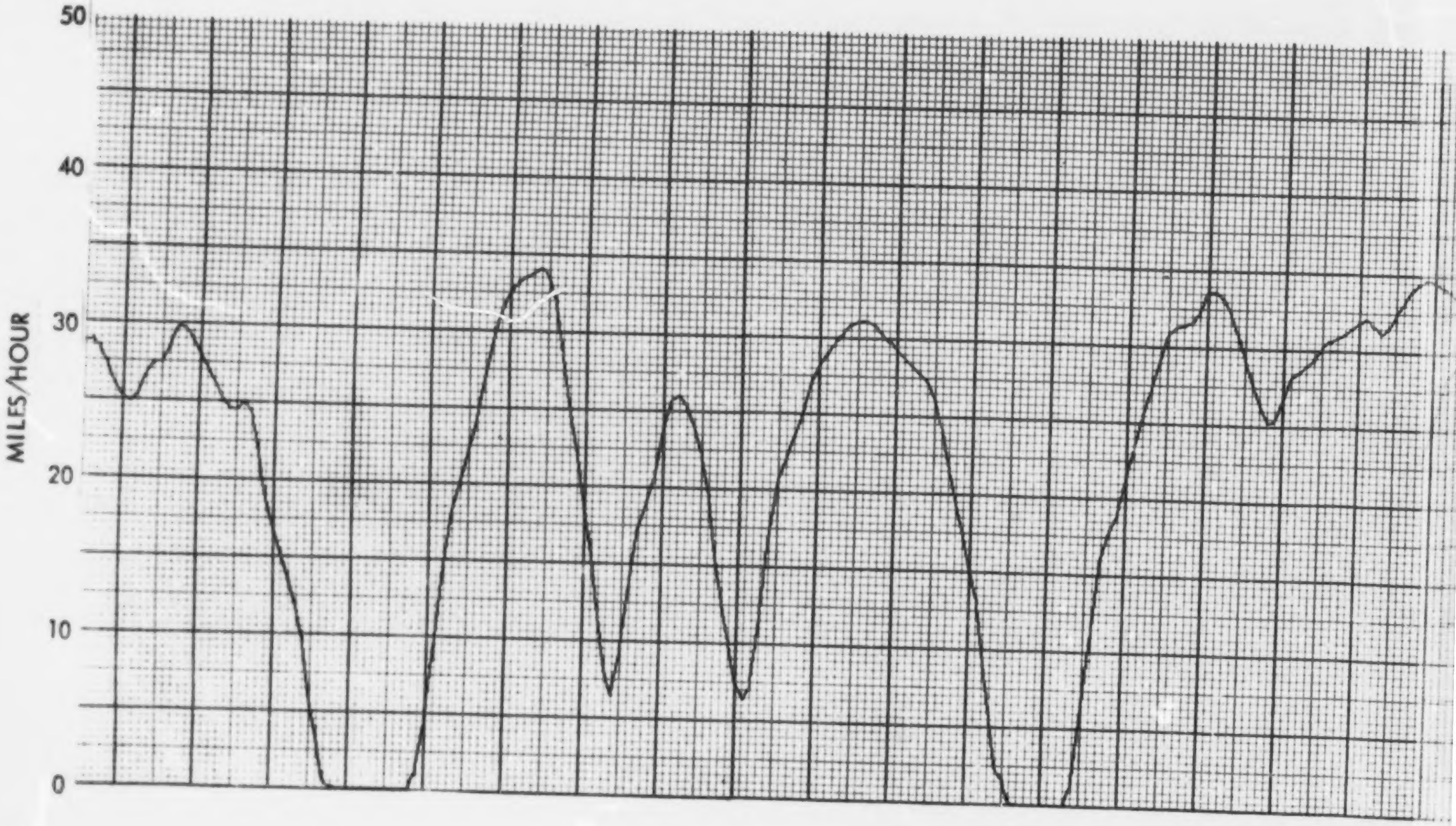

1050 TO 1400

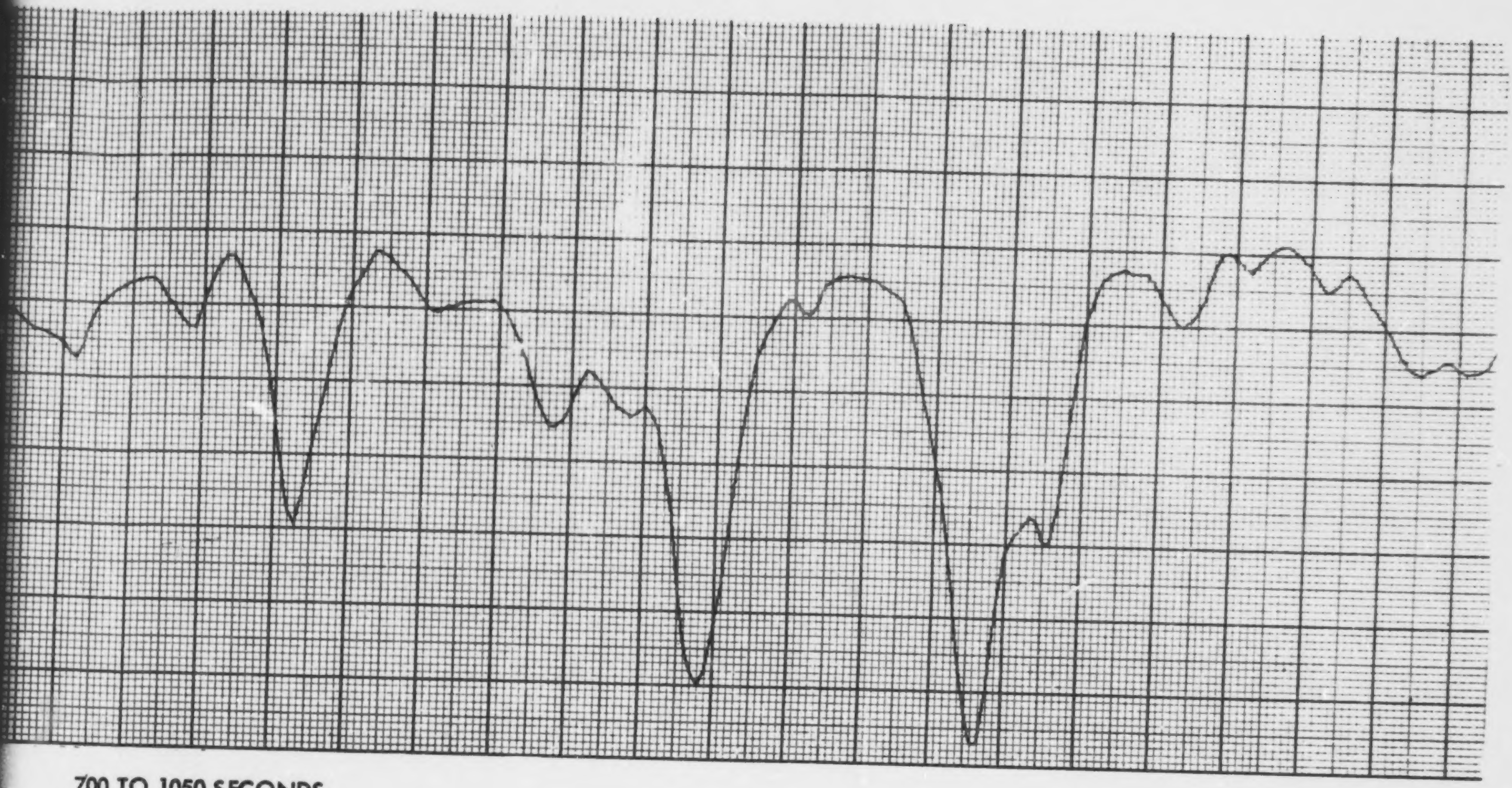

700 TO 1050 SECONDS

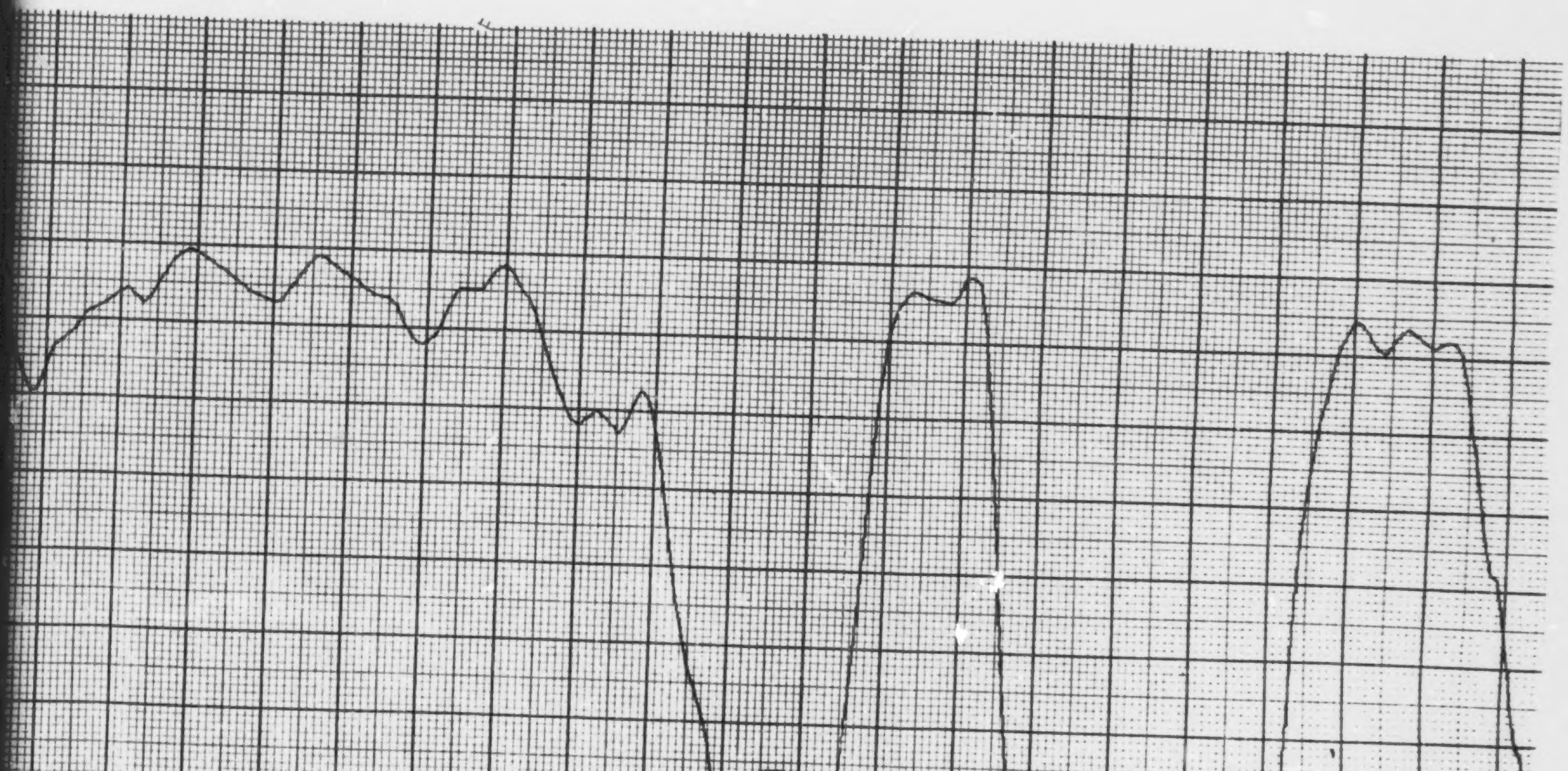

1050 TO 1400 SECONDS

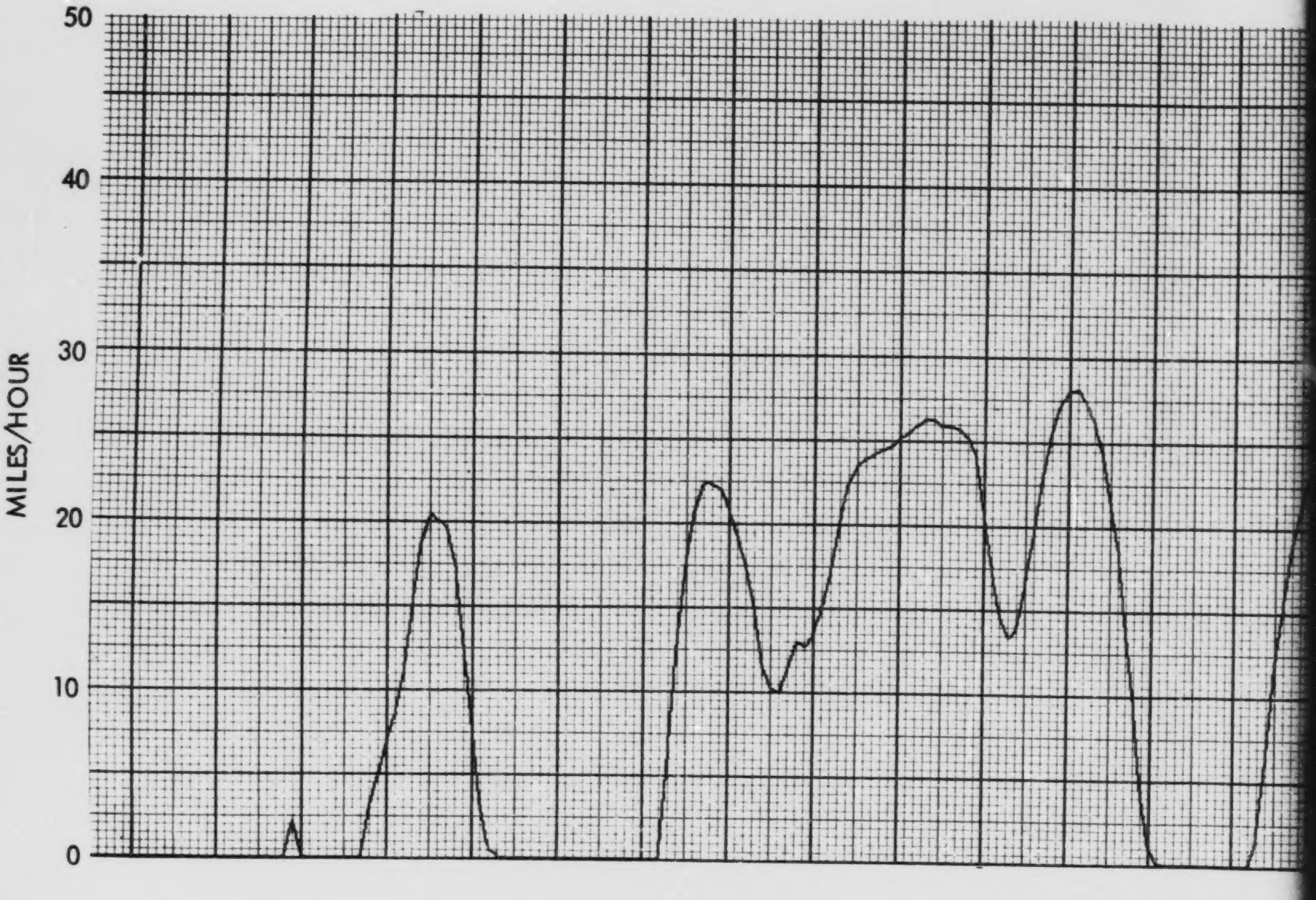

1400 TO 16

FIGURE 5.

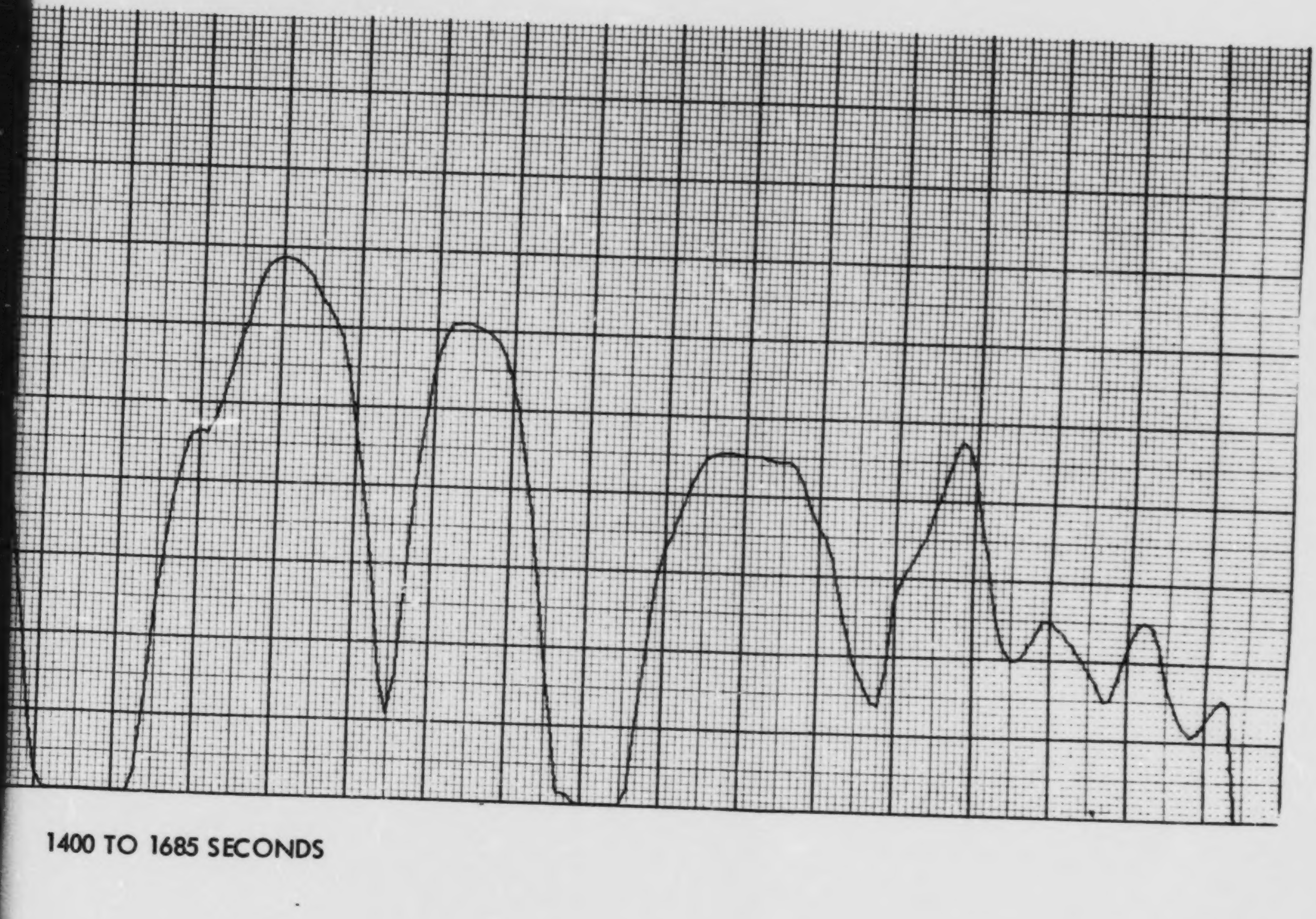

FIGURE 5.4 (Cont'd)

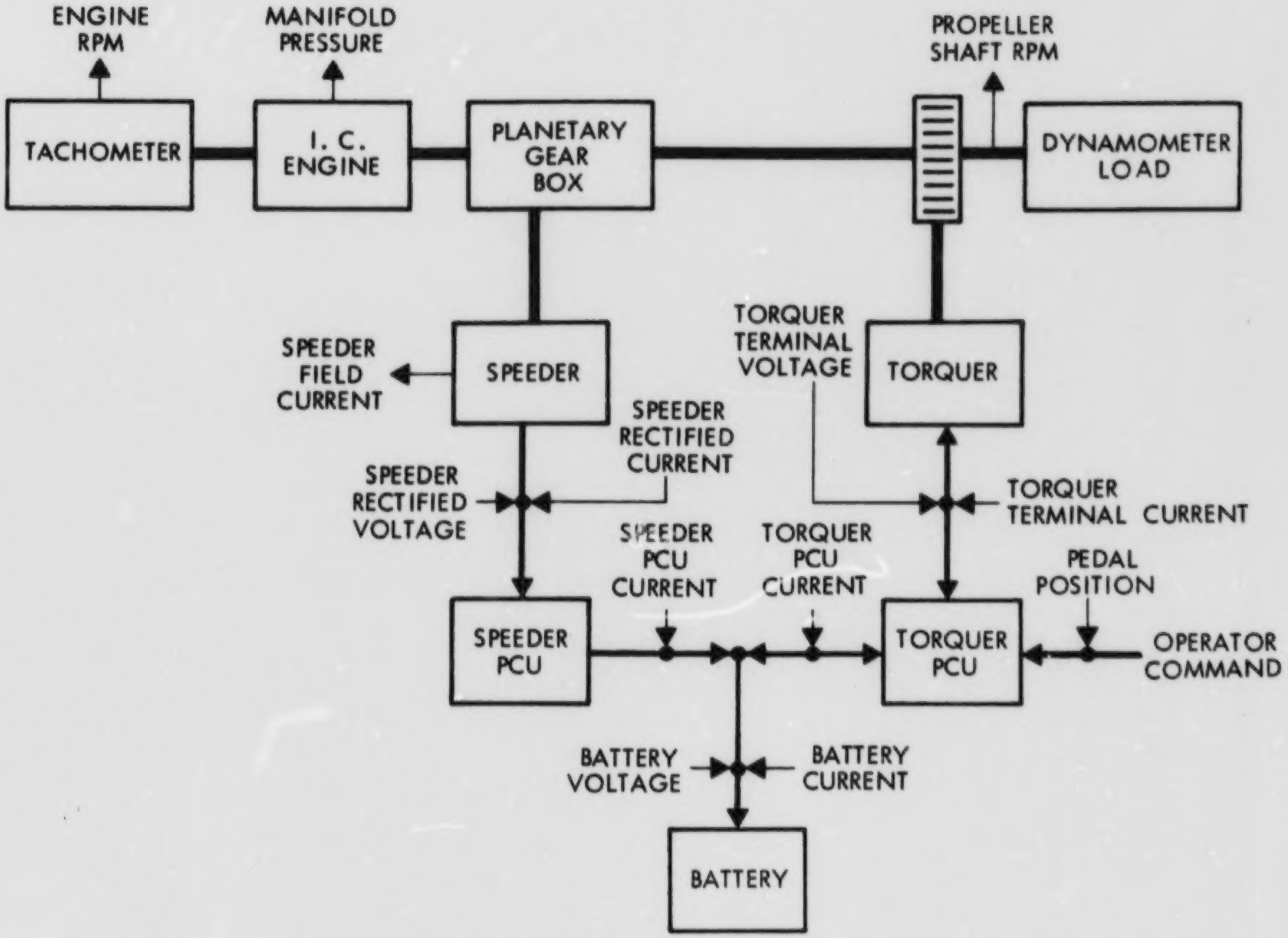
ENGINE RPM
MANIFOLD PRESSURE
PROPELLER SHAFT RPM
TACHOMETER
I. C. ENGINE
PLANETARY GEAR BOX
DYNAMOMETER LOAD
SPEEDER FIELD CURRENT
SPEEDER
TORQUER TERMINAL VOLTAGE
TORQUER
SPEEDER RECTIFIED CURRENT
SPEEDER RECTIFIED VOLTAGE
TORQUER TERMINAL CURRENT
SPEEDER PCU CURRENT
TORQUER PCU CURRENT
PEDAL POSITION
SPEEDER PCU
TORQUER PCU
OPERATOR COMMAND
BATTERY VOLTAGE
BATTERY CURRENT
BATTERY

FIGURE 5.5

## 5.3 Computation Sub-Routines

The high level of radiated electromagnetic noise from the equipment coupled with the long instrumentation lines between the dynamometer stand and the recording equipment required a sizable degree of noise filtering prior to analog recording. The computation of electrical power requires the multiplication of two quantities: current and voltage. However, after filtering signals represent the average waveform values and do not contain all the information of the true "chopped" waveforms associated with TRC. The average electrical power, $\overline{VI}$ is:

$$\frac{1}{T}\int_{0}^{T} V(t)\ I(t)dt$$

where T is a time period associated with the chopper frequency.

For all but very special conditions, it can be shown that:

$$\overline{VI} \neq \overline{V}\ \overline{I}$$

and consequently it was necessary to perform off-line experiments to establish a power coefficient, $K_1$, defined as

$$K_1 = \frac{\overline{VI}}{\overline{V}\,\overline{I}}$$

where $K_1$ can be experimentally correlated with Torquer current, mode of operation (drive or regeneration) and vehicle speed. Waveform oscillograms of the voltages and currents at the terminals of the equipment were taken. Several of these are shown in Figures 5.6 through 5.9. The average power was then determined by the following process. The current and voltage waveforms of the oscillograms were divided into segments, and the instantaneous current, $i_m$, and voltage, $v_m$, measured. The average power, $\overline{VI}$ was determined as:

$$\overline{VI} = \frac{\sum_{m=1}^{m=m} i_m\ V_m}{m}$$

DRIVE MODE

VEHICLE SPEED 15 mph

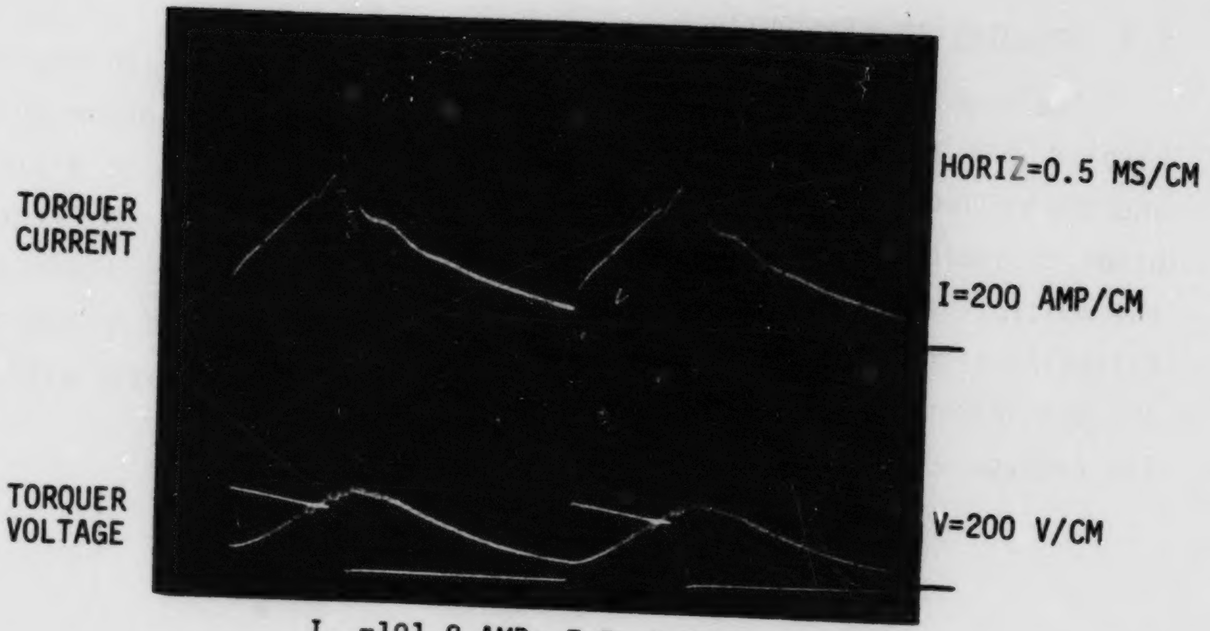

$I_{AV}$=191.8 AMP; F.F.=1.103

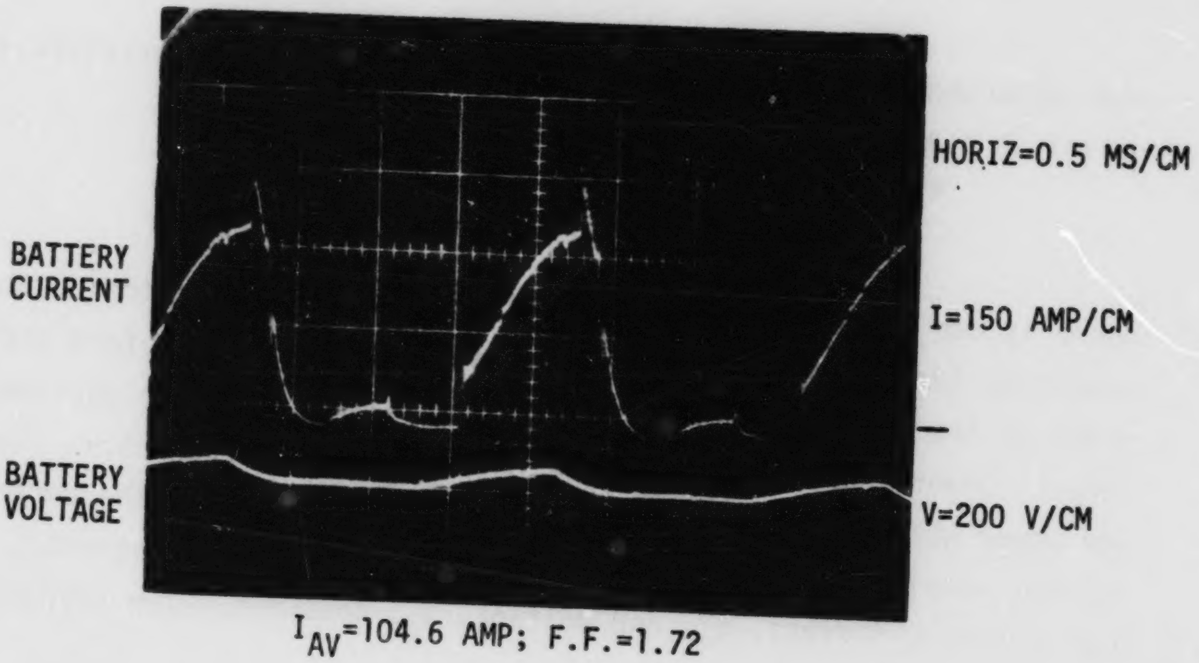

$I_{AV}$=104.6 AMP; F.F.=1.72

FIGURE 5.6

DRIVE MODE

VEHICLE SPEED 45 mph

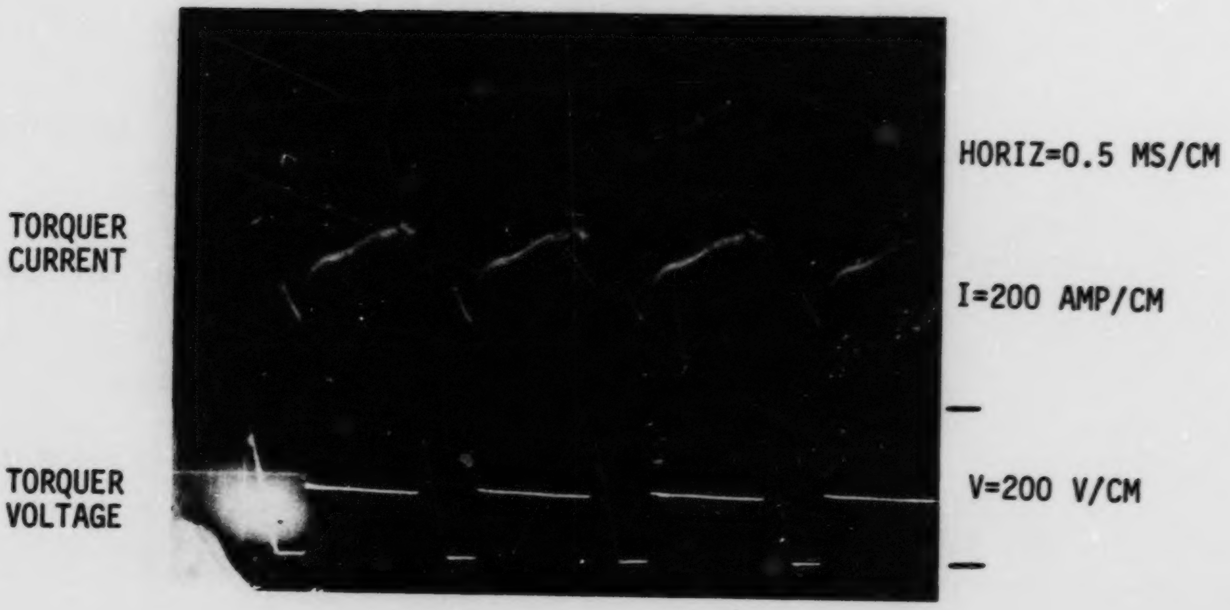

$I_{AV}$=146.4 AMP; F.F.=1.019

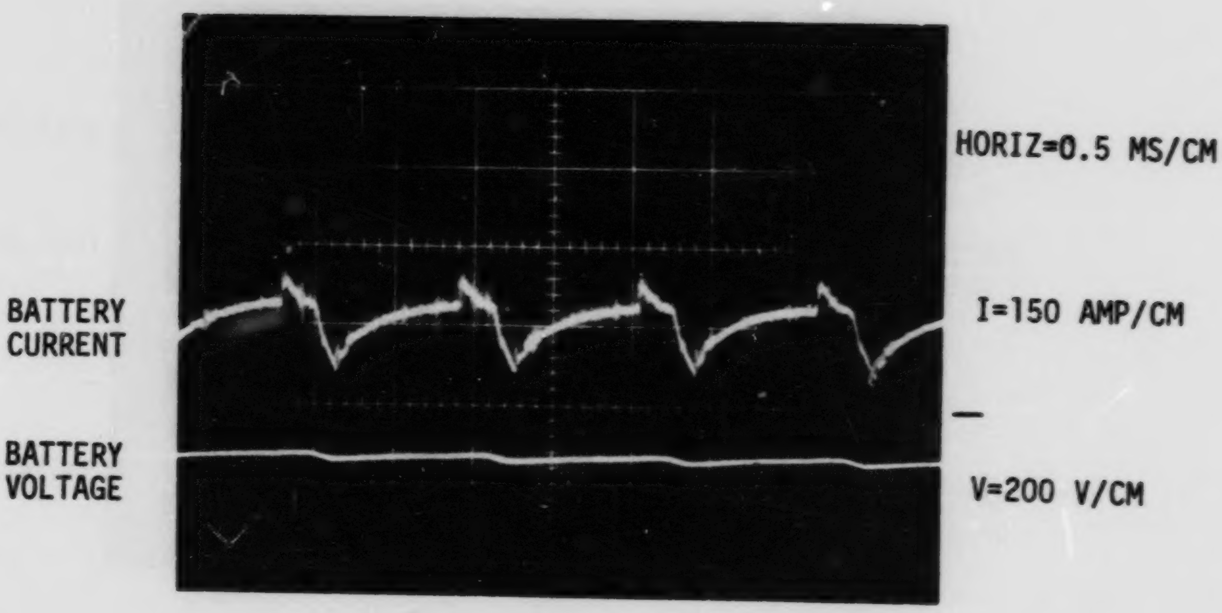

$I_{AV}$=152.5 AMP; F.F.=1.03

FIGURE 5.7

VEHICLE SPEED 30 mph

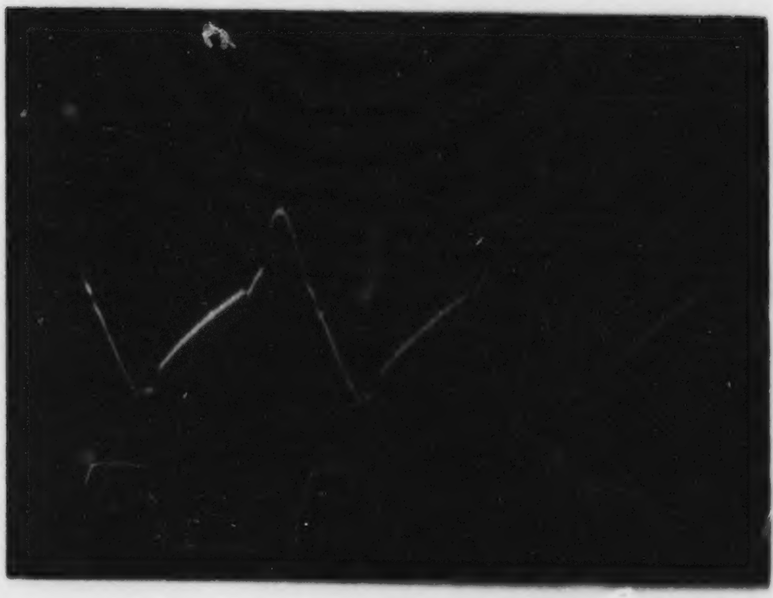

$I_{AV}$=79.3 AMP; F.F.=1.193

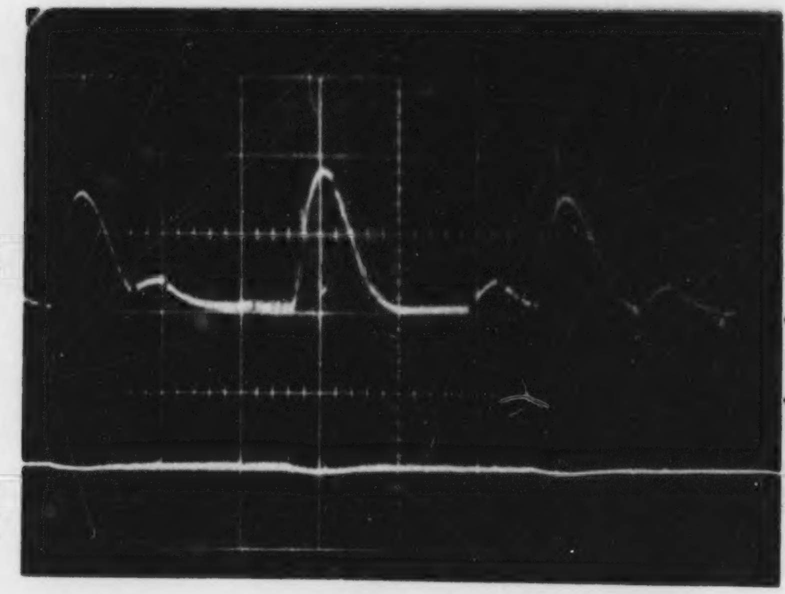

$I_{AV}$=25.3 AMP; F.F.=1.56

FIGURE 5.8

REGENERATION MODE

VEHICLE SPEED 45 mph

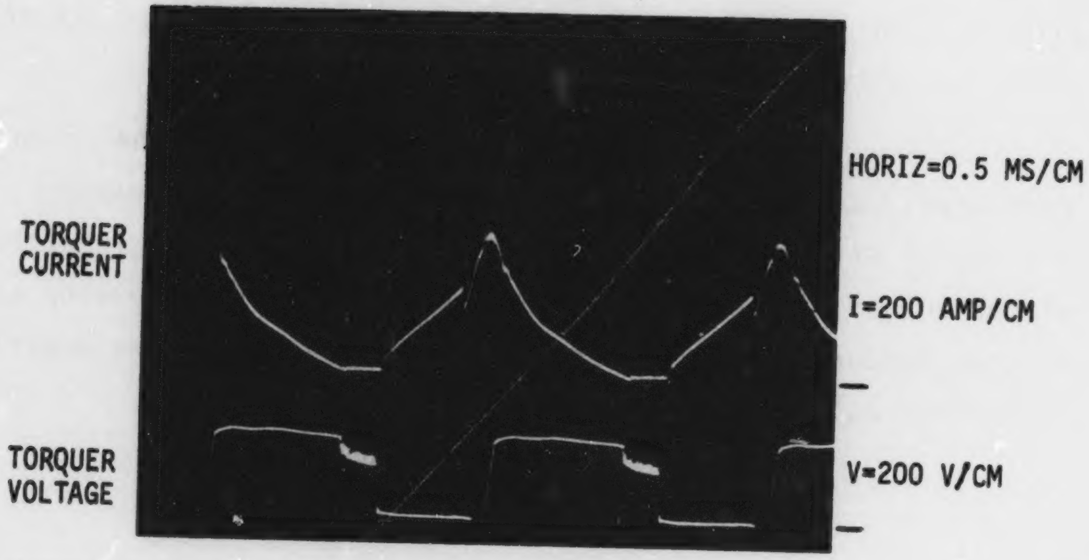

$I_{AV}$=126.3 AMP; F.F.=1.311

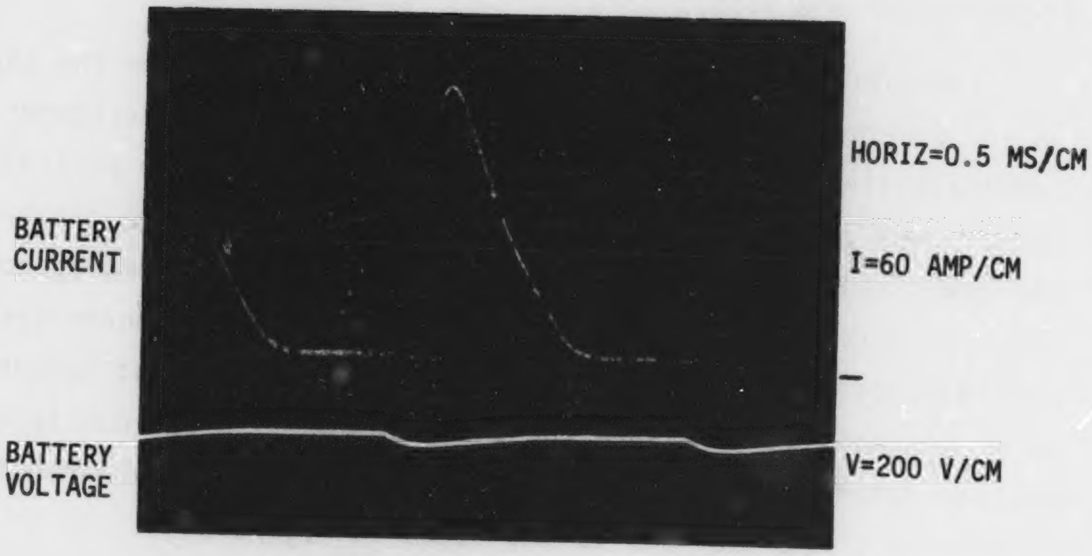

$I_{AV}$=61.7 AMP; F.F.=1.61

FIGURE 5.9

Since the waveforms are periodic, only one cycle needed to be analyzed. Figures 5.10 and 5.11 show the power factor coefficients for the Torquer using two different batteries.

The ohmic losses in the Torquer and battery are the product of the root-mean-squared current and the resistance of the component. Again, the degree of filtering precluded any meaningful digital multiplication of current signals. It was therefore necessary to develop another conversion factor, the form factor, F.F., from the off-line experiments. F.F. is defined as:

$$\text{F.F.} = \frac{I_{RMS}}{\bar{I}}$$

F.F. can be correlated with the average current, mode of operation and vehicle speed. The numerical computation of the form factor was performed in a manner similar to that of the power factor coefficient. The form factors of the Torquer in drive and regeneration for two different batteries are shown in Figures 5.12 and 5.13. The battery form factors are shown in Figures 5.14 and 5.15.

Off-line experiments were also conducted to relate the shaft torques on the Speeder and Torquer to the average current and voltages at their terminals (in the case of the Speeder, the three-phase rectifier) and shaft speeds. The Torquer in drive and the engine were calibrated using the power absorber portion of the Clayton equipment; the Speeder and the Torquer in regeneration were examined using a Ward-Leonard system and a separate, calibrated DC drive motor. The engine output torque was related to engine manifold pressure and shaft speed. The various factors and calibration data was programmed into various computation sub-routines. A summary of these routines is indicated in Figure 5.16.

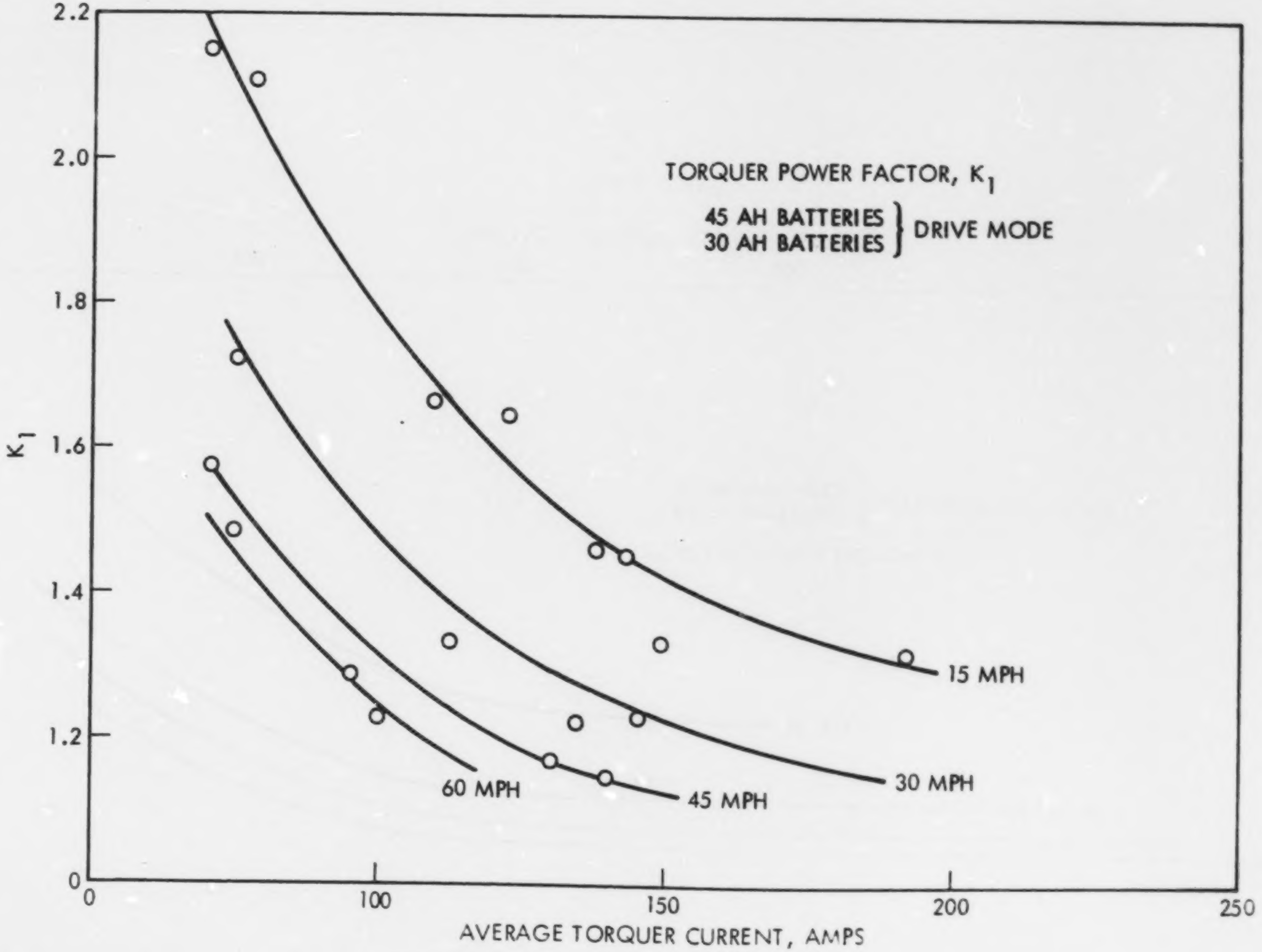
TORQUER POWER FACTOR, $K_1$
45 AH BATTERIES
30 AH BATTERIES
DRIVE MODE
15 MPH
30 MPH
45 MPH
60 MPH
$K_1$
2.2
2.0
1.8
1.6
1.4
1.2
0
0
100
150
200
250
AVERAGE TORQUER CURRENT, AMPS

FIGURE 5.10

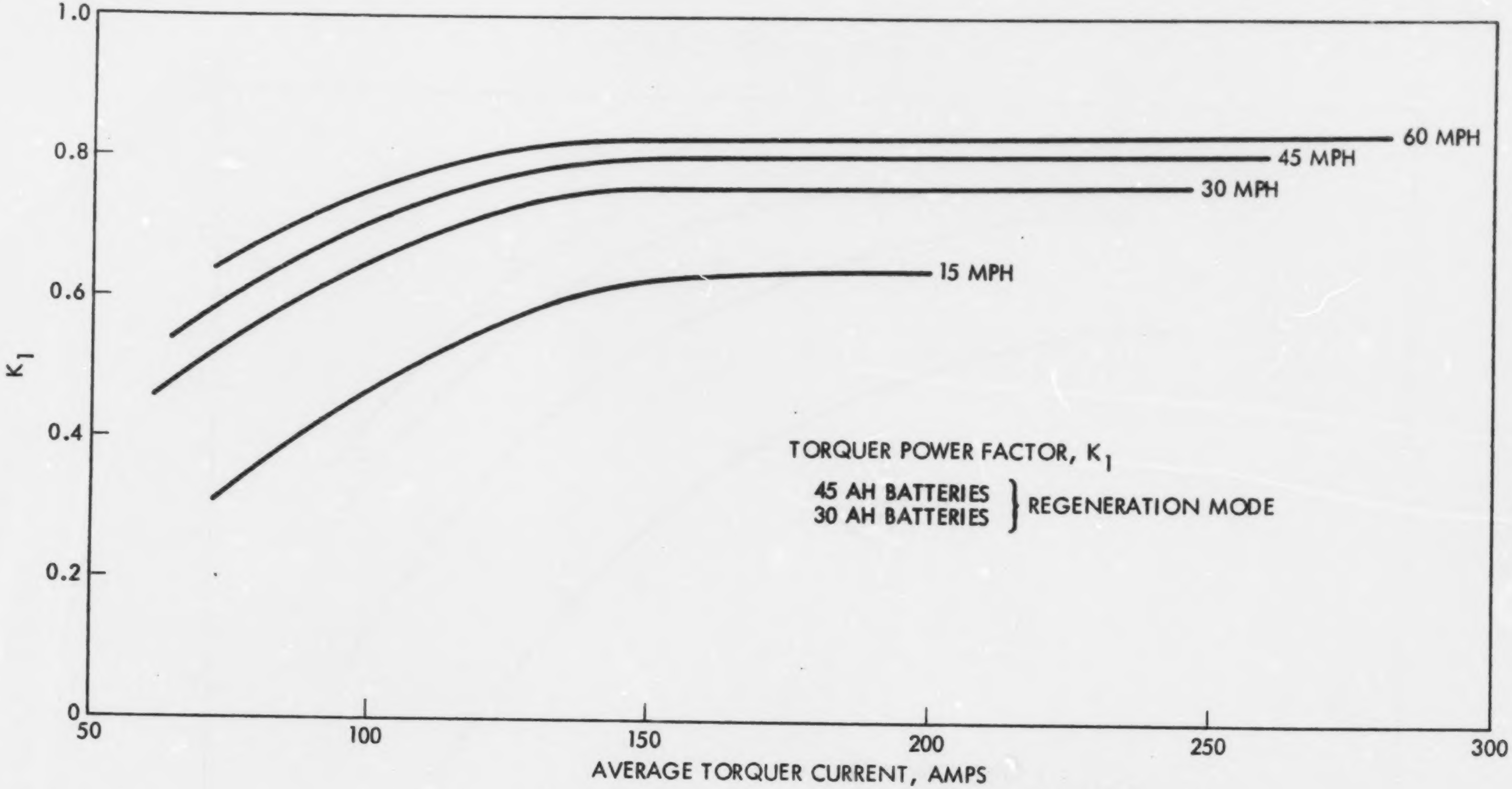
1.0
0.8
0.6
0.4
0.2
0
K1
50
100
150
200
250
300
AVERAGE TORQUER CURRENT, AMPS
60 MPH
45 MPH
30 MPH
15 MPH
TORQUER POWER FACTOR, K1
45 AH BATTERIES
30 AH BATTERIES
REGENERATION MODE

FIGURE 5.11

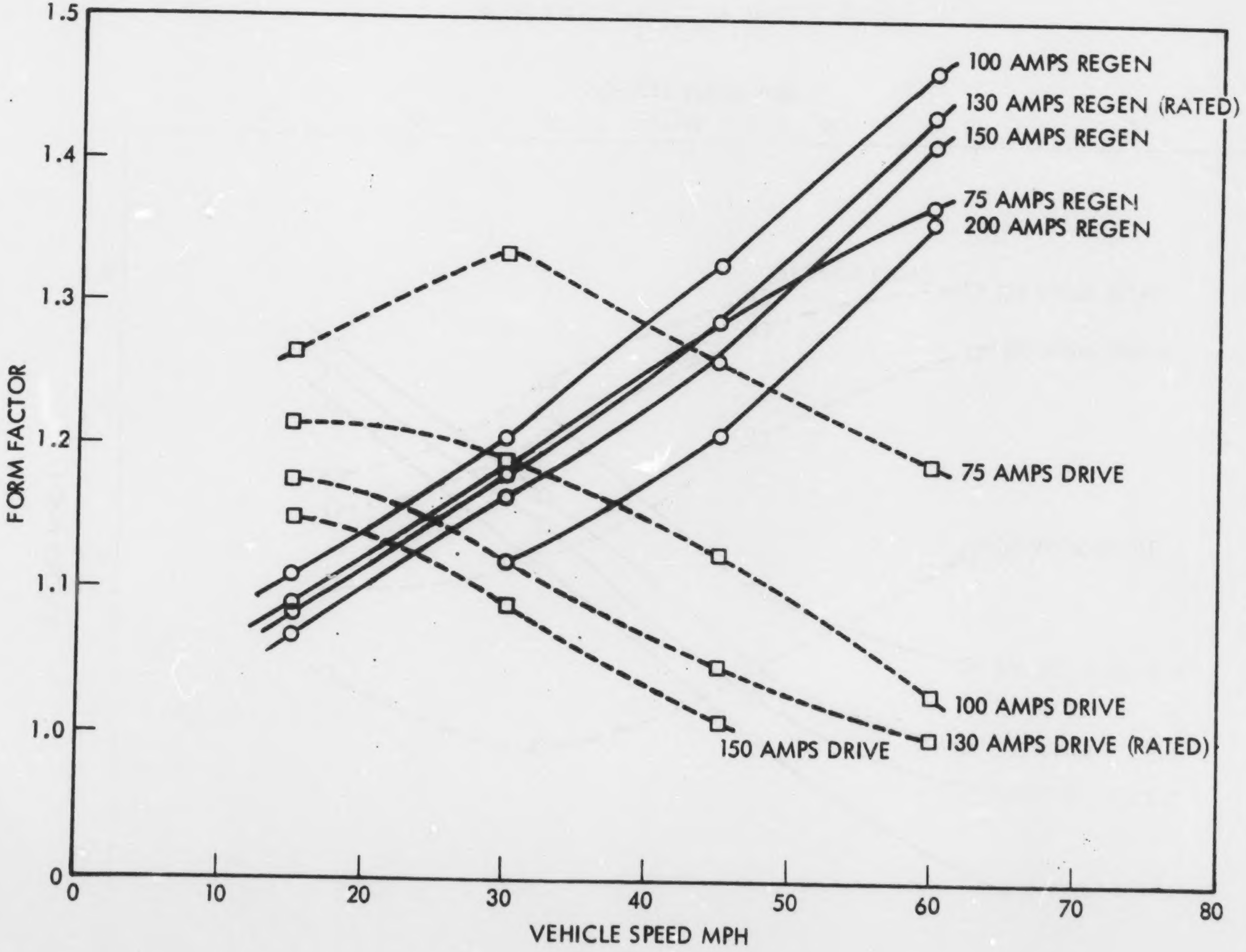

FIGURE 5.12
TORQUER FORM FACTOR VS VEHICLE SPEED
45 AH, SLI BATTERIES

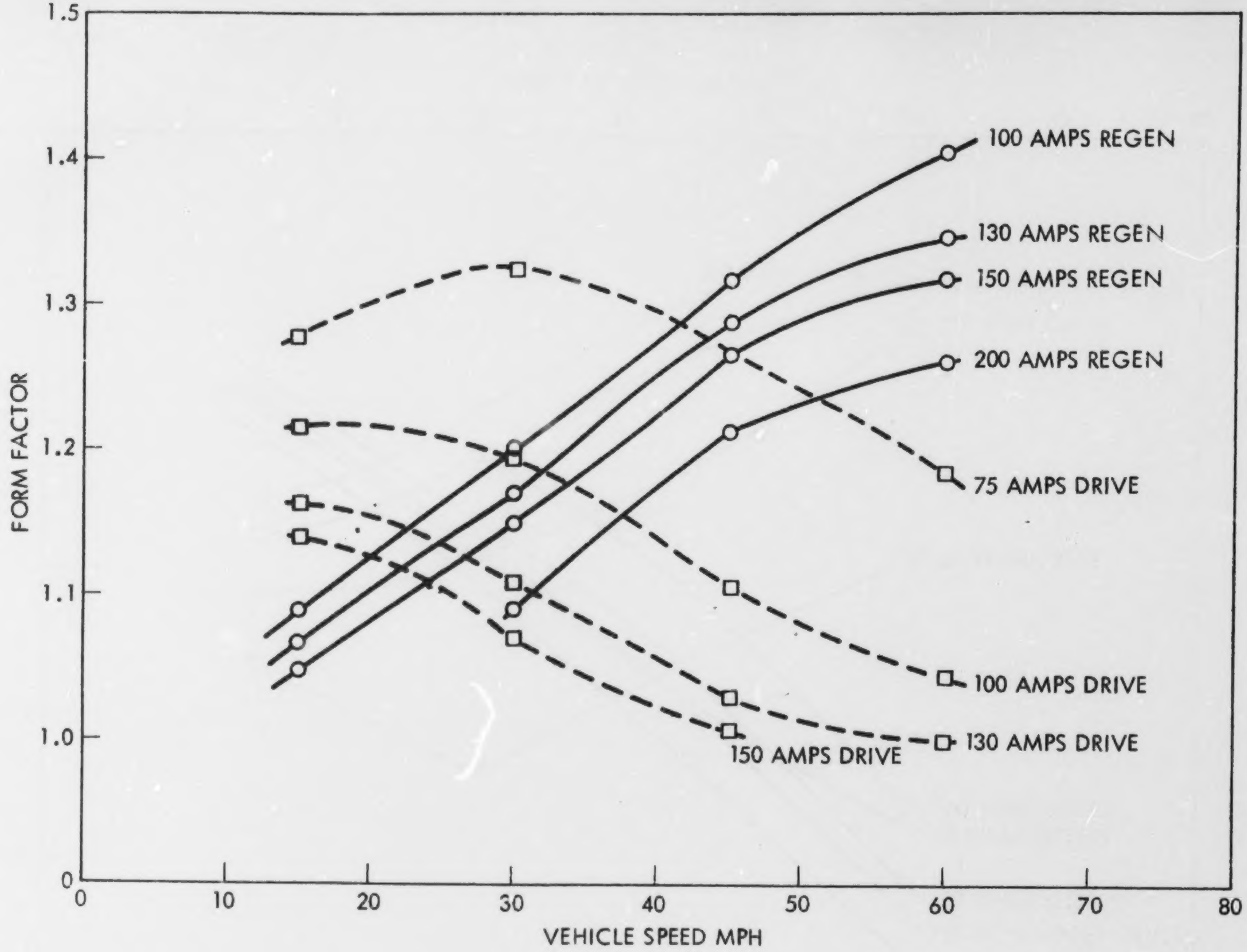

FIGURE 5.13
TORQUER FORM FACTOR VS VEHICLE SPEED
30 AH, SLI BATTERIES

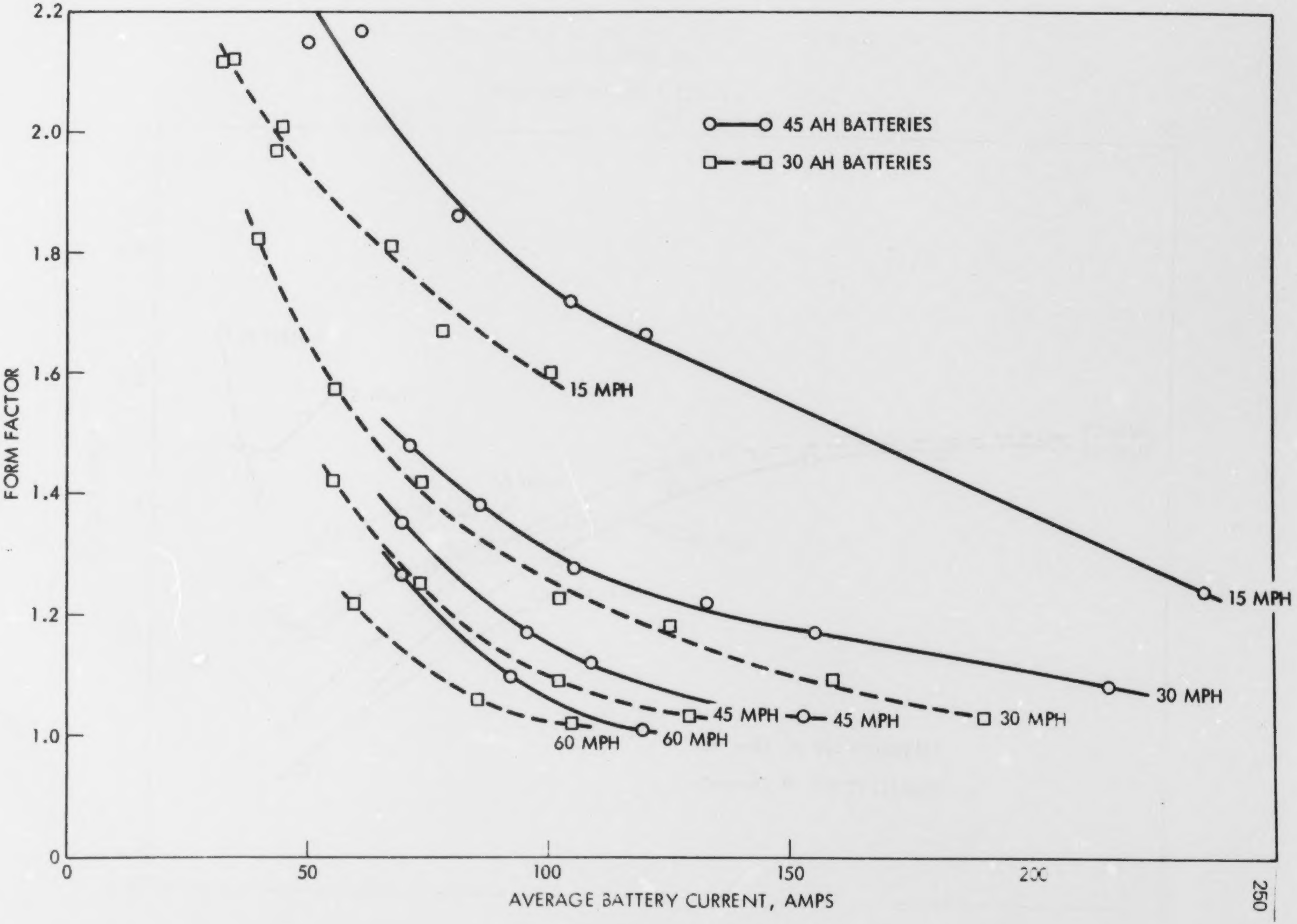

FIGURE 5.14
BATTERY FORM FACTOR VS BATTERY CURRENT IN DRIVE

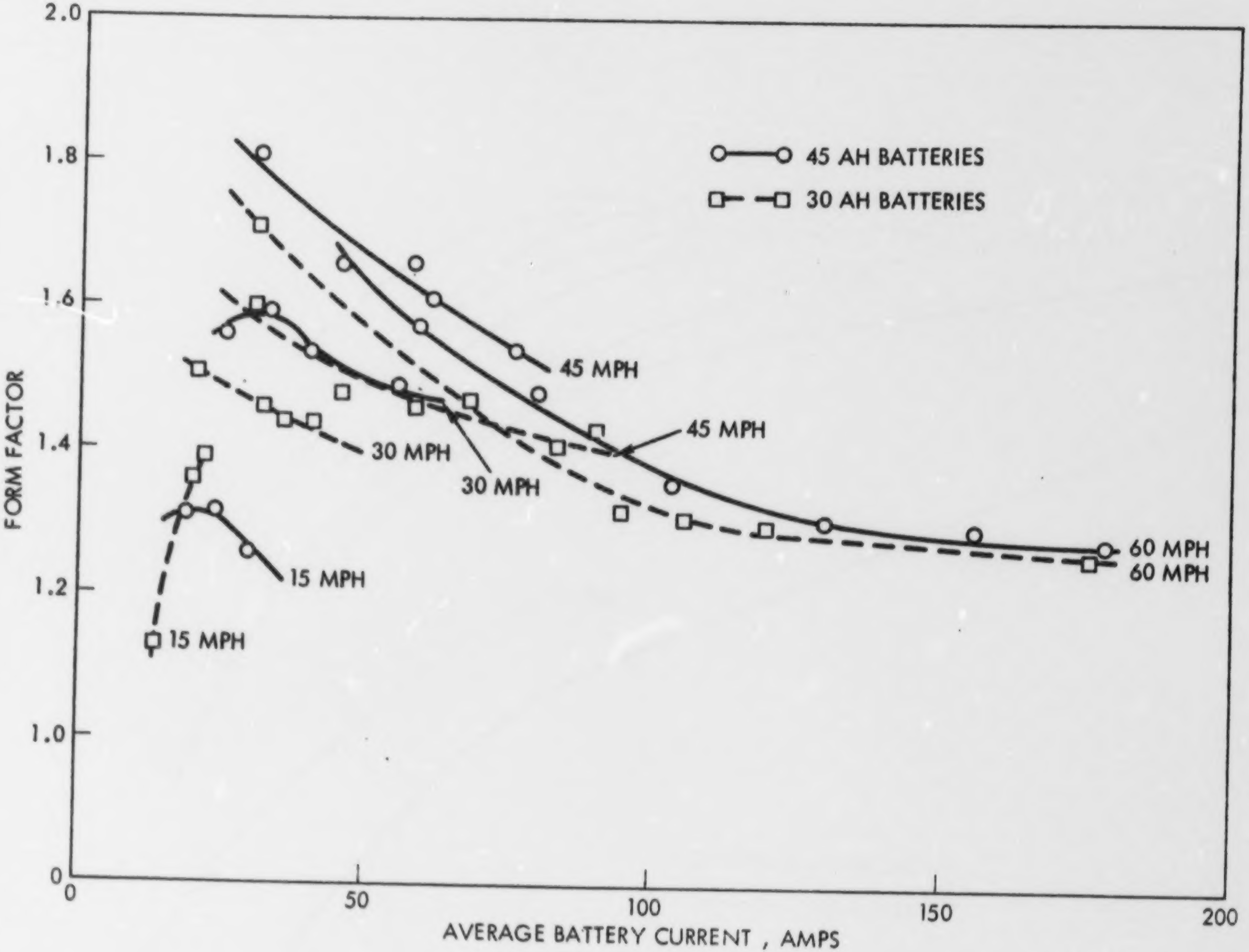

FIGURE 5.15
BATTERY FORM FACTOR VS BATTERY CURRENT IN REGENERATION

FIGURE 5.16

COMPUTATION SUB-ROUTINES

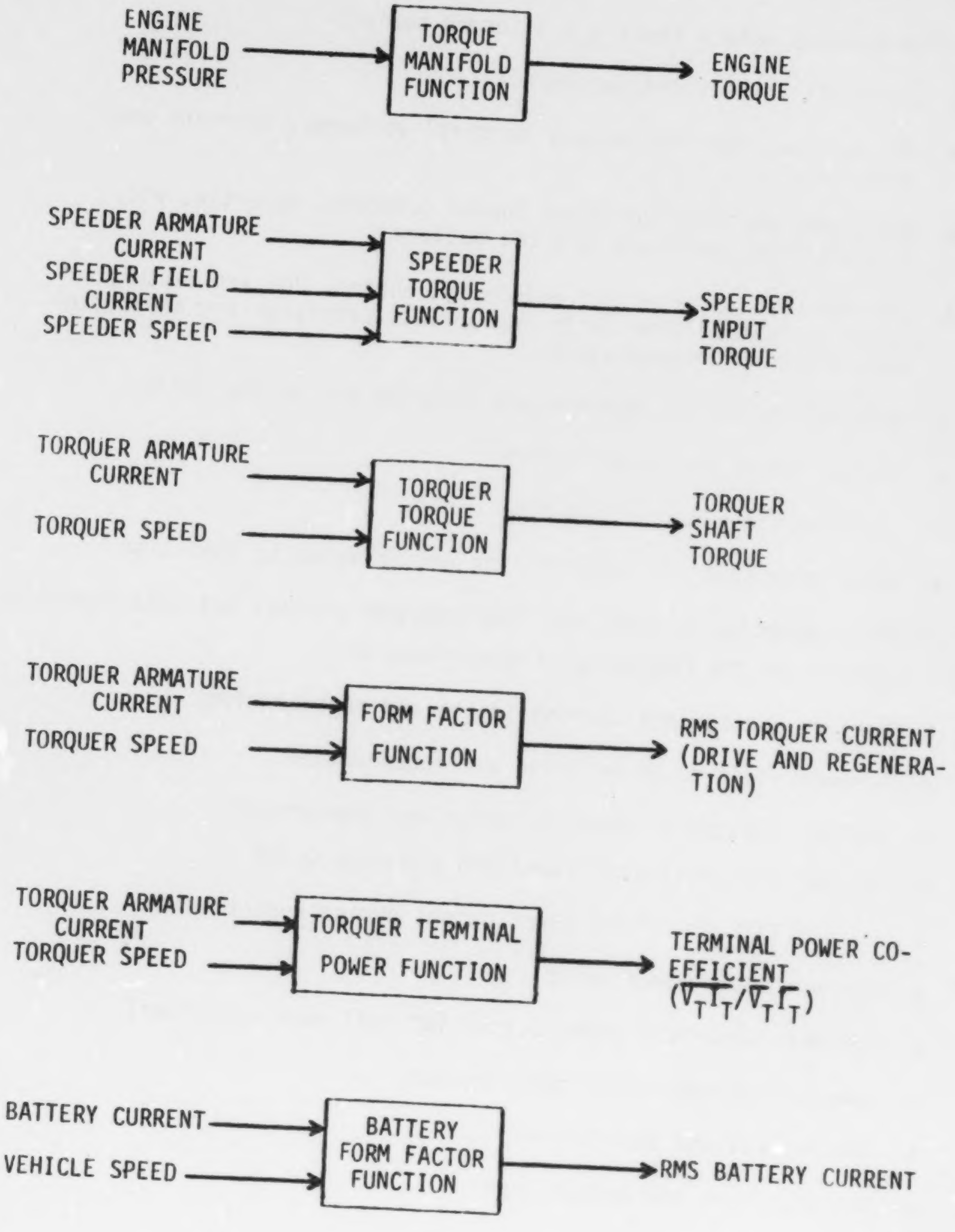
ENGINE MANIFOLD PRESSURE
TORQUE MANIFOLD FUNCTION
ENGINE TORQUE
SPEEDER ARMATURE CURRENT
SPEEDER FIELD CURRENT
SPEEDER SPEED
SPEEDER TORQUE FUNCTION
SPEEDER INPUT TORQUE
TORQUER ARMATURE CURRENT
TORQUER SPEED
TORQUER TORQUE FUNCTION
TORQUER SHAFT TORQUE
TORQUER ARMATURE CURRENT
TORQUER SPEED
FORM FACTOR FUNCTION
RMS TORQUER CURRENT (DRIVE AND REGENERATION)
TORQUER ARMATURE CURRENT
TORQUER SPEED
TORQUER TERMINAL POWER FUNCTION
TERMINAL POWER COEFFICIENT $(\overline{V_T I_T}/\overline{V_T}\,\overline{I_T})$
BATTERY CURRENT
VEHICLE SPEED
BATTERY FORM FACTOR FUNCTION
RMS BATTERY CURRENT

## 5.4 Computer Print-Out and Data Presentaiton

The digitized tapes were processed by computer, programmed to print-out the following information at 5 second intervals:

Instantaneous values (over a 0.1 second period)

- all shaft torques and speeds
- all machine, PCU and battery terminal voltages, currents and power levels
- ohmic and the total of other losses (windage, magnetic, etc.) in electrical machinery and the battery
- the integral value of all machinery, engine, PCU and battery power up to that time (with appropriate provision for separation into drive and regeneration)
- integral values of ampere-hours into and out of the battery
- vehicle speed and acceleration
- distance traveled to that time
- total time spent in regeneration and drive up to that time.

At the completion of each run, the computer printed out data (sampling at 0.1 seconds) on the frequency of occurrence of:

- Torquer voltage and current (drive and regeneration)
- Torquer shaft power in drive and regeneration
- Torquer electrical power in drive and regeneration
- Torquer PCU electrical power input during drive
- Torquer PCU electrical power output during regeneration
- Speeder shaft power input
- Speeder electrical power output (at full wave rectifier)
- Speeder PCU electrical power output
- Battery voltage and current
- Battery input and output power

## 5.5 Data Logging

In addition to the recording of component performance, the following were logged for each run:

- inertia loading (equivalent vehicle weight) and power absorber torque at 50 mph equivalent road speed
- total fuel consumed
- battery used
- specific gravity of selected cells of the battery before and at the end of the run
- battery temperature

## 5.6 EMT Dynamometer Performance on LA-4 Route

Table 5.1 presents a summary of 18 runs of the EMT system over the LA-4 driving route. The major system parameters which were explored were:

- Vehicle weight and drag
    - 2000, 2500, 3000, 3500 and 4000 pounds equivalent inertia settings
    - power absorber settings at an equivalent 50 mph road speed; approximately 10 hp for the 2000 pound vehicle, 19 hp for the 4000 pound vehicle
- Lead-acid batteries
    - 32-217 ampere-hour, 6 volt golf cart batteries weighing approximately 2100 pounds
    - 16-45 ampere-hour, 12 volt SLI batteries weighing approximately 500 pounds
    - 16-30 ampere-hour, 12 volt power supply batteries weighing approximately 320 pounds
- Engine power settings
    - 12-16 output shaft horsepower at 1800 rpm

TABL

PERFORMANCE SUMMA

| RUN IDENTIFICATION NUMBER | HC 56 | HC 52 | HC 49 | HC 47 | HC 55 | HC 53 | HC 50 | HC 32 |
|---|---|---|---|---|---|---|---|---|
| Vehicle Weight | 2000 | 2500 | 2500 | 3000 | 3000 | 3500 | 3500 | 3000 |
| Battery Type | Troj. | Troj. | Troj. | Troj. | Troj. | Troj. | Troj. | Troj. |
| Manifold Press. " Hg | 7.0 | 8.0 | 9.0 | 8.0 | 7.0 | 8.0 | 7.0 | 8.5 |
| Distance (D) - miles | 9.91 | 9.74 | 9.60 | 8.91 | 9.78 | 9.39 | 9.42 | 9.25 |
| EICE/D Kw-Hr/Mi | .565 | .514 | .525 | .529 | .561 | .546 | .579 | .550 |
| ETIR/D Kw-Hr/Mi | .199 | .178 | .182 | .202 | .210 | .178 | .182 | .126 |
| ETOR/D Kw-Hr/Mi | .091 | .081 | .084 | .090 | .107 | .072 | .084 | .066 |
| ETID/D Kw-Hr/Mi | .126 | .202 | .227 | .261 | .234 | .323 | .329 | .287 |
| ETOD/D Kw-Hr/Mi | .065 | .111 | .127 | .153 | .139 | .193 | .198 | .179 |
| Regeneration Time (sec) | 1263 | 1096 | 1073 | 1031 | 1136 | 1025 | 1034 | 807 |
| Drive Time (sec) | 416 | 574 | 606 | 539 | 544 | 665 | 656 | 872 |
| % Regeneration Time | 75.3 | 66.6 | 63.9 | 65.6 | 67.6 | 60.5 | 61.1 | 48.0 |
| % Drive Time | 24.7 | 33.4 | 36.1 | 34.4 | 32.4 | 39.5 | 38.9 | 52.0 |
| EBO/D Kw-Hr/Mi | .091 | .159 | .184 | .212 | .189 | .266 | .279 | .224 |
| EBI/D Kw-Hr/Mi | .199 | .168 | .154 | .181 | .190 | .169 | .182 | .140 |
| AHI/D (calc) Amp-Hr/Mi | .859 | .793 | .716 | .809 | .845 | .790 | .833 | .650 |
| AHO/D (calc) Amp-Hr/Mi | .485 | .979 | 1.100 | 1.330 | 1.130 | 1.750 | 1.740 | 1.433 |
| EGI/D Kw-Hr/Mi | .229 | .217 | .217 | .227 | .224 | .235 | .261 | .194 |
| ESPO/D Kw-Hr/Mi | .140 | .123 | .126 | .128 | .134 | .154 | .154 | .135 |
| ETLR/D Kw-Hr/Mi | .108 | .097 | .098 | .112 | .103 | .106 | .098 | .060 |
| EBLI/D Kw-Hr/Mi | .014 | .008 | .007 | .008 | .008 | .008 | .009 | .008 |
| EBLO/D Kw-Hr/Mi | .008 | .039 | .047 | .065 | .051 | .097 | .100 | .056 |
| ETLD/D Kw-Hr/Mi | .061 | .091 | .100 | .108 | .095 | .130 | .131 | .108 |
| ESL/D Kw-Hr/Mi | .080 | .094 | .091 | .099 | .090 | .081 | .107 | .059 |
| Fuel Consumption miles/gal. | 17.4 | 18.4 | 18.1 | 16.8 | 17.0 | 17.6 | 16.5 | 17.3 |
| ΔAH (calc) (charge) | (.374) | .186 | .324 | .521 | .285 | .960 | .907 | .783 |
| ΔAH (sp. gr.) (charge) | (.440) | .440 | .321 | .761 | .537 | 1.340 | .618 | .986 |
| EROAD/D Kw-Hr/Mi | .210 | .235 | .235 | .264 | .264 | .295 | .295 | .264 |
| ESOTI/D Kw-Hr/Mi | .035 | .043 | .043 | .049 | .045 | .057 | .050 | .063 |
| ESOBI/D Kw-Hr/Mi | .105 | .080 | .083 | .079 | .089 | .097 | .104 | .072 |
| EGI/EICE % | 40.5 | 42.3 | 41.4 | 42.9 | 40.0 | 42.7 | 45.1 | 35.2 |
| ESOTI/EICE % | 6.2 | 8.4 | 8.2 | 9.3 | 8.0 | 10.4 | 8.6 | 11.4 |
| EROAD/EICE % | 37.1 | 45.7 | 44.8 | 51.8 | 48.8 | 53.0 | 51.0 | 48.0 |
| ETOR/D + ESOBI/D Kw-Hr/Mi | .196 | .161 | .167 | .167 | .196 | .169 | .186 | .138 |
| [EBI - (ETOR+ESOBI)]/EBI % | 0 | +4.2 | -8.5 | +7.7 | -3.2 | 0 | -2.2 | +1.4 |

TABLE 5.1

## SUMMARY OF LA-4 TESTS

| 50 | HC 32 | HC 57 | HC 58 | HC 59 | HC 33 | HC 27 | HC 29 | HC 43 | HC 37 | HC 45 | HC 62 |
|---|---|---|---|---|---|---|---|---|---|---|---|
| 0 | 3000 | 3000 | 3000 | 4000 | 2500 | 2500 | 4000 | 3000 | 3500 | 4000 | 3000 |
| j. | Troj. | G.C. | G.C. | G.C. | Willard | Willard | Willard | Willard | Willard | Willard | Willard |
| 0 | 8.5 | 7.0 | 9.0 | 8.0 | 8.0 | 9.0 | 7.5 | 7.0 | 7.0 | 6.5 | 8.0 |
| 42 | 9.25 | 9.79 | 9.75 | 8.34 | 9.59 | 9.55 | 9.44 | 9.75 | 9.70 | 8.05 | 9.69 |
| 79 | .550 | .514 | .480 | .509 | .535 | .504 | .569 | .567 | .686 | .569 | .545 |
| 82 | .126 | .199 | .172 | .204 | .124 | .116 | .140 | .217 | .164 | .212 | .208 |
| 84 | .066 | .098 | .077 | .091 | .067 | .089 | .066 | .096 | .085 | .100 | .111 |
| 29 | .287 | .252 | .289 | .391 | .209 | .203 | .450 | .248 | .296 | .346 | .244 |
| 98 | .179 | .138 | .153 | .232 | .119 | .135 | .287 | .135 | .196 | .208 | .154 |
| 4 | 807 | 1114 | 1041 | 830 | 895 | 929 | 811 | 1132 | 953 | 815 | 1074 |
| 6 | 872 | 571 | 639 | 545 | 775 | 751 | 864 | 544 | 718 | 510 | 606 |
| 1 | 48.0 | 66.1 | 61.9 | 60.4 | 53.6 | 56.2 | 48.5 | 67.6 | 57.0 | 61.5 | 64.0 |
| 9 | 52.0 | 33.9 | 38.1 | 39.6 | 46.4 | 43.8 | 51.5 | 32.4 | 43.0 | 38.5 | 36.0 |
| 279 | .224 | .206 | .237 | .337 | .156 | .175 | .361 | .199 | .242 | .292 | .212 |
| 82 | .140 | .188 | .164 | .126 | .147 | .137 | .164 | .204 | .184 | .199 | .180 |
| 33 | .650 | .901 | .798 | .881 | .681 | .632 | .780 | .894 | .859 | .900 | .816 |
| 40 | 1.433 | 1.110 | 1.280 | 1.895 | .854 | .985 | 2.290 | 1.082 | 1.420 | 1.720 | 1.270 |
| 61 | .194 | .202 | .188 | .191 | .180 | .174 | .187 | .244 | .222 | .235 | .211 |
| 54 | .135 | .123 | .114 | .116 | .134 | .076 | .188 | .147 | .135 | .137 | .068 |
| 98 | .060 | .101 | .095 | .113 | .047 | .027 | .074 | .121 | .079 | .112 | .097 |
| 09 | .008 | .006 | .005 | .006 | .007 | .005 | .008 | .005 | .019 | .006 | .004 |
| 00 | .056 | .049 | .023 | .043 | .011 | .014 | .056 | .018 | .090 | .038 | .026 |
| 31 | .108 | .114 | .136 | .159 | .090 | .090 | .163 | .113 | .100 | .138 | .090 |
| 07 | .059 | .079 | .074 | .075 | .046 | .098 | .000 | .097 | .087 | .098 | .143 |
|  | 17.3 | 18.3 | 18.4 | 18.9 | 17.9 | 17.0 | 17.9 | 17.2 | 17.1 | 17.5 | 18.3 |
| 07 | .783 | .209 | .482 | 1.014 | .173 | .353 | 1.510 | .108 | .561 | .820 | .450 |
| 18 | .986 | (.051) | .693 | .750 | .350 | .472 | .705 | .210 | .780 | .802 | .775 |
| 95 | .264 | .264 | .264 | .330 | .235 | .235 | .330 | .264 | .295 | .330 | .264 |
| 50 | .063 | .046 | .052 | .054 | .053 | .028 | .089 | .049 | .054 | .054 | .032 |
| 04 | .072 | .077 | .062 | .062 | .081 | .038 | .099 | .098 | .081 | .083 | .036 |
|  | 35.2 | 39.3 | 39.2 | 37.6 | 33.7 | 34.5 | 32.9 | 42.9 | 32.4 | 41.3 | 38.8 |
|  | 11.4 | 9.0 | 10.8 | 10.6 | 9.9 | 5.5 | 15.6 | 8.6 | 7.9 | 9.5 | 5.9 |
|  | 48.0 | 51.4 | 55.0 | 64.8 | 44.0 | 46.0 | 58.0 | 46.5 | 43.1 | 58.0 | 48.5 |
| 86 | .138 | .175 | .139 | .153 | .148 | .127 | .165 | .194 | .166 | .183 | .147 |
| .2 | +1.4 | +6.9 | +15.4 | -21.4 | -0.7 | +7.4 | -0.6 | +3.4 | +9.8 | +8.0 | +18.3 |

BLANK PAGE

# NOMENCLATURE FOR TABLE 5.1

EICE/D - energy from engine shaft per mile

ETIR/D - energy into Torquer shaft in regeneration per mile

ETOR/D - energy out of Torquer PCU (to battery terminals) in regeneration per mile

ETID/D - energy into Torquer PCU in drive per mile

ETOD/D - energy out of Torquer shaft in drive per mile

EBO/D - energy out of battery terminals per mile

EBI/D - energy into battery terminals per mile

AHI/D - integral ampere-hours into battery terminals per mile

AHO/D - integral ampere-hours out of battery terminals per mile

EGI/D - energy into Speeder shaft per mile

ESPO/D - energy out of Speeder PCU per mile

ETLR/D - losses in Torquer system during regeneration per mile

EBLI/D - losses in battery during charge per mile

EBLO/D - losses in battery during discharge per mile

ETLD/D - losses in Torquer system during drive per mile

ESL/D - losses in Speeder system per mile

$\Delta$AH(calc) - ampere-hour change of battery as measured terminals per mile

$\Delta$AH(sp. gr.) - ampere-hour change of battery as measured by specific gravity readings per mile

EROAD/D - road energy requirement per mile (computed during previous computer simulations)

ESOTI/D - energy out of Speeder which flows directly to Torquer per mile

ESOBI/D - energy out of Speeder which flows directly into battery

### 5.6.1 Distance and Time

The dispersion of distances the simulated vehicle traveled during the tests is very small, less than 10% of the average. Variations can be attributed to; the variability of various drivers in accurately following the driver's aid, and small errors in the computing process.

Total trip time variations are very small, related to the detailed time of starting and stopping the data recording. Two runs, columns 11 and 17 are much shorter; during these tests the vee-belts driving the inertia wheels became dislodged and the tests were stopped short of the full duration.

### 5.6.2 Regeneration and Battery Charging

The time spent in regeneration; i.e., the Torquer acting as a generator, is always greater than 60% of the total driving time. The battery therefore receives energy more than 60% of the time or is being charged almost twice as often as it is being discharged. Battery charging comes from two sources, directly from the engine by way of the Speeder and from the propeller shaft through the Torquer acting as a generator. In the latter case, energy comes from two sources: the engine's torque contribution and kinetic energy of the vehicle as it slows down. The contribution of the two machines' outputs to battery charging are close to one another, thus accounting in each case for about 50% of the total battery charging power.

The contribution of regenerative braking to battery charging is difficult to determine--no instrumentation or computation technique was available for that measurement. However, there is no apparent correlation between vehicle weight and Torquer regenerative output as would be expected if regenerative braking were a substantial portion of the Torquer's total regenerative output. Indeed, qualitative observations as to the need for the mechanical disc brake during LA-4 decelerations would indicate that as the vehicle weight increased, more mechanical braking was necessary, probably negating the effect of the additional kinetic energy. The Torquer system used during the tests had a constant, limited maximum braking torque capability in it. A redesign would tailor this limited capability to reflect vehicle size--higher limits for higher vehicles.

### 5.6.3 Drive and Battery Discharge

The EMT system spent approximately 35% of its time in the drive mode, i.e., the Torquer acting as a motor. (An exception to this is the 2000 pound vehicle run of column 1. In this case, the engine output was too high, and additional regeneration time was used to absorb the excess energy.) Figure 5.17 shows the average Torquer electrical input and mechanical output are approximately proportional to the vehicle weight. Acceleration power requirements are proportional to vehicle weight; the relatively constant engine output of the tests can only provide base traction loads and in all cases the Torquer had to provide the peaking power.

The energy output of the Speeder is constrained (for a fixed engine output power) by the speed relationships of the engine, Speeder and propeller shafts and the driving cycle. Speeder energy available to the Torquer is therefore invariant with vehicle weight or battery type.

In the tests, the engine power settings were not increased enough with vehicle weight and as a result the depth of battery discharge increases with increasing vehicle weight. (In column 1, the excess engine power shows up as a net charging of the battery during the test.)

### 5.6.4 Battery Operation

Figure 5.18 summarizes the effect of battery capacity and vehicle weight on the performance of the battery. There is a strong difference in the percent loss (or discharge efficiency) of the smallest (30 A-H) batteries and the SLI and golf cart batteries. Since the battery energy requirement for a given vehicle weight is relatively constant, it must be concluded that the discharge efficiency is related to battery construction. To a first approximation, the plate area of the batteries should be proportional to the capacity. Plate area establishes (to a first order)

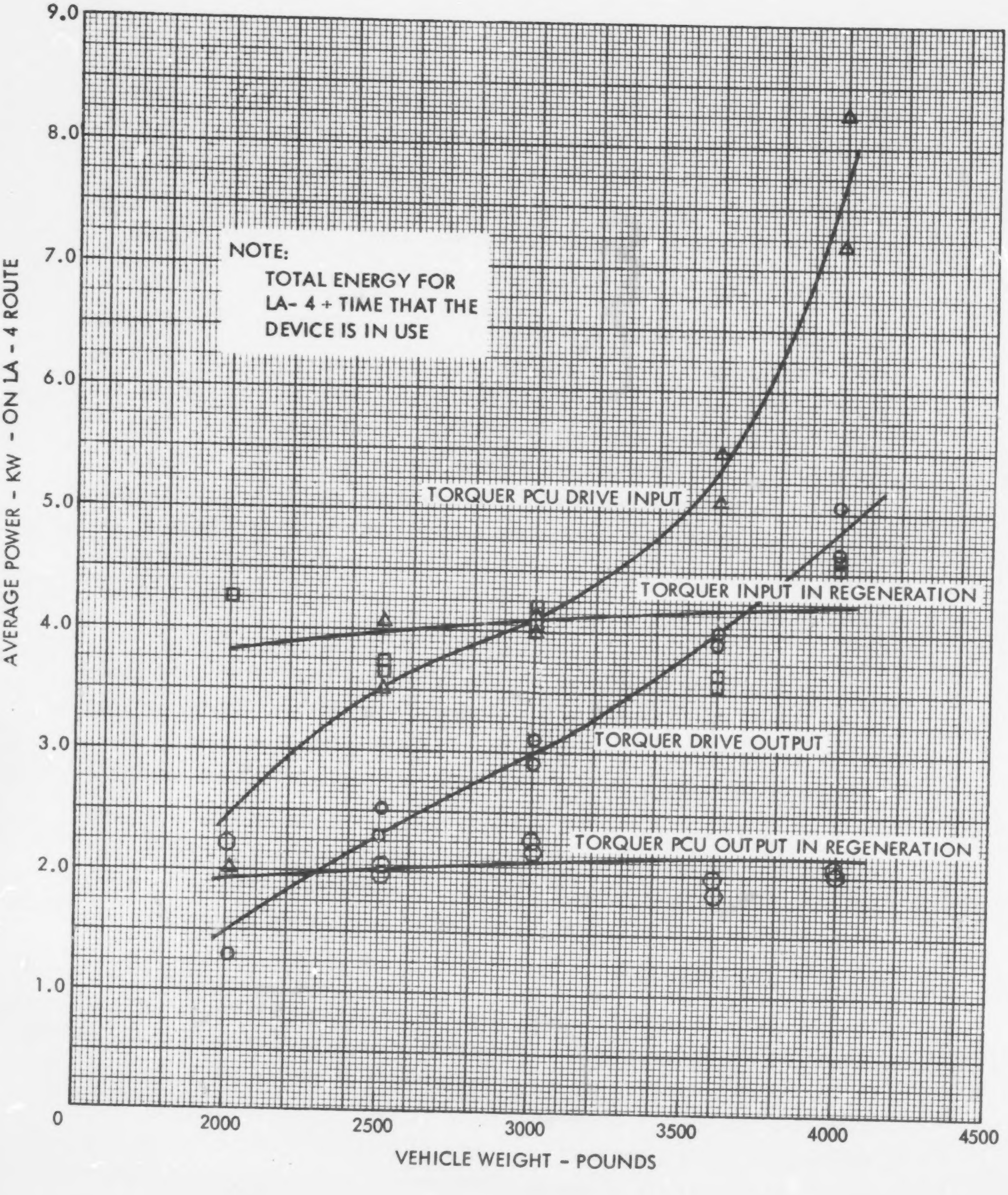
9.0
8.0
7.0
6.0
5.0
4.0
3.0
2.0
1.0
0
2000
2500
3000
3500
4000
4500
AVERAGE POWER - KW - ON LA - 4 ROUTE
VEHICLE WEIGHT - POUNDS
NOTE:
TOTAL ENERGY FOR LA- 4 ÷ TIME THAT THE DEVICE IS IN USE
TORQUER PCU DRIVE INPUT
TORQUER INPUT IN REGENERATION
TORQUER DRIVE OUTPUT
TORQUER PCU OUTPUT IN REGENERATION

FIGURE 5.17

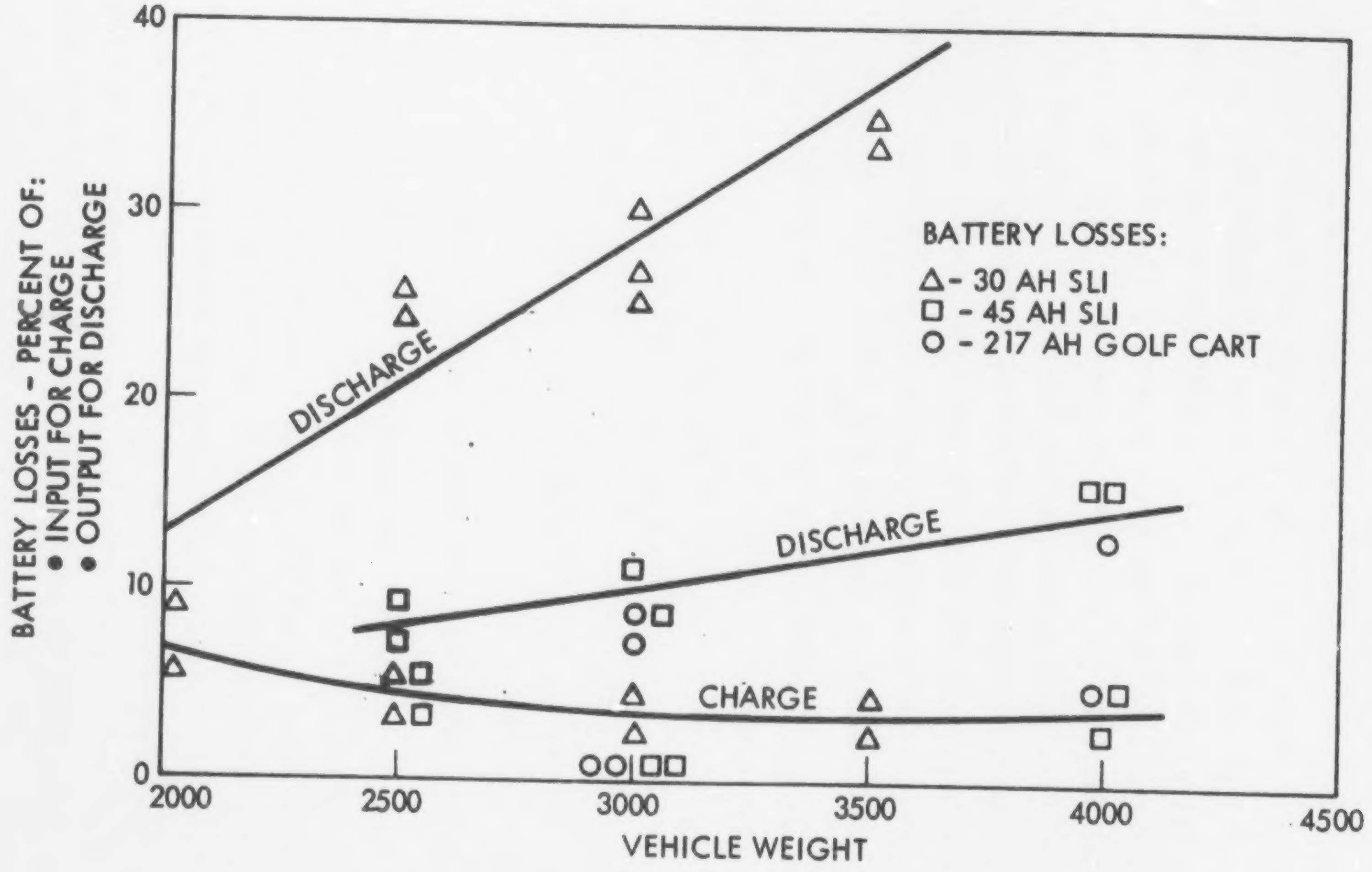

FIGURE 5.18
EFFECT OF BATTERY CAPACITY ON BATTERY LOSSES

the current density and polarization losses; losses are generally proportional to current density. The construction forms of the 30 A-H and 45 A-H batteries are similar, both designed for SLI duty, and the poorer performance of the 30 A-H batteries is expected on the basis of capacity. The comparison with the golf cart batteries is more difficult. These batteries are designed for deep discharge service and thus their thickness to surface area is higher than the SLI batteries. It is probable that the useful surface area of the golf cart batteries under high loads is no more than that of the lower capacity, 45 A-H batteries and the additional capacity is of no use in hybrid service. All the batteries exhibit similar performance during charge. The charging power is low (relative to discharge) and invariant with vehicle weight (as long as the engine power remains approximately the same). The difference in plate construction is not as important as in discharge because of the lower currents and less dependence on electrolyte diffusion.

The calculated ampere-hour change of the batteries (ampere-hours in minus ampere-hours out) varies in a similar manner with the charge state changes as measured by specific gravity readings. These are, however, no good correlation between them or their relative differences. It had been hoped that the difference would be a good measurement of Faradiac efficiency, that is, the amount of current charge which went into the parasitic gassing reactions.

### 5.6.5 Energy Flow Paths and Component Efficiencies

A summary of average component and system efficiencies for a 3000 pound EMT vehicle is given in Table 5.2. The overall system efficiency for any decreases in battery charge state brings this number even lower. A certain amount of caution must be applied to this number in that the road demand is based on earlier computer simulations of an EMT system in which the road energy for LA-4 operation was computed using inertia, drag and a LA-4 velocity profile.[4] There is no way at present by which the road load required on the dynamometer to perform the same profile can be compared to these computer numbers.

The energy which flows from the engine shaft is distributed to the road through various paths, each of which contain dissipative elements which degrade the total energy flow. For example only a small percentage (∿10%)

TABLE 5.2 AVERAGE EFFICIENCIES OF SUBSYSTEMS OF VARIOUS 3000 POUND EMT VEHICLES ON LA-4 MISSION

| | |
|---|---|
| OVERALL EFFICIENCY - $\left(\frac{EROAD}{EICE}\right)$ | 50% |
| GEAR BOX EFFICIENCY | 75% |
| SPEEDER EFFICIENCY | 70% |
| SPEEDER PCU | 95% |
| TORQUER MACHINE EFFICIENCY (DRIVE) | 67% |
| TORQUER PCU EFFICIENCY (DRIVE) | 88% |
| TORQUER MACHINE EFFICIENCY (REGENERATION) | 65% |
| TORQUER PCU EFFICIENCY (REGENERATION) | 88% |
| BATTERY UTILIZATION $\frac{\text{Power out}}{\text{Power in} + (AH\text{-}V_B)}$ | 64% |

of the engine energy flows directly from the Speeder to the Torquer. Since the combined Speeder and Speeder PCU operate at an average efficiency of about 65%, the 40% of the engine energy available at the Speeder input is degraded to 26% at the Speeder PCU output, leaving only 16% of the engine output for the battery.

A major source of inefficiency in all engine paths is the gear box. Off-line experiments indicate that the present gear box operates around 75% efficiency. The gearing was designed about an existing planetary gear system and contains idler gears that would not be needed in a redesigned system. The box is completely filled with heavyweight oil to insure proper lubrication--a better design would use sling or mist lubrication.

## 5.7 Statistical Representation of EMT-Dynamometer Operation

Section 5.4 described the distributional information computed at the end of each test. Figure 5.19 through 5.28 present histograms for the run of column 5 of Table 5.1, representative of the data. There are various ways of describing this statistical data; this section will treat several of them.

### 5.7.1 Cumulative Energy Distributions and Through-Put Power Levels

Cumulative energy distributions of some of the histograms were computed and are presented in Figures 5.29 through 5.33. The distributions were calculated by multiplying the value of the mid-point value of each interval of the histogram by its probability of occurrence and summing the result with the sum of all the products starting with the lowest power level interval. The summation was then divided by the sum of products over the entire power range.

The distributions of battery discharge and charge energy exhibit characteristics primarily dependent on the vehicle weight. As the vehicle weight increases, the range of charge and discharge power increases, related to the increasing available deceleration energy and the increasing acceleration effort required. The discharge power capability of the battery is the ultimate limiting factor and the distributions indicate that the peak power density (watt/pound) of the golf cart batteries is far less than that of the SLI type. For the required peaking power of hybrid operation, the excess golf cart battery capacity has little effect in providing additional power.

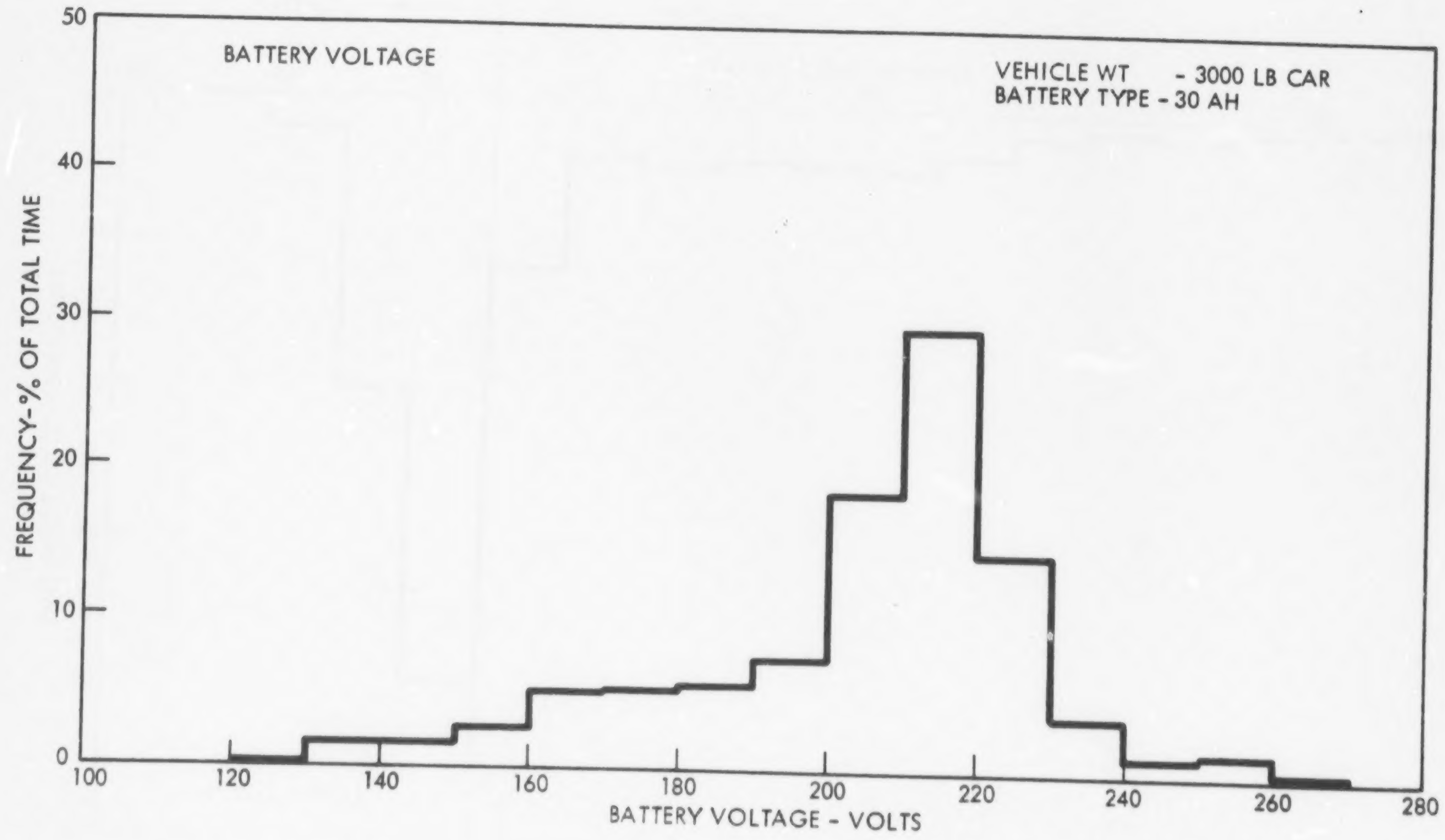
BATTERY VOLTAGE
VEHICLE WT - 3000 LB CAR
BATTERY TYPE - 30 AH
FREQUENCY-% OF TOTAL TIME
50
40
30
20
10
0
100
120
140
160
180
200
220
240
260
280
BATTERY VOLTAGE - VOLTS

FIGURE 5.19

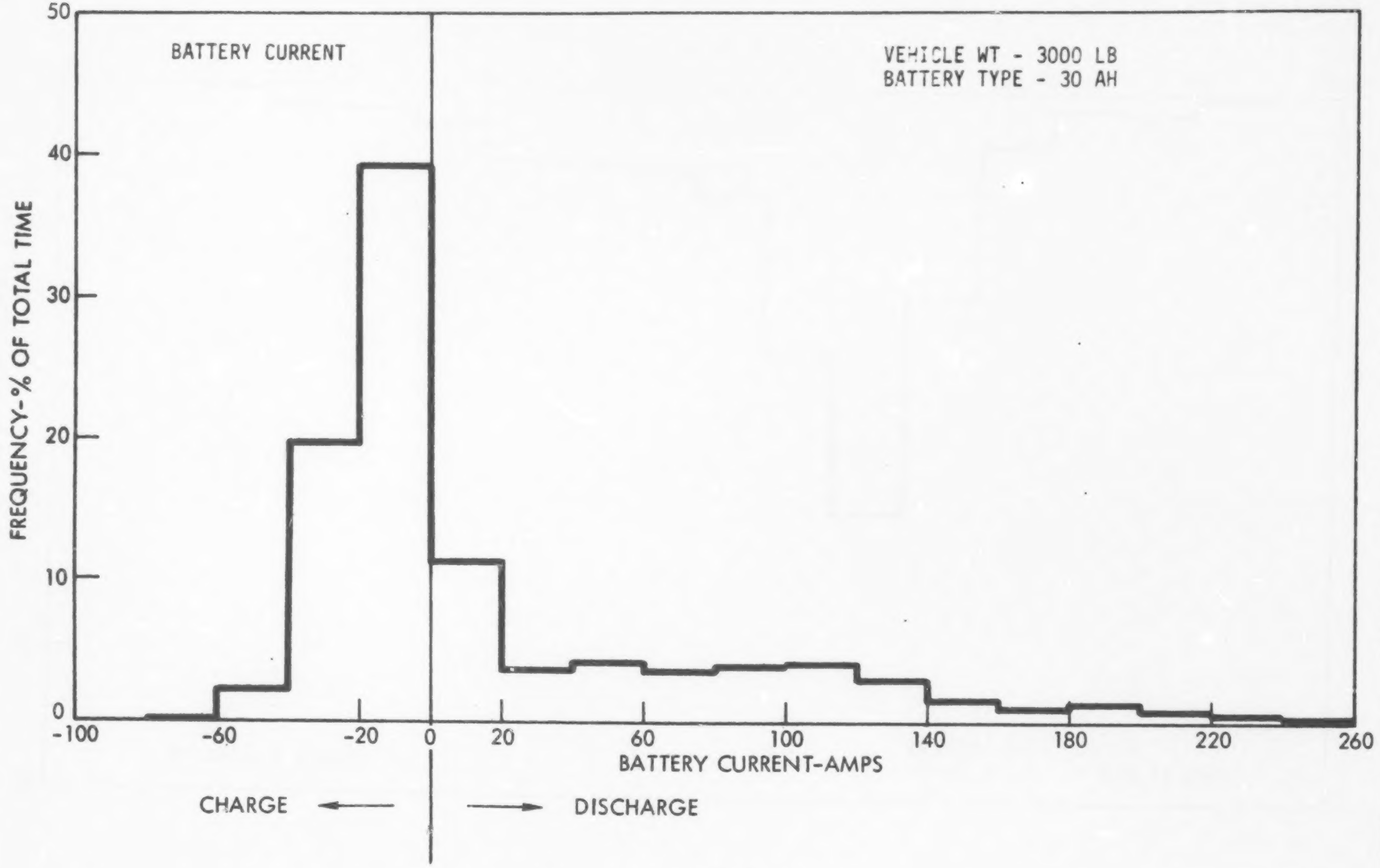
BATTERY CURRENT
VEHICLE WT - 3000 LB
BATTERY TYPE - 30 AH
FREQUENCY-% OF TOTAL TIME
50
40
30
20
10
0
-100
-60
-20
0
20
60
100
140
180
220
260
BATTERY CURRENT-AMPS
CHARGE
DISCHARGE

FIGURE 5.20

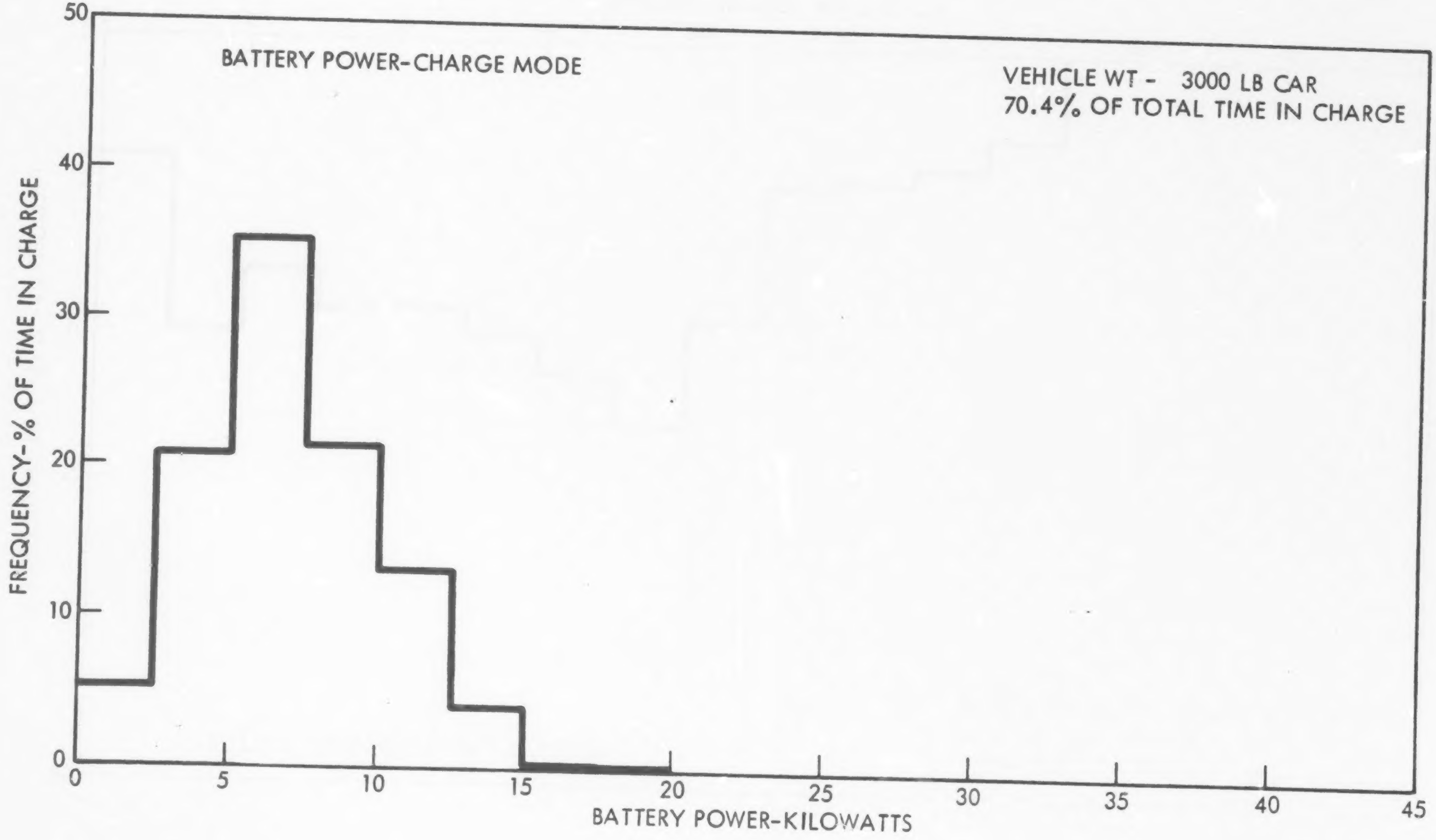
BATTERY POWER-CHARGE MODE
VEHICLE WT - 3000 LB CAR
70.4% OF TOTAL TIME IN CHARGE
FREQUENCY-% OF TIME IN CHARGE
0
10
20
30
40
50
0
5
10
15
20
25
30
35
40
45
BATTERY POWER-KILOWATTS

FIGURE 5.21

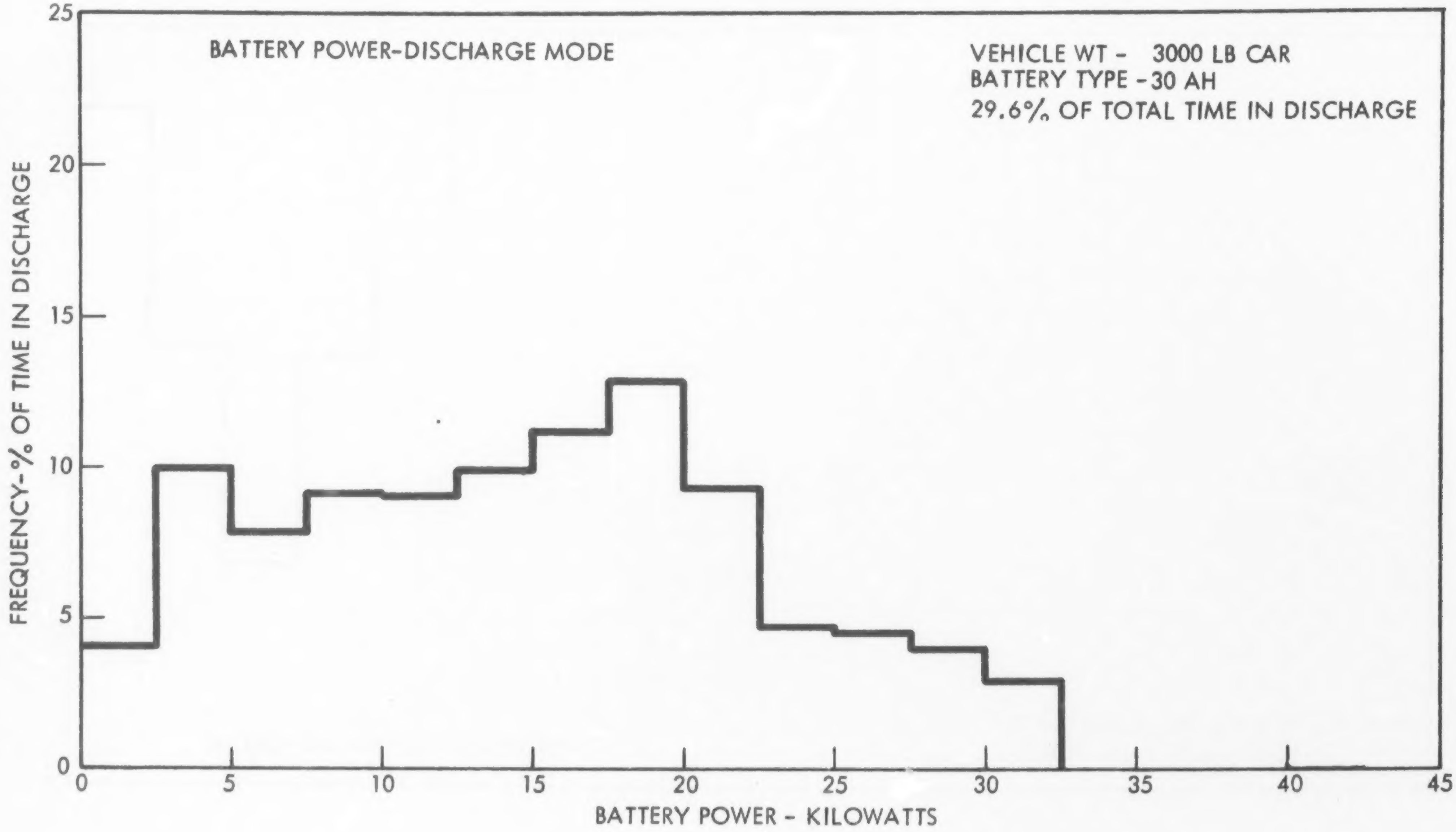
BATTERY POWER-DISCHARGE MODE
VEHICLE WT - 3000 LB CAR
BATTERY TYPE - 30 AH
29.6% OF TOTAL TIME IN DISCHARGE
FREQUENCY-% OF TIME IN DISCHARGE
25
20
15
10
5
0
0
5
10
15
20
25
30
35
40
45
BATTERY POWER - KILOWATTS

FIGURE 5.22

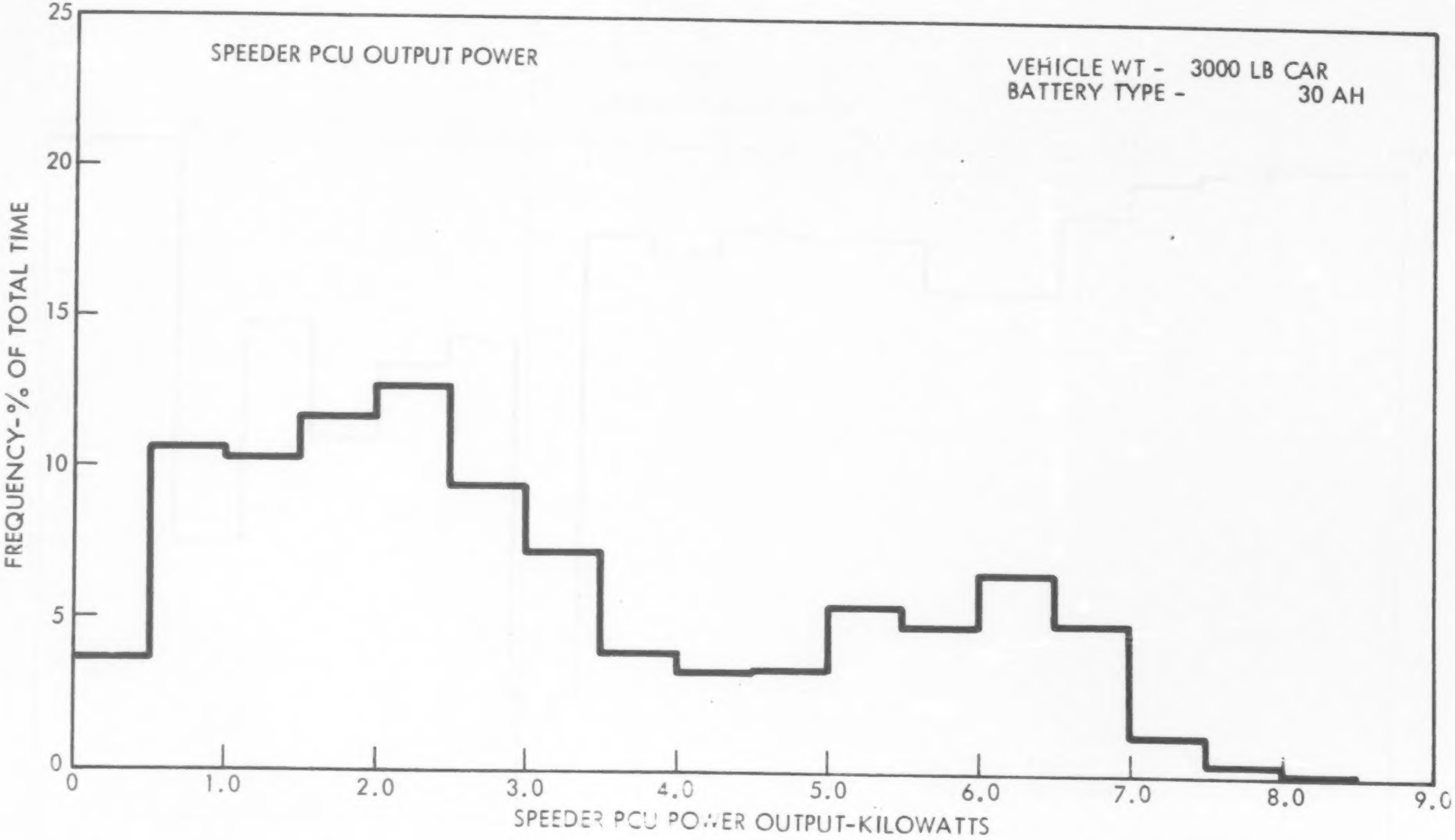
SPEEDER PCU OUTPUT POWER
VEHICLE WT - 3000 LB CAR
BATTERY TYPE - 30 AH
FREQUENCY-% OF TOTAL TIME
25
20
15
10
5
0
0
1.0
2.0
3.0
4.0
5.0
6.0
7.0
8.0
9.0
SPEEDER PCU POWER OUTPUT-KILOWATTS

FIGURE 5.23

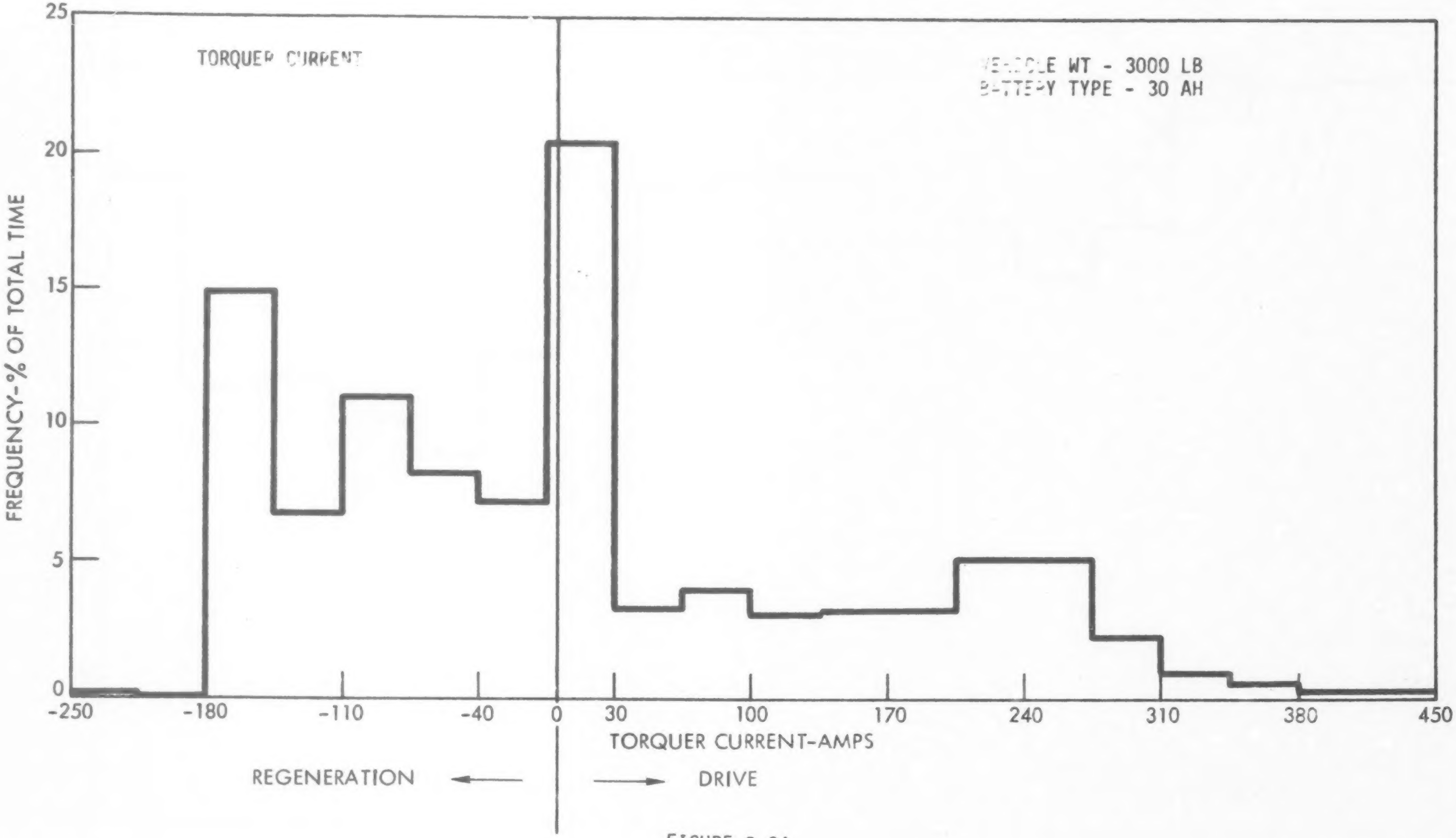
TORQUER CURRENT
VEHICLE WT - 3000 LB
BATTERY TYPE - 30 AH
FREQUENCY-% OF TOTAL TIME
25
20
15
10
5
0
-250
-180
-110
-40
0
30
100
170
240
310
380
450
TORQUER CURRENT-AMPS
REGENERATION
DRIVE

FIGURE 5.24

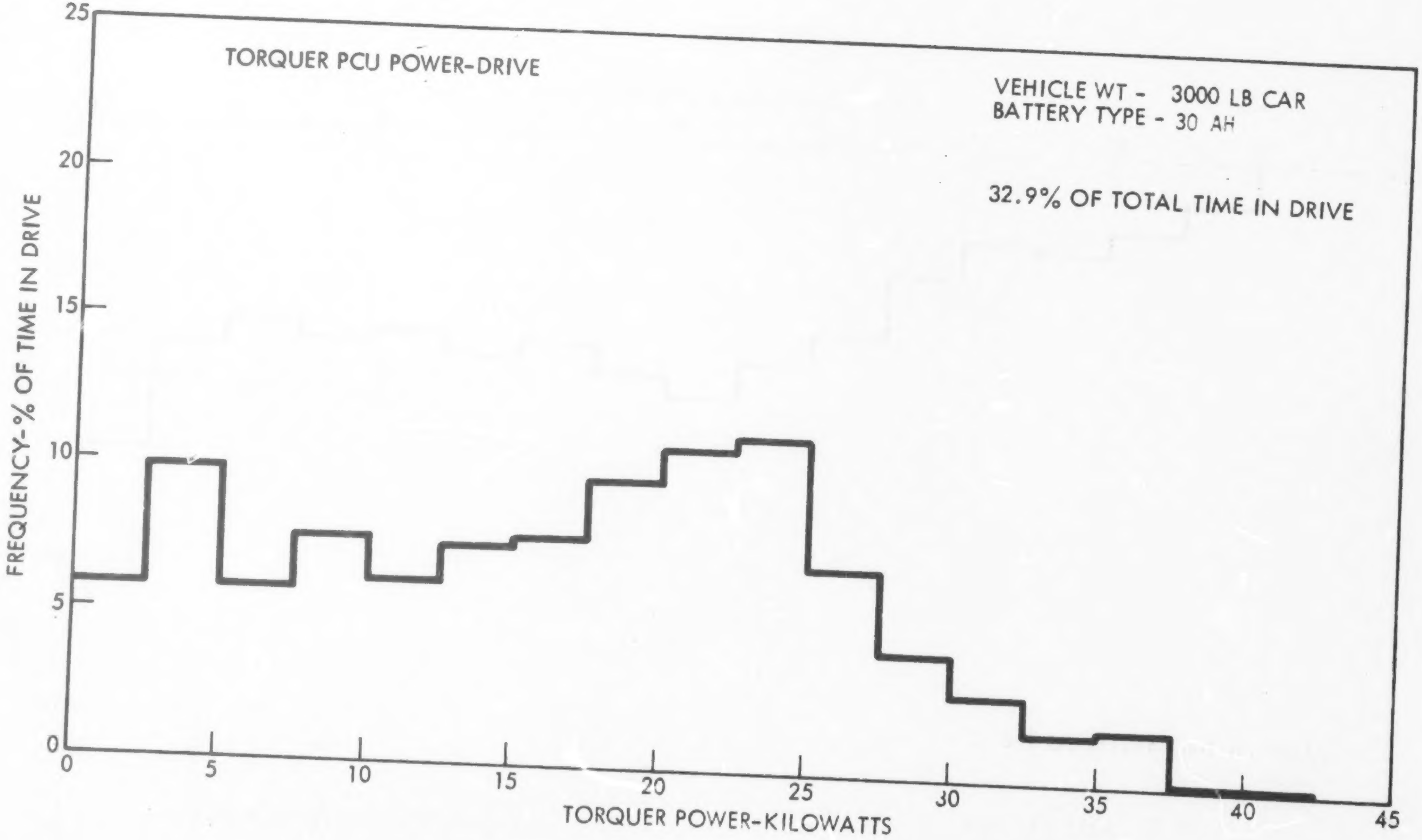
TORQUER PCU POWER-DRIVE
VEHICLE WT - 3000 LB CAR
BATTERY TYPE - 30 AH
32.9% OF TOTAL TIME IN DRIVE
FREQUENCY-% OF TIME IN DRIVE
0
5
10
15
20
25
0
5
10
15
20
25
30
35
40
45
TORQUER POWER-KILOWATTS

FIGURE 5.25

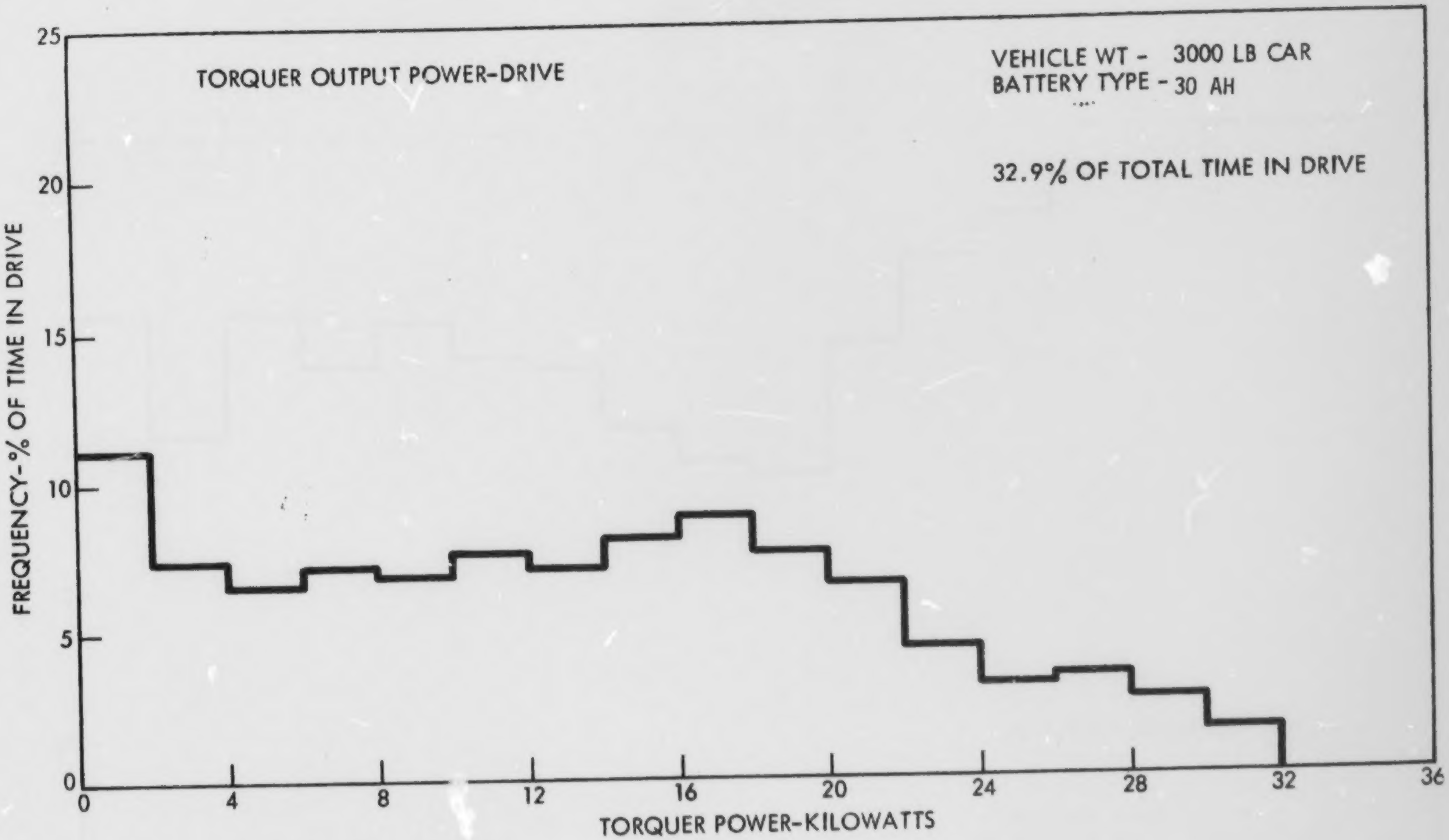
TORQUER OUTPUT POWER-DRIVE
VEHICLE WT - 3000 LB CAR
BATTERY TYPE - 30 AH
32.9% OF TOTAL TIME IN DRIVE
FREQUENCY-% OF TIME IN DRIVE
25
20
15
10
5
0
0
4
8
12
16
20
24
28
32
36
TORQUER POWER-KILOWATTS

FIGURE 5.26

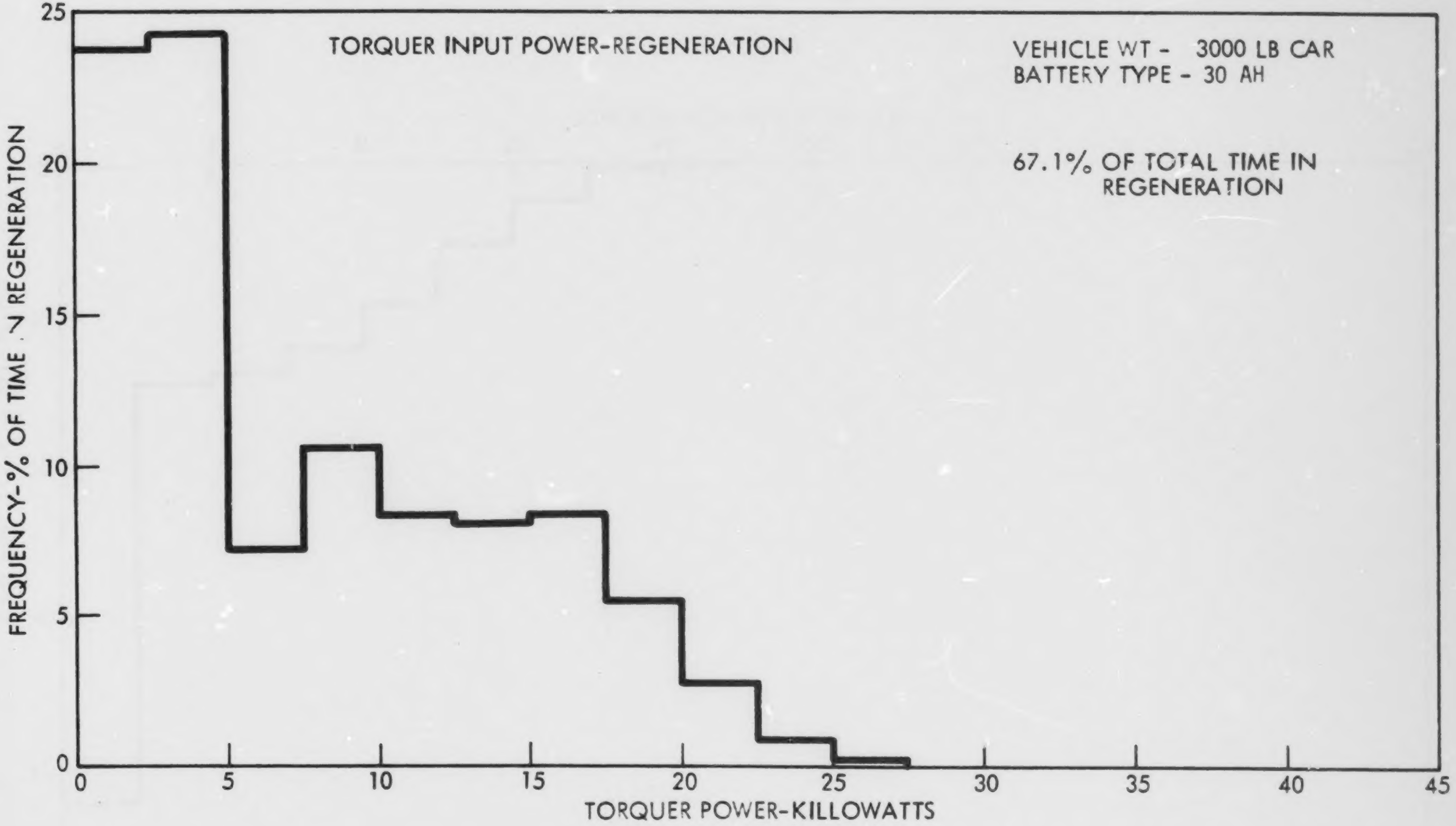
TORQUER INPUT POWER-REGENERATION
VEHICLE WT - 3000 LB CAR
BATTERY TYPE - 30 AH
67.1% OF TOTAL TIME IN REGENERATION
FREQUENCY-% OF TIME IN REGENERATION
0
5
10
15
20
25
0
5
10
15
20
25
30
35
40
45
TORQUER POWER-KILLOWATTS

FIGURE 5.27

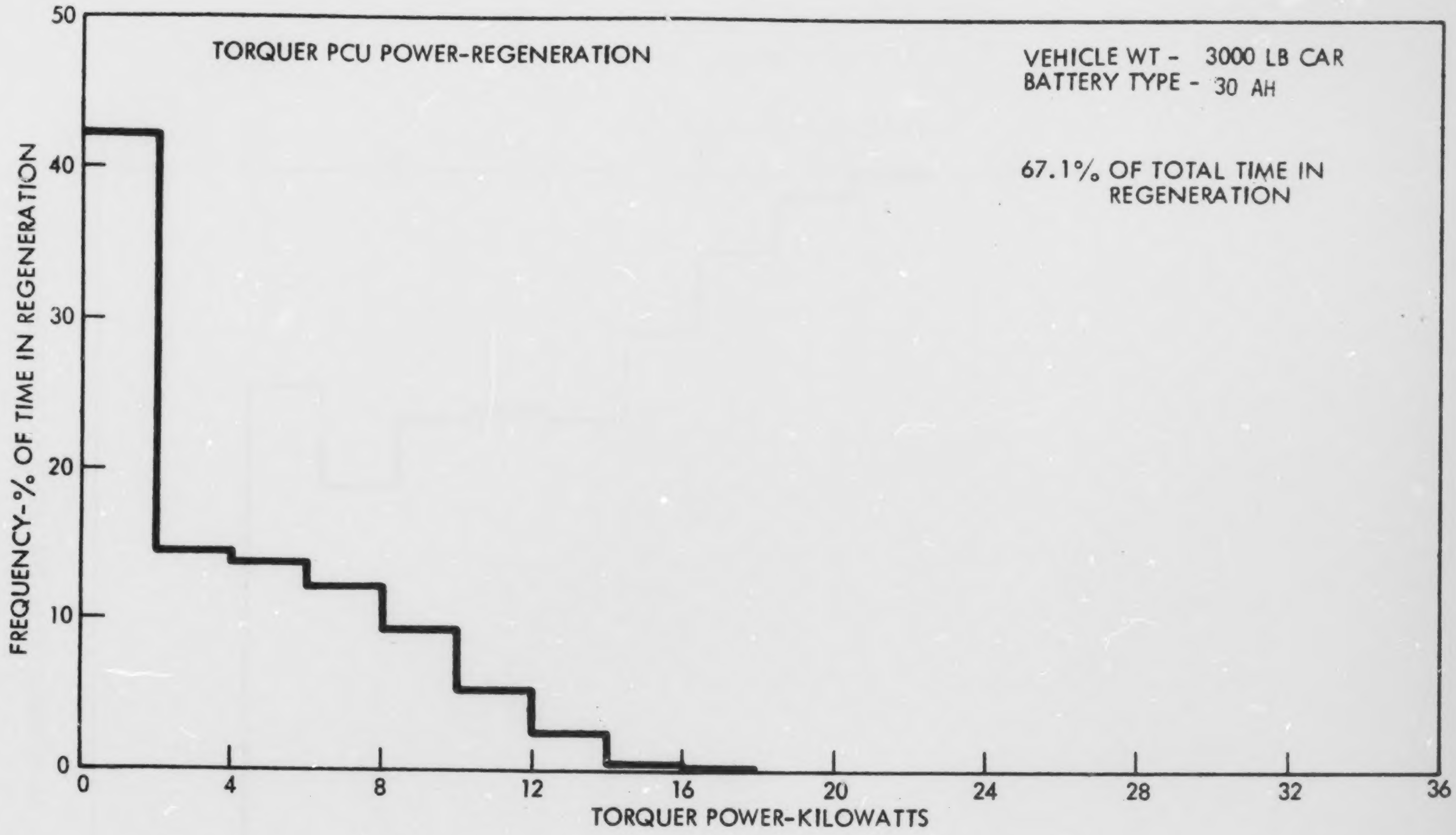
TORQUER PCU POWER-REGENERATION
VEHICLE WT - 3000 LB CAR
BATTERY TYPE - 30 AH
67.1% OF TOTAL TIME IN REGENERATION
FREQUENCY-% OF TIME IN REGENERATION
50
40
30
20
10
0
0
4
8
12
16
20
24
28
32
36
TORQUER POWER-KILOWATTS

FIGURE 5.28

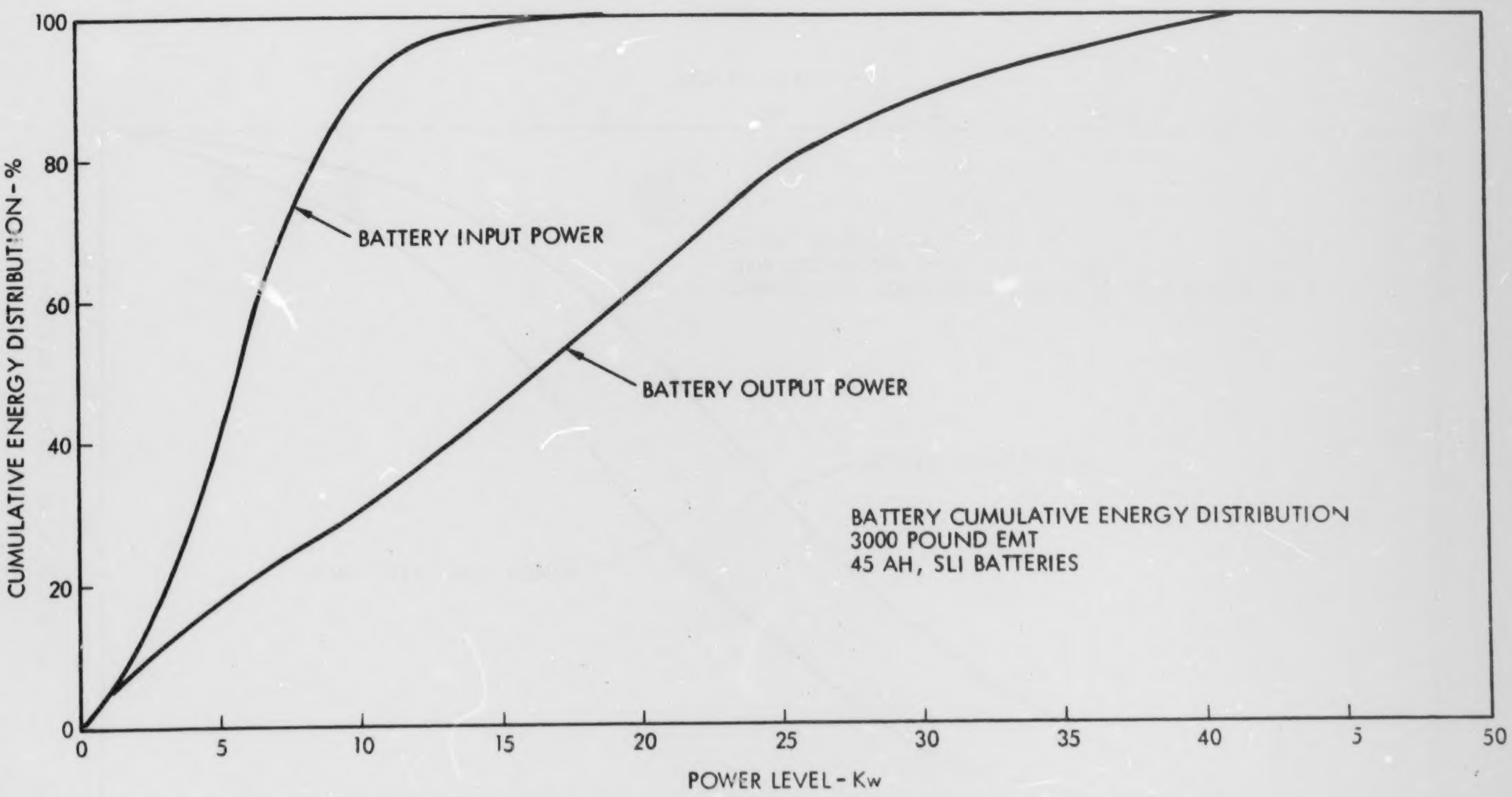
BATTERY INPUT POWER
BATTERY OUTPUT POWER
BATTERY CUMULATIVE ENERGY DISTRIBUTION
3000 POUND EMT
45 AH, SLI BATTERIES
CUMULATIVE ENERGY DISTRIBUTION - %
0
20
40
60
80
100
POWER LEVEL - Kw
0
5
10
15
20
25
30
35
40
5
50

FIGURE 5.29

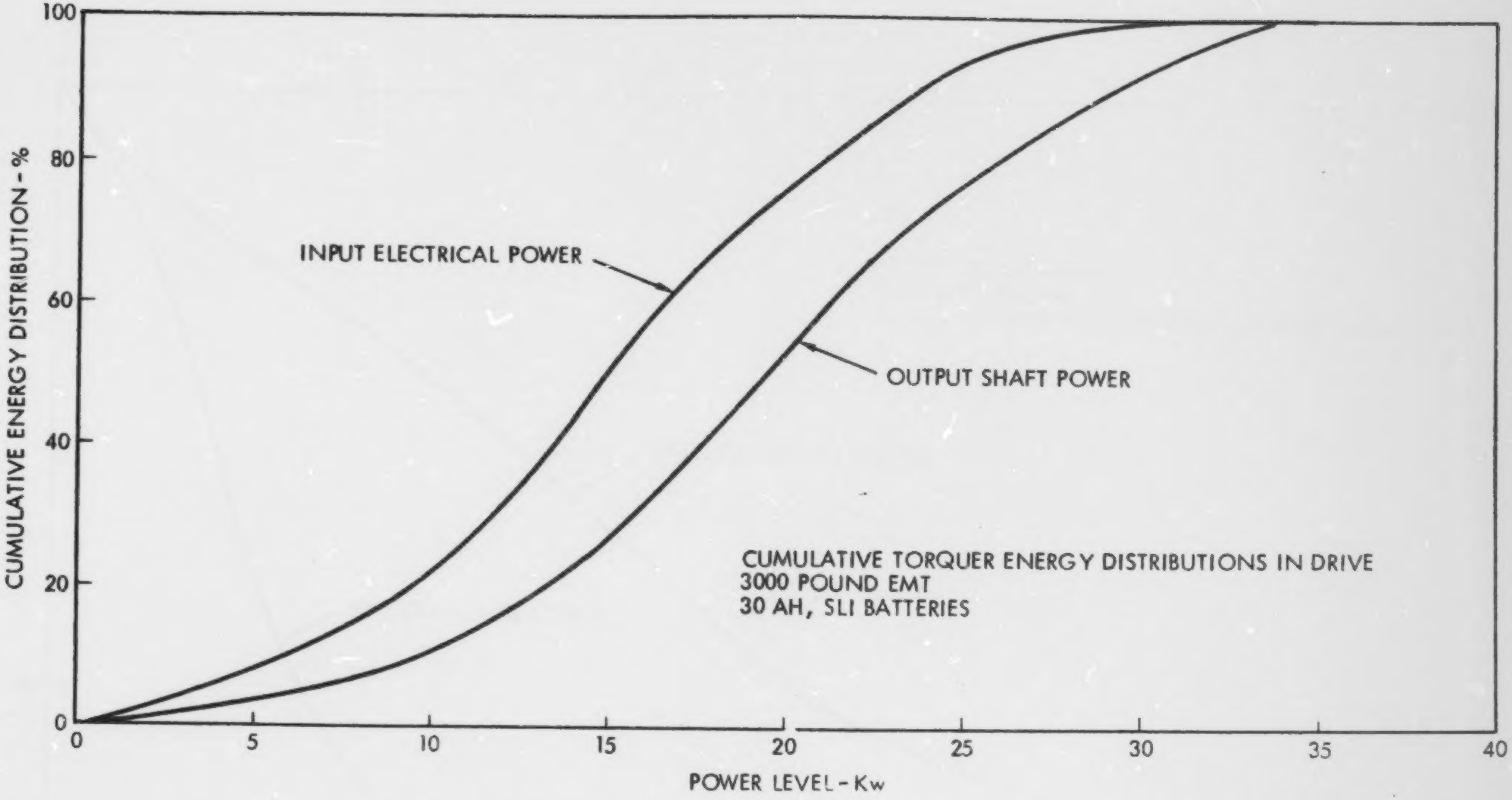
CUMULATIVE ENERGY DISTRIBUTION - %
0
20
40
60
80
100
INPUT ELECTRICAL POWER
OUTPUT SHAFT POWER
CUMULATIVE TORQUER ENERGY DISTRIBUTIONS IN DRIVE
3000 POUND EMT
30 AH, SLI BATTERIES
0
5
10
15
20
25
30
35
40
POWER LEVEL - Kw

FIGURE 5.30

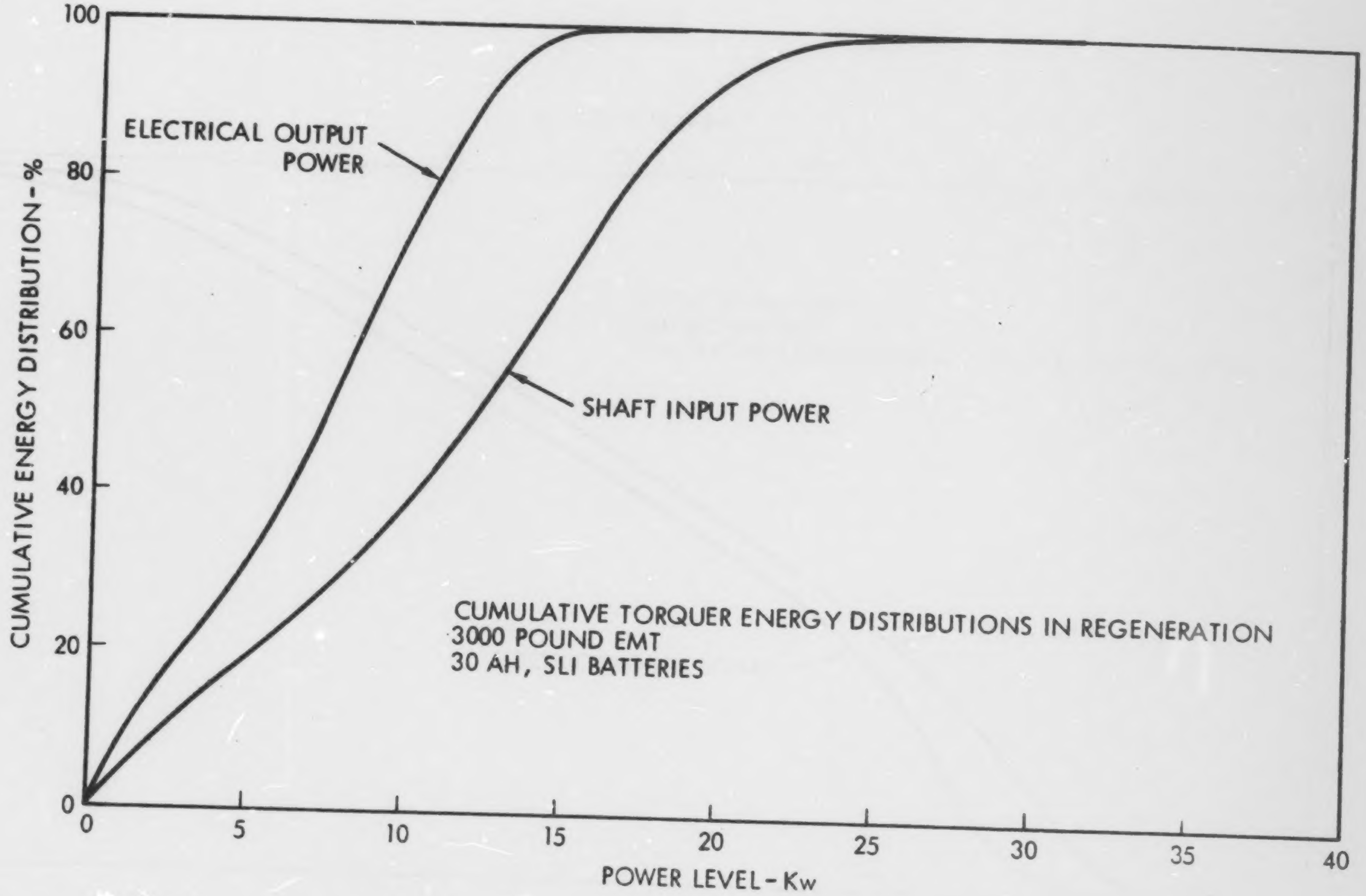

CUMULATIVE TORQUER ENERGY DISTRIBUTIONS IN REGENERATION
3000 POUND EMT
30 AH, SLI BATTERIES

FIGURE 5.31

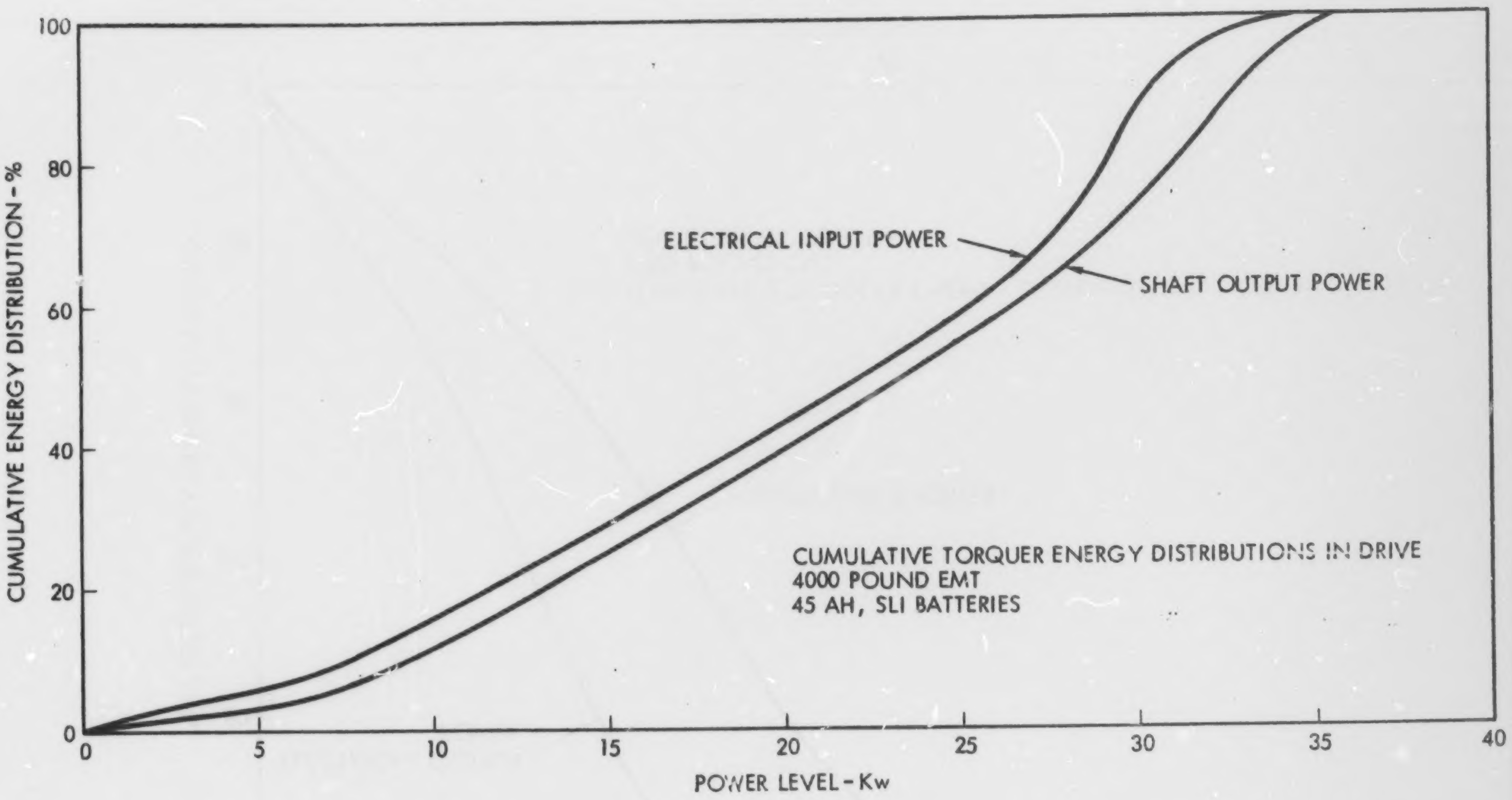
100
80
60
40
20
0
CUMULATIVE ENERGY DISTRIBUTION - %
0
5
10
15
20
25
30
35
40
POWER LEVEL - Kw
ELECTRICAL INPUT POWER
SHAFT OUTPUT POWER
CUMULATIVE TORQUER ENERGY DISTRIBUTIONS IN DRIVE
4000 POUND EMT
45 AH, SLI BATTERIES

FIGURE 5.32

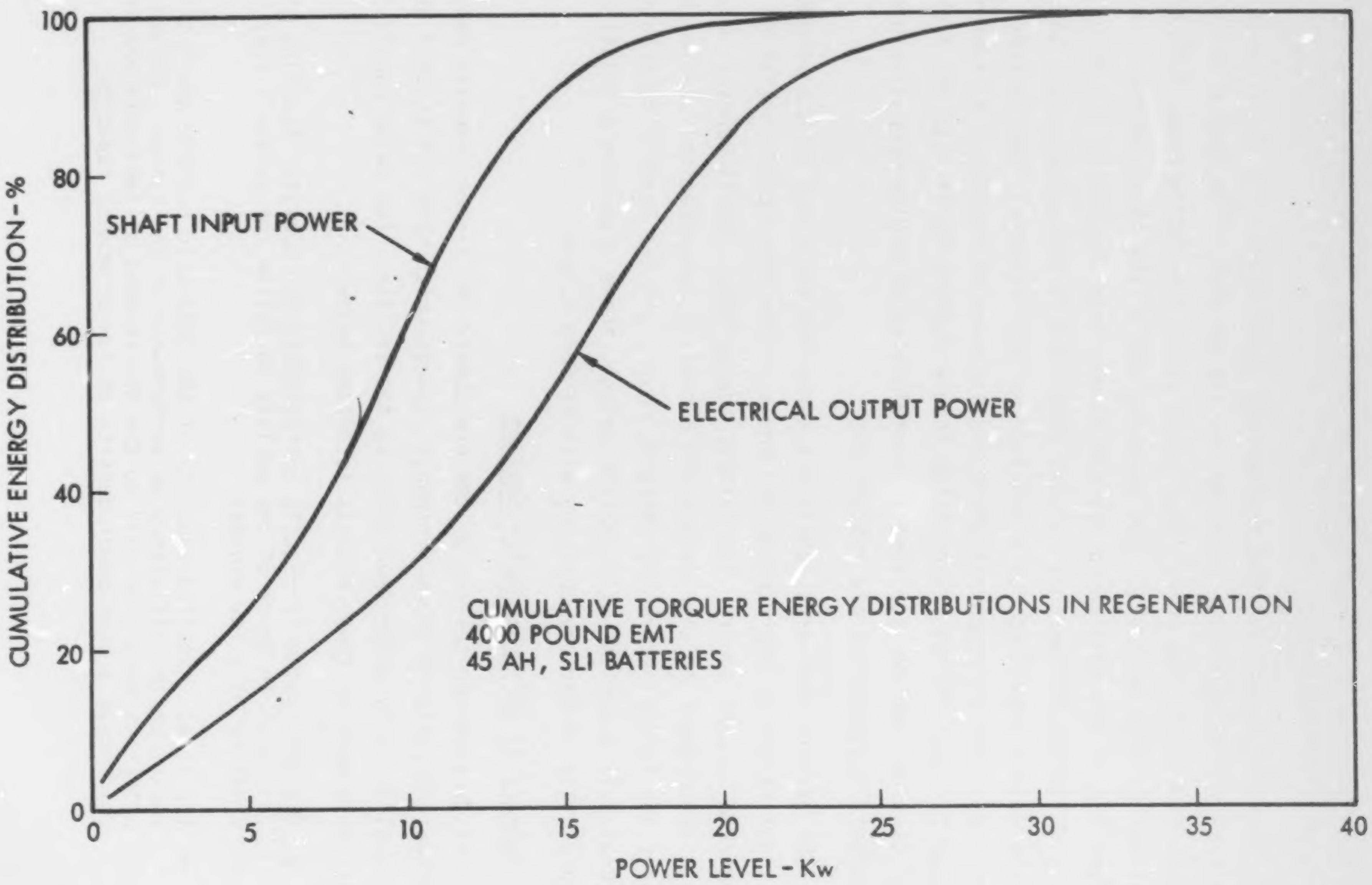

CUMULATIVE TORQUER ENERGY DISTRIBUTIONS IN REGENERATION
4000 POUND EMT
45 AH, SLI BATTERIES

FIGURE 5.33

The Torquer drive and regeneration distributions for several vehicle weights and batteries follow similar patterns as the battery charge and discharge distributions.

Table 5.3 summarizes the through-put power levels for the Torquer and batteries for an aggregate of three vehicle weights. The number in the columns represents the power level below which the indicated percent of the total energy flow occurred. For example, 50% of the total energy into the Torquer PCU of the 2000 pound vehicle flowed into the PCU at 8.5 kw or less. While the 50% and 90% Torquer power levels are proportional to vehicle weight (doubling for a two-fold weight increase), the Torquer power levels during regeneration do not increase as rapidly. As suggested previously, the limited regeneration torque command built into the operator pedal control, and the substantial contribution of engine-propeller power to Torquer regeneration are responsible.

The battery discharge levels are approximately equal to the Torquer PCU input values as expected on the basis of the small contribution of Speeder-to-Torquer power. The battery charge power levels however, bear little resemblence to the Torquer PCU output in regeneration. Since the Speeder and Torquer share the charging power, and the Speeder contribution is relatively invariant with vehicle weight, there should be a relative insensitivity of battery charging with vehicle weight.

## 5.8 Summary of EMT-Dynamometer Testing

The dynamometer testing of the breadboard EMT system revealed many important operational and performance aspects which were not evident or only qualitatively understood prior to the testing. The major conclusions relative to each of these aspects is listed below.

- The EMT system is readily controllable and operator learning time (at least in terms of the ability to follow the driver's aid) is a matter of a few minutes.
- The total installed capacity of the lead-acid battery has little impact on the efficiency or performance of the system. Rather, attention should be paid to the development of lead-acid batteries which have a high power density at low or modest capacity.

## TABLE 5.3 THROUGHPUT POWER LEVELS (KW) FOR THE TORQUER AND BATTERIES AS A FUNCTION OF VEHICLE WEIGHT ON THE LA-4 ROUTE

| Vehicle Weight | Torquer PCU Input-Drive | | Average Power KW | Torquer Shaft Output-Drive | | Average Power KW | Torquer Shaft Input-Regen. | | Average Power KW | Torquer PCU Output-Regen. | | Average Power KW | Battery Discharge | | Battery Charge | |
|---|---|---|---|---|---|---|---|---|---|---|---|---|---|---|---|---|
| | 50% | 90% | | 50% | 90% | | 50% | 90% | | 50% | 90% | | 50% | 90% | 50% | 90% |
| 2000 | 8.5 | 18.5 | 2.5 | 7.0 | 15.9 | 1.5 | 3.5 | 12.5 | 3.8 | 3.0 | 7.9 | 1.9 | 10.5 | 21.5 | 4.9 | 7.3 |
| 3000 | 14.5 | 32.5 | 4.1 | 10.8 | 25.6 | 3.0 | 4.8 | 16.5 | 4.1 | 2.8 | 9.6 | 2.1 | 13.8 | 30.3 | 6.5 | 11.5 |
| 4000 | 20.0 | 40.0 | 7.8 | 15.8 | 31.4 | 4.8 | 5.8 | 19.0 | 4.2 | 2.4 | 8.8 | 2.2 | 21.0 | 38.0 | 6.5 | 12.5 |

- The charging energy to the battery is split almost equally between the Speeder and the Torquer used as a generator. Improvements in both of these systems are equally important in terms of charge maintenance.

- The amount of energy delivered to the Torquer directly from the Speeder is presently a small portion of the total engine output. This is due to the large inefficiency of the planetary gearing and the Speeder system. With improvements in these latter sub-subsystems, the Torquer will be able to draw more energy directly from the engine path, and less will be demanded from the battery.

- Improvement in the gear box will allow a greater contribution of direct engine to wheel power thereby reducing the electrical traction demands and providing more energy for battery charging through Torquer generator action.

- To insure good controllability at low speeds in both drive and regeneration, the present Torquer system must utilize variable frequency operation. Methods for implementing the more desirable constant frequency system (see 2.2.2) should be explored.

- Component heating did not present any particular problems during the testing. The Speeder was the only device requiring a cooling fan and this requirement might be relaxed with a more efficient machine. The Torquer was not actively cooled but did run quite close to its rated temperature. Improvements in that machine's efficiency plus installation in the ram air environment of an automobile suggest auxiliary cooling may not be needed. The major power electronics of the breadboard equipment were cooled by natural convection. In a vehicle installation, the closer packaging might aggravate the cooling problem, but this is not expected to be severe.

- Battery thermal behavior was better than expected in that the battery temperature rise (in still air) was about 40-60°F/hour of operation for the smallest (30 A-H) batteries. With improved components requiring less battery drain and in a ram air environment battery cooling would not appear to be a major problem. Gassing losses in the batteries was small; the 30 A-H cells required weekly topping off based on a ten-to-twenty hours per week operating schedule. Typical charging currents are less than the 1C rate.

- There is a strong impact of battery behavior on the design of the electromechanical and electronic equipment. As the voltage stiffness of the battery is increased (lower internal impedance) commutation requirements, Speeder and Torquer losses are reduced and subsystem controllability is increased.

- Regenerative braking of the vehicle does not contribute substantially to charge maintenance. However, the high current battery loading associated with regenerative braking appears to provide a driving force necessary to prevent serious acid depletion in the pores of the plates.

- The electrical braking capability of the present EMT system did not adequately reflect the various vehicle weights explored. The operator pedal controls should be modified so that the maximum braking effort of the "accelerator pedal" is similar to that braking of conventional cars, while the brake pedal should control both the mechanical and electrical braking of the vehicle. In the latter case, the braking effort should be raised nearer to the maximum capability of the electronic/electromechanical components.

- The present Speeder is a relatively poor machine, with excessive windage and magnetic losses. A reduction in its peak speed of operation and a modification of motor construction and material would reduce some portion of these losses. Reduction of maximum speed will also reduce those losses internal to the gear box.

- The operation of the Torquer with a TRC controller introduces additional losses in the machine. Redesign of the machine to minimize these losses for EMT service is required.

## 6.0 ADVANCED DESIGN STUDY OF TORQUER SYSTEM

### 6.1 Torquer Drive System Analysis

A simplified schematic of the Torquer system is shown in Figure 6.1 Both drive and regeneration mode use essentially the same components and power control is based on the similar principles. Appendix A-2 presents the details of the analysis leading to the programming of the circuit equations on a digital computer. The analysis divides the total chopper period, T, into several subdivisions. The dynamic circuit equations for each interval are derived and integrated. The resulting equations for the current flow during each time interval contains several coefficients whose values are established through an iterative solution. Once a continuous current solution is found, the program computes the following information:

- the time from period initiation for the commutating SCR to turn on
- the time from period initiation for the commutating and power SCR to be turned off
- the time from period initiation for the commutating capacitor to discharge
- peak and average current in the machine
- power output of the battery
- ohmic losses in the battery
- losses in the commutating circuit of the PCU
- theoretical power output of the Torquer (average current times back emf)
- Torquer efficiency (theoretical power output/power output plus machine ohmic losses)
- overall Torquer system efficiency (theoretical power output/power output plus battery, PCU and machine ohmic losses)
- Fourier analysis of the Torquer current waveform

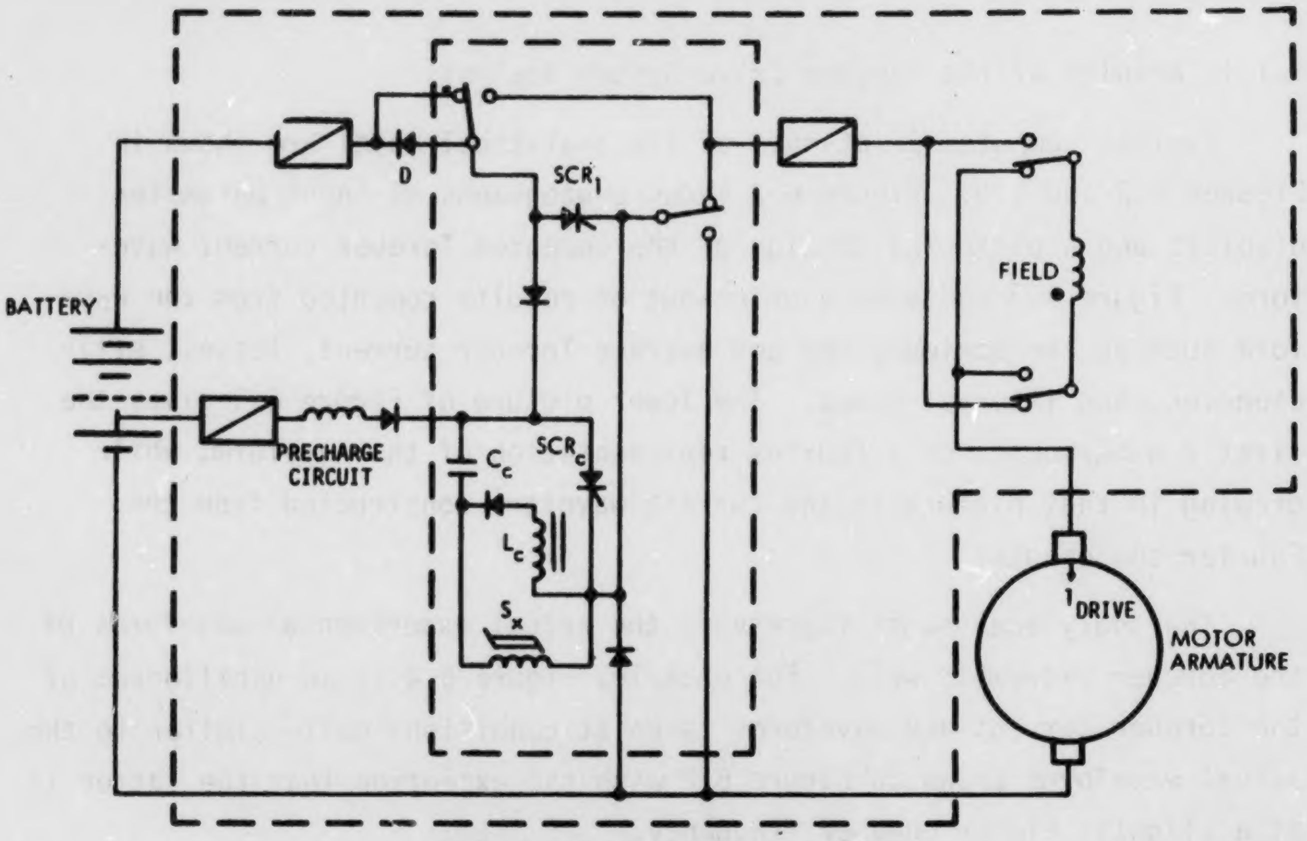
D
SCR₁
FIELD
BATTERY
PRECHARGE CIRCUIT
$C_c$
$SCR_c$
$L_c$
$S_x$
$I_{DRIVE}$
MOTOR ARMATURE

TORQUER SYSTEM IN DRIVE MODE

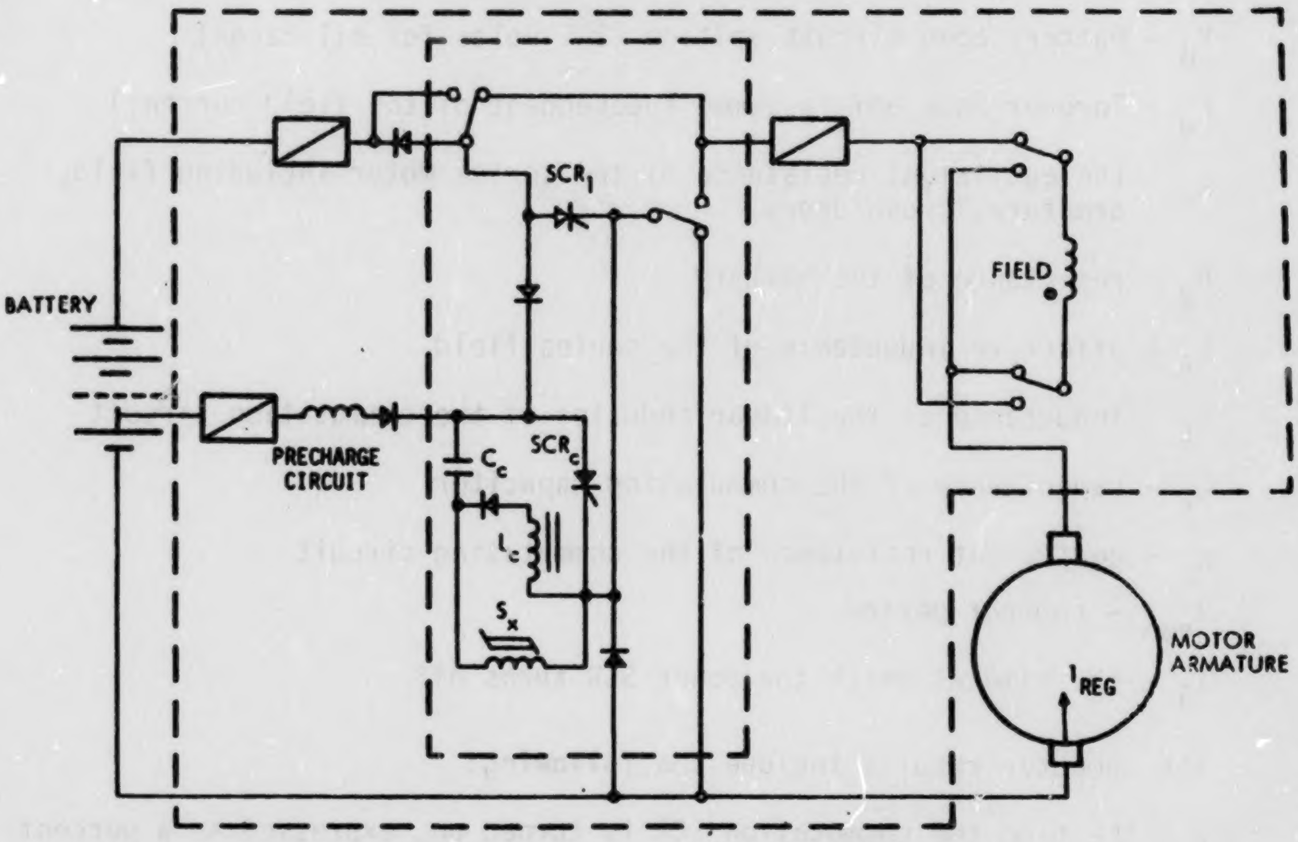
SCR₁
FIELD
BATTERY
PRECHARGE CIRCUIT
$C_c$
$SCR_c$
$L_c$
$S_x$
MOTOR ARMATURE
$I_{REG}$

FIGURE 6.1 TORQUER SYSTEM IN REGENERATION MODE

### 6.1.1 Results of the Torquer Drive System Analysis

Typical computer print-outs of the analytical model are shown in Figures 6.2 and 6.3. Figure 6.2 shows photographs of input parameter displays and a pictorial display of the computed Torquer current waveform. Figure 6.3 contains a print-out of results computed from the waveform such as the maximum, rms and average Torquer current, losses, efficiencies, and interval times. The lower picture of Figure 6.3 gives the first few harmonics of a Fourier representation of the waveform, while drawing in that picture is the current waveform constructed from the Fourier components.

The analytical model represents the actual experimental waveforms of the Torquer extremely well. For example, Figure 6.4 is an oscillogram of the Torquer current and waveforms taken at conditions quite similar to the actual waveforms shown in Figure 6.2 with the exception that the latter is at a slightly higher chopper frequency.

The program input variables consisted of:

$V_B$ - battery open circuit voltage (200 volts for all cases)

$E_g$ - Torquer back emf (assumed independent of the field current)

$R_m$ - the equivalent resistance of the series motor including field, armature, brush drops

$R_B$ - resistance of the battery

$L_A$ - effective inductance of the series field

$L_C$ - inductance of the linear inductor of the commutation circuit

$C_c$ - capacitance of the commutating capacitor

$R_c$ - equivalent resistance of the commutating circuit

$T_{max}$ - chopper period

$t_1$ - the time at which the power SCR turns off

The computer results include the following:

$\beta$ - the time the commutation SCR is turned on, expressed as a percent of the total period

TORQUER MODEL INPUT PARAMETERS

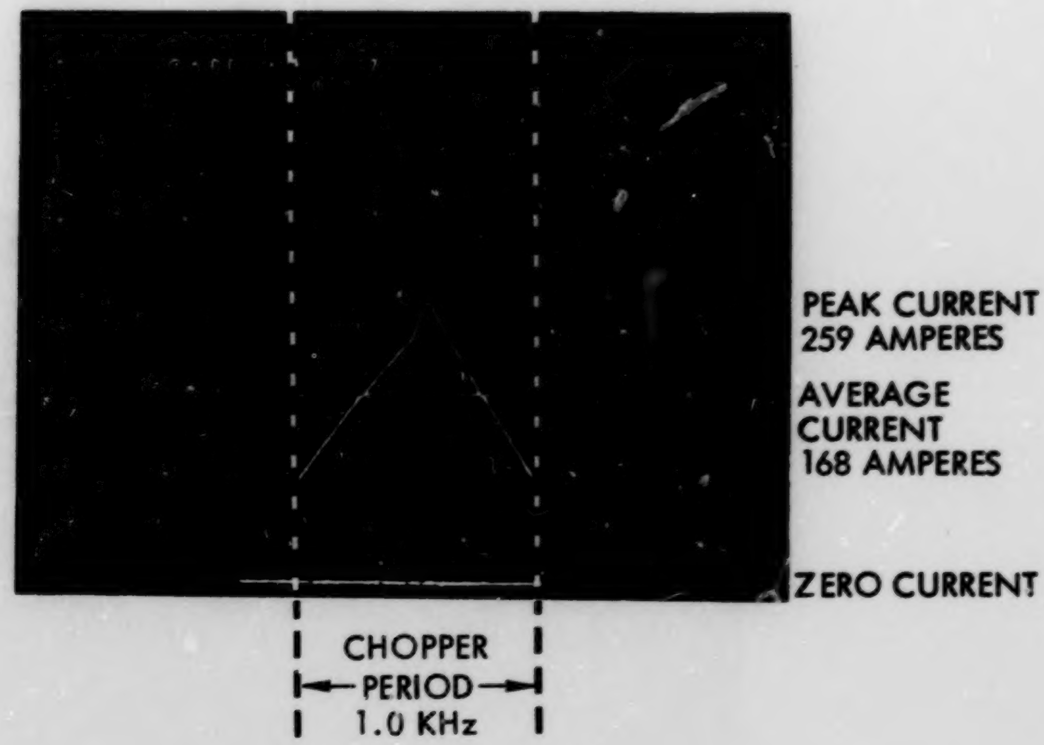

TORQUER CURRENT WAVEFORM SOLUTION

FIGURE 6.2
COMPUTER MODEL OF TORQUER SYSTEM

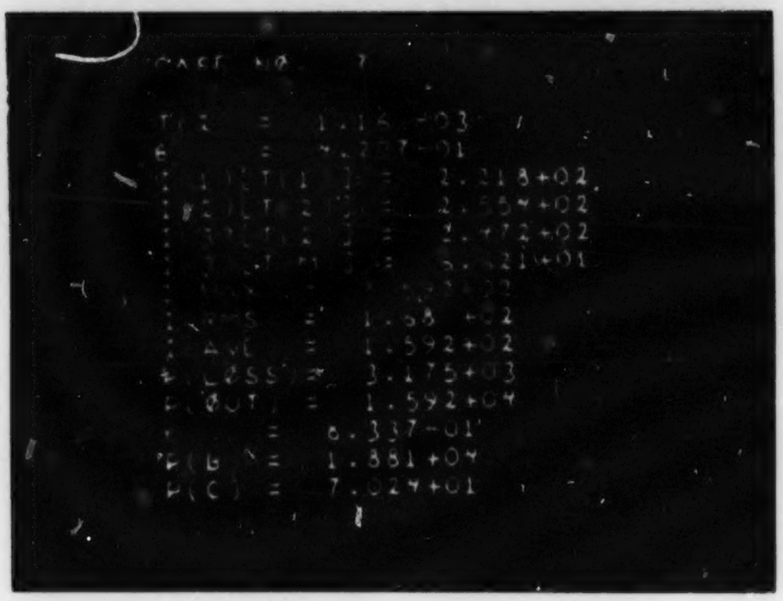

```
CASE NØ. [illegible]

T[illegible] = 1.16[illegible]+03
[illegible] = [illegible]-01
[illegible] = 2.[illegible]18+02
[illegible] = 2.55[illegible]+02
[illegible] = 2.[illegible]72+02
[illegible] = 5.[illegible]21+01
[illegible]
I RMS = 1.[illegible]68 +02
I AVE = 1.592+02
P(LØSS) = 3.175+03
P(ØUT) = 1.592+04
[illegible] = 6.337-01
P(B) = 1.881+04
P(C) = 7.024+01
```

TORQUER SYSTEM PERFORMANCE

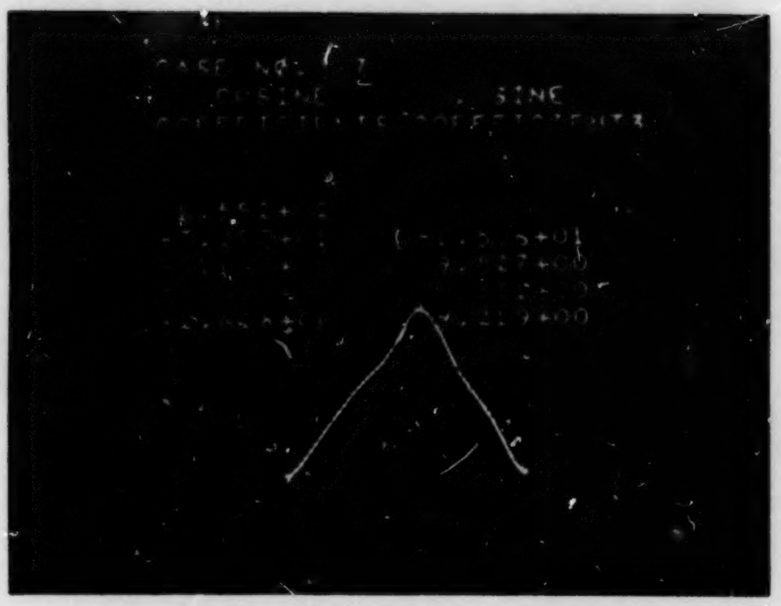

```
CASE NØ. 1
     COSINE          SINE
COEFFICIENTS   COEFFICIENTS
[illegible]
```

FOURIER COEFFICIENTS & RECONSTRUCTED CURRENT WAVEFORM

FIGURE 6.3
NUMERICAL PRINT-OUT OF TORQUER SYSTEM ANALYSIS

VEHICLE SPEED - 30 MPH
TORQUER SPEED - 1/2 RATED

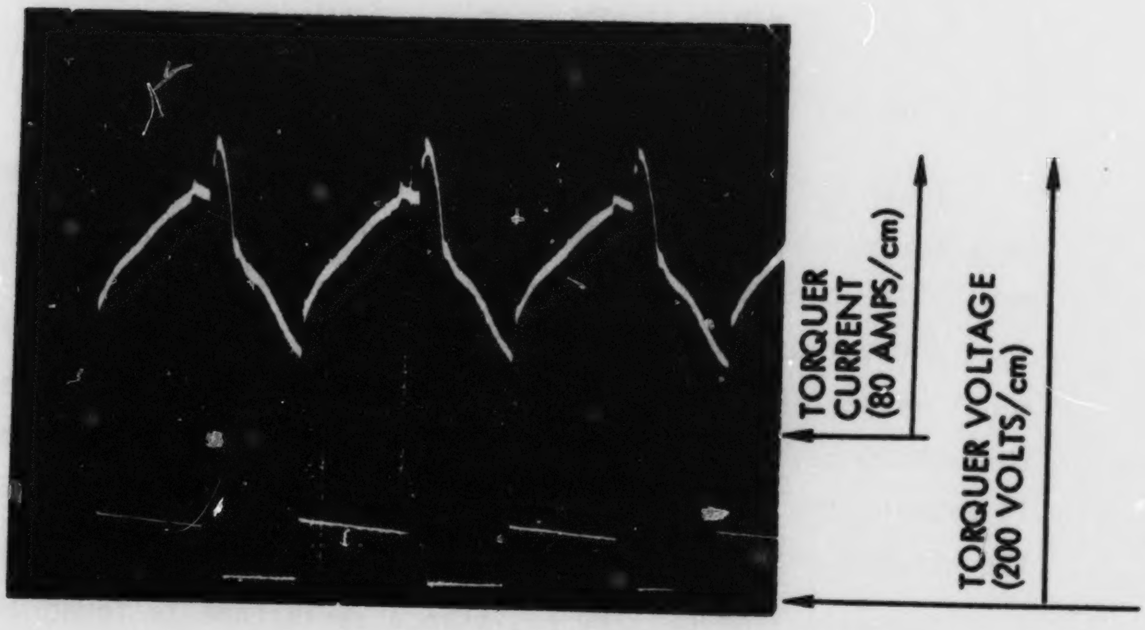

AVERAGE CURRENT - 166 AMPERES
PEAK CURRENT - 280 AMPERES
CHOPPER PERIOD - 750 Hz

FIGURE 6.4

$I_{max}$ - maximum armature current

$I_{RMS}$ - root mean squared armature current

$I_{ave}$ - average armature current

Form Factor - $I_{RMS}/I_{ave}$

$P_{ohmic}$ - total power loss in battery, Torquer and commutation circuit

$P_{out}$ - theoretical power output of motor, $E_g \, I_{ave}$

$\eta_{theoret} - \dfrac{P_{out}}{P_{out} + P_{ohmic}}$

Table 6.2 presents data on the system for various parameter changes at a Torquer back emf of 100 volts (approximately 1/2 rated speed or 30 mph). The parameter values selected represent those of the present equipment and variations about the nominal levels. Columns 1 through 5 have equal parameter values except for varying battery resistance. Columns 6 through 10 have varying inductance in the armature, while columns 11 through 14 examine the effect of changing duty cycle. In columns 15, 16 and 17 the chopper period is changed.

The effect of battery resistance variations is found in Figure 6.5. The figure shows that variation in resistance has little effect on overall system efficiency. However, this result is misleading since decreasing resistance increases the average machine current and increases the power output of the machine. For equal torque output, the duty cycle must be increased with increasing battery resistance and efficiency falls. Note also the relative influence of battery resistance must be duty cycle dependent. At very low duty cycle, the battery is connected to the machine for only a small fraction of the time and the ohmic losses in the armature predominate. At high duty cycles, the battery resistance is in the circuit more often and may outweigh armature resistance losses.

## TABLE 6.2

### ANALYSIS OF TORQUER SYSTEM PARAMETER INFLUENCE

| Run Number | 1 | 2 | 3 | 4 | 5 | 6 | 7 | 8 | 9 | 10 | 11 | 12 | 13 | 14 | 15 | 16 | 17 |
|---|---|---|---|---|---|---|---|---|---|---|---|---|---|---|---|---|---|
| $V_B$(volts) | 200 | 200 | 200 | 200 | 200 | 200 | 200 | 200 | 200 | 200 | 200 | 200 | 200 | 200 | 200 | 200 | 200 |
| $E_g$(volts) | 100 | 100 | 100 | 100 | 100 | 100 | 100 | 100 | 100 | 100 | 100 | 100 | 100 | 100 | 100 | 100 | 100 |
| $R_m$(ohm) | 0.05 | 0.05 | 0.05 | 0.05 | 0.05 | 0.05 | 0.05 | 0.05 | 0.05 | 0.05 | 0.05 | 0.05 | 0.05 | 0.05 | 0.05 | 0.05 | 0.05 |
| $R_B$(ohm) | 0.05 | 0.01 | 0.15 | 0.10 | 0.20 | 0.10 | 0.10 | 0.10 | 0.10 | 0.10 | 0.10 | 0.10 | 0.10 | 0.10 | 0.10 | 0.10 | 0.10 |
| $L_A$(henry) | $2x10^{-3}$ | $2x10^{-3}$ | $2x10^{-3}$ | $2x10^{-3}$ | $2x10^{-3}$ | $10^{-4}$ | $5x10^{-4}$ | $1x10^{-3}$ | $2x10^{-3}$ | $5x10^{-3}$ | $1x10^{-3}$ | $1x10^{-3}$ | $1x10^{-3}$ | $1x10^{-3}$ | $5x10^{-4}$ | $5x10^{-4}$ | $5x10^{-4}$ |
| $L_c$(henry) | $2x10^{-5}$ | $2x10^{-5}$ | $2x10^{-5}$ | $2x10^{-5}$ | $2x10^{-5}$ | $2x10^{-5}$ | $2x10^{-5}$ | $2x10^{-5}$ | $2x10^{-5}$ | $2x10^{-5}$ | $2x10^{-5}$ | $2x10^{-5}$ | $2x10^{-5}$ | $2x10^{-5}$ | $2x10^{-5}$ | $2x10^{-5}$ | $2x10^{-5}$ |
| $C_c$(farad) | $10^{-4}$ | $10^{-4}$ | $10^{-4}$ | $10^{-4}$ | $10^{-4}$ | $10^{-4}$ | $10^{-4}$ | $10^{-4}$ | $10^{-4}$ | $10^{-4}$ | $10^{-4}$ | $10^{-4}$ | $10^{-4}$ | $10^{-4}$ | $10^{-4}$ | $10^{-4}$ | $10^{-4}$ |
| $R_c$(ohm) | 0.01 | 0.01 | 0.01 | 0.01 | 0.01 | 0.01 | 0.01 | 0.01 | 0.01 | 0.01 | 0.01 | 0.01 | 0.01 | 0.01 | 0.01 | 0.01 | 0.01 |
| $T_{max}$(sec) | $2x10^{-3}$ | $2x10^{-3}$ | $2x10^{-3}$ | $2x10^{-3}$ | $2x10^{-3}$ | $2x10^{-3}$ | $2x10^{-3}$ | $2x10^{-3}$ | $2x10^{-3}$ | $2x10^{-3}$ | $1x10^{-3}$ | $1x10^{-3}$ | $1x10^{-3}$ | $1x10^{-3}$ | $1x10^{-3}$ | $1.25x10^{-3}$ | $2.5x10^{-3}$ |
| $T_1$(sec) | $1x10^{-3}$ | $1x10^{-3}$ | $1x10^{-3}$ | $1x10^{-3}$ | $1x10^{-3}$ | $1x10^{-3}$ | $1x10^{-3}$ | $1x10^{-3}$ | $1x10^{-3}$ | $1x10^{-3}$ | $2x10^{-4}$ | $4x10^{-4}$ | $6x10^{-4}$ | $6x10^{-4}$ | $5x10^{-4}$ | $6.25x10^{-4}$ | $1.25x10^{-3}$ |
| $\alpha$ (%) | 50 | 50 | 50 | 50 | 50 | 50 | 50 | 50 | 50 | 50 | 20 | 40 | 50 | 80 | 50 | 50 | 50 |
| $\beta$ (%) | 43 | 43 | 43 | 43 | 43 | 43 | 43 | 43 | 43 | 43 | 5.95 | 25.95 | 45.95 | 65.95 | 35.95 | 38.76 | 44.38 |
| $I_{max}$(amp) | 243 | 287 | 202.4 | 224.3 | 184.6 | 598.5 | 259.2 | 227.1 | 224.3 | 200.6 | 135.1 | 227.1 | 419.6 | 588.7 | 315 | 299 | 284 |
| $I_{rms}$(amp) | 217.8 | 261.6 | 180 | 201.2 | 162.4 | 319.5 | 168 | 179.1 | 201.2 | 190.7 | 108.8 | 201.7 | 399.3 | 576.8 | 266 | 240 | 175 |
| $I_{Ave}$(amp) | 217.4 | 261.2 | 179.6 | 200.8 | 162 | 253.6 | 159.2 | 177.1 | 200.8 | 190.6 | 107.3 | 201.1 | 399.2 | 576.8 | 265 | 238 | 162 |
| Form Factor | 1.0 | 1.0 | 1.0 | 1.0 | 1.0 | 1.26 | 1.06 | 1.01 | 1.00 | 1.00 | 1.01 | 1.00 | 1.00 | 1.0 | 1.0 | 1.01 | 1.08 |
| $P_{ohmic}$(kw) | 3.83 | 3.89 | 4.59 | 4.48 | 4.59 | 13.16 | 3.18 | 3.59 | 448 | 4.08 | 1.39 | 4.54 | 19.16 | 45.63 | 8.17 | 6.53 | 3.29 |
| $P_{out}$(kw) | 21.74 | 26.12 | 17.96 | 20.1 | 16.2 | 25.36 | 15.92 | 17.71 | 20.1 | 19.06 | 10.73 | 20.11 | 39.92 | 57.68 | 26.51 | 23.82 | 16.23 |
| $\eta = \frac{P_{out}}{P_{out}+P_{ohmic}}$ % | 85 | 87.1 | 29.6 | 81.8 | 77.91 | 65.8 | 83.4 | 83.20 | 81.8 | 82.4 | 88.5 | 81.6 | 67.56 | 55.82 | 76.4 | 78.48 | 83.15 |

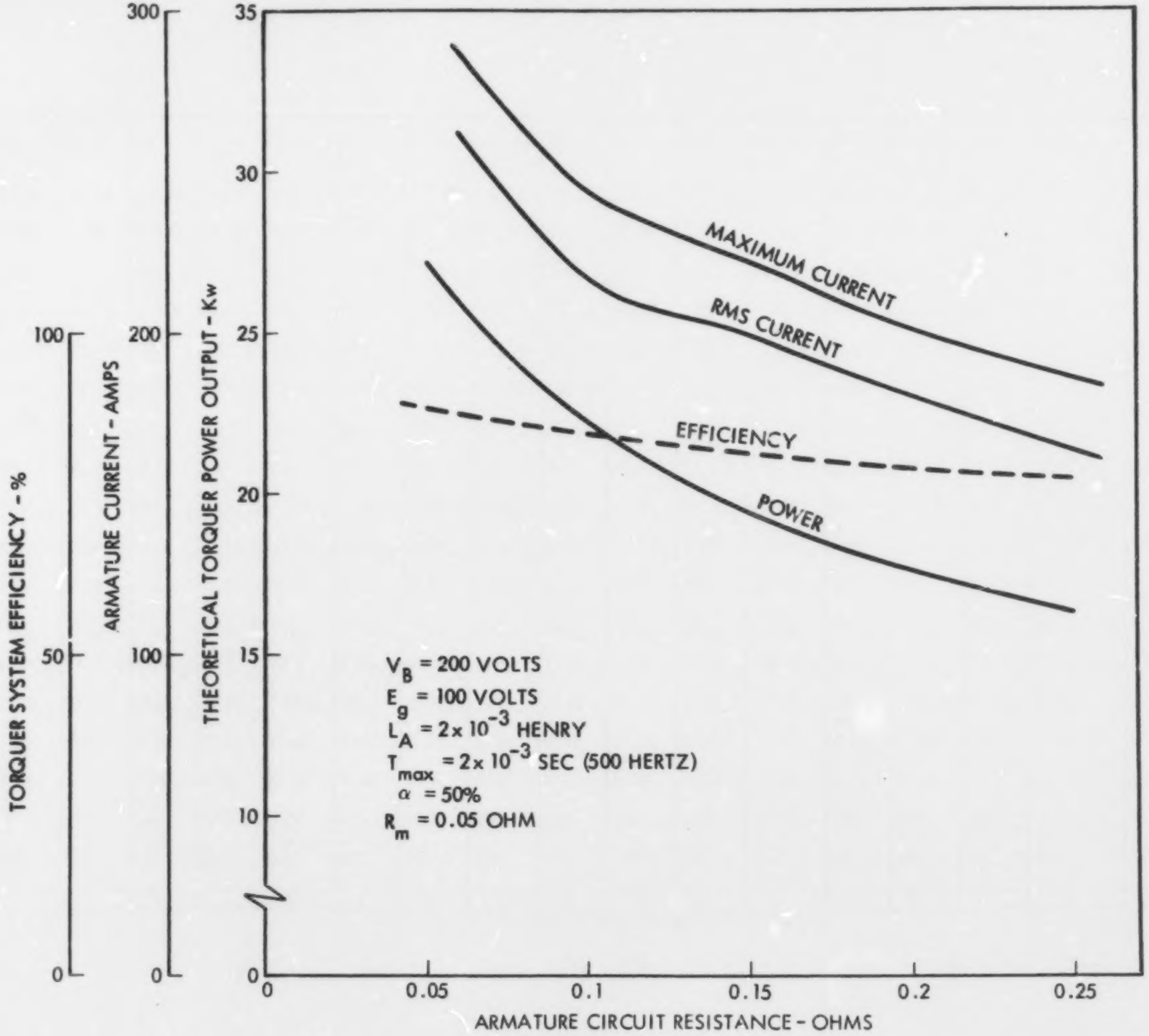

FIGURE 6.5
ARMATURE CURRENT & EFFICIENCY AS A FUNCTION OF
BATTERY RESISTANCE

Figure 6.6 shows the effect of armature circuit inductance on theoretical power, efficiencies and form factor. At low inductance levels, the current in the inductor is not strongly opposed by the $L \frac{di}{dt}$ of the inductor and the peak current is limited only by the resistance of the battery-machine circuit. A large amount of power is transferred but at poor form factor and low efficiency. As the inductance increases, the form factor and efficiency improve, but the peak and average current are reduced. Further inductance increases beyond $10^{-3}$ henrys do not substantially affect the system's performance. As the current variations decrease, power drawn from the battery is utilized more efficiently giving rise to a higher average power and current in the machine. In contrast to this, the increased current level increases ohmic losses with a slight degradation of overall efficiency.

The above observations do not take into account hysteresis and eddy losses. Table 6.3 presents the first three Fourier components of the current waveforms associated with the various inductance levels. Examining the magnitude of the sine and cosine vectors ($c_m$'s), demonstrates the rapid decrease in harmonic content with increasing inductance. In Section 7.2 it is suggested that the hysteresis and eddy current losses are related to the flux density and frequency of operation. Using relations cited in that section, one would predict that the eddy losses of the fundamental using the $5 \times 10^{-3}$ henry inductor would be $(\frac{7.3}{268})^2$ that of the $10^{-4}$ henry inductor. Hysteresis loss reduction would also occur, although the amount would be a function of the exponent of the hysteresis function of Section 7.2.

Figure 6.7 shows the effect of increasing duty cycle on the system. As expected, increased power SCR on-time increases the power output of the system. However, as the current levels increase the system ohmic losses also increase and system efficiency degrades.

Figure 6.8 shows the effect of chopper frequency on system behavior. In the Torquer (as well as the Speeder) the electromagnetic torque is proportional to the average armature current. For conditions of constant average current, the form factor increases as the frequency is decreased, and ohmic losses in the copper conductors increase. Hysteresis losses associated with the flux variations in the magnetic paths also increase

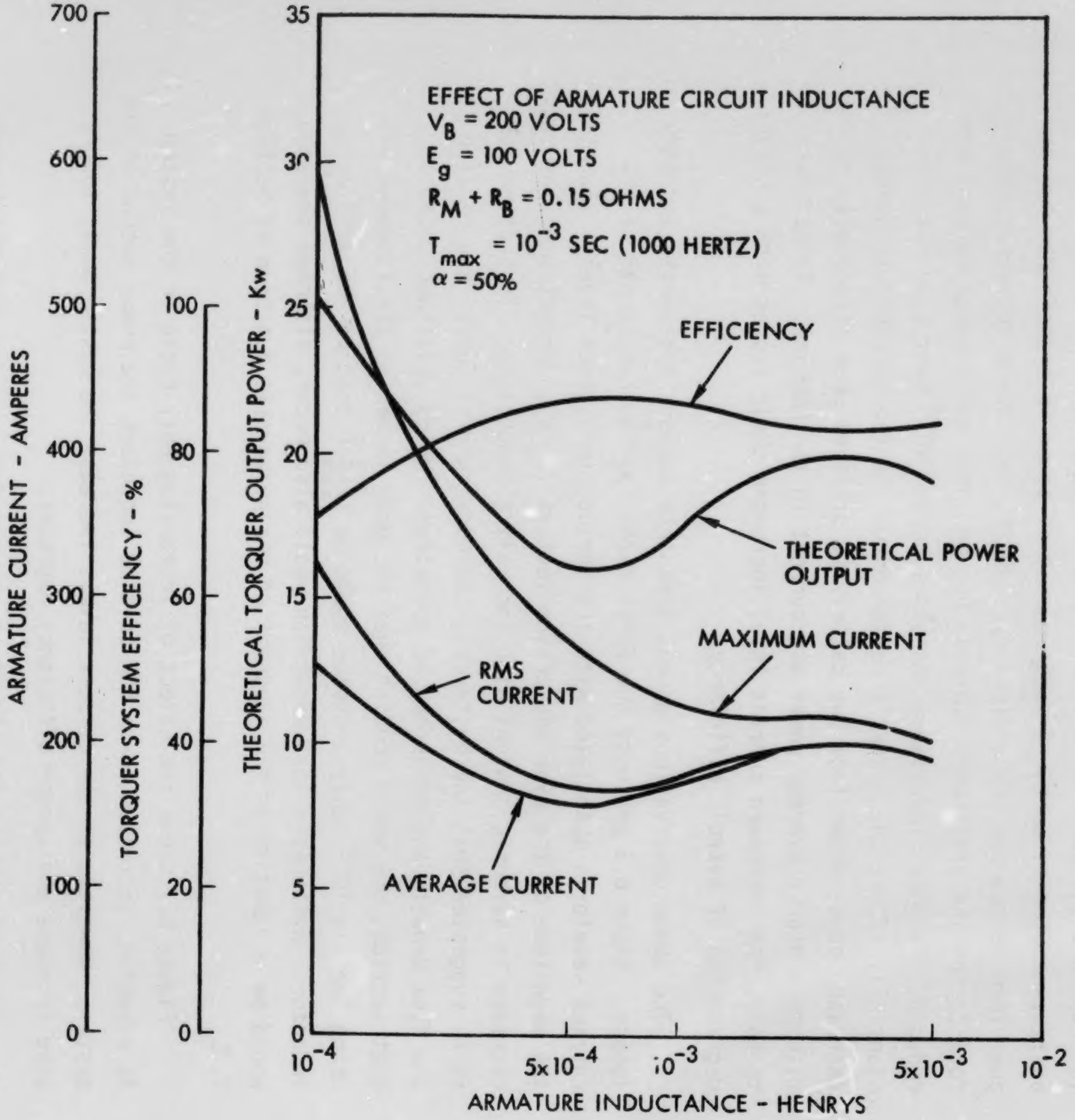
EFFECT OF ARMATURE CIRCUIT INDUCTANCE
$V_B$ = 200 VOLTS
$E_g$ = 100 VOLTS
$R_M + R_B$ = 0.15 OHMS
$T_{max}$ = $10^{-3}$ SEC (1000 HERTZ)
$\alpha$ = 50%
EFFICIENCY
THEORETICAL POWER OUTPUT
MAXIMUM CURRENT
RMS CURRENT
AVERAGE CURRENT
ARMATURE CURRENT - AMPERES
0
100
200
300
400
500
600
700
TORQUER SYSTEM EFFICENCY - %
0
20
40
60
80
100
THEORETICAL TORQUER OUTPUT POWER - Kw
0
5
10
15
20
25
30
35
$10^{-4}$
$5\times10^{-4}$
$10^{-3}$
$5\times10^{-3}$
$10^{-2}$
ARMATURE INDUCTANCE - HENRYS

FIGURE 6.6

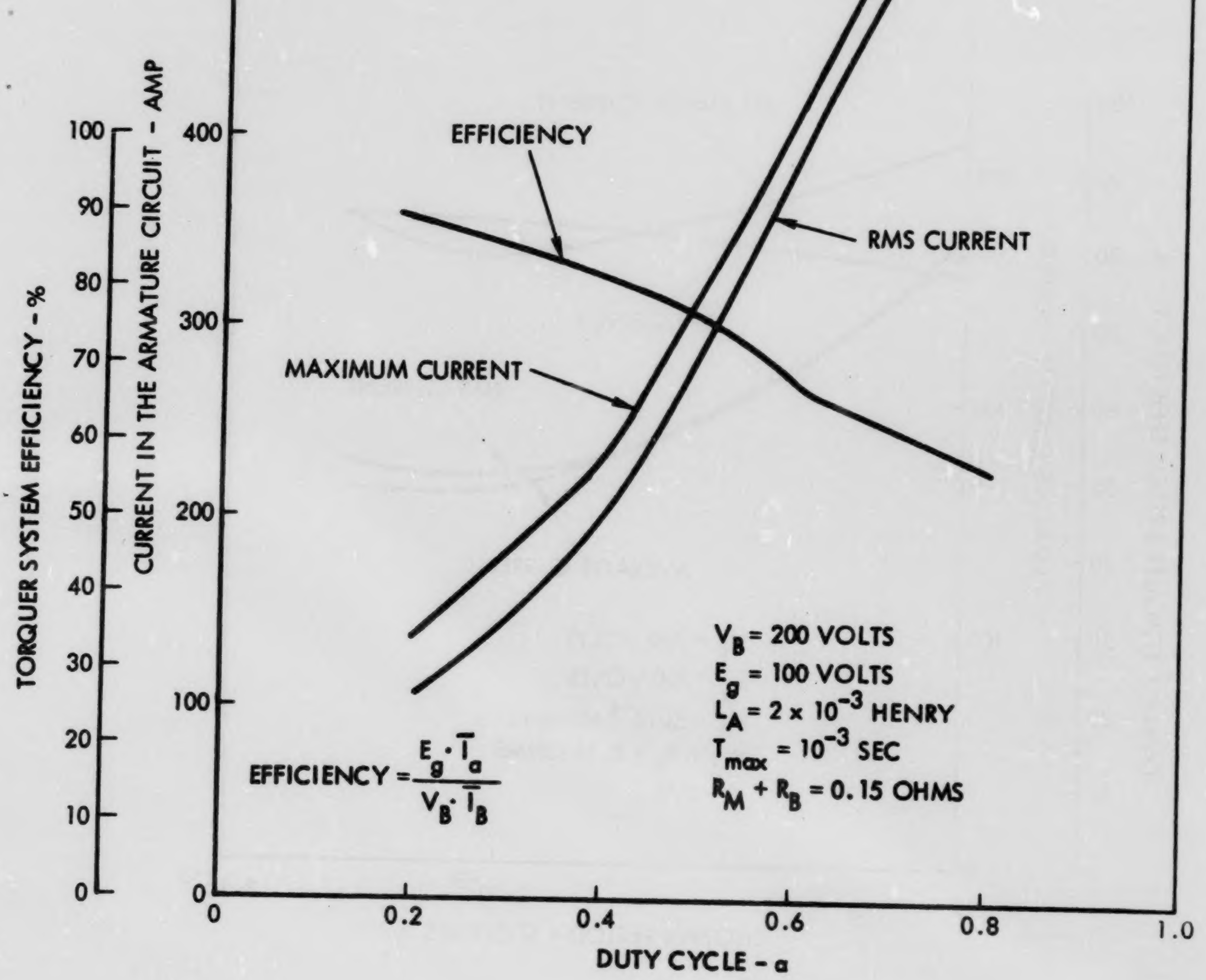

FIGURE 6.7
ARMATURE CURRENT & EFFICIENCY AS A FUNCTION OF
DUTY CYCLE

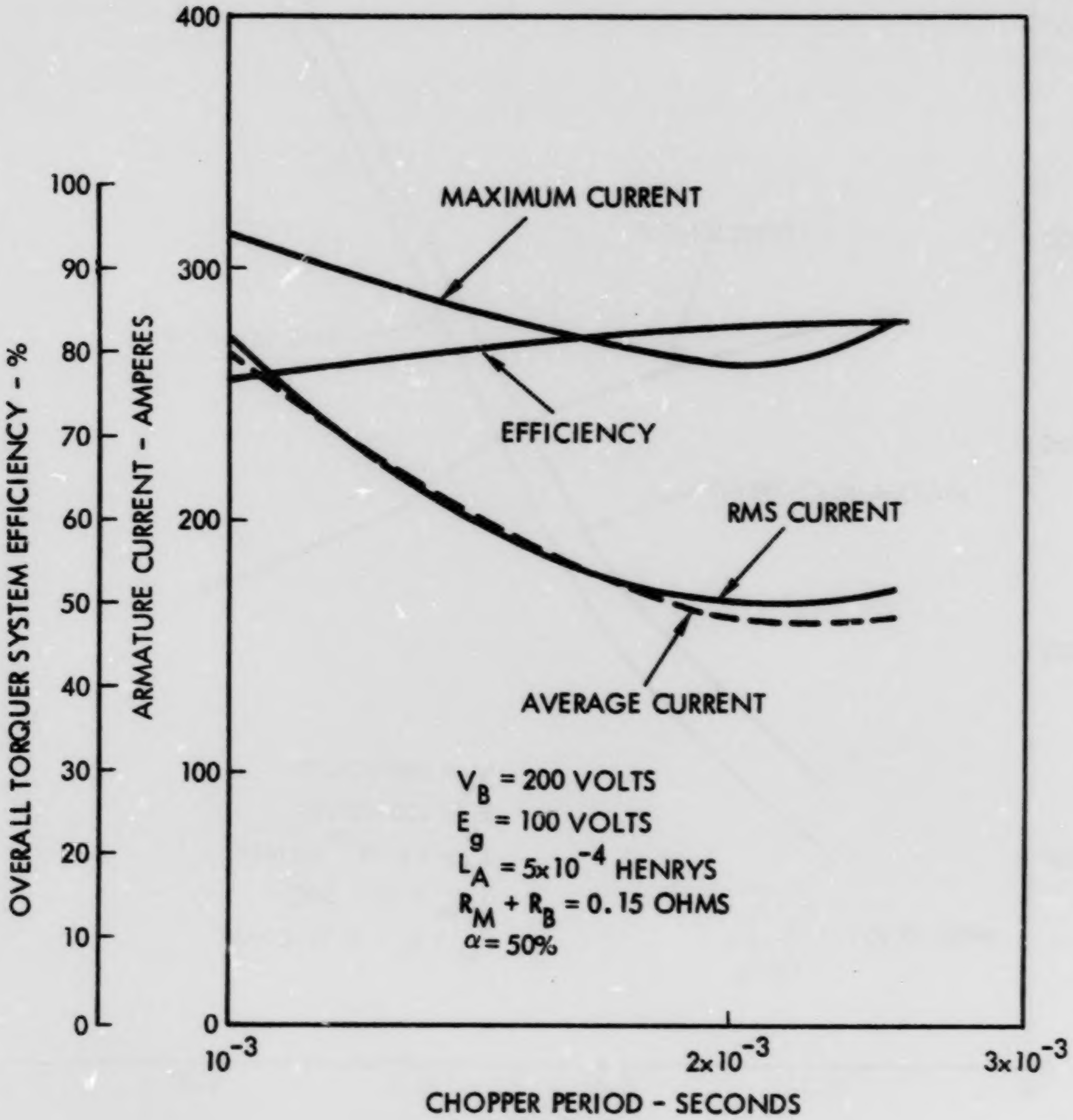
OVERALL TORQUER SYSTEM EFFICIENCY - %
0
10
20
30
40
50
60
70
80
90
100
ARMATURE CURRENT - AMPERES
0
100
200
300
400
MAXIMUM CURRENT
EFFICIENCY
RMS CURRENT
AVERAGE CURRENT
$V_B$ = 200 VOLTS
$E_g$ = 100 VOLTS
$L_A = 5 \times 10^{-4}$ HENRYS
$R_M + R_B$ = 0.15 OHMS
$\alpha$ = 50%
$10^{-3}$
$2 \times 10^{-3}$
$3 \times 10^{-3}$
CHOPPER PERIOD - SECONDS

FIGURE 6.8

## TABLE 6.3

## FOURIER COMPONENTS OF ARMATURE CURRENTS FOR DIFFERENT VALUES OF SERIES INDUCTANCES

| Inductance<br>Fourier Coefficient | $L_A=10^{-4}$ henry | $L_A=5\times10^{-4}$ henry | $L_A=10^{-3}$ henry | $L_A=2\times10^{-3}$ henry | $L_A=5\times10^{-3}$ henry |
|---|---|---|---|---|---|
| $a_o$(average) | 253.6 | 159.2 | 177 | 201 | 191 |
| $a_1$ (cos wt) | -241 | -73 | -35.6 | -17 | -6.9 |
| $b_1$(sin wt) | 117 | -15.1 | -9.9 | -5.9 | -2.4 |
| $a_2$(cos 2wt) | 33.8 | -3.2 | -1.8 | -1.2 | -0.38 |
| $b_2$(sin 2wt) | 38.6 | 9.5 | 5.3 | 2.8 | 1.1 |
| $a_3$(cos 3wt) | -17 | -5.9 | -2.5 | -1 | -0.46 |
| $b_3$(sin 3wt) | -22 | -5.9 | -3.3 | -1.6 | -0.77 |
| $c_1=\sqrt{a_1{}^2+b_1{}^2}$ | 268 | 74.5 | 37.1 | 18 | 7.3 |
| $c_2=\sqrt{a_2{}^2+b_2{}^2}$ | 51.3 | 10 | 5.6 | 3.05 | 1.17 |
| $c_3=\sqrt{a_3{}^2+b_3{}^2}$ | 27.8 | 8.35 | 4.15 | 1.88 | 0.89 |
| $c_1/a_o$ (%) | 106% | 46.7% | 21% | 9% | 3.8% |
| $c_2/a_o$ (%) | 20% | 6.3% | 3.16% | 15% | 0.61% |
| $c_3/a_o$ (%) | 11% | 5.25% | 2.35% | 0.93% | 0.47% |

$$i_{(t)} = a_o + a_1 \cos wt + b_1 \sin wt + a_2 \cos 2wt + b_2 \sin 2wt + a_3 \cos wt + b_3 \sin 3wt \; t \ldots$$

with poorer form factor as the B-H magnetic loop covers a larger area. The hysteresis loss per cycle may increase, but the number of cycles per unit time decreases. The overall loss at any frequency also depends on the magnetic material used in the machine. (The magnetic losses in the PCU are related directly to frequency, since they undergo a constant magnetic loop per commutation cycle.)

### 6.1.2 Summary of Torquer Drive System Analysis

The following conclusions can be drawn from the above results:

- Overall system efficiency is a strong function of battery resistance. The importance of battery impedance as it affects the duty cycle per Torquer power output should be recognized.

- The filtering effect of the armature circuit inductance impacts in two ways, affecting the resistive losses for a given power output as well as the magnetic losses. For the present system an overall inductance of $1 \times 10^{-3}$ to $2 \times 10^{-3}$ henrys is desired.

- Increased duty cycle at constant circuit parameter values increases the power output but also increases system losses. The relative gains (and therefore system efficiency) are functions of battery and armature circuit impedance.

- Lowering the chopper frequency increases the form factor at constant current resulting in higher ohmic losses.

## 6.2 Torquer Design

### 6.2.1 Loss Mechanisms in the Torquer

There are several sources of losses in the Torquer: windage, bearing losses, brush friction, brush drop and ohmic losses, hysteresis and eddy current losses. Of these, the first three are primarily mechanical design considerations, and little flexibility is allowed in them. The brush drop loss is associated with the contact of brushes and commutator. The first four losses are estimated by General Electric (and in some areas supported by TRW tests) to be:

- windage, bearings, and brush friction - 400 total watts at 7200 rpm
- brush drop - 200 watts at 130 amperes DC, 7200 rpm

If the machine is fed from a pure DC power source, the remaining losses at 130 amperes, 7200 rpm are:

- ohmic losses
  - armature, 320 watts
  - commutation windings, 130 watts
  - series field, 170 watts
- hysteresis and eddy current losses, 700 watts.

The total estimated losses at rated current and speed amount to 1.92 kw, giving an anticipated efficiency slightly over 90%. The reasons for the much lower average machine efficiency are given below.

In the breadboard equipment, the Torquer does not see a DC source or load but rather a chopped voltage due to the Torquer PCU. As previously stated, this pulsating terminal voltage gives rise to a pulsating current which increases both ohmic and magnetic losses. The former effect was described in terms of the form factor in Section 5.3. Form factor losses are aggravated by the high current levels required in the Torquer's operation. Figure 6.9 shows a distribution of Torquer drive current levels taken at 5 second intervals for the first few minutes of one of the LA-4 runs. Differing vehicle speeds are associated with each point. The Torquer current exceeds its rated level most of the time and increased ohmic losses and an efficiency less than rated must be expected.

The current variations also produce strong flux variations in the stator and armature structure. These flux variations tend to induce eddy currents and produce a magnetic cycling in the iron paths. While the armature is comprised of laminated, low loss iron typical of DC motor design, the field structure (stator) is not. In classical machine design, the machine frame or yoke and pole cores are solid pieces and only the pole faces are laminated to reduce the losses due to the localized effect of armature slot flux ripple.

FIGURE 6.9
TORQUER EFFICIENCY ON THE LA-4 RUN

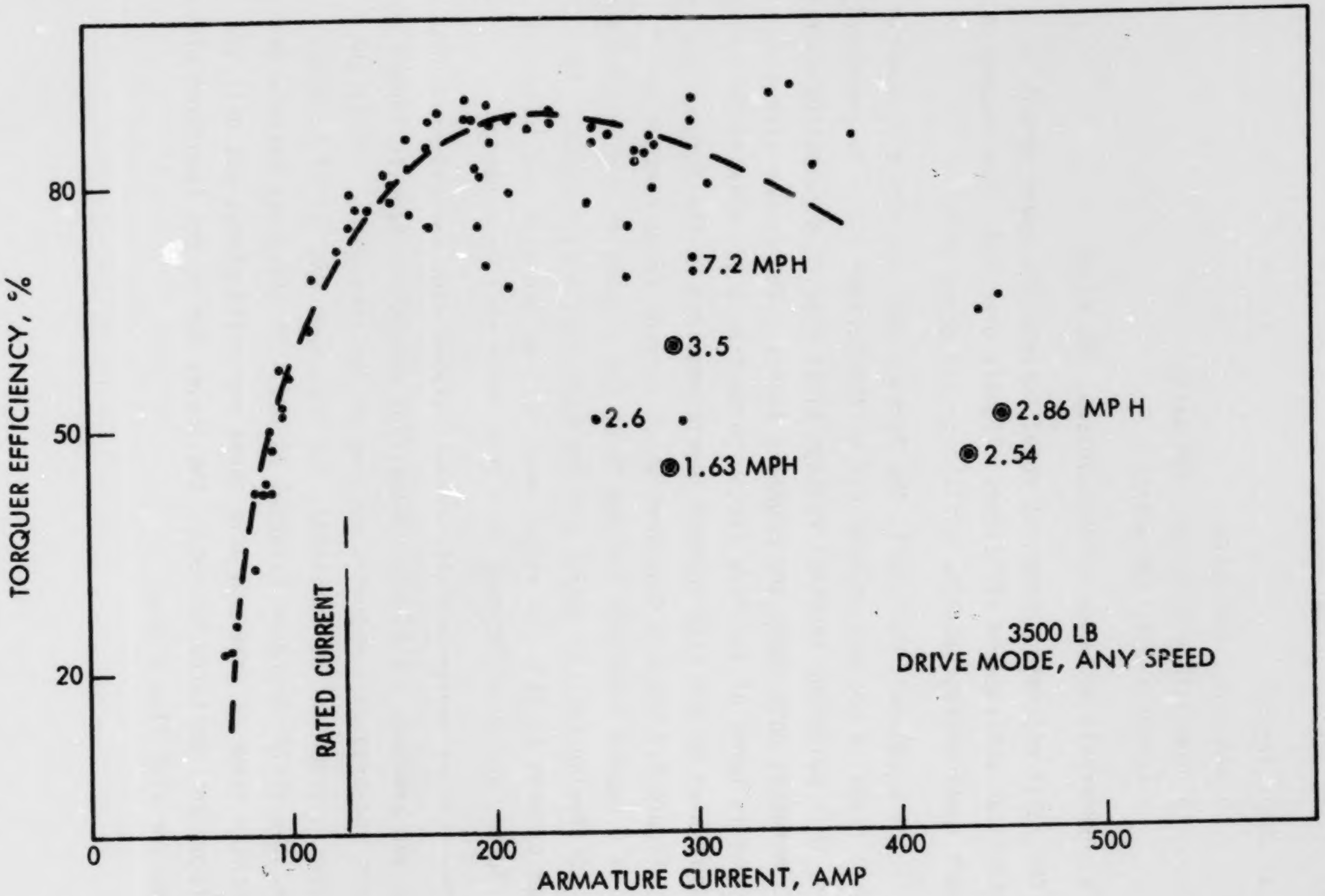

## 6.3 Torquer Design Improvements

There are two approaches to reducing the losses in a DC motor operating from (into) a chopped voltage source (load). Both approaches may have additional cost penalties associated with their use. This section will discuss these possible design changes and describe some problems which may occur with their adoption.

### 6.3.1 Addition of Armature Circuit Inductance

Additional armature circuit inductance could be added in the series winding and/or in an external inductor. If the field winding were increased, there would probably be an increased penalty of machine weight and cost. On the other hand, use of an external inductor allows the total inductance to increase without affecting the motor design. The addition of an external inductor represents an additional costly item that takes up additional space and produces losses and heat.

No matter what the cost or weight penalty, additional inductance has a dramatic effect on Torquer system behavior. A test of the Torquer system in regeneration was made with and without an external choke. The choke was a duplicate of the energy storage inductor used in the breadboard Speeder PCU, having DC inductances as follows:

$1.8 \times 10^{-3}$ henrys at 50 amperes
$1.20 \times 10^{-3}$ henrys at 130 amperes

It was used in this test as a swinging choke; that is, it was expected to be saturated at the rated Torquer current. Tests on the Torquer alone under chopper control indicated the machine's inductance was drastically reduced from the DC design levels (see Section 4.2). The following inductance values were determined at low speed (approximately 25-33% of rated machine speed) for 500 hertz chopper operation:

$0.75 \times 10^{-3}$ henrys at 60 amperes average
$0.35 \times 10^{-3}$ henrys at 130 amperes average
$0.25 \times 10^{-3}$ henrys at 200 amperes average

With the addition of the external inductor a dramatic change was made in the Torquer system's performance.

Table 6.4 summarizes the results of the test. The computations were made by numerically integrating values from armature current oscillograms. For an equal average current, the output torque of the machine with the inductor is nearly double that without it, and the machine efficiency is over twice as large. The inductor losses are included in the PCU efficiency calculation and thus the PCU with the inductor shows a slightly lower efficiency; still the overall effect is to raise Torquer system regeneration efficiency from 39.6% to 80.9%. The results for the drive mode are similar.

TABLE 6.4
EFFECT OF AN EXTERNAL CHOKE ON TORQUER SYSTEM PERFORMANCE
IN REGENERATION (2/3 rated speed)

| | Without Inductor | With Inductor |
|---|---|---|
| Average Torquer Current | 76 | 76 |
| Average Torquer Voltage | 84.7 | 94.5 |
| Shaft Torque, ft-lbs | 13.0 | 10.2 |
| Shaft Power, kw | 10.0 | 7.8 |
| Torquer Output Power, kw | 4.0 | 7.2 |
| Machine Efficiency, % | 40 | 92 |
| Battery Input Power, kw | 3.78 | 6.25 |
| Torquer PCU Efficiency, % | 95.1 | 86.1 |
| Torquer System Efficiency, % | 39.6 | 80.9 |

The impact of additional external inductance is lessened at higher speeds and currents. In either case the chopper duty cycle is increased, resulting in a better current waveform. The added inductor therefore need not remain unsaturated at these higher levels; indeed saturation may be desirable to automatically decrease the armature circuit time constant whenever fast response is required at high output power levels. The use of a small, highly efficient swinging choke may be quite adequate for satisfactorily improving the present machine's performance.

Another possible design effect of additional circuit inductance would be the reduction in the size of the present machine. With a better form factor, the machine losses would be reduced, and a higher torque output could be achieved for the same average current. Since losses and torque output determine the machine size, improvement in these areas might result in a smaller machine capable of the same power performance.

It is probable that the external choke would improve the machine's commutation. (It might be noted in passing that the present Torquer has never exhibited any detrimental sparking and the commutator seems in excellent condition after more than one year in service.) Reduction in the peak current levels would reduce the reactance voltage and the lessened current swings in the interpoles should make these latter elements perform more satisfactory.

### 6.3.2 Lamination of the Poles and Yoke of the Machine

A second method of effectively increasing the DC machine's inductance (and thus efficiency) in pulsating service is to laminate the poles and yoke of the machine with low hysteresis iron. Such an approach is more like that used in AC commutator motor design where the stator must operate under pulsating flux conditions.

The problem of operating a DC machine from a pulsating voltage source has arisen in railroad service where the power source is rectified AC. In the field of industrial motor control many times the power source is a polyphase thryistor bridge. When conventional DC motors are operated from such sources, results similar to those in the EMT are observed: loss in efficiency and heating. In some cases additional commutation problems can arise due to the introduction of transformer emfs in the armature coils and the inability of the interpoles to compensate for these induced voltages.

The approach to the pulsation problem generally has been as follows:

- Redesign the motor yoke and series field pole cores to include low loss iron laminations.
- Laminate the interpoles with low loss iron.
- Minimize spurious eddy current paths through bolts, rivets, pole attachments, etc.

Some concern may be expressed that the increased inductance of the field winding will increase the transformer emf in the armature and degrade the commutation process (shrink the black band current range of sparkless machine operation). This need not present a problem, however, if the interpoles are properly designed to insure that the interpole flux is in phase with the armature current being commutated. While it is possible that a spark developed by transformer emf action may act as hot spot to discharge the reactance voltage, it seems quite likely that a machine designed to minimize reactance effects which are most severe at high speeds and currents, will not spark because of transformer emf at lower speeds and currents.

A recent work by Byrne, et al,[5] reports the design and testing of a modified 3 hp, 1830 rpm, 24 volt machine. The machine was rebuilt using transformer grade steel sheet laminations for the yoke and additional modifications were made to the armature and pole shapes. No interpoles were used. Using data presented in the paper, the following conclusions can be drawn:

- The new design increased the pole flux per ampere by 40% and increased the rating of the machine from 3 Bhp to 5.6 Bhp.
- The specific power density (kw/lb) was raised by 136%.
- The machine's efficiency was increased at all torque and speed levels above that of the conventional machine.
    - 167% increase at half rated torque, 10% rated speed
    - 123% increase at rated torque, 10% rated speed
- The machine's efficiency was made to be almost independent of torque level indicating an almost complete absense of any waveform induced losses.

Another work reported by Kawai and Myake[6] report the modification of a traction motor for use on the Japanese Tokaido Railroad. The authors report that lamination of the yoke, main pole and interpoles produced dramatic reduction in the machine's temperature rise, the effect being more pronounced as the harmonic content of the waveform increased. While it appeared to be necessary to reintroduce some dampening (shunt resistor) in the main winding to completely insure sparkless operation, it is not clear that a modification of the machine interpoles or armature would not have served the same purpose without the parasitic loss in the main winding.

### 6.3.3 Advanced Design Conclusions

It has been demonstrated by TRW and reported in the literature that major efficiency increases can be realized by incorporating modifications of a DC machine design/circuit inductance. While it is not confirmed at this time which approach (or combination of approaches) is the best from the standpoint of highest efficiency per unit cost (at fixed torque and power performance), the laminated motor approach is favored. Further, information must be gathered from machinery vendors before a final design can be selected.

## 6.4 Speed Charging of the Torquer

The present Torquer runs about 1/3 rated speed for LA-4 operation (∿20 mph average speed). Its average power level is nearly rated and thus its currents generally exceed its design level. One means of increasing efficiency is to reduce the average current demand and increase the chopper duty cycle by allowing the machine to run closer to its design speed. It is possible to incorporate a gear ratio shift between the Torquer and the propeller shaft so that the Torquer runs at higher average speed during Mode One and thus is near rated speed at mode transition. Assuming the limit case of rated speed at mode transition (∿40 mph), the Torquer would then run on the average at 1/2 rated speed in Mode One. For the same power delivery, the current would decrease from 300% of rated to 200% of rated and neglecting any changes in form factor, the new ohmic losses would be approximately 4/9 of the present losses.

The gear shifting could be incorporated with the automatic functions of mode transition; however, even under these conditions there would be an increased weight and cost penalty due to the added mechanical and control elements. Also, the higher speed would result in higher back emfs, limiting the ability to overload the machine for acceleration maneuvers. It is probable that the advanced machine designs indicated in the previous section will result in substantial Torquer system improvement. If the level of performance can be raised using those techniques, the need for speed changing may disappear.

## 6.5 Chopper Frequency Selection and Power Control Improvements

The analysis of the Torquer drive system (Section 6.1) demonstrated the desirability of high (chopper) frequency (1 khz). There are several qualitative advantages in that choice of frequency. Some of these are:

- Generally the size and weight of filter components having an equivalent filtering effect vary inversely with operating frequency. Higher frequency will afford easier packaging and mechanical design.
- As the operating frequency increases, the chopper period diminishes with respect to the electrical time constants of the motor and the form factors and efficiency improve. For equal power output schedules, the motor size, weight and cost can be reduced.

On the other hand, there are advantages to the PCU design in using a low frequency:

- The PCU efficiency is improved as the frequency is lowered. The losses associated with the turn-on and turn-off of the semiconductors is fixed and as the period increases, these losses assume a lessened role relative to losses associated with saturated state conduction.
- The times required to turn the power SCR on and off is fixed by the device's characteristics. As the chopper period increases, these times become relatively smaller and the dead-band of controllability decreases. A long period is desirable in order to generate low (approaching zero) and high (approaching 100%) duty cycles.

The advantages of high frequency operation outweigh those of low frequency since the improvement of machine performance and potentially lower cost equipment outweigh those of a higher efficiency and dead-band elimination in an already efficient PCU, particularly if other control techniques can be used.

The present Torquer PCU conducts some power to the Torquer through the action of the commutation circuit even under minimum torque command. The continuous operation of the existing commutation circuit has the advantage of reliability since the commutation SCR gate is always triggered and allows commutation power to be utilized in the motor. On the other hand, the commutation energy delivered per cycle is fixed and as the chopper frequency increases, the commutation power increases, increasing the minimum torque which can be controlled.

The desire for a high chopper frequency is therefore at odds with the problem of commutation power control and in the present system, both are compromised by shifting the chopper frequency as shown in Figure 6.10. In assessing ways of circuit improvement it is worthwhile to examine quantitatively the impact of the 1 kHz chopper frequency.

The commutation circuit provides power to the motor by delivering energy stored in the commutation capacitor (see Appendix A-2). In addition to the current flow to the capacitor during recharge, there is a path for current to flow from the battery to the motor via $SCR_2$ during the period of oscillation just preceding the recharge. However, calculations show the maximum level this current can obtain in the present configuration is 13 amperes--a value incapable of producing usable motor torque. There is no reason to add additional or modify the existing circuitry to isolate the commutation circuit during the oscillation period and prevent this current from flowing.

On the other hand, it can be shown that at very low speeds the average armature current due to the discharge of the commutating capacitor is inversely proportional to the Torquer speed and directly proportional to the PCU switching frequency. For example, with the present commutating capacitor (80 μF), commutation power develops rated current in the Torquer at 340 Hz at 5 mph and at 1 kHz at 15 mph. If the commutating capacitor could be reduced, rated Torquer current due to commutation energy would be produced at a higher frequency and lower speed. Thus, if the capacitor could be reduced to 20 μF, rated current would be produced at 1 kHz and 5 mph, and a constant frequency system would be more practical. (The lower capacity of the commutating capacitor would also reduce the size and cost of that device.)

The principle obstacle to a lower capacity commutation capacitor is that enough charge must be stored on it to turn the SCRs off. For example, in dropping from 80 to 20 μF, the turn-off time of the SCRs must fall from 40 to 10 μ seconds. Such high speed characteristics are presently available in SCRs as long as the $\frac{dv}{dt}$, $\frac{di}{dt}$, voltage levels and dissipation are relatively low as they are in the EMT. In an upgraded Torquer PCU, these faster semiconductors will be used.

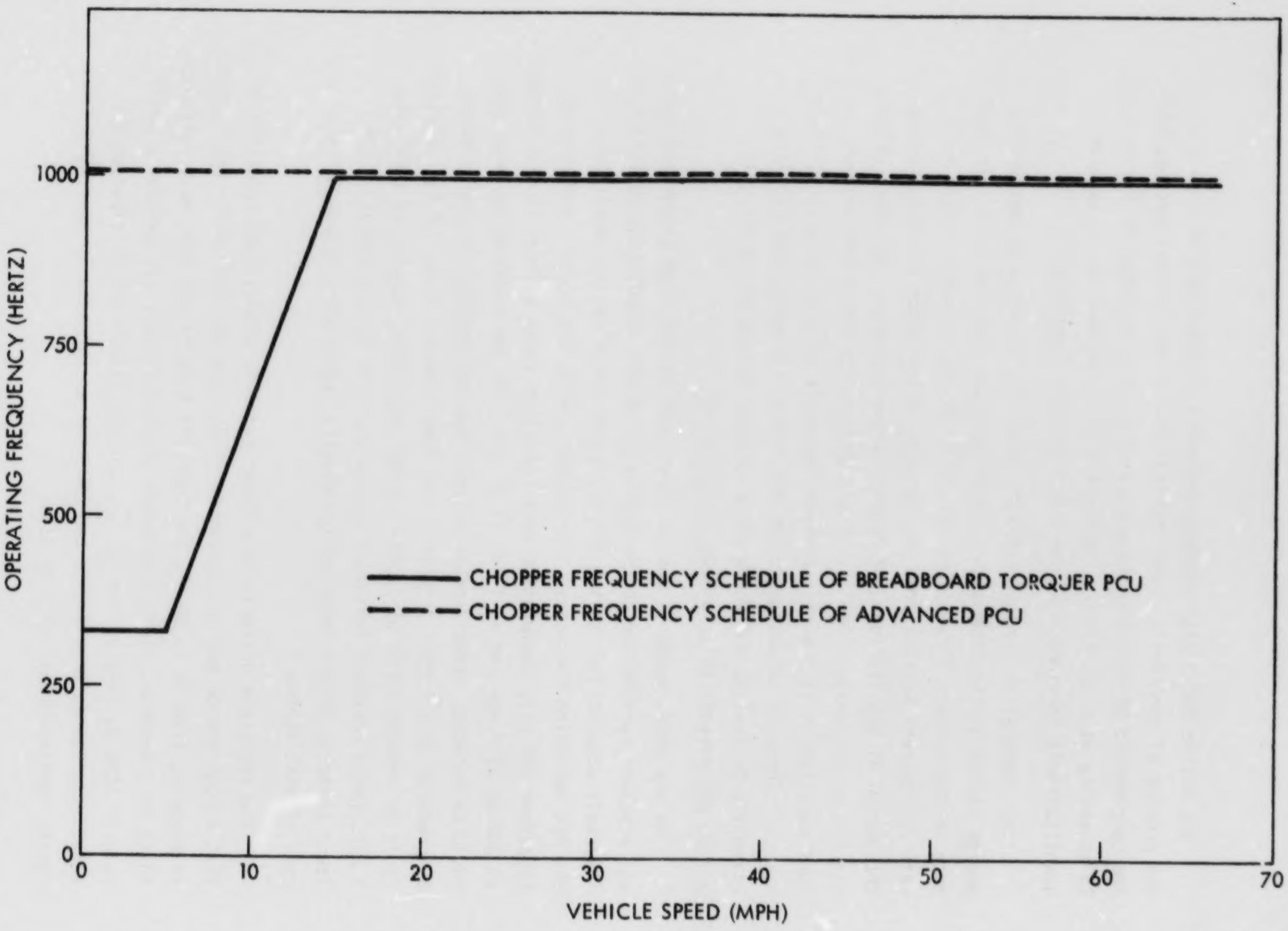

FIGURE 6.10
TORQUER PCU FREQUENCY SCHEDULES

## 6.6 Torquer System Failure Analysis

The EMT dynamometer system was designed and constructed to prove the basic EMT concept. Safety systems were provided to protect the personnel and equipment within the context of a research and development environment. Due to the continuous close monitoring and supervision of the equipment during testing, automatic self-resetting features were not incorporated so that manual control of the many functions of the system was preserved in contrast to the turn key operation essential for a vehicle.

The types of possible failures are grouped roughly into three basic categories, dependent upon their final effect on the vehicle system. The three types range from a malfunction almost undetected by the operator to a failure which disables the vehicle entirely. The three types are as follows:

- abnormal performance (automatic recovery)
- abnormal performance (degraded functional performance)
- catastrophic component failure (vehicle disabled)

Abnormal performance with automatic recovery is that type in which there is no degree of disability relative to the driver or vehicle; rather the operator will feel a momentary deviation (less than 1 second) from the expected vehicle behavior. The third type of failure is the extreme opposite in that the vehicle cannot operate on its own and must be towed to a garage. The degree of this disability is total. Between the two extremes mentioned above there are a few types of abnormal performances which only degrade vehicle functions, but still allow the vehicle to be operated under limited conditions until service is reached. The degree of disability can range from almost undetectable decrease in drive power to no drive at all. For example, even with no power from the Torquer the vehicle can still creep forward on the engine so that this is not a total disability relative to total vehicle function.

### 6.6.1 Advanced Torquer Systems Incorporating Failure Protection

An advanced Torquer system is indicated in block diagram form in Figure 6.11. It reflects the advanced solid state switching system for drive-regeneration configuration changes (see Section 8.1) and incorporates

FIGURE 6.11
ADVANCED TORQUER CIRCUITRY WITH SAFETY PROTECTION & DETECTION

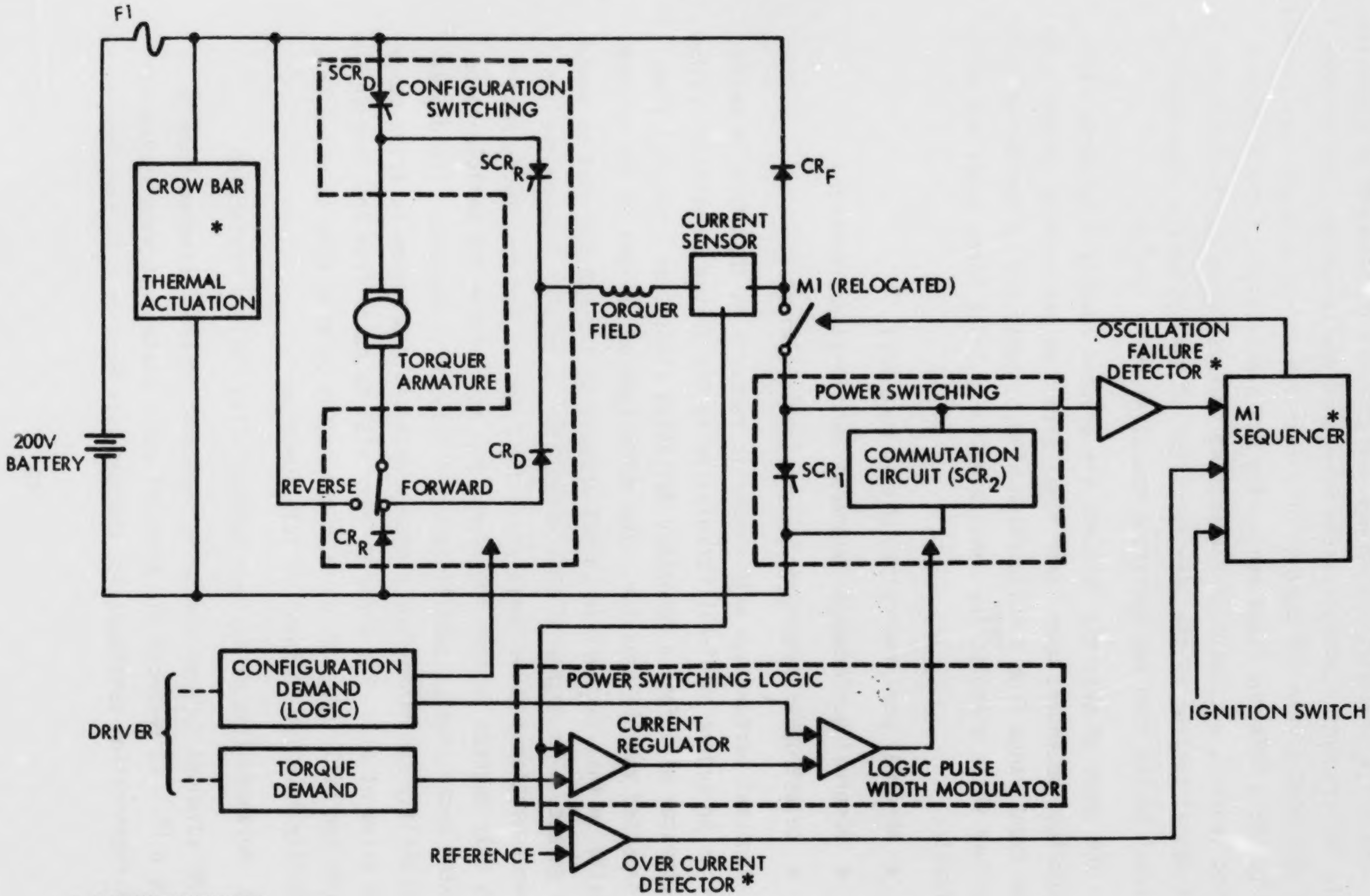
F1
CROW BAR
*
THERMAL ACTUATION
200V BATTERY
SCR$_D$
CONFIGURATION SWITCHING
SCR$_R$
TORQUER ARMATURE
CR$_D$
REVERSE
FORWARD
CR$_R$
TORQUER FIELD
CURRENT SENSOR
CR$_F$
M1 (RELOCATED)
POWER SWITCHING
SCR$_1$
COMMUTATION CIRCUIT (SCR$_2$)
OSCILLATION FAILURE DETECTOR *
M1 SEQUENCER *
IGNITION SWITCH
DRIVER
CONFIGURATION DEMAND (LOGIC)
TORQUE DEMAND
POWER SWITCHING LOGIC
CURRENT REGULATOR
LOGIC PULSE WIDTH MODULATOR
REFERENCE
OVER CURRENT DETECTOR *

* ADDED CIRCUITRY

additional automatic safety and protection circuits. In the block diagram power handling devices are separated into four basic groups:

- power switching (with commutation circuit)
- configuration switching
- Torquer
- safety devices

The operation of the power handling groups is controlled by three basic groups of logic elements:

- power switching logic
  - current regulator
  - logic pulse switch modulator
- configuration switching logic
- M1 sequencing control (with thermal overload actuation)

While these groups of control logic do interact to some slight degree they can be treated as independent blocks, i.e., a failure of a part of one logic group only affects that group. For example, if the power switching logic current regulator fails and demands current above the rating of the PCU or motor, the M1 sequencing control is still operational and can perform its function to correct the overcurrent condition. The power handling elements are subjected to greater stresses, and their various modes of malfunction must be considered on an individual basis.

The protection for a vehicle system must be effective both for the vehicle as well as the driver. Uncontrolled acceleration or deceleration cannot be tolerated, since either could place the vehicle and driver into a condition where an accident can result. In addition to preventing undesired vehicle behavior, the equipment cannot be allowed to destroy itself by exceeding its power rating. This implies two basic methods of protection, one to restore normal operations to the driver, if at all possible, and another to prevent destructive power internal to the circuit.

At this point, thought should be given to two methods of fault correction which have found a place in other applications. These are the use of redundant circuits and manual overrides to bypass a failed component or circuit. The use of redundancy is both costly and complex and should be used only where the failure of a component would directly create a potential for bodily injury. The dual braking system presently used in automobiles is such an example. Redundance where the component failure is merely an inconvenience is not anticipated in this type of vehicle. Manually bypassing a failed device or overriding a safety mechanism until help can be reached is somewhat impractical due to the complexity of the system and the resultant large number of such bypass possibilities. However, it is possible with future on-the-road experience one or two such overrides may be installed if a pattern of uncontrollable failures is determined and the overall safety is not jeopardized.

### 6.6.2 Abnormal Performance - Automatic Recovery

#### 6.6.2.1 Torquer PCU Power Switching SCRs Fail to Commutate Off

If the Torquer PCU SCRs fail to commutate while in regeneration, the present circuit will affect the vehicle behavior in a manner dependent on the speed of the vehicle. The specific speed at which one or the other of two possible malfunction conditions can occur is a function of the wiring, Torquer and semiconductor impedances as well as the actual burn-open current of the fuse located in the Torquer circuit. All these components have relatively large tolerances associated with them so that roughly below 30 mph one action takes place, and above 40 mph another.

Below 30 mph if the power switching pulse width modulator stops operating, a 100% duty cycle is commanded and maximum braking current will be generated. At this speed the current will be too small to open the 400A fuse in the Torquer armature. The vehicle will decelerate with maximum braking torque. This condition cannot be corrected until the vehicle is completely stopped at which time the drive configuration can be selected and normal operation resumed. If drive is selected before the vehicle is completely stopped, the configuration switching circuit will hang-up, the consequence of which is described in the next section. Above 40 mph the hang-up of the power switching SCRs will cause regeneration with current sufficient to open the Torquer fuse, disabling the vehicle in both configurations until a new fuse is inserted.

The above discussion indicates the need to locate M1 in the circuit so that a simple failure to commutate in either drive or regeneration can be corrected without the driver having to act. The proposed circuit shown in Figure 6.11 provides this protection for all SCRs under both configurations.

If the Torquer power switching SCRs ($SCR_1$ and $SCR_2$) fail to shut-off to a misfire or temporary overload, a detection circuit will be provided which will sense that the pulsewidth modulator has stopped operating. This detection circuit will then open the main contactor M1 for a minimum of 100 ms and close M1 again. The contactor will interrupt the current in the SCRs and allow the semiconductors to turn-off. The effect on the driver will be a momentary (less than .5 seconds) drop in power (in drive) or drop in braking torque (in regeneration).

#### 6.6.2.2 Torquer PCR Configuration Switching SCRs Fail to Commutate Off

If the Torquer PCR configuration switching SCRs ($SCR_D$ and $SCR_R$) fail to turn-off during the transition between drive and regeneration, or are turned on out of sequence, there will be an uncontrolled surge of current which will be detected by the overcurrent sensing circuit. This will activate the fault clearing sequence of M1, so that within 100 msec the contactor will have opened, interrupting the current and closed again reestablishing normal operation. If this occurs during configuration switching the driver will only feel a slight (less than .5 seconds) delay in transfer to the new configuration.

### 6.6.3 Abnormal Performance - Degraded System Functioning

#### 6.6.3.1 Torquer PCU Current is Not Fully Controlled

If the current control (torque control) in the Torquer PCU fails slightly off design conditions it is virtually impossible to detect. When this occurs the power handling devices will work properly, but the commands to the SCR gate drive amplifiers will not perform properly. These problems can be caused by the following:

- The accelerator pedal command does not call for the proper current.
- The current regulator does not regulate properly. The regulator may provide for more or less current than that which the driver desires. (This can be detected electronically by a redundant

monitor, which can tell the operator and/or try to correct the error itself. This circuit adds to the complexity and could also malfunction, interferring with a properly working regulator.) Although this is not a catastrophic failure, the operator will probably observe a changing "feel" to the accelerator pedal and should be relied upon to call for service.

- If the logic pulsewidth modulator misinterprets the regulator the effect and cure are the same as above.

If the current in the PCU reaches an uncontrolled level sufficient to cause commutation failure, the procedures as described in 6.6.2 occur. A sensor may have to be provided to warn the operator of the repeated cycling of the $M_1$ contactor after a prescribed number of openings in any given period.

### 6.6.4 Catastrophic Logic Failure Leaving the Vehicle Completely or Partially Disabled

#### 6.6.4.1 Torquer PCU Does Not Switch Configuration

If the Torquer PCU fails to switch between the drive and regeneration configuration one of three conditions is responsible:

- The configuration switching logic does not start to initiate the sequence to transfer, so that the PCU stays in the previous configuration but under full control. If this happens in drive the vehicle will behave normally in drive and the vehicle can proceed until service is found. The mechanical brakes will have to do more work to control vehicle speed. If the PCU is in regeneration, the vehicle can be operated up to a maximum speed corresponding to a balance between road load torque and engine-propeller shaft torque less the contribution of regenerative commutation current in the PCU.

- The configuration switching logic completes the first step in the sequence to transfer, i.e., commands minimum power. This will allow only commutation energy to flow. If this occurs in regeneration or drive, the effect will be the same as in the previous situation.

- If the configuration switching logic sequences to the neutral position and stops the PCU will handle no power at all. The vehicle will be able to proceed similar to the previous situations without commutation power.

### 6.6.5 Catastrophic Component Failure Leaving the Vehicle Completely or Partially Disabled

#### 6.6.5.1 Torquer PCU SCRs, $SCR_1$ and $SCR_2$, Short or Fail to Turn-Off Due to Commutation Degradation

The failure of $SCR_1$ and/or $SCR_2$ to be turned off by the commutation circuit, or the direct short of these SCRs will cause full current in the system. This might result in full acceleration or deceleration. One of two detection circuits will respond to open $M_1$. Either the oscillation detector will indicate a failure, or the high current will cause the sequencer to open $M_1$ for its prescribed length of time. $M_1$ will close again having assumed the fault is cleared, but the failure will repeat and an operator warning will be given. The above condition will totally disable the Torquer system. However, the vehicle will still retain its basic torque contribution from the ICE since the Speeder system will not be affected and the vehicle can move slowly as in the last case of 6.6.4.1.

#### 6.6.5.2 Torquer PCU Blocking Diode Short or Open

The Torquer PCU blocking diode, $CR_F$, is one of the links from the PCU to the traction battery. The path $CR_F$-$SCR_1$ is the only one which does not have the Torquer's impedance to limit the battery current when $CR_F$ develops a short. Therefore, it cannot utilize a relay to interrupt the rapidly rising currents which could develop. For this type of failure a fuse must be used to halt the current before unreasonably high levels are reached and thus $F_1$ is provided for this purpose. The fuse rating must be such that faults in other semiconductors which can be cleared by $M_1$ should not open the fuse and disable the PCU.

In a circuit with an inductive element such as the Torquer field winding, a path must be provided for the current flowing in the inductor to dissipate itself in a load external to the inductor. Normally in the Torquer system the inductive energy of the field passes through the flyback diode, armature and/or battery. If the flyback diode, $CR_F$, is open the inductor will develop whatever voltage is required to preserve a path for its current. This will result in an increase in the forward voltage across $SCR_1$ until an avalanche breakdown occurs and current flows through $CR_R$ and

$CR_D$ to complete the circuit. A large amount of commutation energy is still available because the commutation capacitor will charge to the avalanche voltage of $SCR_1$ and the system may go on operating in this manner until the current activates the overcurrent sensor or causes a failure in the switching SCRs. In either case the $M_1$ sequencer will continue to cycle and warn the operator.

### 6.6.5.3 Torquer PCU Configuration Switching Devices, $SCR_D$, $SCR_R$, $CR_D$, $CR_R$ Open Circuited

To change the configuration of the Torquer system from drive to regeneration requires four semiconductors. The four devices are made up of two diodes ($CR_D$ and $CR_R$) and two SCRs ($SCR_D$ and $SCR_R$). Since the Torquer is a series machine, it requires regeneration current to flow before its voltage can build-up. This inherent feature provides a degree of self protection for failures if the semiconductor devices fail in the open position. Since there will be no voltage generated, there is no need to provide protection for driver, vehicle or PCU for this type of failure. However, if the configuration switching semiconductors are not capable of conducting current, the Torquer is completely disabled. If the fault occurs during regeneration, there will be a lack of electrical braking power and the driver must rely on his mechanical brakes.

### 6.6.5.4 Torquer PCU Configuration Switching Devices Shorted

The effect of developing a short in $SCR_D$ and $SCR_R$ are identical in nature, so they can be treated as a group. In drive, current normally flows through $SCR_D$, armature, $CR_D$, and the field. If a short develops at zero vehicle speed in $SCR_R$, the path of current from the battery will be $SCR_D$, $SCR_R$ (shorted), and field. The current flow will be limited by the impedance of the field, the cable and terminal impedances, the semiconductors and the battery impedance. Using values associated with the present Torquer PCU, the current could rise to 760 amperes in 12 milliseconds. Similarly if $SCR_R$ is conducting during regeneration, and $SCR_D$ develops a short the same conditions can occur as those caused by a shorted $SCR_R$. The manner of protection for both failures is to open $M_1$.

In Section 6.6.2.2 it was stated that if either $SCR_D$ or $SCR_R$ fail to commutate off, then contactor $M_1$ would clear the fault. The fuse $F_1$ must be properly rated so that the current can flow through it until $M_1$ has opened if automatic recovery is to be achieved during a commutation failure in the configuration switching circuit. The $M_1$ protection circuit cannot differentiate an actual short from a commutation failure. The differentiation must be established through the repeated operation of the $M_1$ sequencer and operator warnings.

A short in $CR_R$ will produce extremely high current levels. The armature will have almost no back EMF to oppose the potential of the battery because the shorted $CR_R$ will bypass the current which normally flows through the series field. Since the path for current when $CR_R$ shorts has only $F_1$ for interruption, this device must be relied upon to clear this fault.

In regeneration a short in $CR_D$ will deprive the field of current and no armature voltage can be developed. The fault sensors cannot detect this difficulty since none of the fault conditions have been reached. The PCU will keep operating but no breaking torque will be developed. In drive, a short in $CR_D$ will cause no problems as it never has to assume a blocking state.

### 6.6.5.5 Torquer Field or Armature Open

An open circuit in either the field or armature will not allow current to flow from the battery in either portion of the motor or the PCUs while in drive. The series connection of armature, field, configuration switching devices and power switching devices are inherently self-protected if any of the elements develop an open circuit. Similarly in regeneration there can be no destructive voltages or currents developed.

### 6.6.5.6 Torquer Field or Armature Shorted

Shorted turns in the power handling elements will produce an excessive current and the development of hot spots. The amount of disability depends on the percentage of turns shorted. Conceivably if only one is affected the unit could continue to operate with only a small decrease in efficiency which neither the sensors or the driver could detect. As more turns are shorted, internal heating will increase, and efficiency will decrease until one or more events occurs:

- The driver detects the decreased power
- The need for higher power to produce the same mechanical work activates the overcurrent circuit
- The motor thermal protection limit is reached by the internal heating.

The current in the affected turns melts and the circuit opens.

### 6.6.6 Summary of Torquer System Failure Analysis

Table 6.5 presents a concise listing of possible Torquer system failures, degree of disability and manner of protection. While this list seems excessive it is to be noted that the majority of failures are self-correcting or at least allow a small degree of vehicle mobility due to the basic parallel configuration of the EMT.

No analysis of the impact of these electronic/electrical failures on engine operation has been included. In the breadboard equipment the engine throttle is tied to the Torquer current flow during Mode Two. Failures which result in excessive current flows in either direction would cause the throttle to open to its full position or completely close. Complete loss of current would disable the throttle feedback system and the engine would be left in its prefailure position. In any case, the operator could use his brakes or ignition switch to bring the car under control and back into the Mode One regime of operation. Since the engine control system is still in its early development, further design effort is needed to establish procedures and circuits which could be incorporated into the system to prevent or override such failures.

## TABLE 6.5
## TYPE OF FAILURES, PROTECTION & STATUS FOR THE TORQUER PCU

| COMPONENT OR CIRCUIT | TYPE OF FAILURE | METHOD OF PROTECTION | DEGREE OF DISABILITY |
|---|---|---|---|
| Torquer PCU | | | |
| SCR1<br>SCR2<br>$SCR_R$ &<br>$SCR_D$ | Failure to Commutate | Automatic Reset | None |
| | Shorted or Degradation of Commutation Ability | PCU will turn off by M1 | Total |
| | Open | None needed | Total |
| $CR_R$ | Shorted | Fuse F1 will open, to turn PCU off. | Total |
| | Open | None needed | No Regeneration |
| $CR_D$ | Shorted | None needed | No Regeneration |
| | Open | None needed | No Drive |
| $CR_F$ | Shorted | Fuse F1 will open, to turn PCU off. | Total |
| | Open | M1 will open & PCU turns off | Total |
| Commutation Circuit | Does not provide adequate reverse bias to turn-off SCR1 & SCR2 | PCU will turn off by M1 | Total |
| Driver Foot Pedal Command | Generates low current command | None needed | Drive & Regeneration Power Degraded |
| | Generates high current command | PCU will turn off if current exceeds over current limit by M1. | Total |
| Configuration Switching Logic | Does not transfer to drive | None needed | No Drive |
| | Does not transfer to regeneration | None needed | No Regeneration |
| Current Regulator | Regulates at lower than commanded | None needed | Drive & Regeneration Power Degraded |
| | Regulates at Higher than commanded | PCU will turn off if current exceeds over current limit by M1. | Total |

## TABLE 6.5
(Cont'd)

| COMPONENT OR CIRCUIT | TYPE OF FAILURE | METHOD OF PROTECTION | DEGREE OF DISABILITY |
|---|---|---|---|
| Logic Pulse Width Modulator | Range Limited to Low Duty Cycle | None needed | Drive & Regeneration power degraded |
| | Range Limited to High Duty Cycle | PCU will turn off if current exceeds over current limit by M1. | Total |
| M1 Contactor & Logic | Does not open | Crow Bar Circuit will turn PCU off. | Total |
| | Does not close | None needed | Total |
| Torquer Motor | | | |
| Armature | Open | None needed | Total |
| | Shorted Turns | None needed | Performance degraded. Ranging from undetectable to total disability |
| Field | Open | None needed | Total |
| | Shorted Turns | None needed | Performance degraded. Ranging from undetectable to total disability |

## 7.0 ADVANCED DESIGN OF THE SPEEDER SYSTEM

### 7.1 Review of Speeder Performance on LA-4 Tests

The present Speeder system was shown to have an overall efficiency of about 65% on the LA-4 route. The Speeder PCU has a relatively high efficiency around 95%, while the Speeder itself is a poor performer. Figure 7.1 shows several points of machine operation at various speeds and power levels taken during LA-4 operation. The machine's efficiency never exceeds 70%.

There are several contributors to the low machine efficiency; they are

- windage losses
- ohmic losses
- losses due to magnetic interactions.

Each of these contributors will be examined to assess their relative magnitude and to suggest means for their reduction.

### 7.2 Machine Losses

Figure 7.2 shows the losses in the Speeder due to windage and the rotating magnetic field of the unloaded machine. Ignoring the latter, the windage losses amount to 1.5 hp at 10,000 rpm and even at the speed corresponding to the average vehicle speed (5000 rpm at 20 mph) these losses are in excess of 0.5 hp.

The methods for reducing windage losses are well known. The machine should be more aerodynamically designed to approximate a smooth rotor. The present Lundell construction is particularly lossy and means should be explored for filling in the interpole area. In addition, thought should be given to running the machine at a lower top speed. Since windage losses vary approximately with the cube of the rotational speed, a small speed reduction would reduce aerodynamic losses substantially. The lower speeds would also reduce gear box losses. On the other hand, a reduction in speed would increase the torque (and current) rating of the machine with some increase in machine weight.

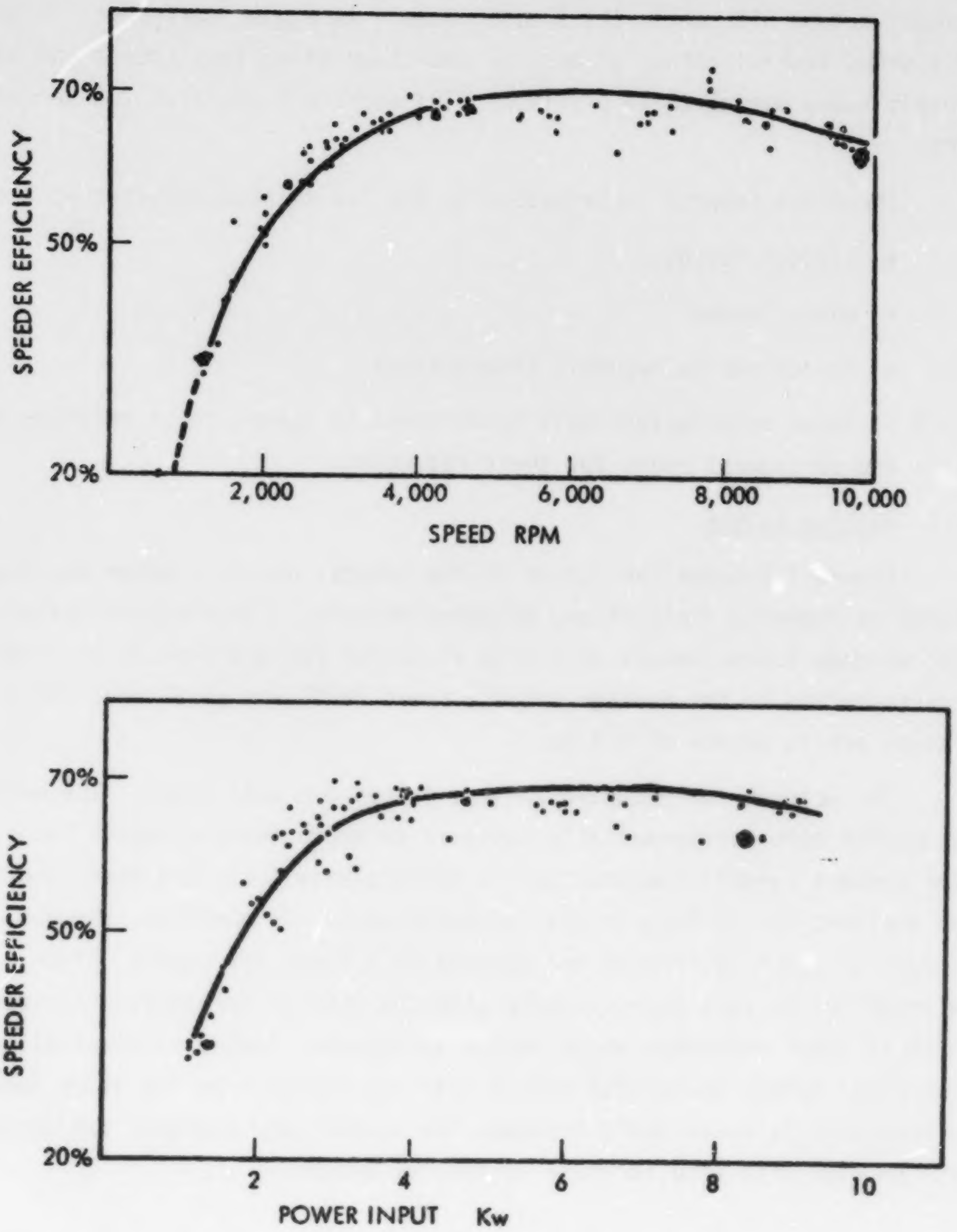

FIGURE 7.1

SPEEDER SYSTEM EFFICIENCY

FIGURE 7.2

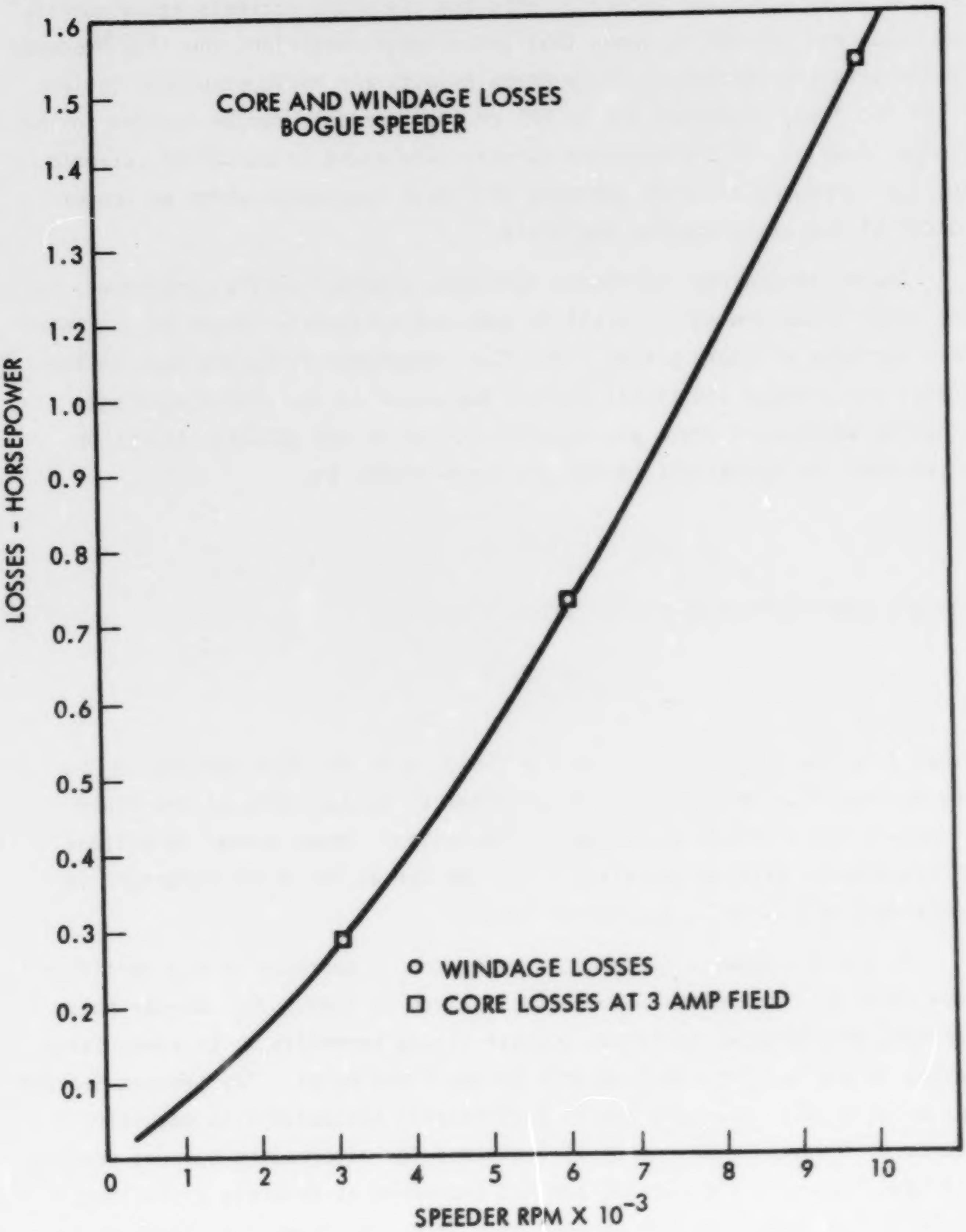
CORE AND WINDAGE LOSSES
BOGUE SPEEDER
LOSSES - HORSEPOWER
1.6
1.5
1.4
1.3
1.2
1.0
0.9
0.8
0.7
0.6
0.5
0.4
0.3
0.2
0.1
0
1
2
3
4
5
6
7
8
9
10
SPEEDER RPM X $10^{-3}$
○ WINDAGE LOSSES
□ CORE LOSSES AT 3 AMP FIELD

The electrical and magnetic losses are more difficult to analyze. When a polyphase synchronous generator is used to supply power to balanced passive loads, both the generated EMFs and the phase currents are sinusoidal and balanced. It can be shown that under these conditions the flux produced by the armature current is in synchronism with the field structure (pole faces and field windings) and no EMF or eddy currents can be induced in the field. However, if the armature carries unbalanced or pulsating currents, the flux produced by these currents will have components which no longer rotate at the same speed as the field.

The stator current harmonics introduce alternating flux components in the rotor structure which result in eddy and hysteresis losses in the rotor pole surfaces and pole pieces. The flux components reflected back to the stator can produce additional current harmonics in the stator windings, creating additional ohmic and magnetic losses in the stator. It can be shown that the hysteresis losses are proportional to:

$$fB_m^{\ x}; \quad (0.5 < x < 2.3)$$

and the eddy-current losses are proportional to:

$$\sigma\ t^2\ f^2\ B^2$$

where f is the frequency seen by the field, B is the flux density, $B_m$ is the maximum flux density, $\sigma$ is the electrical conductivity of the field structure and t is the thickness of lamination. Under normal conditions of synchronous machine operation $f = 0$ (as far as the field structure is concerned) and these losses do not occur.

In the EMT-Speeder system, the generator is operated into a rectifier load which in turn delivers power to a switching load. The Speeder phase currents and voltages therefore contain strong harmonics which cause large losses in the machine, particularly in the field poles. The present Speeder has a solid pole structure and is particularly susceptable to magnetic losses. (The stator of course is laminated for alternating current service and thus losses in the element are not increased as severely as in the field.) Examination of the Speeder pole faces has shown discoloration of of the pole tips where flux crowding is expected. While the exact nature of the discoloration was not determined to be merely the overheating of the dip varnish or actual "bluing" of the metal, the losses apparently are severe in this region.

### 7.2.1 Analysis of the Effect of the Rectifier on Speeder Performance

An analysis of the effect of the full-wave rectifier was made. In the model, it was assumed that the rectifiers are ideal, i.e., turn on and off instantaneously, and the load has infinite inductance so that the phase currents appear as square waves. The conclusions of the analysis are:

- Due to rectification, the armature currents are non-sinusoidal. As a result, an alternating current is induced in the field winding. The upper bound of this current is approximately 20% of the rated field current (defined as the field current which produces rated induced voltage at rated speed). The ohmic loss due to this current is not severe. However, it may induce a fairly high voltage at the terminals of the field winding.

- If the rotor surface is not properly laminated, excessive ohmic loss and local heating is produced. The frequency of the equivalent damper winding current is six times the fundamental frequency of the machine. (A damper winding is a short circuited winding on the field poles of a synchronous machine. It is normally used in larger machines as an aid in preserving synchronism by induction action. In the analysis, the pole faces are assumed to act as shorted circuits and thus can be replaced by an equivalent single turn winding having the same effective resistance of the pole faces.) At rated speed (10,000 rpm), the fundamental frequency is about 600 hertz hence the damper winding current frequency is about 3600 hertz. At this frequency, the skin depth of the eddy currents on the pole faces is less than one millimeter. The resistance of the eddy current path thus becomes very high and in a very crude calculation, the ohmic loss of the equivalent d-axis damper winding is estimated to be eight or nine times the field winding loss at rated current.

- There are strong 5th and 7th harmonic components in both the internal and terminal voltages on the stator side. The 5th harmonic is approximately 30% and the 7th harmonic 65% of the fundamental component.

- The electromechanic torque in the absence of any damping contains pulsating components at six and twelve times the fundamental frequency of the induced EMF. Its magnitude (the 6th harmonic) is approximately 18% of the steady-state torque. The damping torque of the present Speeder design is a function of the rotor pole resistance. It is estimated to be less than 5% of its steady-state component.

- By introducing a low loss (high conductivity) damper winding on the rotor side, the A-C component of the field current could be substantially reduced resulting in a better waveform of the induced voltage and a smoother electromechanical torque.

Typical phase current and line to line voltage waveforms for the Speeder are shown in Figure 7.3. The Speeder and rectifier are operating into a pure resistive load and the waveforms are symmetrical about the zero axis. The waveforms were analyzed by the TRW on-line computer and Fourier representations made. The analyses indicated the existence of strong 5th and 7th harmonics in the current waveforms. The magnitude of the 5th harmonic amounts to nearly 10% of the fundamental harmonic.

With the addition of the boost PCU, additional mechanism for Speeder losses is introduced. The load on the rectifier is no longer passive but contains reactive elements. When the Speeder power SCR is on, the storage inductor charges and presents an inductive load. When the SCR opens and the inductor current flows to the battery the load takes on a capacitive reactance character. The relative effects of these loads on current waveform and machine losses are further complicated by the necessity to vary the PCU duty cycle with machine voltage, battery voltage and engine torque variations.

Phase current and voltage waveforms for the Speeder-rectifier-PCU system are shown in Figure 7.4. Speeds and average currents are the same as in Figure 7.3. The lack of waveform symmetry about the zero axis is apparent as well as the cycle to cycle variation of waveform. While a Fourier analysis of these waveforms on a single cycle basis does not completely represent the total waveform, it serves to identify the major harmonics. (There are undoubtedly subharmonics which would show up in terms of a beat frequency between the machine frequency and the chopper frequency.)

Table 7.1 presents the ratio of the various Fourier components to the fundamental for the three waveforms of Figure 7.4. As in the case of the pure resistive load, the 5th harmonic content is very high, approximately 10% of the fundamental. The effect of the rectifier appears to dominate even with the addition of the PCU. However, the PCU does introduce

FIGURE 7.3

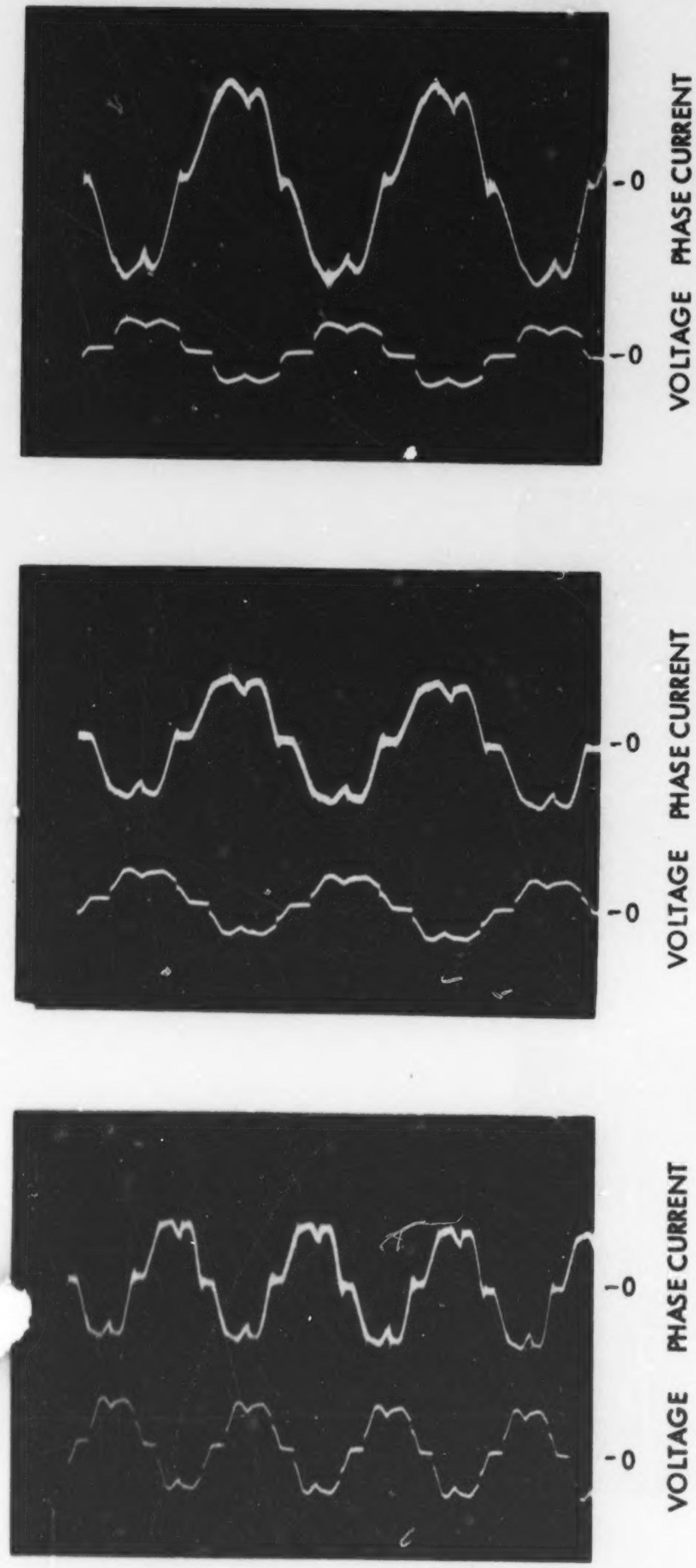

50 AMPERES DC
93 VOLTS DC
5000 RPM

30 AMPERES DC
97 VOLTS DC
5000 RPM

30 AMPERES DC
141 VOLTS DC
7500 RPM

ALL SCALES
30 AMPERES/cm
200 VOLTS/cm
1.0 MILLISECONDS/cm

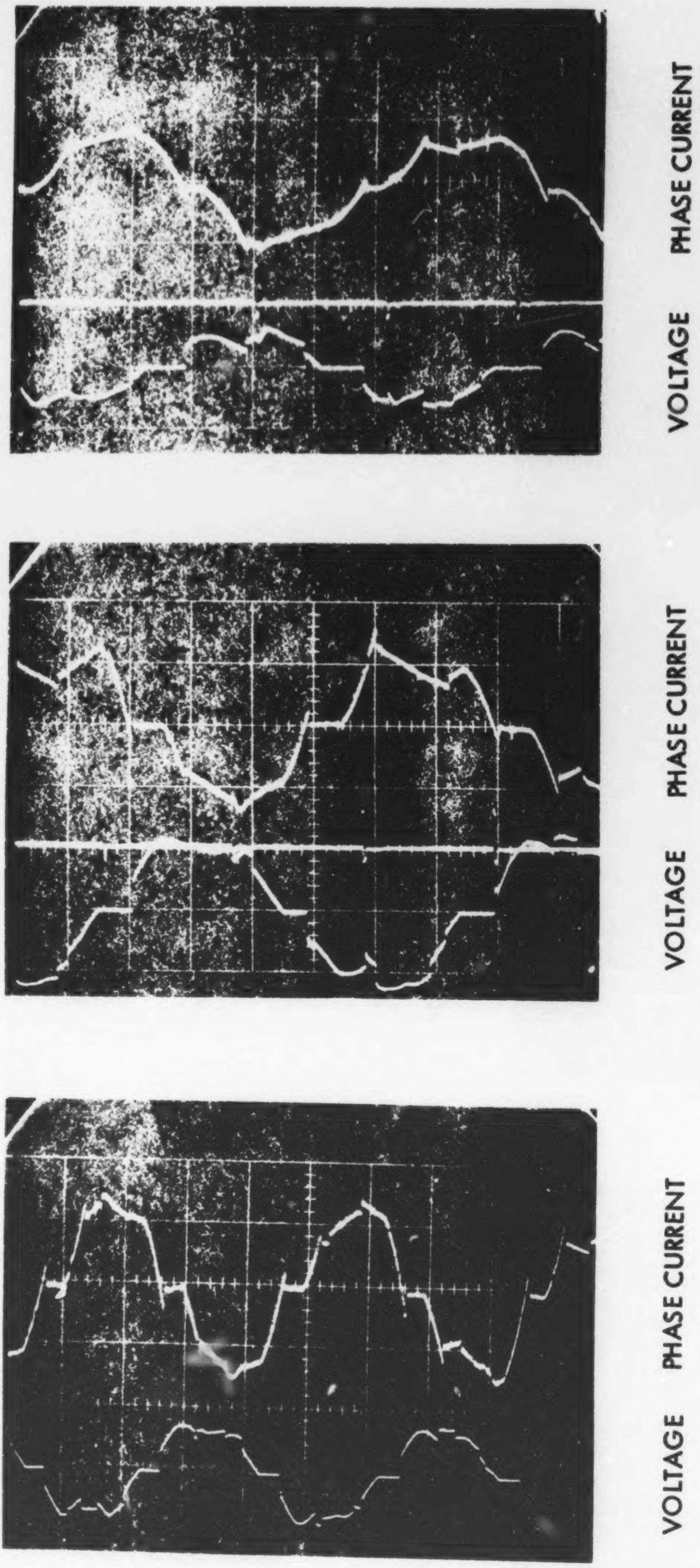

50 AMPERES DC
5000 RPM
75 AMPERES/cm
200 VOLTS/cm
0.5 MILLISECONDS/cm

30 AMPERES DC
5000 RPM
30 AMPERES/cm
200 VOLTS/cm
0.5 MILLISECONDS/cm

30 AMPERES DC
7500 RPM
30 AMPERES/cm
200 VOLTS/cm
0.5 MILLISECONDS/cm

FIGURE 7.4

## TABLE 7.1

## RATIO OF FOURIER COMPONENT TO FUNDAMENTAL (%) IN FIGURE 7.4

| | TOP FIGURE | MIDDLE FIGURE | BOTTOM FIGURE |
|---|---|---|---|
| 1st | 100 | 100 | 100 |
| 2nd | 6.6 | 4.3 | 4.5 |
| 3rd | 1.3 | 9.3 | 6.6 |
| 4th | 5.7 | >1.0 | 2.3 |
| 5th | 9.6 | 11.7 | 12.5 |
| 6th | 2.1 | 1.0 | 2.0 |
| 7th | 3.6 | 10.6 | 9.8 |
| 8th | 2.0 | 5 | 1.2 |
| 9th | 2.0 | 2 | 2.3 |
| 10th | <1.0 | 1.5 | 1.9 |
| 11th | 2.2 | 3.0 | 2.2 |
| 12th | 2.7 | 1.3 | 1.3 |

---

*ratio defined as $\frac{c_n}{c_1}$ ; where $c_n = \sqrt{a_n^2 + b_n^2}$

additional higher harmonics. These higher harmonics, although of lesser magnitude than the 5th, occur at such high frequencies that their resultant eddy currents are restricted extremely thin layers on the pole face.

Up to this point hysteresis losses have not been considered. These losses relate to the variations of the flux density, the frequency of variation and the magnetic material itself. The pole magnetic flux is always dominated by the main DC flux and the iron should be near or in saturation. The harmonic flux variations in the pole faces are restricted to a small layer due to the skin effect and their magnitude cannot be expected to produce a large B-H area.

### 7.2.2 Summary of Machine Analysis

The Speeder operates in an environment where windage and magnetic losses are extremely important. An advanced Speeder should be designed along the following guidelines:

- lower speed range to reduce windage and gear box losses as well as frequency of operation (the use of lower frequencies will also allow the use of slower diodes in the full wave rectifier)
- higher air gap flux density to minimize the effects of armature reaction
- introduction of low electrical conductivity pole faces by
    - using laminated pole faces
    - grooved pole faces on a solid pole
    - anisotropic iron (having a grain orientation with a high resistivity to eddy current flow).

## 7.3 Speeder PCU Improvements

The breadboard Speeder PCU control circuit was examined with respect to possible improvements. A number of such improvements were identified which would:

- employ control circuitry with linear characteristics
- permit the Speeder output to go to zero output
- utilize a constant frequency boost PCU
- minimize the current rating of the commutation SCR

- minimize the commutation capacitor requirement
- employ the inherent short circuit safety of the alternator design
- delete the requirement for field control and thus provide true constant field operation
- provide "back-up" overcurrent protection for the alternator above and beyond that possible duty cycle control only.

### 7.3.1 Linear Control Circuitry

The present Speeder PCU uses a variable time pulser (VTP) control logic. This logic, shown in Figure 7.5, utilizes a controlled current source to charge a capacitor which is connected to the emitter of a unijunction transistor (UJT). When the voltage on the capacitor equals the UJT trip voltage ($V_\eta$), the UJT transmits a pulse to the gate of the Speeder power SCR. The power SCR then conducts until commanded off by a 1.0 kHz sync pulse which also clears the timing capacitor. The power SCR off time is thus coincident with the period during which the capacitor is charging from zero to $V_\eta$ and may be varied by adjusting the magnitude of the charging current. The off time for this stage is given by:

$$t_{off} = \frac{(C)\ (V_\eta)}{I} = \frac{K_1}{I}$$

where C and $V_\eta$ are constants and I is the controlled variable. It is apparent from this expression that the controlled period ($t_{off}$) does not vary in a linear manner with the controlling parameter, I. Another circuit, the ramp and pedestal (RAP) control circuit, appears an attractive linear system. A simple form of the circuit is shown in Figure 7.6. The RAP circuit utilizes a constant current source to charge a capacitor which is connected to the input of a voltage controlled trigger circuit. When the voltage on the capacitor equals the trigger voltage ($V_{PED}$) a pulse is transmitted to the gate of the power SCR. The power SCR then conducts until commanded "OFF" by a 1.0 kHz sync pulse which also clears the timing capacitor. The power SCR "OFF" time is then coincident with the period during which the capacitor is charging from zero to $V_{PED}$ and may be varied by adjusting the magnitude of $V_{PED}$. The off time for this stage is:

FIGURE 7.5
VARIABLE TIME PULSER CONTROL

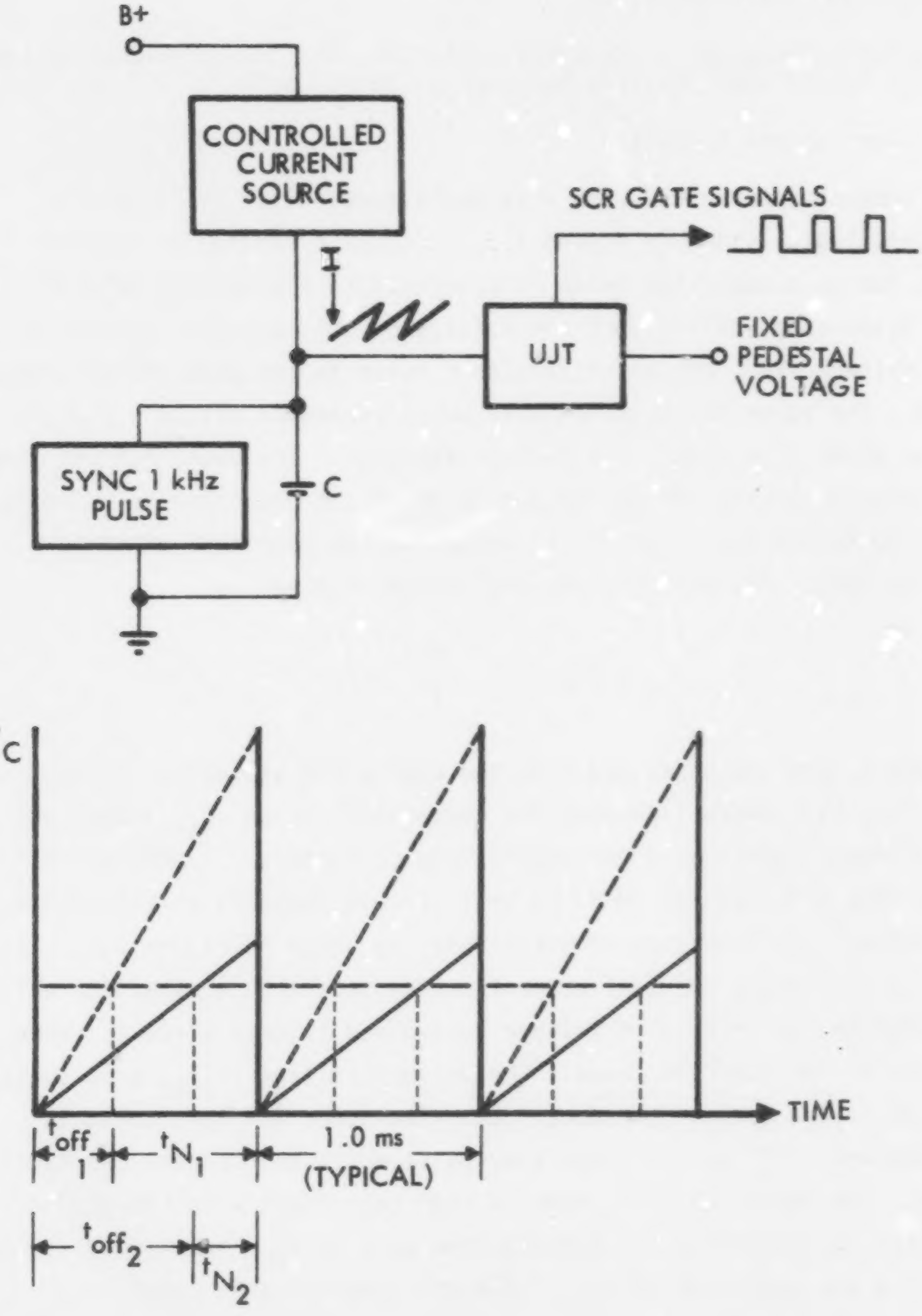
B+
CONTROLLED CURRENT SOURCE
I
SCR GATE SIGNALS
UJT
FIXED PEDESTAL VOLTAGE
SYNC 1 kHz PULSE
C
V_C
TIME
t_off1
t_N1
1.0 ms (TYPICAL)
t_off2
t_N2

FIGURE 7.6
RAMP & PEDESTAL CONTROL

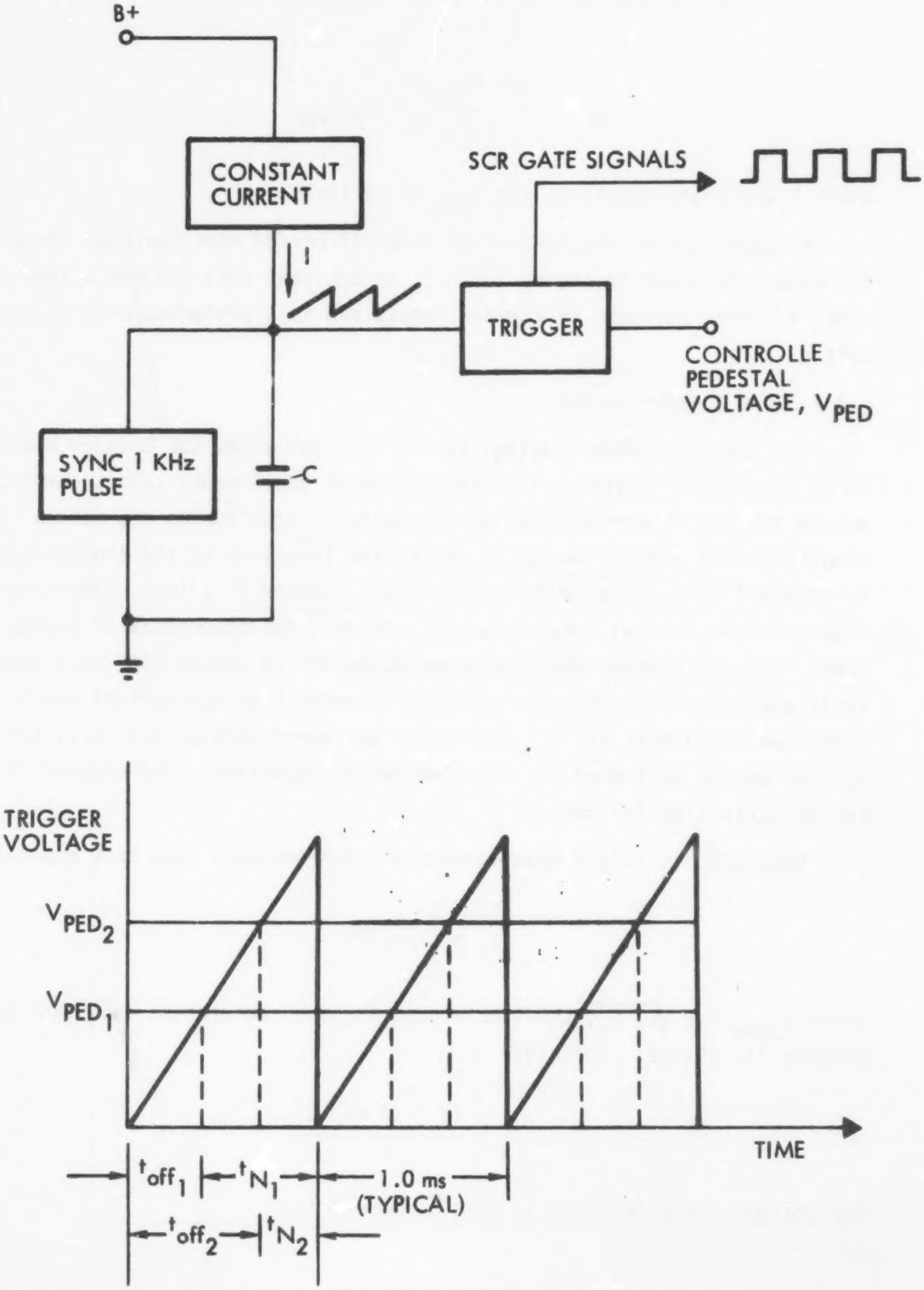
B+
CONSTANT CURRENT
I
SCR GATE SIGNALS
TRIGGER
CONTROLLE PEDESTAL VOLTAGE, $V_{PED}$
SYNC 1 KHz PULSE
C
TRIGGER VOLTAGE
$V_{PED_2}$
$V_{PED_1}$
TIME
$t_{off_1}$
$t_{N_1}$
1.0 ms (TYPICAL)
$t_{off_2}$
$t_{N_2}$

$$t_{off} = \frac{(C)\ (V_{PED})}{I} = K_2\ V_{PED}$$

where C and I are constants and $V_{PED}$ is variable.

A comparison of the controlled time-off period (for constant frequency operation) is shown in Figure 7.7. It is apparent that the RAP system provides a linear response to command inputs and is a preferred control circuit.

### 7.3.2 Zero Speeder Output

The present Speeder control system does not allow the Speeder output to go completely to zero. This in turn means the Speeder cannot completely unload the engine during cranking or engine control during operation. The problem of the present design is due to the inability of the present system to shut-off commutation when a zero output command is given. Examining Figure 3.1 of Section 3.4, it can be seen that two components of energy are drawn from the Speeder when the commutation SCR is pulsed "ON" once each cycle whether or not the power SCR was in conduction during that cycle. These two components are $E_L$--the energy delivered through SCR to L, and $E_C$--the energy delivered via the commutation capacitor. The components can be derived as follows:

When $SCR_C$ is pulsed into conduction, current will flow in L equal to:

$$I_s = \frac{V_s\ t_{comm}}{L}$$

where $t_{comm} = \Pi \sqrt{L_c\ C_c}$, the time needed for the commutation capacitor to reverse its charge. Therefore

$$I_s = \frac{(V_s)\ (\Pi \sqrt{L_c C_c})}{L}$$

The energy stored in L due to this component is:

FIGURE 7.7
COMPARISON OF VTP & RAP CONTROL RESPONSE

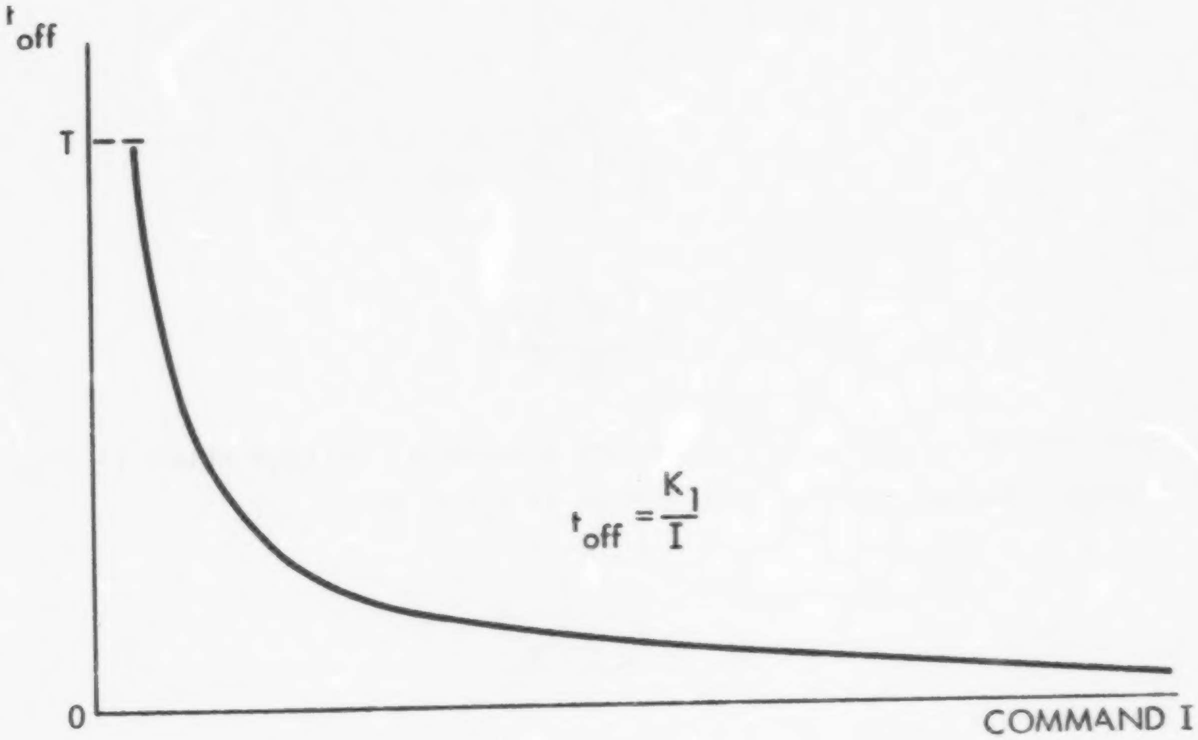

VTP COMMAND CURVE

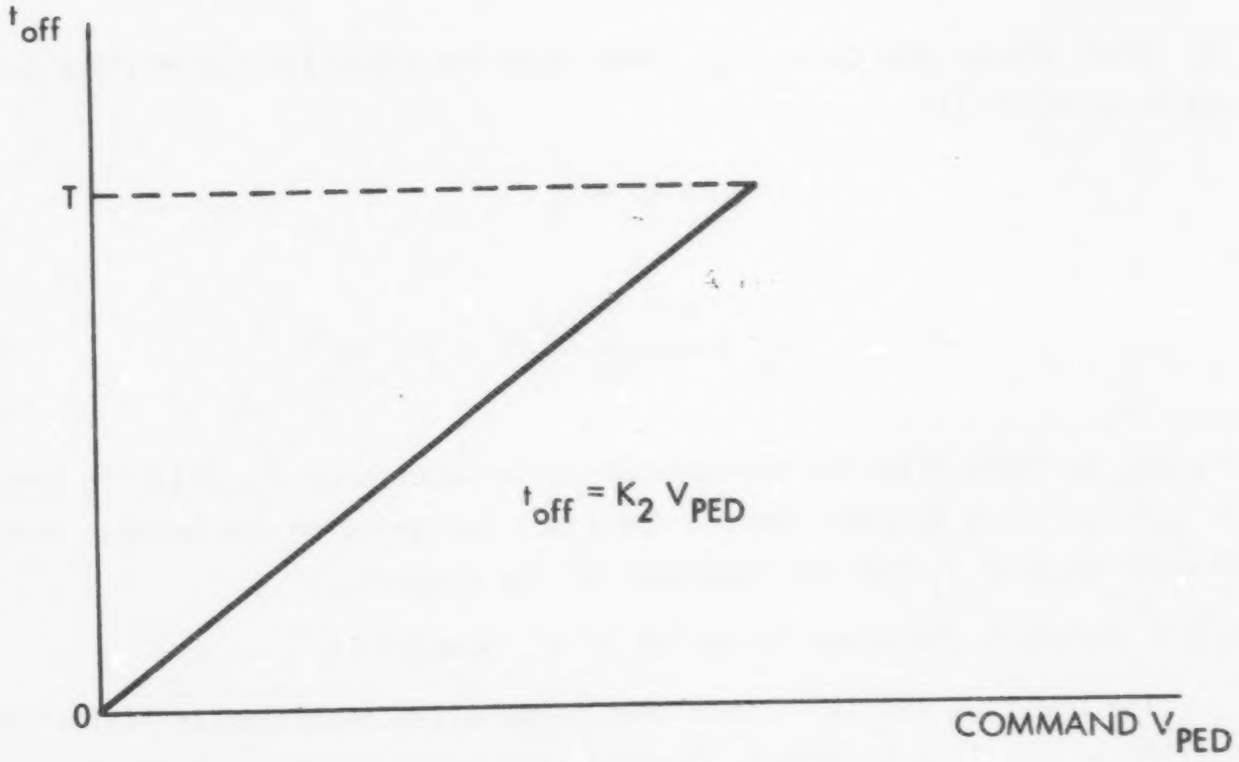

RAP COMMAND CURVE

$$E_L = \frac{L\ I_s^2}{2} =$$

$$E_L = \frac{L}{2}\left[\frac{(V_s)\ (\pi)\ (\sqrt{L_c C_c})}{L}\right]^2$$

$$E_L = \frac{V_s^2\ \pi^2\ L_c C_c}{2L}$$

The commutation capacitor $C_c$ traverses a terminal voltage equal to $2V_B$. The energy consumed during this action is equal to

$$E_C = \frac{C_c\left[2V_B\right]^2}{2}$$

$$E_C = 2\ C_V\ V_B^2$$

The total energy per cycle ($E_s$) taken from the alternator at minimum duty cycle is equal to:

$$E_s = E_L + E_C$$

$$E_s = \frac{V_s^2\ \pi^2\ L_c C_c}{2L} + 2\ C_c\ V_B^2$$

The energy taken from the Speeder per cycle depends on $V_s$, which in turn is a function of Speeder speed. The power delivered by the Speeder thus depends on both $V_s$ and the frequency of the chopper.

### 7.3.3 Constant Frequency Operation of the Speeder PCU

The previous section showed that commutation requirements limited the ability of the Speeder output to go to zero. The present Speeder PCU compensates for this limitation by adjusting to a lower frequency of operation if low outputs are needed. This variable frequency mode of operation has the disadvantages outlined in Section 2.2.2.2. Advanced Speeder PCU techniques should incorporate means for constant frequency operation while retaining the capability of low power control.

### 7.3.4 Commutation SCR Rating

If the commutation SCR in the present system is pulsed "On" when the power SCR is not conducting, a parasitic current, $I_s$, flows in the commutation SCR as described in 7.3.2. In turn the commutation SCR must be capable of carrying an additional current above the normal commutation current, and the higher rating means higher dissipation and cost.

An upgraded Speeder control circuit must include a logic gating network which will always cause the power SCR to be gated on whenever the commutating SCR receives a turn-on command. This technique will insure that the power SCR conducts the load (inductor L) component of current, while the commutating SCR will never carry more than its design commutation load.

### 7.3.5 Minimize the Commutation Capacitor Requirement

If the commutation capacitor does not have a sufficient charge when the commutation SCR is pulsed on, the commutation will not succeed and both the commutation SCR and the power SCR will remain in conduction. In this case, both devices will have excessively large currents from the Speeder. The present system has no protection against this mode of failure.

An upgraded PCU should include a voltage detector which monitors the voltage on the commutation capacitor and compares it to a fixed reference. Whenever the capacitor voltage is below a minimum required value, a lockout signal should insure that neither the power SCR nor the commutation SCR can be turned on.

### 7.3.6 Utilize the Inherent Short Circuit Design Features of the Speeder

When the armature of an alternator draws current, a reaction component of flux is induced in the field structure which tends to oppose the main field flux. This effect, termed armature reaction, reduces the terminal voltage. Under short circuit conditions, the armature reaction flux can be so large in comparison to the main field flux that the net induced armature voltage is very small. The short circuit current is the induced voltage divided by the winding impedance. The short circuit current of the Speeder should be included as a major parameter in the selection and rating of Speeder PCU components and in methods of fault protection.

### 7.3.7 Elimination of Field Control

The terminal voltage of the battery in the EMT system varies widely due to changing load and charge state conditions. Voltages from 140 to 260 VDC have been observed. In order to work into this voltage range and provide Speeder torque and yet preserve the boost mode of PCU operation, the present Speeder PCU incorporates a field control circuit which adjusts the alternator field so as to maintain the Speeder output voltage below battery voltage. This method has two shortcomings: (1) it requires additional control circuitry, and (2) the capacity of the machine is not properly utilized and thus it is larger than might otherwise be required.

The Speeder should be designed to have an output voltage at rated speed and saturated field less than the minimum anticipated battery voltage. This redesign would allow the additional controls to be eliminated and insure the machine is always used at full field. The disadvantages of this approach is the more stringent current requirements on the remaining control and power circuits as well as a slightly higher current rating of the machine.

### 7.3.8 Overcurrent Control

The present control circuit employs a current sensing network plus a field current regulator to limit the current drawn from the alternator. This requires a complex circuit containing many components and is not effective in the event a failure occurred in the control circuit.

An advanced system is needed containing a current sensing network which operates a sequencer in series with the field. If the current rises above a predetermined level, the circuit is opened for a fixed length of time and then reset. This action will occur repeatedly for a predetermined number of sample cycles, after which some fault indication should be provided to the vehicle operator.

## 7.4 Preliminary Design of an Advanced Speeder PCU Control Circuit

A block diagram of an advanced Speeder PCU control circuit is shown in Figure 7.8. The essential elements are:

- ramp generator
- clock oscillator
- pedestal comparator
- L-multiplier
- error amplifier
- SCR gate drives
- commutation lock-out.

The signal inputs to the control circuit are:

- engine tachometer speed
- Speeder alternator current
- commutation capacitor voltage.

The output signals are:

- power SCR gate drive
- commutation SCR gate drive.

The system employs a constant frequency ramp and pedestal comparator in conjunction with a fixed reference and an error amplifier to control the fraction of the ramp period during which the battery presents a load to the Speeder. A network termed the "L-multiplier" is incorporated to enhance system stability by preventing the Speeder current from changing until commanded to do so by the tachometer signal. A protection network denoted the "commutation lock-out" is provided to prevent either the power SCR or the commutation SCR from conducting in the event an insufficient charge is stored in the commutation capacitor immediately prior to SCR conduction.

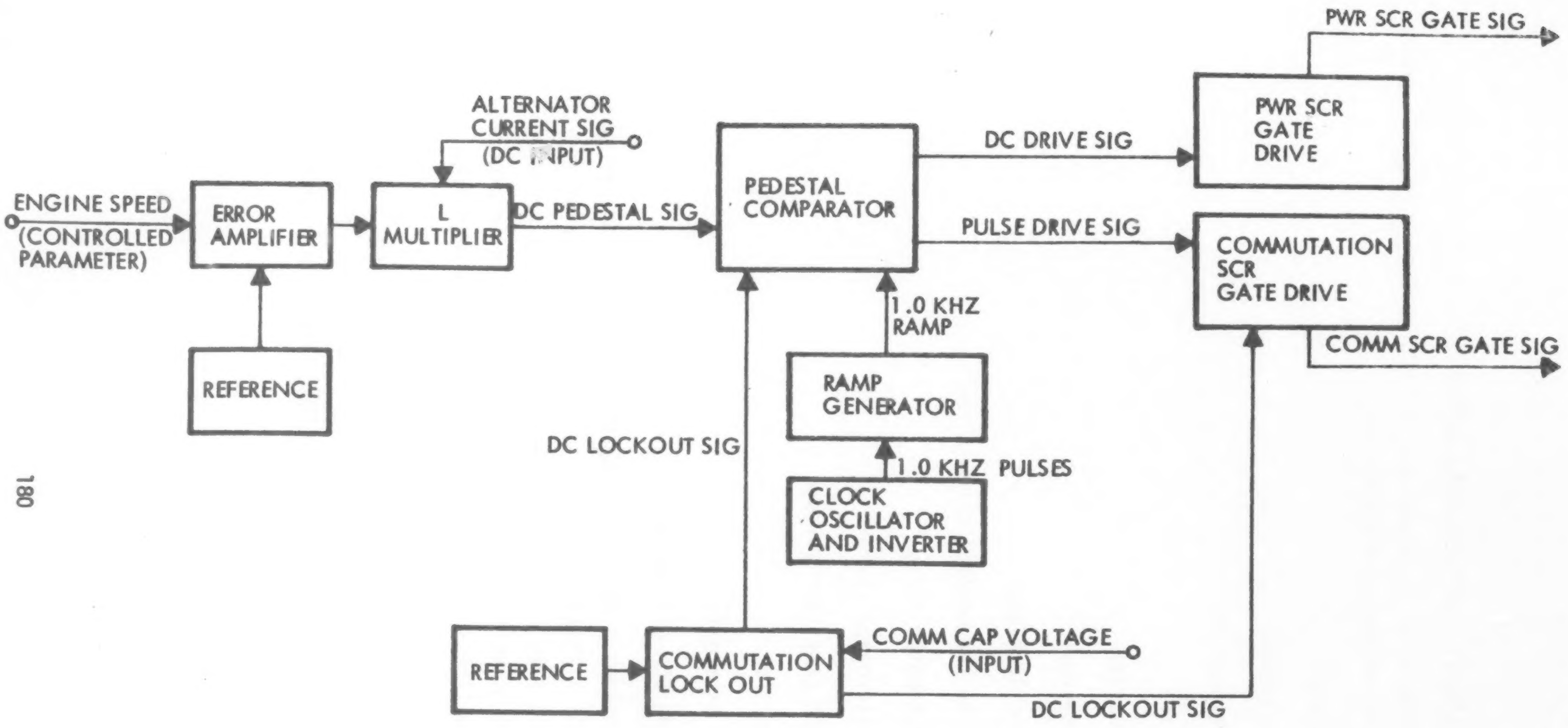
PWR SCR GATE SIG
ALTERNATOR CURRENT SIG (DC INPUT)
PEDESTAL COMPARATOR
DC DRIVE SIG
PWR SCR GATE DRIVE
ENGINE SPEED (CONTROLLED PARAMETER)
ERROR AMPLIFIER
L MULTIPLIER
DC PEDESTAL SIG
PULSE DRIVE SIG
COMMUTATION SCR GATE DRIVE
1.0 KHZ RAMP
COMM SCR GATE SIG
REFERENCE
RAMP GENERATOR
DC LOCKOUT SIG
1.0 KHZ PULSES
CLOCK OSCILLATOR AND INVERTER
COMM CAP VOLTAGE (INPUT)
REFERENCE
COMMUTATION LOCK OUT
DC LOCKOUT SIG

FIGURE 7.8
BLOCK DIAGRAM OF ADVANCED SPEEDER PCU

### 7.4.1 Ramp Generator

The ramp generator circuit consists of a constant current source which charges a capacitor at a fixed rate. The capacitor is discharged by means of the clock oscillator at a rate much faster than the rate of capacitor charging.

### 7.4.2 Clock Oscillator

The clock oscillator is composed of components which form a saturable magnetic multivibrator whose operating frequency is adjusted to and held constant at 500 Hz by the output of a positive voltage regulator. The output of the clock is differentiated and rectified thereby producing a 1.0 kHz pulse train.

### 7.4.3 Pedestal Comparator

Duty cycle control is accomplished by applying the constant frequency ramp signal to the sensing base of a trigger circuit while maintaining the reference base at the pedestal voltage of the error amplifier. When the ramp voltage is below the pedestal voltage, the comparator outputs a gate signal and the power SCR is programmed "on". When the ramp rises above the pedestal voltage, the comparator puts out a signal which turns on the commutation SCR. The commutation circuit then turns the commutation and power SCRs off. The SCRs remain off until the power SCR is again commanded "on" by the next clock pulse.

### 7.4.4 L-Multiplier

The L-multiplier is a minor servo-loop which maintains the Speeder current constant with respect to any EMT parameter changes which do not cause the engine tachometer signal to change. This minor control loop is employed since it can response much faster than the main error amplifier. Because the minor loop attempts to hold the alternator current constant, the energy storage inductance of the Speeder system appears to be much larger than it actually is; hence, the name "L-multiplier". The output of the L-multiplier determines the value of the pedestal voltage and is phased such that changes in the Speeder current signal cause a change in the power stage duty cycle so as to restore the reference current signal.

### 7.4.5 Error Amplifier

The error amplifier monitors the tachometer signal and compares it with a fixed reference. The output of the error amplifier is the reference voltage for the L-multiplier. When the tachometer signal departs from the desired value, the error amplifier transmits a corresponding voltage change to the L-multiplier which in turn causes a shift in the pedestal voltage.

### 7.4.6 SCR Gate Drive Stages

The gate of the commutating SCR is turned on by signals from the commutating SCR gate drive. The drive in turn receives its command signal from the pedestal comparator. The drive stage is also connected to the power SCR gate drive in such a manner as to pulse the power SCR "on" whenever the commutation SCR receives an "on" command. The power SCR gate drive receives its initial command pulse from the clock by way of the pedestal comparator. The drive puts out a steady "on" gate signal until the ramp voltage crosses the pedestal voltage again when the gate signal is removed.

To reduce the effect of commutation on the lower limits of power control a pulse skipping feature is used. When the pedestal voltage goes to zero, commanding a zero power output, no gate signal is applied to the power SCR. Since the previous function of the pedestal comparator was to turn off the commutation SCR, both SCRs are turned off and remain in that state until a finite pedestal voltage is applied.

### 7.4.7 Commutation Lock-Out

The voltage of the commutation capacitor is monitored and compared to a fixed reference. If the capacitor voltage is below the required minimum value, the pedestal voltage is forced to zero and holds the commutation SCR gate pulse circuit inoperative.

## 7.5 Speeder System Failure Analysis and Protection

### 7.5.1 Speeder System Operation and Protection

The basic requirements of the Speeder PCU is to regulate the speed of the engine by providing a variable torque load on it. The design of the PCU is such that it cannot operate unless the traction battery is connected to its output. With regard to the Speeder system, the battery is not a source of power as it is the Torquer, but is the output load which must be present to absorb the inductive energy stored in the PCU.

A block diagram of the Speeder system is shown in Figure 7.9 which includes the elements which are required to control the Speeder system in the event of failure within that group. The power handling elements, alternator, PCU, batteries and logic directly related to the PCU operation are essentially the same as those used in the breadboard equipment. The fault protection circuit allows power to flow from the alternator only when all safety conditions are satisfied. In the protection system the power from the Speeder is controlled entirely by the presence or absence of the field current. The conditions to be satisfied for field current to flow are:

- the battery voltage must be above a preset level
- $SCR_1$ and $SCR_C$ must not be permanently on
- the Speeder current must exceed a preset level
- the engine ignition switch must be on
- the PCU or Speeder cannot be overheated.

The field sequencer portion of the fault protection circuit monitors the above conditions and decides whether or not field current should flow. (This element also is used to defeat the Speeder field during engine cranking.) It functions by momentarily removing the possibility for electric power generation and thereby allows the current flow in the SCRs to decay and recover. The sequencer also decides when, after a series of unsuccessful attempts to establish normal operation, to signal the operator that the system may be failing and should be shut down.

The only other source of energy into the Speeder PCU is that which could flow from the battery. Relays are of no use in this application since a reverse current flow indicates a serious Speeder system failure. Fuses are therefore preferred. Since the protection system operates by field control it is important that it be tied to the engine throttle contro Any extended field removal must also cause the throttle to cut-back or unacceptable engine (and Speeder) speeds may occur.

FIGURE 7.9
ADVANCED SPEEDER CIRCUITRY WITH FAILURE DETECTOR
& SAFETY PROTECTION

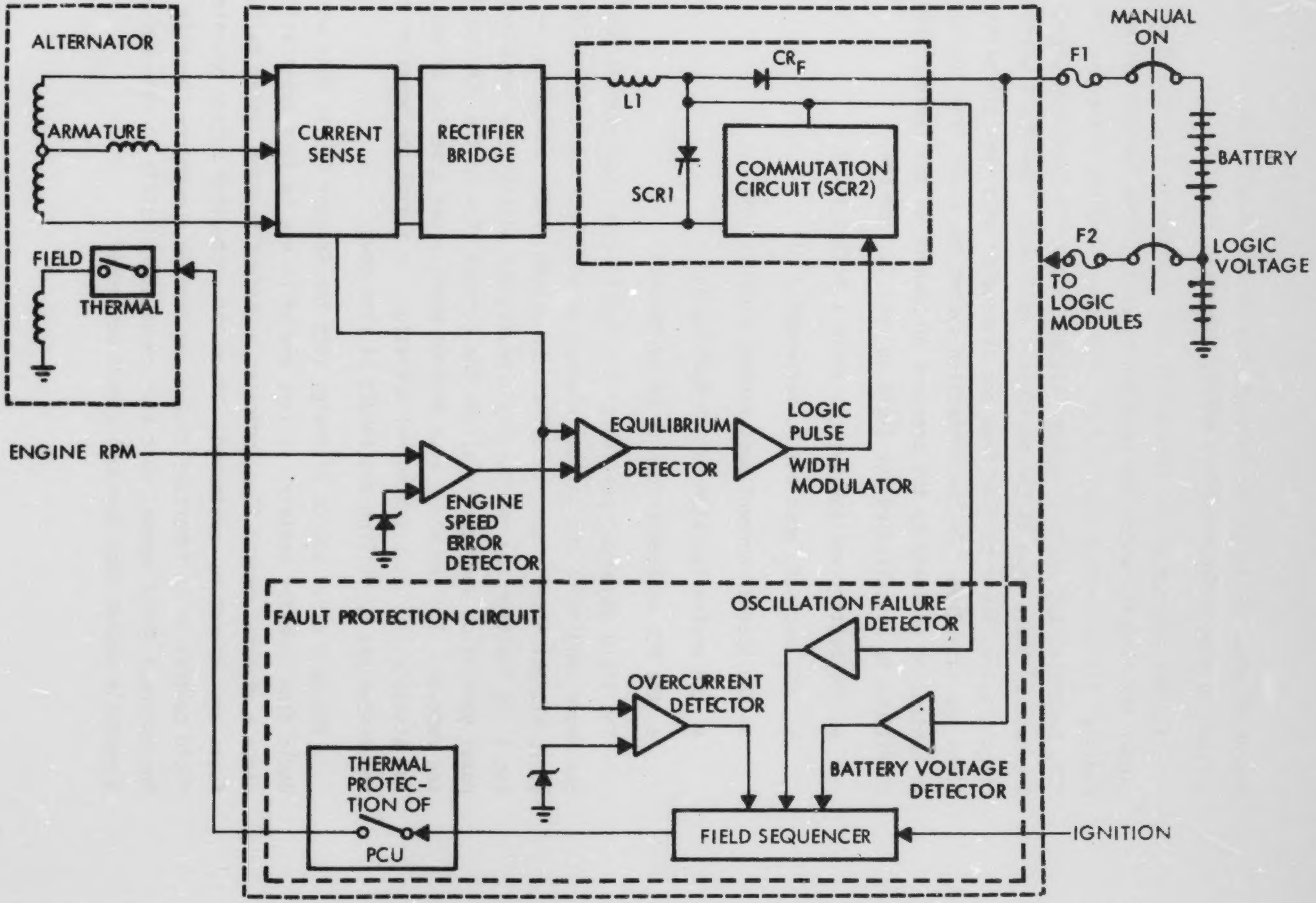
ALTERNATOR
ARMATURE
FIELD
THERMAL
CURRENT SENSE
RECTIFIER BRIDGE
L1
CR_F
SCR1
COMMUTATION CIRCUIT (SCR2)
F1
MANUAL ON
BATTERY
F2
LOGIC VOLTAGE
TO LOGIC MODULES
ENGINE RPM
ENGINE SPEED ERROR DETECTOR
EQUILIBRIUM DETECTOR
LOGIC PULSE WIDTH MODULATOR
FAULT PROTECTION CIRCUIT
OSCILLATION FAILURE DETECTOR
OVERCURRENT DETECTOR
BATTERY VOLTAGE DETECTOR
THERMAL PROTECTION OF PCU
FIELD SEQUENCER
IGNITION

### 7.5.2 Abnormal Performance with Automatic System Recovery

#### 7.5.2.1 Speeder PCU SCRs Fail to Commutate Off

If the Speeder PCU SCRs fail to commutate off due to misfire, temporary overload, or temporary battery voltage collapse, a detection circuit senses that the pulse width modulator has stopped oscillating. When this is detected the field and logic current are disconnected for a minimum of 200 milliseconds and then reapplied. During this time the current in the SCRs will go to zero and, as there are no gate pulses, they will turn-off. The external effect will be a momentary increase in engine speed followed by normal operation in about 0.5 seconds.

### 7.5.3 Abnormal Performance with Degraded System Functioning

#### 7.5.3.1 Speeder PCU Does Not Control the Engine Speed Properly (within 25% of reference speed)

The Speeder PCU might not be able to regulate the engine speed for the following reasons:

- the logic amplifiers do not operate correctly
- the PCU does not transmit the Speeder power
- the Speeder does not produce torque
- the engine torque increases or decreases to a level the Speeder system cannot control. This failure would be associated with the engine control or the engine itself and will not be considered here.

If the speed error detector, equilibrium detector, or logic pulse-width modulator fail to perform their required function the regulated speed of the engine can be affected. If the PCU attempts to regulate the engine at a higher speed, the PCU would not recognize the engine's departure from its reference speed. For example, a high engine speed implies a low current in the Speeder and there is no protection for this condition. If the Speeder forces the engine speed down the PCU would have to operate at a higher current. In order to prevent a continued overcurrent condition, a thermal interlock would remove the field current and the engine speed would increase.

#### 7.5.3.2 Engine Controller Fails in Mode One

If the engine controller allows the engine power to rise, the Speeder PCU will increase the Speeder armature current. Even if the Speeder does not close torque due to armature reaction, a prolonged heating of the Speeder or Speeder PCU will cause the thermal protection system to dump the field current.

In the event that the engine power falls the PCU will decrease its load as far as its control range allows. This of course may keep the engine under control, but sustained low engine power will ultimately cause the battery to deplete its charge.

### 7.5.4 Abnormal Performance with Complete System Stoppage

If the Speeder is unable to produce a reaction torque on the engine, engine torque cannot be transmitted to the rear wheels and the engine must be throttled down or another means for reaction torque must be provided. If the engine is throttled down or shut off the vehicle can still proceed for a short distance using the battery and Torquer if the engine can be uncoupled from the drive train.

#### 7.5.4.1 Shorted or Opened Windings

If the Speeder develops an interwinding short it will dissipate some of the power which normally passes through the PCU. The speed regulator will continue to adjust the duty cycle to keep the engine speed constant, and there will be no apparent effect on the system operation until the alternator overheats and is turned off and/or burns open the effected winding. Similarly if a winding opens up due to vibration or abrasion, the Speeder will lose torque and the engine must be shut down.

#### 7.5.4.2 Shorting of Speeder PCU SCRs

A direct short of the Speeder SCRs ($SCR_1$ and $SCR_2$) will produce the same immediate effect as a hang-up, described in Section 7.5.2.1 except that the reapplication of power will not succeed in establishing normal operation. Rather the logic sequencer will try again to apply power, and after a series of attempts the timing network will permanently turn-off the alternator power. A warning signal will have to be presented to the operator.

### 7.5.4.3 Speeder PCU Block Diode Open

The Speeder PCU blocking diode ($CR_F$) is the only direct link with the battery. If this link is opened the energy in storage inductor will produce whatever voltage is required to provide a path for its current. With $CR_F$ open the only possibility is to force $SCR_1$ or $SCR_2$ to breakdown and conduct in the forward direction.

### 7.5.4.4 Speeder PCU Blocking Diode Shorted

A short circuit in $CR_F$ will allow the battery current to flow backward through $CR_F$ (shorted), and $SCR_1$. The fuse between the PCU and the battery, $F_1$, will open and the alternator power will be removed.

### 7.5.5 Summary of Speeder Failure Analysis

Table 7.2 summarizes the above failure modes and contemplated courses of action. Almost all Speeder failures result in the possibility of engine overspeed and it is obvious that some means of overspeed protection must be provided. In no case would a Speeder system failure present a real hazard to the operator or vehicle.

## TABLE 7.2
## SPEEDER PCU FAILURE DETECTION & PROTECTION SYSTEM

| COMPONENT OR CIRCUIT | TYPE OF FAILURE | METHOD OF PROTECTION | DEGREE OF DISABILITY |
|---|---|---|---|
| Speeder PCU | | | |
| SCR1<br>SCR2 | Failure to Commutate | Automatic Reset | None |
| | Shorted or Degradation of Commutation Ability | Field Sequencer will turn Power off | Engine will Speed up |
| | Open | None needed | " |
| $CR_F$ | Short | Fuse F1 will Open, to turn PCU off. | " |
| | Open | Field Sequencer will turn Power off | " |
| Commutation Circuit | Does not provide adequate reverse bias to turn off SCR1 & SCR2 | " " | " |
| L1 | Open | None needed | " |
| | Shorted turns | " "<br>Overcurrent sense will eventually actuate field sequencer. | Peak current in the PCU will rise, possibly beyond the commutation capability. |
| Rectifier Bridge | Open | None needed | Engine will Speed up |
| | Short | Field Sequencer will turn power off | " " |
| Current Sense | Indicates high current | None needed | " " |
| | Indicates low current | Thermal protection will turn power off | Engine may drop in speed until thermal protection activates, then engine will speed up |

## TABLE 7.2
(Cont'd)

| COMPONENT OR CIRCUIT | TYPE OF FAILURE | METHOD OF PROTECTION | DEGREE OF DISABILITY |
|---|---|---|---|
| ICE Speed Error Detector,<br>Current Regulator<br>Pulse Width Modulator | Commands less then required current | None in PCU (Engine should be self-protected) | Engine speed will increase, depending on the degree of failure |
| | Commands more then required current | Field sequencer will turn power off if over-current is reached | Engine speed will decrease depending on the degree of failure |
| Speeder Alternator | | | |
| Armature, Field | Open | None needed | Engine will speed up |
| | Shorted turns | " " | " " |

## 8.0 ADVANCED EMT POWER TRAIN OPERATIONAL CONCEPTS

This section describes work associated with three areas of advanced system design:

- Solid state switching of the Torquer PCU between the drive and regeneration configurations
- EMT power train start-up concepts
- System override approaches

### 8.1 Solid State Switching System

#### 8.1.1 Three-Power Relay System

The original design of the Torquer PCU used three power relays to switch the semiconductors and motor elements between drive and regeneration. The power elements of that circuit are shown in Figures 8.1 and 8.2. The three relays are termed $M_3$, $M_4$ and $M_5$. The relay $M_3$ is used to establish the configuration of the power unit of the pulsewidth modulator; relays $M_4$ and $M_5$ operate on the Torquer field to direct the current flow in either drive or regeneration.

Flyback diodes are used in both configurations to provide a path for the inductive energy of the Torquer. These flyback diodes are presently two separate devices, but they also could be combined into one semiconductor switched by a double-pole double-throw relay. However, their low cost relative to high current relays and their impedance from commutator requirements favors the two device approach. The main power switching element $SCR_1$ and its associated circuitry are of such a cost that it is desirable to use a relay to connect it to the PCU in order that it can be used both in drive and regeneration.

$M_3$ must be capable of conducting peak currents up to 400A. To reduce the size and rating of this relay, a sequence of events during switching was established so that current never flows through its contacts while they are open. If this condition can be guaranteed, then a low standoff voltage contactor (one which can only switch low voltage, but still has high isolation capability during the non-ionized periods across the contacts) can be used. The difference in volume and weight between a contactor which can interrupt 24 VDC inductive load and a contactor for 200 V inductive load is approximately 5 to 1.

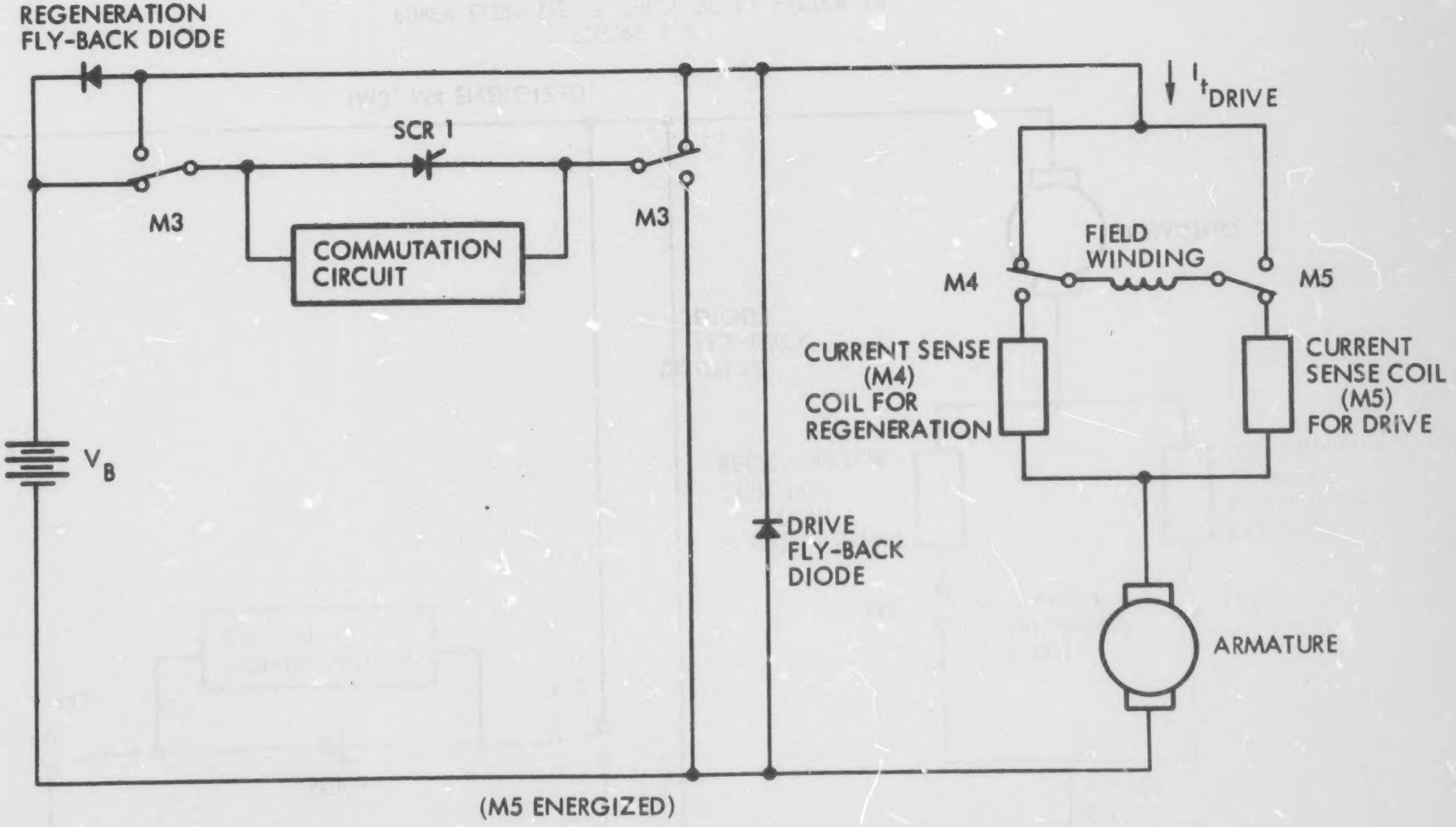
REGENERATION
FLY-BACK DIODE
SCR 1
M3
COMMUTATION
CIRCUIT
M3
$I_{t_{DRIVE}}$
FIELD
WINDING
M4
M5
CURRENT SENSE
(M4)
COIL FOR
REGENERATION
CURRENT
SENSE COIL
(M5)
FOR DRIVE
$V_B$
DRIVE
FLY-BACK
DIODE
ARMATURE
(M5 ENERGIZED)

FIGURE 8.1
POWER ELEMENTS OF THREE RELAY SYSTEM IN DRIVE

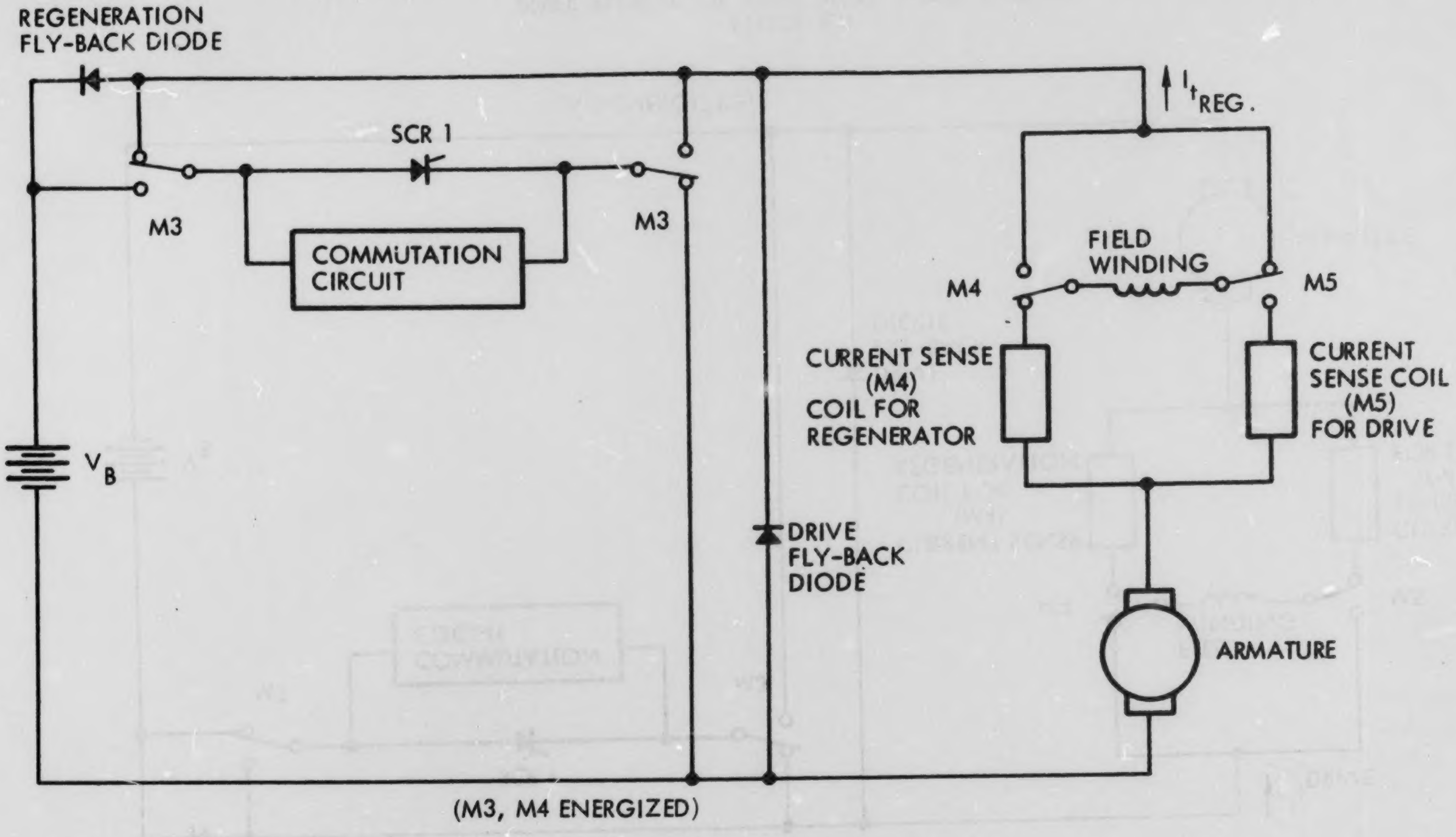
REGENERATION FLY-BACK DIODE
SCR 1
M3
M3
COMMUTATION CIRCUIT
$I_{t_{REG.}}$
FIELD WINDING
M4
M5
CURRENT SENSE (M4) COIL FOR REGENERATOR
CURRENT SENSE COIL (M5) FOR DRIVE
$V_B$
DRIVE FLY-BACK DIODE
ARMATURE
(M3, M4 ENERGIZED)

FIGURE 8.2
POWER ELEMENTS OF THREE RELAY SYSTEM IN REGENERATION

The present EMT system never operates in reverse on the dynamometer. In an actual vehicle application, reverse driving can be done by gear shifting or by reversal of the motor terminal polarity. Assuming as a first case, the motor will always rotate in the same direction, the armature voltage must retain the same polarity in drive and regeneration, and therefore the polarity of the field with respect to the armature must change. In the three relay system, the armature remains permanently wired to the ground side of the battery, whereas the field is switched. Two single pole double-throw relays, $M_4$ and $M_5$, are used to invert the field of the motor, so that it can act as a generator. $M_4$ and $M_5$ have 24 volt activating coils used to pull the relays open and closed. In addition, both coils have a current coil of five turns which carries the load current of each relay when it is energized. Even if the voltage coil is deenergized, the relay will be held in the energized position until the load current drops to a low level. This interlock prevents the relay contacts from opening while a certain minimum allowable current is still flowing through the contacts.

The sequence of operation of the three relay system upon the operator commanding a transfer from drive to regeneration or vice versa is as follows:

- The duty cycle of the chopper circuitry is reduced to a minimum.
- The power to the logic system of the chopper is turned off, insuring that commutation ceases and power cannot flow through the commutation circuit.
- The power to the 24 V coil on $M_4$ and $M_5$ is removed.
- As the current through the five turn coil of $M_4$ or $M_5$ (depending on direction of the transfer) decays below a minimum level, that relay drops out.
- When the relay drops out, it disconnects or connects, the 24 volt coil on $M_3$, establishing the configuration of the power module.
- Contacts on $M_3$ reestablish the 24 volts to $M_4$ or $M_5$ which operate and transfer the configuration of the series field.
- The power to the logic is reconnected and commutation oscillation starts.
- Finally the command signal to the chopper is allowed to build-up to the desired value.

### 8.1.2 Two Relay System

The number of relays in the switching operation can be reduced if instead of switching the position of the field and $SCR_1$, they are left in a fixed position and the armature switched. Figure 8.3 shows such a scheme. $SCR_1$ must be located at all times with its cathode at a potential closer to ground than the anode. In drive it conducts from the high potential of the battery to ground, and in regeneration from the armature to ground. Instead of using a relay to switch it from battery potential to ground level, it can be permanently connected to ground. If in addition the field is connected in series with $SCR_1$, then its magnetic flux is always in the same direction in both configurations. The remaining requirement is to locate the armature in drive so that it can accept battery power by way of $SCR_1$ yet be capable of relocation in regeneration.

A single double-pole, double throw could be used in the application; however, to insure that there cannot be an opening of the contacts under load it is safer to retain the two separate relay configurations. This way transfer in either direction cannot occur until the current has decayed to low level.

The primary differences between the three and two relay systems are associated with the PCU's total system interface and the need to sequence two relays instead of three relays between drive and regeneration. Note that with the two relay system transition time between drive to regeneration is shorter and vehicle controllability is better.

### 8.1.3 One Relay System

The diagram of Figure 8.3 shows that the flow of current through the contacts of $M_4$ and $M_5$ are unidirectional. A single SCR or rectifier could be inserted instead of the four contacts and still retain the circuit functions if the characteristics of the solid state devices can be mated to the circuit. The application of semiconductors would decrease transfer switching times, but at some loss in efficiency due to the inherent conduction and switching losses of the devices.

Figure 8.4 shows a modification of the two relay systems. The $M_4$ relay is replaced by two rectifiers, $CR_R$ and $CR_D$. $CR_R$ blocks current flow during drive and conducts during regeneration. $CR_D$ conducts during

FIGURE 8.3
TWO RELAY SYSTEM

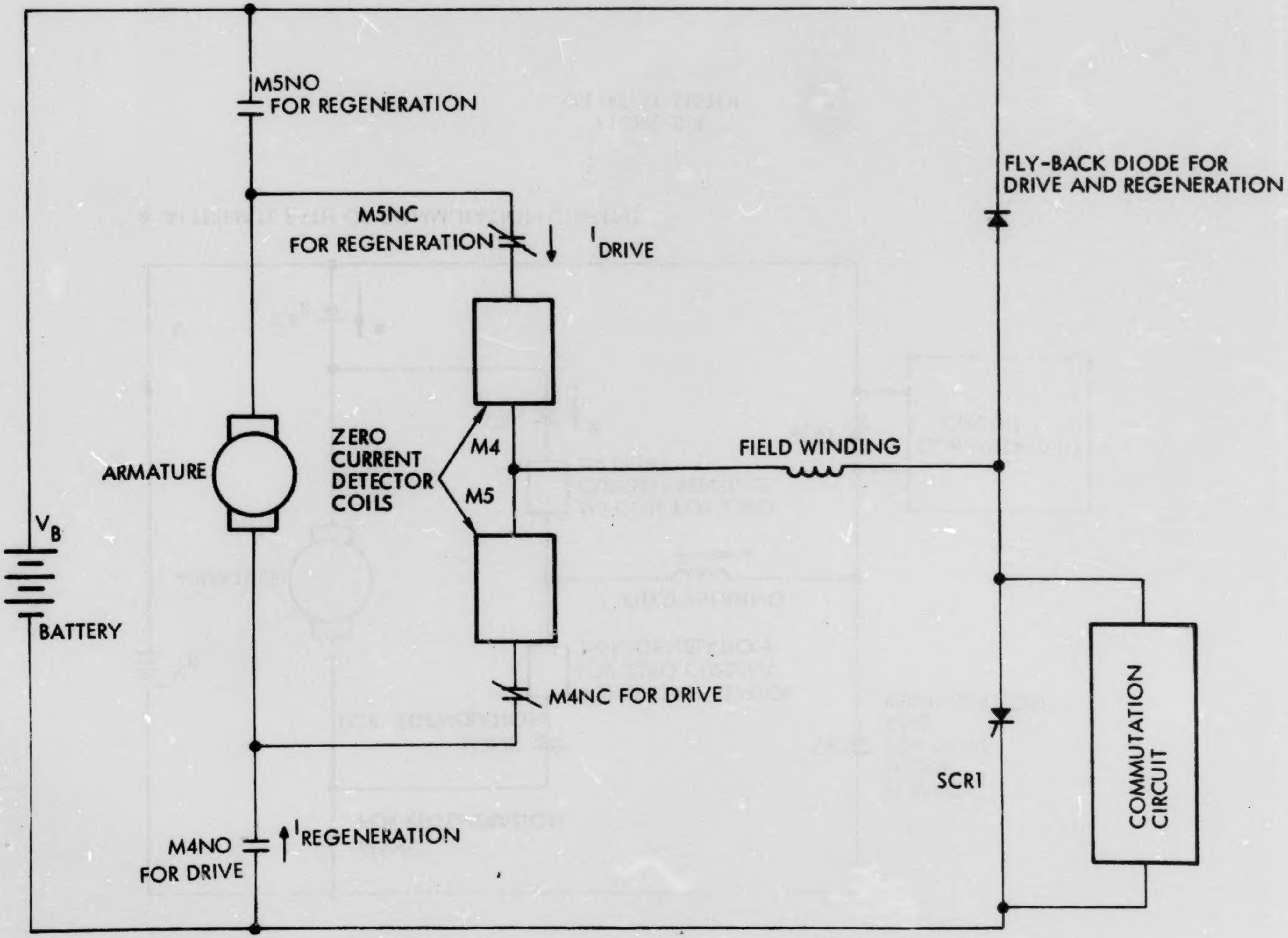
M5NO
FOR REGENERATION
FLY-BACK DIODE FOR
DRIVE AND REGENERATION
M5NC
FOR REGENERATION
$I_{DRIVE}$
ZERO
CURRENT
DETECTOR
COILS
M4
M5
ARMATURE
FIELD WINDING
$V_B$
BATTERY
M4NC FOR DRIVE
SCR1
COMMUTATION
CIRCUIT
M4NO
FOR DRIVE
$I_{REGENERATION}$

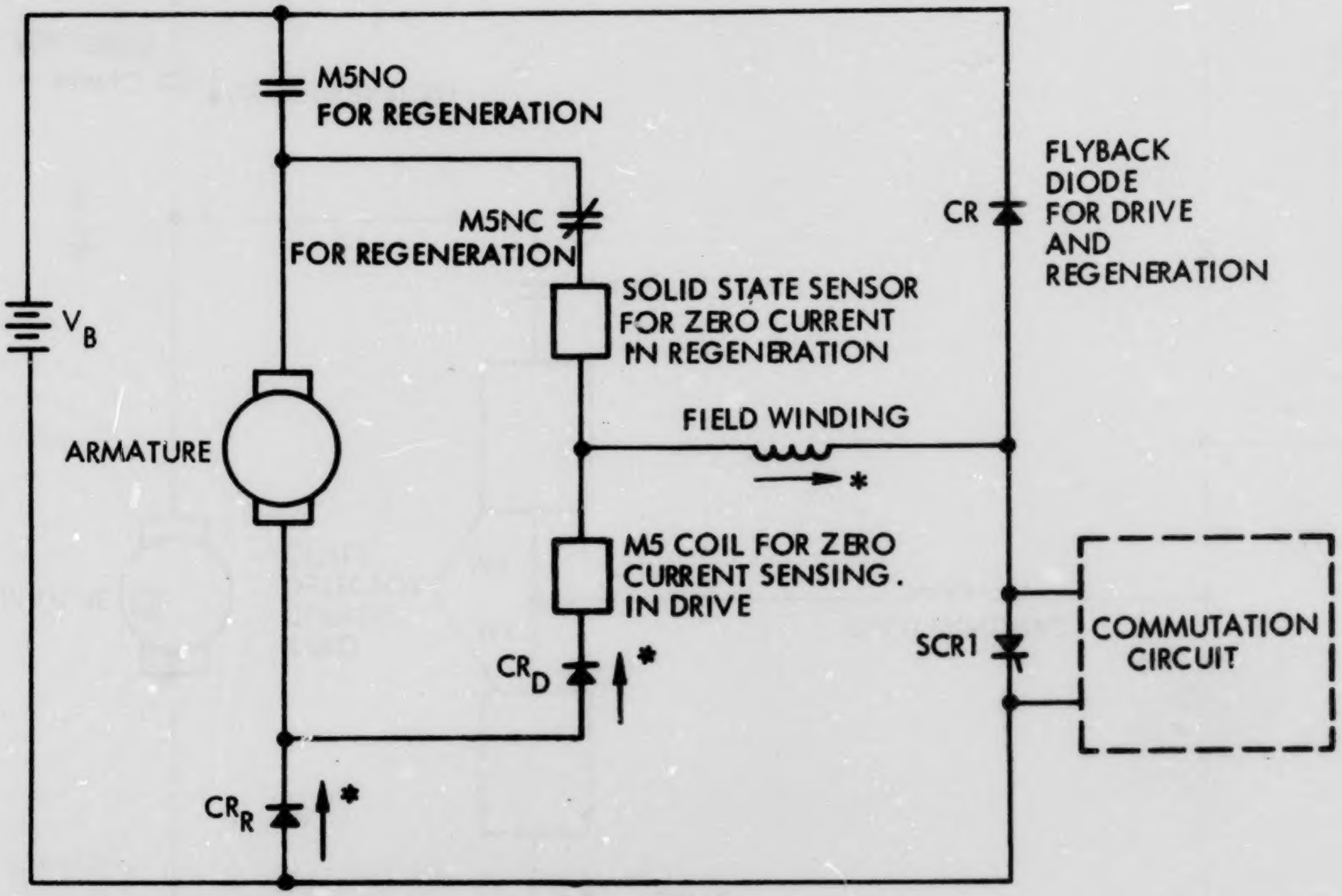
M5NO
FOR REGENERATION
M5NC
FOR REGENERATION
$V_B$
ARMATURE
SOLID STATE SENSOR
FOR ZERO CURRENT
IN REGENERATION
FIELD WINDING
*
M5 COIL FOR ZERO
CURRENT SENSING.
IN DRIVE
$CR_D$
*
$CR_R$
*
CR
FLYBACK
DIODE
FOR DRIVE
AND
REGENERATION
SCR1
COMMUTATION
CIRCUIT

* ALTERNATE PATH OF COMMUTATION CURRENT

FIGURE 8.4
ONE RELAY SYSTEM

drive and blocks during regeneration. There is no need to use an SCR in place of $CR_R$ since no forward voltage is applied across that path during regeneration.

The normal operation of this one relay system is as follows. During drive, $SCR_1$ conducts with M5NO closed (M5NC open) and the full battery voltage is impressed across the motor. Note the blocking voltage of $CR_R$ is less than battery voltage. When $SCR_1$ is commutated off, current continues to circulate through the flyback diode and the commutation circuit, resetting the latter.

Several tests were performed on the one relay system to insure proper operation before final installation of the all-solid state system. The following tests were performed:

- Determination of voltages and voltage rise rates. The rate of change of voltage, $\frac{dv}{dt}$, is an important parameter for sizing the SCRs, while the diodes are rated in terms of their current carrying ability and the reverse bias voltages they encounter in service.
- Determination of the impact of the location of the Torquer armature inductance on the semiconductor ratings. If the inductance from the armature is large compared to that of the series field, then the commutation current through $CR_R$ (or $CR_D$) can be large and the device must be rated at a higher current level.
- Confirm that the precharge circuit is disconnected during switching to insure all currents decay to zero during transfer. The replacement of $M_5$ by an SCR hinges on the SCR being turned off by complete elimination of its current flow. If this is not done an auxiliary commutation circuit is required.
- Confirmation of switching logic sequences.

### 8.1.4 Solid State System

$SCR_R$ and $SCR_D$ were installed in place of the $M_5$ relay and the new circuit is shown in Figure 8.5. In the drive configuration, $SCR_D$ and $SCR_1$ are gated on the current, $I_D$, flows through the armature, $CR_D$, the field and $SCR_1$. When $SCR_1$ is turned off, current continues to flow through the free-wheeling diode. During regeneration the current flows through $CR_R$, the armature, $SCR_R$, the field and $SCR_1$ to charge the series field.

FIGURE 8.5
SOLID STATE SYSTEM

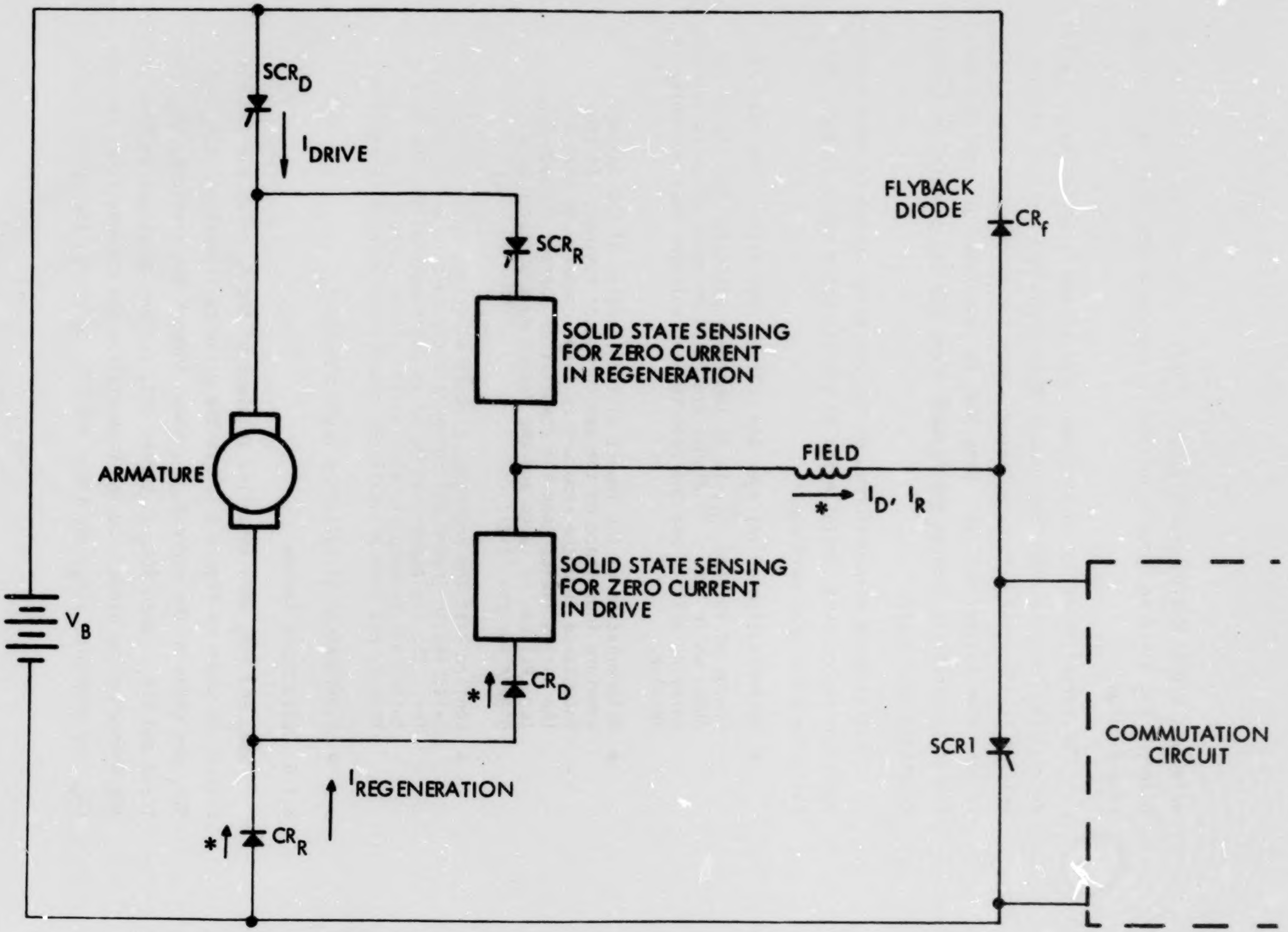
$SCR_D$
$I_{DRIVE}$
FLYBACK DIODE
$CR_f$
$SCR_R$
SOLID STATE SENSING FOR ZERO CURRENT IN REGENERATION
ARMATURE
FIELD
* $I_D$, $I_R$
SOLID STATE SENSING FOR ZERO CURRENT IN DRIVE
$V_B$
* $CR_D$
SCR1
COMMUTATION CIRCUIT
$I_{REGENERATION}$
* $CR_R$

* ALTERNATE PATH OF COMMUTATION CURRENT

When $SCR_1$ is turned off, the discharge current continues through $CR_F$ into the battery.

A number of tests were performed to confirm the solid state design and to gain greater insight into the dynamic requirements of the SCRs used in this application. The tests included:

- Configuration switching logic characteristics--drive-to-regeneration and regeneration-to-drive
- Blocking voltage stresses on $SCR_D$ and $SCR_R$ as well as the diodes of the one relay system
- Measurement of the transfer time for mode switching.

The conversion from the three relay system to the solid state system increases the speed of switching and it becomes extremely important that the logic characteristics are rapid enough to keep pace with the quicker system. All the tests conducted indicated that the logic transfer speed is satisfactory, about 100 milliseconds. This speed is sufficiently fast so that the operator, when starting to transfer from say drive to regeneration can be insured that logic switching is completed before he is able to change his mind and command the previous configuration. If transfer was not completed, a large number of improperly timed sequences could occur. Figure 8.6 shows an oscillogram of the sequencing from drive to regeneration at a power train speed of 10 mph (1200 rpm for the Torquer). The upper trace shows the command duty cycle which reduces the duty to cycle minimum (10 volts) at the start of the sequence. At the same time, the 24 volt SCR gate drive power is reduced to zero. Note that the Torquer current starts falling immediately. Current continues until the 24 volts for the commutating SCR gate goes to zero, after which it decays to zero by virtue of the 20 millisecond motor time constant. After transfer, the reverse process takes place and drive operation is attained. The total transfer time is on the order of 100 milliseconds. Previous measurements using the three relay system showed at transfer time of approximately 400 milliseconds, a period longer than operator response time.

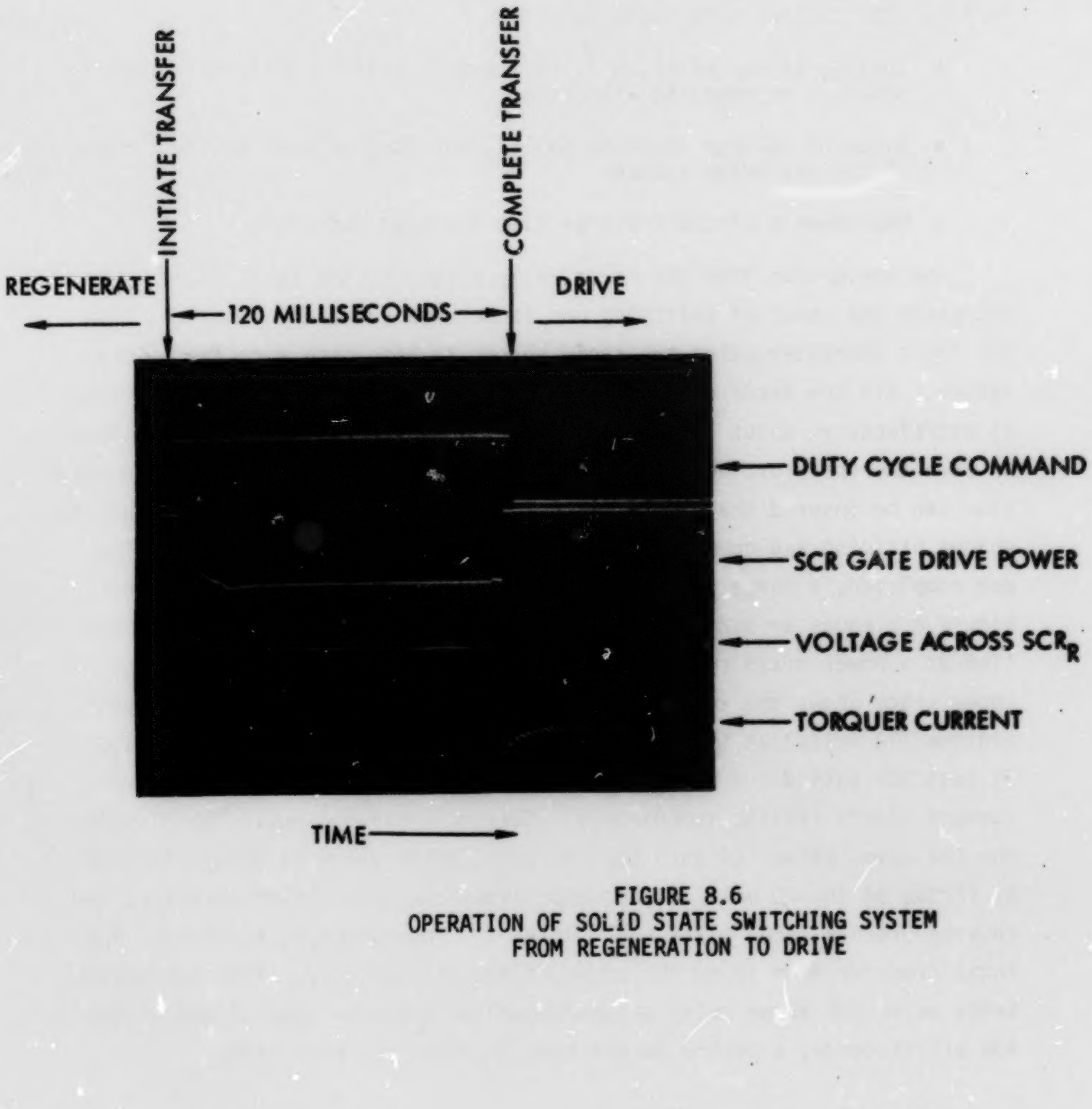

FIGURE 8.6
OPERATION OF SOLID STATE SWITCHING SYSTEM
FROM REGENERATION TO DRIVE

### 8.1.5 Summary of Solid State Switching Activities

An all solid state switching system was developed in a series of steps starting with a three relay system through two and one relay stages. While the digital logic is still implemented with low power level pilot relays, these have no effect on the behavior of the circuits and could be replaced in the future by low cost integrated circuits.

The solid state system possesses the following advantages:

- Speed of transfer between the configurations is considerably faster than with relays, with total transfer time less than operator response time.
- The weight and volume of semiconductors for equal rating is less than relays.
- The price of SCRs can be reduced by mass production, whereas the reduction of price for relays is limited by their use of finite amounts of materials.
- SCR service life is many times longer than that of an equivalent relay.

On the other hand, the solid state system suffers the following disadvantages:

- The power dissipation in semiconductors is considerably higher than relays. Typical diodes and SCRs have 1.5 V forward drop, whereas relays in the range of current used have approximately .2 V drop across the contacts.
- The packaging of semiconductors is more critical due to the need for greater effective cooling. The peak operating temperature of SCRs is much lower than relays compounding the cooling problem.
- Semiconductors have considerably lower overload capabilities; misuse will generally destroy them in circumstances where a relay would not be damaged.
- Relays can be repaired; semiconductors cannot be salvaged after damage.

These disadvantages reveal that the use of the all solid state system may not be the optimum for vehicular use. Instead, further attention should be paid to the one relay approach which seems to combine the good points of both switching methods while diminishing the undesirable properties of each. Some of the advantages in compromising on the one relay approach are:

- The high dissipation semiconductors, $SCR_D$ and $SCR_R$, are replaced by a relay $M_5$.
- Diodes which require no logic to control them replace $M_4$, a device which must be sequenced in the two and three relay systems.
- $M_5$ can be called upon to clear low current level faults, a property which SCRs do not have (with $M_5$ the PCU can be made to malfunction in regeneration at less than 30 mph and the unit will recover by itself. With SCRs the PCU will blow a fuse requiring the operator to stop the vehicle.)
- The $M_5$ relay replaces only the higher priced semiconductors, $SCR_R$ and $SCR_D$.
- Diodes can operate up to 200°C junction temperature, whereas SCRs are limited to 100°C junction temperature. Diodes are thermally closer to relays than SCRs.

## 8.2 EMT Power Train Start-Up Concepts

The breadboard EMT system was started by unclutching the VW engine from the planetary gear train and turning the engine over by a conventional VW starter. Once the engine was started, the throttle was advanced and the clutch engaged. The engine was then brought up to the control speed of the Speeder.

This approach, while quite satisfactory for the demonstration equipment, is not suited for vehicle use for the following reasons:

- Requires an additional starter motor, starter solenoids, battery or battery tap.
- Engagement of the engine-gear box is not smooth and engine is apt to stall. This is particularly troublesome for a lean, quick relief choked engine needed for reduced starting emissions.

Two approaches for system start-up are suggested; use of the Torquer as a starting motor and use of the Speeder as a starting motor. Each concept will be described below.

### 8.2.1 Torquer Starter Motor

In this concept the Torquer-drive wheel connection is broken so the Torquer can rotate the propeller shaft without moving the car. There is no clutch between engine and gearing. Using the existing Torquer circuitry and current transducer, a drive command is given, establishing a torque output of the Torquer. The motor rotates the engine and Speeder. At an appropriate engine speed, the Speeder tachometer signals the Torquer to go to normal operation; i.e., full regeneration. The propeller shaft is held at a low speed and the engine is automatically controlled by the Speeder. During this period, the Speeder is not operated (the boost PCU is not turned on), reducing the cranking load of the Torquer. When the operator wants to move, he engages clutch, making the propeller shaft-rear wheel connection.

Advantages of the Concept

- Torquer is used as a low speed traction motor
- All cranking torque control is already built into Torquer PCU
- The clutch function can be combined with reversing gears
- The Speeder retains its present configuration and function.

Disadvantages of the Concept

- The engine is always connected to the gearing and Speeder; design flexibility for gear shifting (see Section 8.3) may be reduced.
- If the Speeder system fails, the vehicle cannot run on battery power alone without rotating the Speeder.

### 8.2.2 Speeder Starter Motor

With the propeller shaft braked, the Speeder is used as a starter motor. It cranks the engine over to a given speed; once there it reverts back to its normal generator function. To go forward, the operator releases the propeller shaft and operates the vehicle normally.

Advantages of the Concept

- The need for a clutch between the Torquer and rear wheels is eliminated.

Disadvantages of the Concept

- The Speeder must be capable of motor operation. Several ways of doing this are possible:
    - use a DC motor/generator as the Speeder with the Torquer PCU controlling it as a motor, or with a different Speeder PCU similar to that of the Torquer. The cost of a DC Speeder would be much greater than an alternator.

- use the Speeder as an AC motor.

The control of an alternator as a motor from a battery requires an expensive polyphase inverter and some means of commutating the position of the rotor.

The most attractive method of combining the EMT with engine starting is to use the DC Torquer with a slightly modified form (engine speed sensing and mode transfer control) of the Torquer PCU.

## 8.3 Override Options to the EMT System

A drawback of the EMT system in its breadboard form is its inability to provide sustained low speed (lower than mode transition speed), high power (greater than the Mode One engine power). This section suggests several options which could be included in an advanced EMT system. They are restricted to overrides during Mode One and would be either manually or automatically controlled.

### 8.3.1 Option A

In this option, the engine speed increases at relatively constant engine torque. This is done by increasing the engine throttle while simultaneously increasing the engine control speed level of the Speeder. As the Speeder and engine increase their power output, the incremental power is delivered to the Torquer for traction. The limiting factor is the design speed of the Speeder. In the present system, there is very little reserve Speeder speed at very low road speeds; near mode transition, there is almost the full Speeder design speed available and the engine output can be approximately doubled.

### 8.3.2 Option B

This option lets the engine torque increase at constant engine speed. Increasing the throttle, increases the torque which the Speeder must accept; however, it also increases the torque delivered directly to the propeller shaft. The former effect means more power can be converted by the Speeder for use in the Torquer. The limit of usable engine power is set by the sustained torque capability of the Speeder PCU. At speeds near mode transition where the Speeder voltage is low, the increased current output can be limited by the lack of storage capacity in the boost inductor.

### 8.3.3 Option C

In this option the combined techniques of options A and B are used. It is estimated that the combined technique could increase the factor of engine output from the normal Mode One level by about 2.5 to 3.

### 8.3.4 Option D

This option relies on a gear ratio changing between the engine and the rear wheels; in effect, down-shifting the transmission with an associated engine throttle increase. One method of doing this is to manually instruct the transmission to go into Mode Two (shut the Speeder off-line) while simultaneously changing the gear ratio between the engine shaft and the planetary input or the planetary output and propeller shaft. For the present system this would be equivalent to shifting from 4th gear (the approximate overall gear ratio of the breadboard equipment) to something between 1st and 2nd gear. Near mode transition, the engine output could approach its maximum level without overloading or overspeeding the Speeder.

### 8.3.5 Conclusions

Of the options offered, A, B and C will not require substantial redesign of the EMT system but rather modification of existing Speeder and engine throttle subsystems. On the other hand, these options will not allow the full power output of the engine to be utilized without excessive weight and cost penalties to the Speeder system. Option D, while requiring a secondary gear ratio allows full engine output to be developed near mode transition. Further tradeoffs must be made to establish on one hand the degree and frequency of sustained power demand in Mode One and on the other hand the detailed design implications of each option.

# 9.0 EFFECT OF SELECTED PARAMETERS ON EXHAUST EMISSIONS FROM AN INTERNAL COMBUSTION ENGINE

## 9.1 Introduction

This study was undertaken to determine the effects of various engine parameters during the start-up period of engine operation. In particular, emphasis was placed on defining the boundaries of choke scheduling, timing and power so that the engine would deliver stable power with minimum emissions. The EMT system is a particularly attractive system to conduct the experiments as the Speeder load control completely frees the engine from the driveability requirements of normal automotive operation.

The work performed falls into three categories. The first deals with a series of experiments in which the cold start emissions of the engine were measured under a variety of controlled start conditions. Measurements were made using both the proportional sampling technique and continuous on-line concentrations.

The second data set defines engine operation beyond the cold period. Particularly lean engine operation and the effect of timing and power level were explored. Data was again gathered by both "bag" and concentration measurements.

Finally, some data was experimentally obtained on the performance of a three-component catalyst operating under steady hot emission load.

## 9.2 Determination of Engine Emissions During Cold and Hot Operation

### 9.2.1 Experimental Equipment and Procedures

The test engine used was a 1968 VW 1600 cc engine equipped with intake port fuel injection. It is the same engine used in the dynamometer work of Section 5 and was operated into the power train described in the earlier sections. The fuel injection control system was modified in two ways. First, the injection pulse duration circuitry was adapted so that the mixture ratio of the engine could be varied over a wide range from flood to lean misfire. These modifications affected a continuously variable metering jet capability to the engine carburetion. Second, the thermal transducer controlling the choke operation was removed and a manually controlled signal was added in its place so that the "choke" could be varied over a wide range of settings and time schedules.

The engine was instrumented as follows:

Engine air flow - a Meriam Laminar flowmeter was used to monitor the engine intake air flow. The pressure drop across the flowmeter was monitored by an inclined manometer and recorded using a pressure transducer.

Fuel flow - a turbine meter calibrated in-situ monitored the fuel flow.

Manifold pressure - the manifold pressure was indicated by a mercury manometer and pressure transducer.

Engine temperatures - two thermocouples were placed in the exhaust manifold about one inch from the manifold flange on the number 3 and 4 cylinders. Additional thermocouples sensed the temperature of; the outer portion of one cylinder lead, the crankcase oil and the mid-point of the muffler.

Engine speed - engine speed was monitored by a tachometer-generator driven off the engine cooling fan. This tachometer is currently used as a primary sensor for the Speeder control system.

Engine timing and control - the engine timing was adjusted by two means. First, the distributor was manually rotated from the manufacturer's specified position ($0^{o}$ TDC) with engine off. Additional timing control was affected by using the vacuum advance diaphram on the distributor in conjunction with an external vacuum pump. All timing was checked with an electronic stroboscopic tachometer.

Emission measurements were made using two sets of equipment:

- Continuous concentration monitoring of the exhaust was made by drawing a sample from the mid-point of the muffler. The sample line was fed into the following instruments:

| | |
|---|---|
| Beckman Model 315A | NDIR CO Analyzer |
| Beckman Model 315A | NDIR NO Analyzer |
| Beckman Model 400 | FID Hydrocarbon Analyzer |
| Beckman Process Oxygen Analyzer | |

- Proportional sampling (1972 HEW test equipment) was performed by Scott Research Laboratories using their equipment. The technique samples and measures the CO, NO, $NO_2$ and FID hydrocarbons in a bag diluted with ambient air. Additional on-stream records of the NDIR concentrations of CO, $CO_2$, NO and hydrocarbons were taken. Bag measurements were performed on approximately 50% of the cold start tests and 30% of the hot tests.

Power delivered by the engine was determined by recording the voltage and current of the Speeder rectifier output. The values of the inefficiencies of the Speeder and the gear box were derived from the previous experimental work (Table 5.2 and Figure 7.2) and were factored into the computations to reflect the engine shaft output power.

### 9.2.2 Cold Start Test Results

The data gathered during this portion of the study is summarized in Tables 9.1 and 9.2. A total of 14 cold starts were performed.

The mass rates in Tables 9.1, 9.2 and 9.3 of the next section were computed from measured steady state or averaged pollutant concentrations and engine air intake flows. Intake air mass flows were corrected for the addition of fuel to compute the exhaust mass flow rates. The test numbers of Table 9.1 refer to consecutive 1½ min. intervals during which samples were taken. Table 9.1a compares the bag measurements to the computed ("integrated") pollutant mass rates for the samples taken simultaneously. Good agreement is observed in hydrocarbon mass rates, but the integrated CO and NO rates are consistently lower than those obtained by the constant volume bag technique. The discrepancy in CO mass rates is especially high. An investigation of the observed differences revealed that most of the hot test bag measurements of CO and NO were recorded at the least sensitive portion of the NDIR instruments (lower 5% of scale); this can easily be the cause of the observed error during hot work. However, the CO error should not occur to the much higher levels in CO.

For the purpose of this study where trends are more important than absolute values, the integrated mass rate results presented in Tables 9.1 and 9.3 were used to establish relationships between them and engine operation parameters. The choice was dictated by the fact that the integrated mass rates represent a more complete set of data.

## TABLE 9.1 COLD

| | Initial Conditions | | | | | Exhaust Composition (Avg.@1.5Min.intervals for 4.5 Minutes) | | | |
|---|---|---|---|---|---|---|---|---|---|
| Test Nos. | Cold Soak Period (Hours) | Crank-case Temp. (°F) | Timing | Throttle Setting | Choke | HC Gms/Min. | CO Gms/Min. | NOx Gms/Min. | $O_2$ % |
| C-1.1 | 2 | 70 | 10°retard/ Full vac. adv. | 1.69 | Manual Control | 4.18 | 6.45 | 1.14 | 5 |
| 1.2 | | | | | | 1.65 | 1.65 | 0.47 | 5 |
| 1.3 | | | | | | 1.03 | 1.53 | 0.49 | 5 |
| C-2.1 | 2 | 70 | Normal VW | 1.55 | VW | 5.08 | 38.1 | 2.14 | 0.6 |
| 2.2 | | | | | | 1.77 | 2.07 | 5.38 | 1.8 |
| 2.3 | | | | | | 1.18 | 1.30 | 5.38 | 2.4 |
| C-3.1 | Over-night | 70 | 10°retard, VW Vac.adv. | 1.55 | VW | 6.2 | 37.6 | 1.02 | 1.2 |
| 3.2 | | | | | | 1.42 | 1.85 | 2.62 | 2.3 |
| 3.3 | | | | | | 0.66 | 1.40 | 2.54 | 2.5 |
| C-4.1 | 3 | 80 | 10°retard Full vac. adv. | 1.35 | Manual Control | 2.65 | 9.1 | 0.48 | 4.0 |
| 4.2 | | | | | | 0.49 | 1.15 | 0.41 | 4.5 |
| 4.3 | | | | | | 0.38 | 1.11 | 0.30 | 5.0 |
| C-5.1 | 3 | 80 | 10°retard Full vac. adv. | 1.11 | Manual Control | 2.95 | 8.30 | 0.48 | 4.5 |
| 5.2 | | | | | | 0.83 | 1.48 | 0.73 | 4.5 |
| 5.3 | | | | | | 0.60 | 1.32 | 0.73 | 4.5 |
| C-6.1 | Over-night | 60 | 10°retard Full vac. adv. | 1.11 | Manual Control | 2.10 | 16.0 | 0.22 | 2 |
| 6.2 | | | | | | 1.03 | 1.18 | 0.30 | 5 |
| 6.3 | | | | | | 0.58 | 0.95 | 0.49 | 5 |
| C-7.1 | 7 | 75 | 0°retard Full vac. adv. | 1.11 | Manual Control | 3.04 | 32.8 | 0.45 | 5 |
| 7.2 | | | | | | 1.30 | 1.02 | 1.03 | 4.5 |
| C-8.1 | Over-night | 70 | Normal VW | 1.11 | VW | 4.00 | 53.4 | 0.12 | 1.3 |
| 8.2 | | | | | | 3.06 | 23.1 | 1.70 | 1.3 |
| 8.3 | | | | | | 1.52 | 5.1 | 2.36 | 2.0 |
| C-9.1 | 3 | 75 | Normal VW | 1.55 | VW | - | - | - | 1.2 |
| 9.2 | | | | | | 2.06 | 6.54 | 4.58 | 1.6 |
| 9.3 | | | | | | 1.38 | 1.71 | 6.42 | 2.2 |
| C-10.1 | 2 | 80 | 0°retard Full vac. retard | 1.35 | Manual Control | 2.12 | 23.80 | 0.38 | 1.2 |
| 10.2 | | | | | | 0.59 | 4.84 | 0.90 | 3.3 |
| 10.3 | | | | | | 0.52 | 1.41 | 1.28 | 3.5 |
| C-11.1 | 2 | 75 | 0°retard Full vac. adv. | 1.35 | Manual Control | 2.25 | 9.8 | 1.24 | 4.5 |
| 11.2 | | | | | | 1.34 | 1.4 | 4.46 | 3.0 |
| 11.3 | | | | | | 0.91 | 1.25 | 4.42 | 3.2 |
| C-12.1 | Week-end | 70 | Normal VW | 1.35 | VW | 5.78 | 57.0 | 0.33 | 1.2 |
| 12.2 | | | | | | 1.62 | 4.05 | 3.20 | 1.9 |
| 12.3 | | | | | | 1.10 | 1.10 | 4.32 | 2.4 |
| C-13.1 | 4-1/2 | 75 | 10°retard Full vac. adv. | 1.35 | Manual Control | 3.87 | 9.45 | 1.11 | 4 |
| 13.2 | | | | | | 1.09 | 1.89 | 1.22 | 4 |
| 13.3 | | | | | | 0.49 | 1.35 | 1.84 | 3.5 |
| C-14.1 | 3 | 70 | o°retard Full vac. adv. | 1.35 | Manual Control | 2.48 | 5.6 | 1.12 | 4.0 |
| 14.2 | | | | | | 0.81 | 0.9 | 1.06 | 4.6 |
| 14.3 | | | | | | 0.72 | 1.03 | 1.41 | 4.6 |

A

LD START TESTS OF 1600 cc.VW

| | Engine Operating Conditions | | | | | |
|---|---|---|---|---|---|---|
| $O_2$ % | Average Intake Air Flow (cfm) | Exhaust Gas Temp. °F | RPM | Alternator Output (kw) | Manif. Press " Hg. | Remarks |
| 5<br>5<br>5 | 35.6<br>35.8<br>35.8 | 1310 Final<br>1180 @ 20sec. | 1800<br>↓ | 2.06<br>3.7 | 6.3<br>↓ | Choke completely off in 60 seconds. |
| 0.6<br>1.8<br>2.4 | 31.4<br>31.4<br>30.8 | 1260 Final<br>1130 @ 45 sec. | 1800<br>↓ | 5.5<br>6.7 | 8.4<br>↓ | Normal VW start with fixed throttle. |
| 1.2<br>2.3<br>2.5 | 30.8<br>32.2<br>31.2 | 1320 Final<br>1190 @ 45sec. | 1800<br>↓ | 5<br>5<br>5.5 | 8.3<br>↓ | Normal VW with fixed throttle, 10° retard, 6 seconds for engine to start. |
| 4.0<br>4.5<br>5.0 | 24.0<br>25.0<br>25.0 | 1300 Final<br>1170 @ 30sec. | 1800<br>↓ | 2.55 | 12.3<br>12.3<br>12.5 | Engine stumble at 25 & 60 seconds due to under choking leaned during cold start) |
| 4.5<br>4.5<br>4.5 | 24.0<br>32.0<br>32.0 | 1300 Final<br>1170 @ 55sec. | Oscil-lation<br>1800 | 3.22<br>5.5 | 5.8<br>5.8 | Increased throttle @ 28sec., engine too lean, did not re-establish contro until 45 sec.,speed & emission excur. |
| 2<br>5<br>5 | 16.5<br>19.2<br>23.8 | 1275 Final<br>1150 @ 70sec. | 1400<br>1400<br>1800 | <2<br><2 | <12.5<br>~12.5 | Opened throttle in stages @ 1:40,3:00, 3:30. Excessive enrichment during start (3sec.)No regulation till 3:40. |
| 5<br>4.5 | 24.5<br>30.8 | 1250 in 4min.<br>1120 in 50 sec. | | ~4.0 | 9.5<br>@60 sec<br>↓ | Increased throttle at 30sec. through 60sec.;dropped choke @ 45sec.to fully off; engine stable in approx.60sec. |
| 1.3<br>1.3<br>2.0 | 17.0<br>24.0<br>23.0 | 1220 Final<br>1100 @ 80sec. | 1400<br>1800<br>1800 | ~4.0 @2min. | 13.3@2min. | Normal VW start, increase throttle after 30 sec., 1400 rpm till 35sec. (1 minute intervals). |
| 1.2<br>1.6<br>2.2 | 32.4<br>32.4<br>32.4 | 1250 Final<br>1120 @55sec | 1800<br>↓ | 8.15<br>7.40<br>7.05 | 9.0<br>8.86<br>8.6 | 1 minute intervals |
| 1.2<br>3.3<br>3.5 | 24.0<br>24.0<br>26.7 | 1270 Final<br>1140 @48sec. | 1800<br>↓ | -<br>-<br>2.66 | 13.1<br>10.2 | VW choke schedule for 35sec., then rapid decrease to full off in 1:00 mi 1 minute intervals. |
| 4.5<br>3.0<br>3.2 | 33.0<br>36.5<br>35.0 | 1260 Final<br>1135 @45sec. | 1800<br>↓ | -<br>7.4 max.<br>(4) | 3.9max<br>6.5 | After 4-5sec.cranking,leaned down for 10sec.,retarded spark at 30sec., inc. throttle @50sec.,reduced thr.110sec. leaned during full test. |
| 1.2<br>1.9<br>2.4 | 24.6<br>24.5<br>24.4 | 1230 Final<br>1100 @90sec. | 1800<br>↓ | 4.0<br>4.8<br>4.6 | 12.0<br>11.85<br>11.85 | Normal VW start.<br>Engine cranked 10 seconds. |
| 4<br>4<br>3.5 | 39.4<br>41.8<br>37.2 | 1380 Final<br>1240 @55sec. | 1400<br>1800<br>↓ | 6.2(max)<br>5.7 | 2.0 max<br>5.8final | Lean down for 30sec. then retard spark 10° & adv.thr.(Eng.out-of-cont. for 40sec.) Cont.decreasing thr. & leaning. |
| 4.0<br>4.6<br>4.6 | 23.0<br>24.5<br>26.0 | 1200 Final<br>1080 @35sec. | 1800<br>↓ | 2.8<br>3.2 | 12.2<br>12.2<br>12.2 | Rapid leaning. Most choke relief after 20 seconds. |

B

## TABLE 9.1a

## COMPARISON OF CVS AND INTEGRATION PROCEDURE COLD START EMISSION VALUES
grams/min

| Test No. | CVS Method |  |  | Integration Procedure |  |  |
|---|---|---|---|---|---|---|
|  | HC | CO | NO$_x$ | HC | CO | NO$_x$ |
| C-8.1 | 2.57 | 48.37 | 0.31 | 4.00 | 53.4 | 0.12 |
| 8.2 | 1.93 | 24.19 | 2.01 | 3.06 | 23.1 | 1.70 |
| 8.3 | 1.36 | 16.55 | 5.00 | 1.52 | 5.1 | 2.36 |
| C-9.1 | 6.24 | 86.56 | 2.41 | - | - | - |
| 9.2 | 1.85 | 10.18 | 7.57 | 2.06 | 6.54 | 4.58 |
| 9.3 | 2.19 | 5.09 | 9.03 | 1.38 | 1.71 | 6.42 |
| C-10.1 | 2.34 | 54.45 | 0.84 | 2.12 | 23.80 | 0.38 |
| 10.2 | 0.50 | 2.42 | 1.21 | 0.59 | 4.84 | 0.90 |
| 10.3 | 0.50 | 2.42 | 1.69 | 0.52 | 1.41 | 1.28 |
| C-11.1 | 1.76 | 8.47 | 1.75 | 2.25 | 9.80 | 1.24 |
| 11.2 | 0.72 | 2.42 | 4.08 | 1.34 | 1.40 | 4.46 |
| 11.3 | 0.94 | 2.42 | 4.27 | 0.91 | 1.25 | 4.42 |
| C-12.1 | 5.80 | 125.21 | 0.75 | 5.78 | 57.00 | 0.33 |
| 12.2 | 1.72 | 2.46 | 6.01 | 1.62 | 4.05 | 3.20 |
| 12.3 | 1.42 | 1.23 | 5.06 | 1.10 | 1.10 | 4.32 |
| C-13.1 | 3.14 | 8.59 | 1.77 | 3.87 | 9.45 | 1.11 |
| 13.2 | 1.20 | 3.68 | 1.92 | 1.09 | 1.89 | 1.22 |
| 13.3 | 0.58 | 3.68 | 2.82 | 0.49 | 1.35 | 1.84 |
| C-14.1 | 2.70 | 11.05 | 1.25 | 2.48 | 5.60 | 1.12 |
| 14.2 | 1.13 | 2.46 | 1.11 | 0.81 | 0.90 | 1.06 |
| 14.3 | 0.88 | 2.46 | - | 0.72 | 1.03 | 1.41 |

BLANK PAGE

## TABLE 9.2

| TEST NUMBER* | ENGINE PARAMETERS | POWER END OF 3 MIN (HP) | TOTAL POLLUTANTS GRAMS/3 MIN | | | REMARKS |
|---|---|---|---|---|---|---|
| | | | HC | CO | NO | |
| C-2 & C-9 | Normal VW choke and timing High Power Settings | 15-16 | 10.27 | 60.12 | 11.28 | Good start-reproducible tests |
| C-3 | Normal VW choke Mechanically Retarded 10° | 13 | 11.43 | 59.17 | 5.46 | Rough start |
| C-12 | Normal VW choke and timing Medium Power Setting | 12 | 11.10 | 91.58 | 5.30 | Rough start |
| C-8 | Normal VW choke and timing Low Power initially, scheduled throttle** after 35 sec. | 11 | 8.58 | 89.11 | 7.32 | Maximum RPM first 35 sec. 1400 |
| C-10 | Normal VW choke for 35 sec only Full Vacuum Retard Rapid de-choking after 35 sec off choke in 1 min. | 9 | 3.23 | 30.25 | 2.56 | Good start |
| C-1 | Controlled VW (EMT) High Throttle, 10° Mech. Ret. Lean start***, 60 sec. de-choking schedule | 10 | 8.74 | 12.15 | 2.41 | Good start |
| C-4 | EMT - Low Throttle, 10° Mech. Retard, Lean start, 60 sec. de-choking | 9 | 4.71 | 15.37 | 1.34 | Rough engine operation first 60 sec. |
| C-5 | EMT - Same as C-4 but scheduled throttle | 13 | 5.67 | 14.57 | 1.81 | Rough up to 45 sec. |
| C-6 | EMT - Low throttle, 10° Mech. Ret. Rich start Rapid choke relief, stepwise throttle increase | 8 | 4.70 | 25.77 | 0.78 | No speed control during entire test (RPM 1400 rpm) |
| C-7 | EMT - Low throttle, 0° Retard scheduled choke and throttle through first 60 sec. | 11 | 6.51 | 50.73 | 2.22 | Good start |
| C-11 | EMT - High throttle 0° Retard initially 10° Retard after 30 sec (see Table 1 for choke schedule) | 16 | 5.39 | 16.8 | 8.55 | Good start |
| C-13 | EMT - High throttle, 10° Ret. initially - 10° additional retard after 30 sec (see Table 1 for schedules) | 15 | 7.44 | 17.01 | 3.50 | No speed control for 40 sec (1400 RPM) |
| C-14 | EMT - Low throttle, 0° retard Rapid de-choking (20 sec) | 9 | 4.94 | 9.75 | 3.27 | Good start |

---

* Corresponds to Table 9.1

** Implied scheduled increase in manifold pressure

*** "Lean" implies leaner than normal VW

Typical pollutant concentration signatures during the cold period are shown in Figures 9.1 and 9.2. In Figure 9.1, the engine was started with the normal VW choke and timing schedule. The throttle was set to give approximately 9 hp after three minutes of operation. Figure 9.2 shows a cold start test at the same three-minute power level but with a much more rapid choke relief. Figures 9.3 and 9.4 show temperature and air-fuel ratio variations for the respective tests.

Several observations can be made. A low air-fuel ratio ($< 10$) is necessary for engine start. This very rich mixture results in a high hydrocarbon and CO output during the initial period of operation ($\sim$ one minute). Second, the engine reaches a quasi-steady state within three minutes after ignition. Third, rapid choke relief dramatically reduces both the concentration magnitude and duration of hydrocarbon and CO emissions. $NO_x$ concentrations, however, start to buildup earlier in the operating cycle.

Figure 9.5 demonstrates the effect of rapid choke relief on total emissions during the first three minutes after engine start. All major pollutants are decreased by rapid choke relief when contrasted to the normally choked engine. The degree of reduction is a function of the particular pollutant. CO and hydrocarbon show the highest and intermediate percent reductions; NO reduction is considerably less. CO and HC reductions are somewhat independent of engine power level, suggesting they are associated with the earliest period of engine operation where the engine is stabilizing its internal temperature structure. NO levels on the other hand are more related to the three-minute power level. With increasing manifold pressure (increased power) the $NO_x$ concentration and volume flow rate increase once the engine has passed through its initial starting period.

Figure 9.6 indicates the effect of engine timing on total pollutant levels. Better than 50% reduction in $NO_x$ is observed with $10^o$ retard at both power levels. However, spark retard appears to have an adverse effect on hydrocarbon emissions; the effect increasing with power level. The engine is harder to start with a retarded spark and the incremental HC levels may be due to additional fuel injected into the engine during cranking.

NORMAL VW 1600 COLD START
EMT-11 HP (TEST C-8)

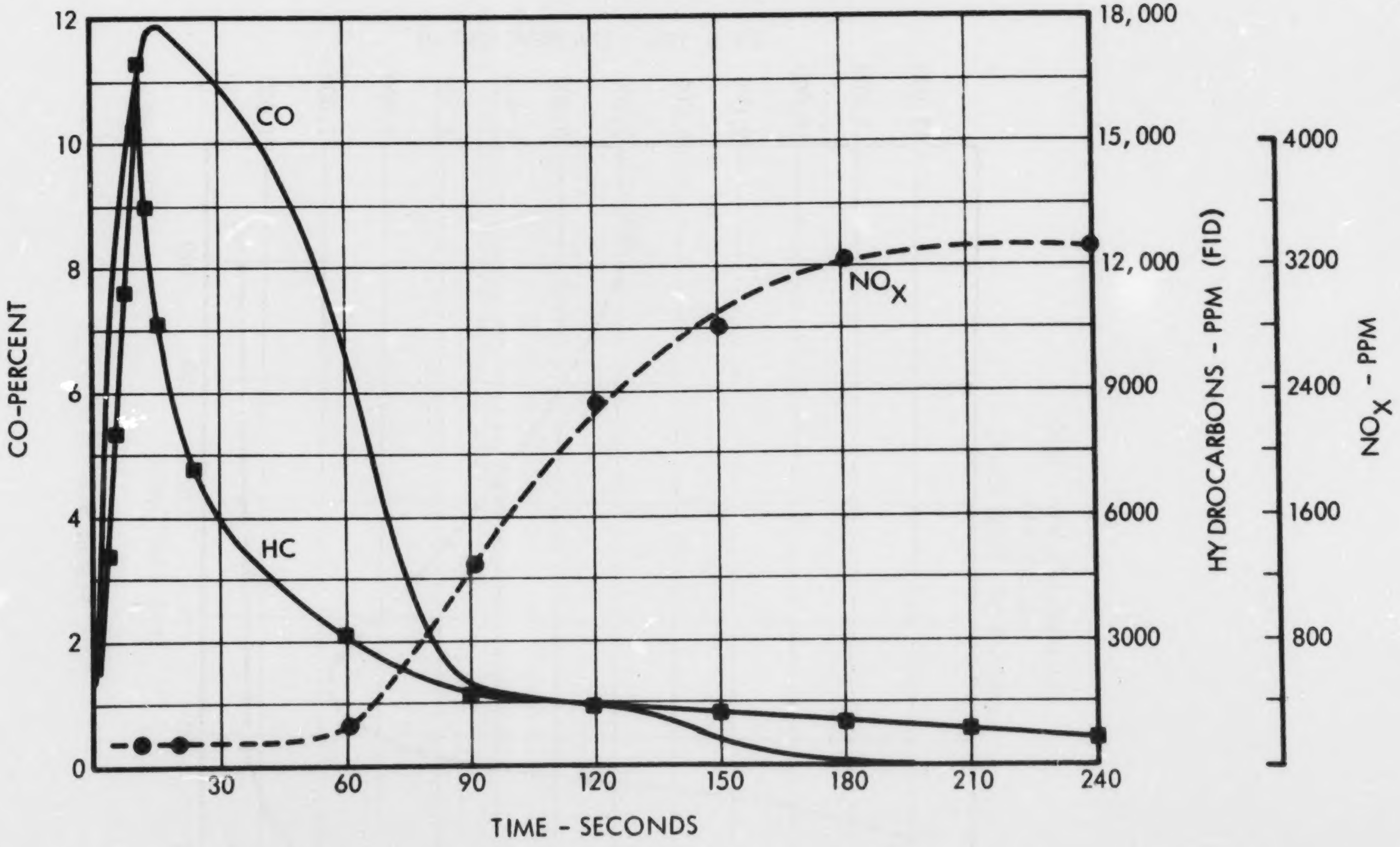

FIGURE 9.1

CONTROLLED VW - 1600
COLD START
EMT - 9 HP (TEST C-14)

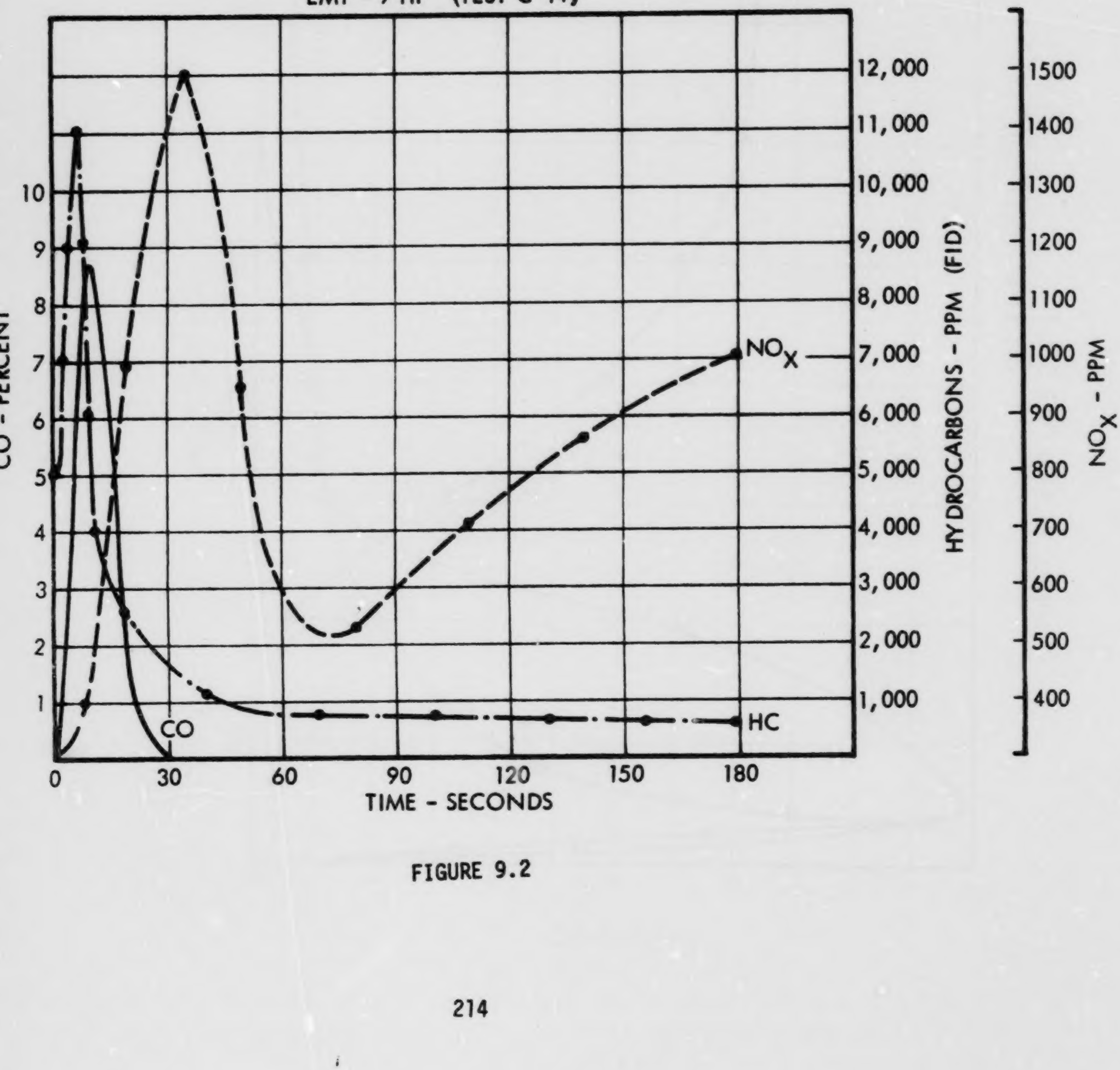

FIGURE 9.2

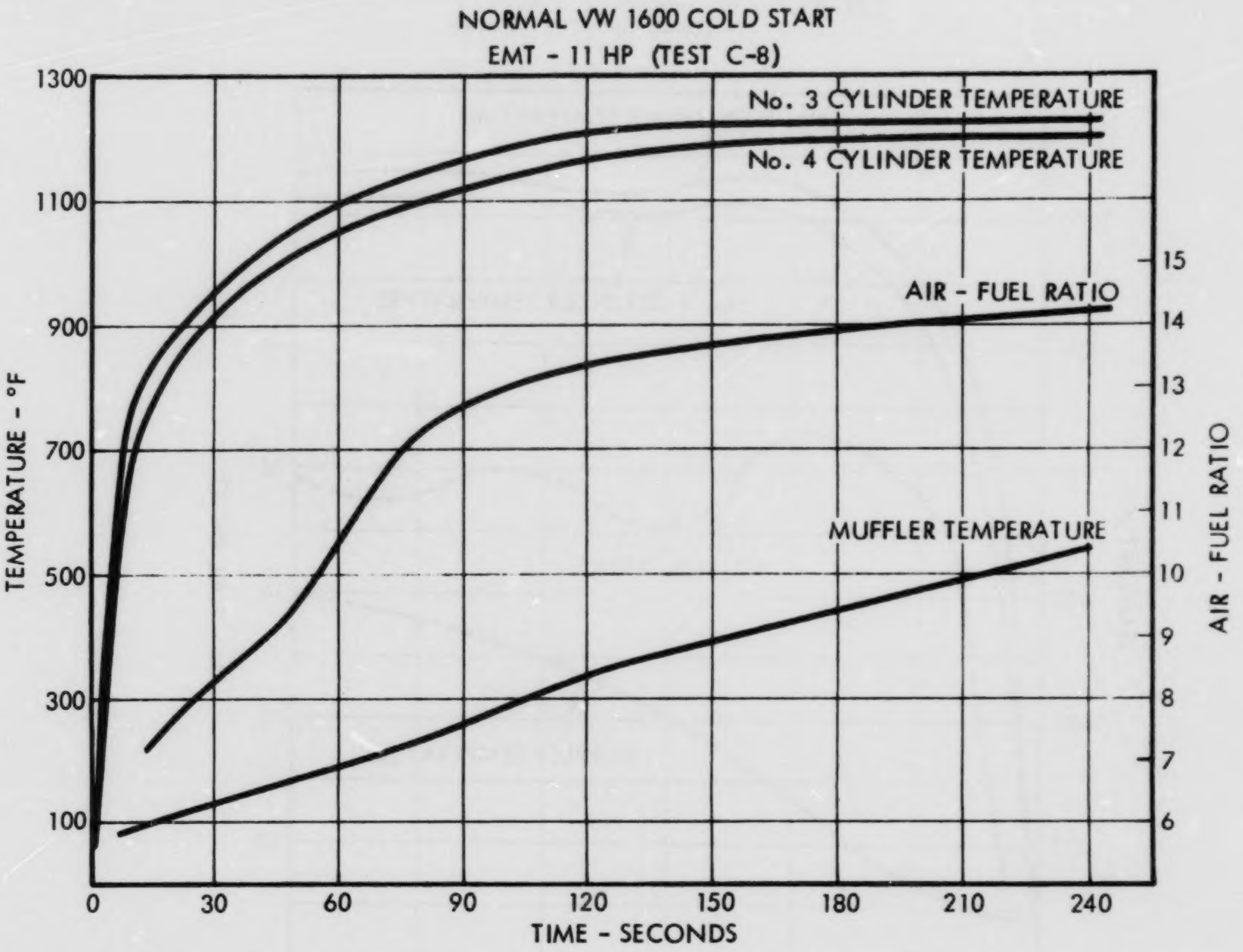

NORMAL VW 1600 COLD START
EMT - 11 HP (TEST C-8)

FIGURE 9.3

CONTROLLED VW-1600 COLD START
EMT-9 HP (TEST C-14)

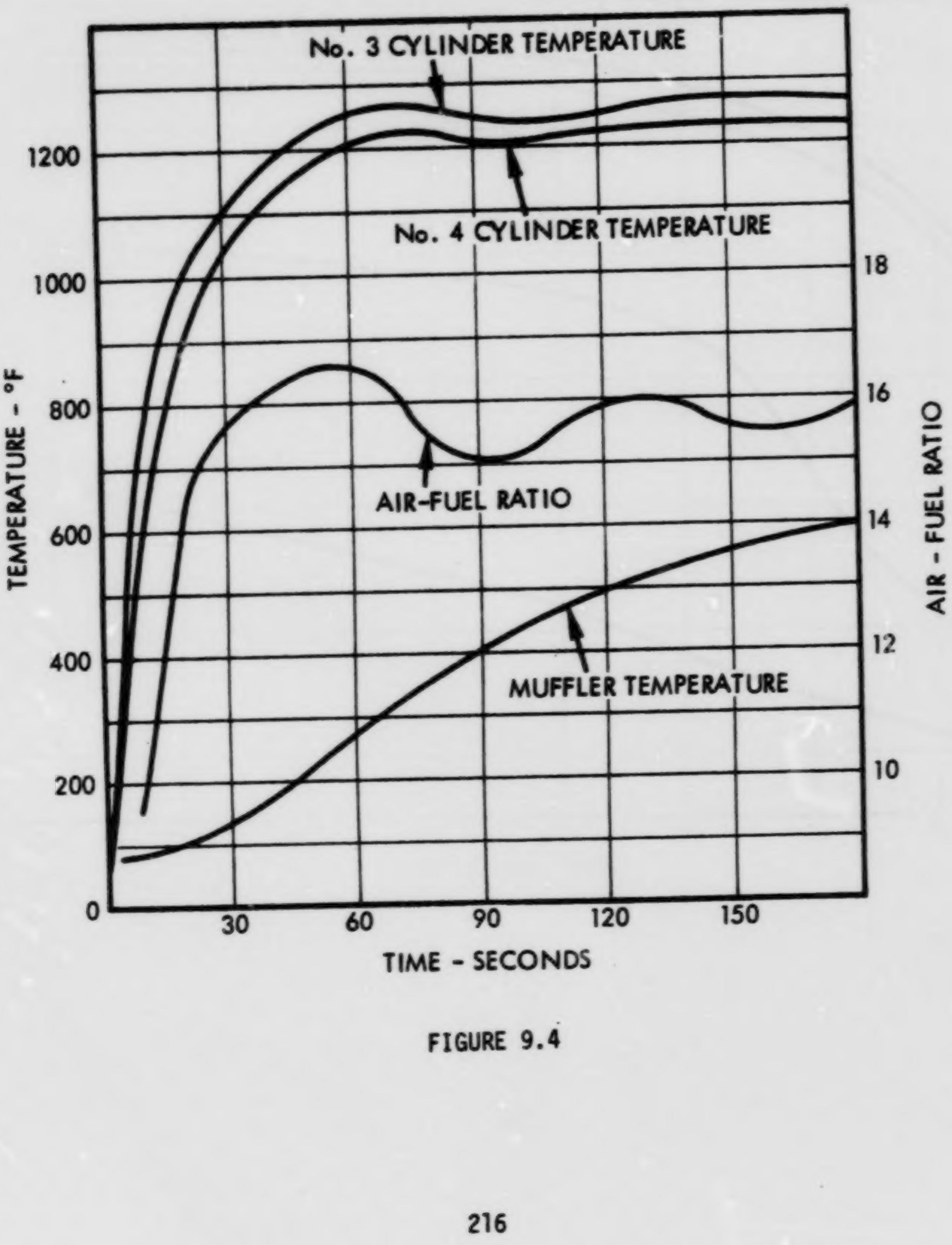

FIGURE 9.4

EFFECT OF CHOKE SCHEDULE ON
3 MINUTE POLLUTANT TOTALS

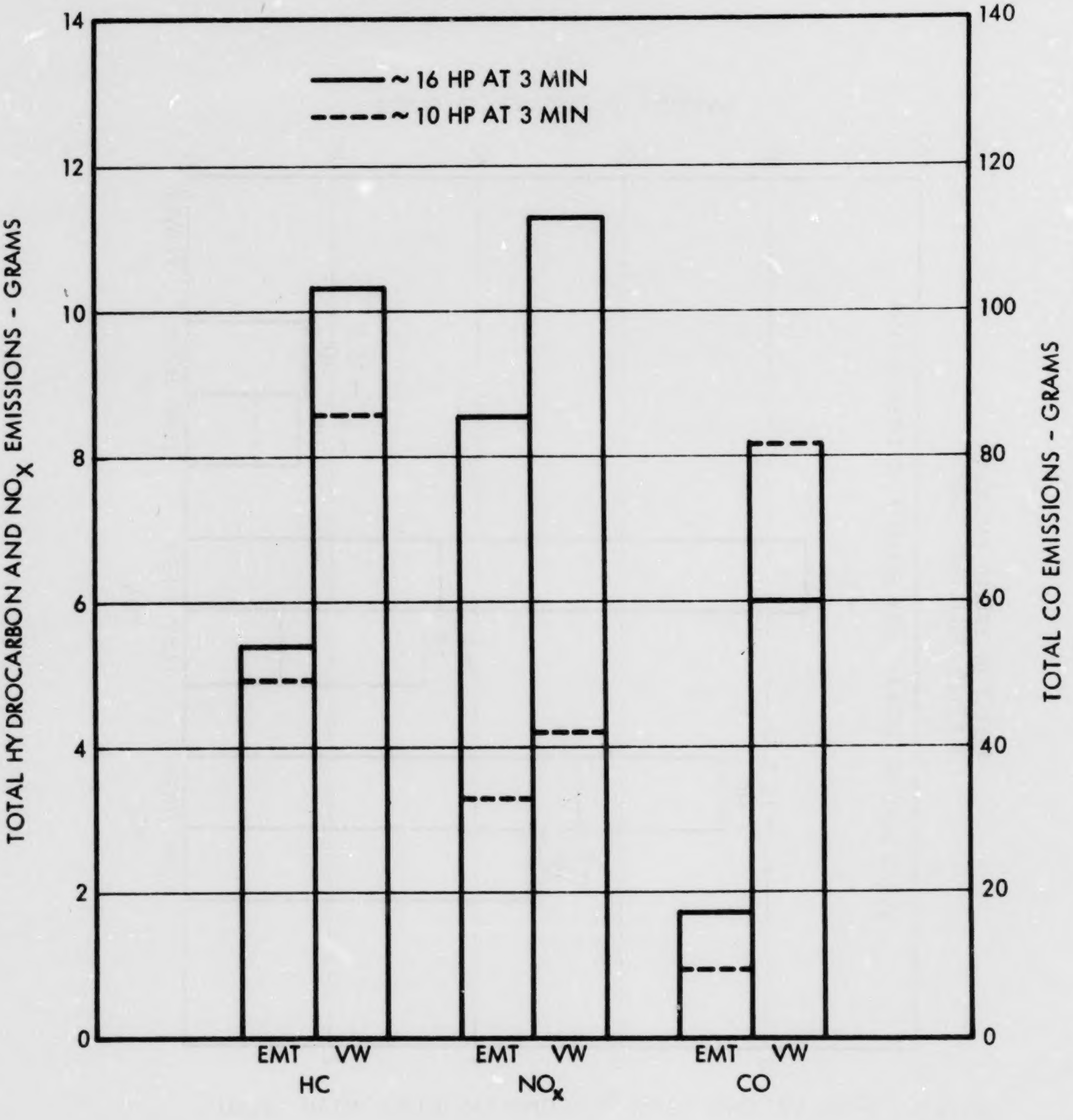

FIGURE 9.5

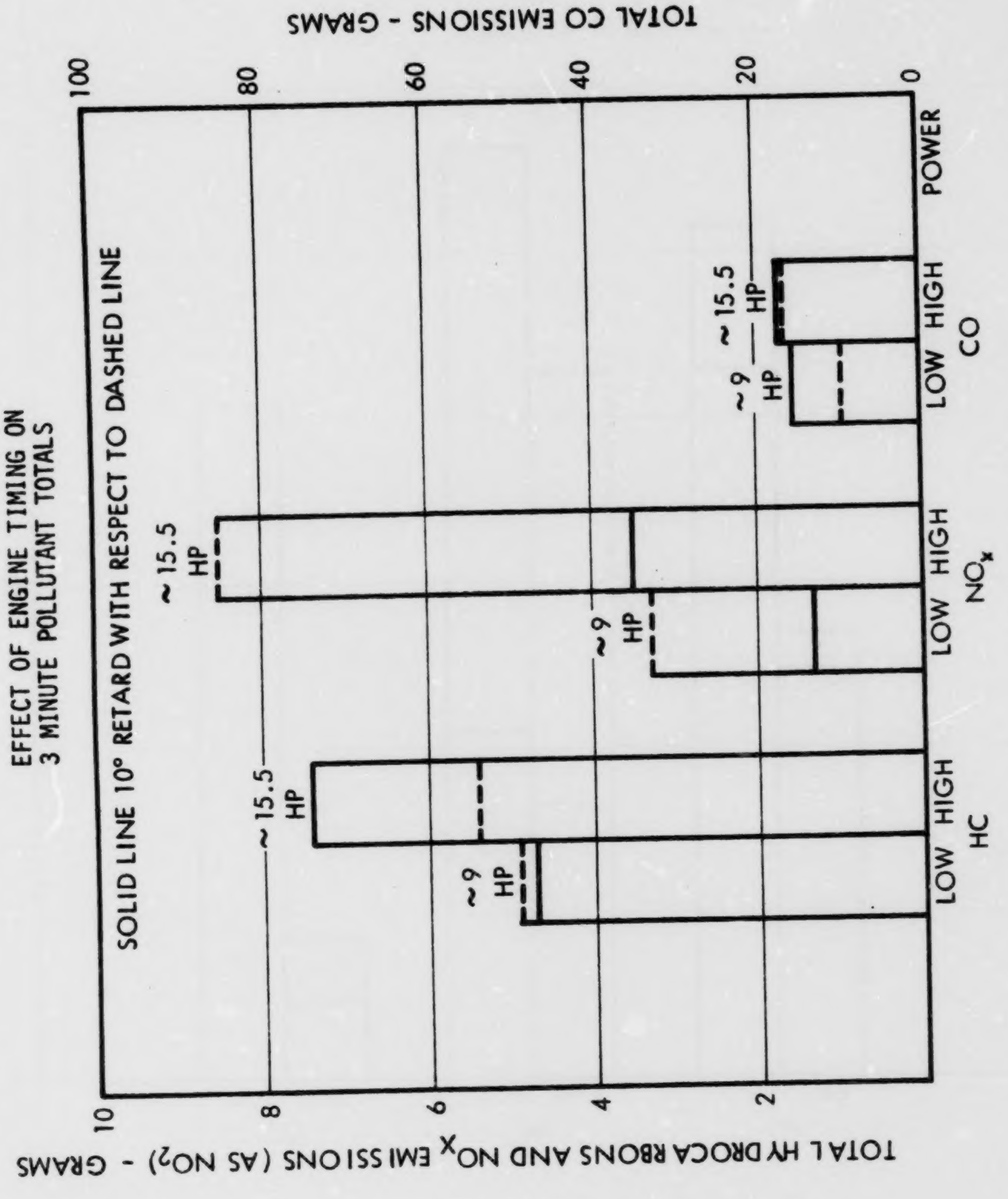
EFFECT OF ENGINE TIMING ON
3 MINUTE POLLUTANT TOTALS
SOLID LINE 10° RETARD WITH RESPECT TO DASHED LINE
TOTAL HYDROCARBONS AND NOx EMISSIONS (AS NO2) - GRAMS
10
8
6
4
2
TOTAL CO EMISSIONS - GRAMS
100
80
60
40
20
0
~9 HP
~15.5 HP
~9 HP
~15.5 HP
~9 HP
~15.5 HP
LOW
HIGH
HC
LOW
HIGH
NOx
LOW
HIGH
CO
POWER

FIGURE 9.6

Several conclusions can be drawn from the cold start test work:

- The internal combustion engine tested exhibits a period of operation after ignition where its temperature, mixture ratio and emission signature vary very rapidly.
- This period is of approximately three minutes duration.
- The cold period can be broadly broken into two portions; the CO and HC portion and the $NO_x$ portion. The former occurs immediately after ignition and lasts for 30 to 60 seconds. During this period the major contribution to the cold start HC and CO emissions results. The $NO_x$ portion builds as the HC and CO portion falls off. While the HC and CO mass totals are relatively unaffected by power level, the $NO_x$ contribution is clearly related to power level.
- Emissions during the cold start period can be greatly reduced by controlled engine operation. Simultaneous rapid dechoking and throttle increase may be the best starting procedure.
- Spark retard reduces the mass emissions during the cold period. Reduction of $NO_x$ levels is particularly sensitive to timing; the effect increases with increasing power level.
- Minimum emissions are obtained from procedures such as followed in tests C-10, C-11 and C-14 of Tables 9.1 and 9.2.

### 9.2.3 Hot Tests Results

A complete summary of hot engine test results is given in Table 9.3. Thirteen tests were performed varying in duration from ten to thrity minutes. During each test a number of engine parameters were varied and their effect on pollutant mass rates was determined. Tables 9.4, 9.5 and 9.6 group a portion of the data of Table 9.3 in a way such that the effects of various engine parameters on emissions are isolated.

The data of Table 9.4 indicates the effect of air-fuel ratio on major pollutant mass rates at constant power, speed and engine timing. Two power settings and two values of ignition timing are examined. The data of Table 9.4 indicates that at both power settings and both spark timings minimum pollutant mass rates are observed at leaner than stoichiometric air-fuel ratios. It is also shown that at constant spark timing the higher the power setting the leaner the fuel mixture should be to keep emissions low. Increased spark retard requires a decrease of the air-fuel ratio for constant power operation. In general, even a five percent change in the

## TABLE 9.3 HOT TESTS (1968 VW)

| Test Nos. | Engine Parameters | | | | Exhaust Composition - Concentration | | | | Emissions - Mass Rate | | | Engine Performance | | |
|---|---|---|---|---|---|---|---|---|---|---|---|---|---|---|
| | Air/ Fuel Ratio | Timing BTDC | Manifold Pressure "Hg | RPM | HC (as $C_3$) (PPM) FID | CO (PPM) | NO (PPM) | $O_2$ (%) | HC gms/ min | CO gms/ min | NO gms/ min | Intake Air Flow (CFM) | Alter- nator (Kw) | Exhaust Gas Temp ($^0$F) |
| 1-1 | 16.1 | 10° | 8.4 | 1800 | 190 | 950 | 980 | 3 | 0.28 | 0.94 | 1.60 | 30 | 2.52 | 1420 |
| 1-2 | 16.1 | 20° | 8.4 | 1800 | 360 | 1400 | 2000 | 2.5 | 0.53 | 1.38 | 3.26 | 30 | 4.0 | 1330 |
| 1-3 | 17.2 | 20° | 6.5 | 1800 | 250 | 1100 | 550 | 3.5 | 0.42 | 1.23 | 1.02 | 34 | - | |
| 1-4 | 14.5 | 20° | 6.7 | 1800 | 370 | 1750 | 2300 | 1.8 | 0.60 | 1.90 | 4.20 | 33 | - | |
| 1-5 | 17.8 | 20° | 6.7 | 1800 | 220 | 1100 | 300 | 4.5 | 0.35 | 1.20 | 0.54 | 33 | 2.91 | |
| 1-6 | 19.0 | 20° | 6.7 | 1800 | 600 | 1420 | 170 | 6.0 | 0.97 | 1.55 | 0.305 | 33 | 1.92 | |
| 1-7 | 17.7 | 20° | 6.7 | 1800 | 200 | 1110 | 900 | 4.0 | 0.32 | 1.20 | 1.61 | 33 | 3.60 | 1380 |
| 2-1 | 19.1 | 20° | 6.2 | 1800 | 300 | 1150 | 750 | 4.5 | 0.53 | 1.36 | 1.46 | 35.8 | 3.70 | 1330 |
| 2-2 | 18.3 | 10° | 6.0 | 1780 | 120 | 750 | 300 | 5.0 | 0.20 | 0.77 | 0.55 | 34.0 | 1.9 | 1430 |
| 2-3 | 16.9 | 20° | 3.0 | 1800 | 170 | 1000 | 1100 | 5.0 | 0.33 | 1.21 | 2.43 | 40.4 | 5.9 | |
| 2-4 | 15.2 | 20° | 3.0 | 1800+ | 330 | 2550 | 2400 | 5.0 | 0.60 | 3.42 | 5.29 | 40.5 | 8.45 | 1400 |
| 2-5 | 16.8 | 20° | 0.9 | 1800+ | 200 | 1100 | 2000 | 5.6 | 0.43 | 1.61 | 4.80 | 44.3 | 9.08 | |
| 2-6 | 16.6 | 20° | 0.9 | 1800+ | 230 | 1130 | 2350 | | 0.51 | 1.68 | 5.73 | 45.0 | - | |
| 2-7 | 17.3 | 20° | 0.9 | 1800+ | 150 | 1000 | 750 | | 0.33 | 1.48 | 1.84 | 45 | 6.96 | |
| 2-8 | 17.7 | 20° | 0.9 | 1800+ | 160 | 1050 | 350 | | 0.35 | 1.56 | 0.85 | 45 | 5.68 | |
| 2-9 | 19.8 | 20° | 0.9 | 1800 | 330 | 1150 | 210 | | 0.73 | 1.70 | 0.51 | 45 | 4.54 | 1360 |
| 3-1 | 12.1 | 30° | 8.2 | 1800 | 1400 | 4150 | 1250 | 0.5 | 2.10 | 4.20 | 2.08 | 30.6 | 5.5 | 1260 |
| 3-2 | 12.3 | 30° | 8.3 | 1800 | 1200 | 2500 | 2000 | 1.2 | 1.80 | 2.52 | 3.32 | 30.6 | 7.5 | 1300 |
| 3-3 | 13.7 | 30° | 8.4 | 1800 | 750 | 3200 | 3250 | 2.5 | 1.12 | 3.23 | 5.40 | 30.6 | 7.4 | |
| 3-4 | 16.2 | 30° | 8.4 | 1800 | 400 | 1250 | 2150 | 3.5 | 0.60 | 1.26 | 3.58 | 30.6 | 5.6 | |
| 3-5 | 18.0 | 30° | 8.4 | 1800 | 350 | 1200 | 600 | 4.6 | 0.52 | 1.21 | 1.00 | 30.6 | 4.5 | |
| 3-6 | 19.4 | 30° | 8.4 | 1800 | 1200 | 1700 | 150 | 6.0 | 1.80 | 1.72 | 0.25 | 30.6 | 2.4 | 1250 |
| 3-7 | 16.8 | 30° | 8.5 | 1800 | 400 | 1250 | 1350 | 3.70 | 0.60 | 1.26 | 2.24 | 30.6 | 5.75 | |
| 3-8 | 16.9 | 20° | 8.4 | 1800 | 230 | 1100 | 650 | 3.70 | 0.34 | 1.11 | 1.08 | 30.6 | 4.55 | 1320 |
| 3-9 | 16.9 | 22° | 8.4 | 1800 | 250 | 1200 | 800 | 3.70 | 0.37 | 1.21 | 1.33 | 30.6 | - | |
| 3-10 | 17.0 | 30° | 8.4 | 1800 | 360 | 1250 | 1300 | 4.00 | 0.54 | 1.26 | 2.16 | 30.6 | - | |
| 3-11 | 16.9 | 30° | 0.90 | 1800+ | 540 | 1200 | 3700 | 3.20 | 1.18 | 1.76 | 8.94 | 44.5 | 11.3 | 1280 |
| 4-1 | 16.1 | 20° | 8.3 | 1800 | 350 | 1350 | 1600 | 2.50 | 0.54 | 1.39 | 2.70 | 31.2 | 5.5 | 1350 |
| 4-2 | 14.9 | 20° | 13.4 | 1800 | 250 | 1200 | 900 | 2.0 | 0.26 | 0.85 | 1.05 | 21.5 | 2.44 | 1320 |
| 4-3 | 14.3 | 20° | 13.4 | 1800 | 250 | 1350 | 1100 | 1.5 | 0.27 | 0.98 | 1.31 | 21.9 | 2.96 | |
| 4-4 | 13.0 | 20° | 13.4 | 1800 | 710 | 11000 | 1300 | 0.5 | 0.76 | 8.00 | 1.55 | 21.9 | 3.80 | |
| 4-5 | 13.3 | 20° | 13.4 | 1800 | 450 | 4000 | 1400 | 0.8 | 0.48 | 2.90 | 1.67 | 21.9 | 3.53 | 1350 |
| 4-6 | 13.3 | 10° | 13.4 | 1800 | 200 | 3000 | 800 | 0.7 | 0.21 | 2.20 | 0.95 | 21.9 | 2.44 | 1430 |
| 4-7 | 13.3 | 20° | 13.4 | 1800 | 450 | 4400 | 1450 | 0.8 | 0.48 | 3.20 | 1.73 | 21.9 | 3.70 | 1350 |
| 4-8 | 15.1 | 20° | 13.4 | 1800 | 200 | 1100 | 900 | 2.2 | 0.21 | 0.80 | 1.07 | 21.9 | 2.61 | |
| 4-9 | 15.6 | 20° | | 1700 | 160 | 1000 | 600 | 3.0 | 0.17 | 0.73 | 0.71 | 21.9 | 2.28 | |
| 4-10 | 15.3 | 20° | 10.4 | 1510 | 150 | 1000 | 300 | 3.7 | 0.15 | 0.70 | 0.35 | 20.9 | 2.23 | 1300 |
| 4-11 | 15.2 | 20° | 9.3 | 1330 | 450 | 1400 | 150 | 5.0 | 0.43 | 0.89 | 0.16 | 20.0 | 0.7 | 1300 |
| 5-1 | 17.1 | 20° | 0.9 | 1800 | 420 | 1250 | | | | | | | | |

| | | | | | | | | | | | | | |
|---|---|---|---|---|---|---|---|---|---|---|---|---|---|
| | | | | | | | [illegible] | [illegible] | [illegible] | [illegible] | 1.07 | 21.9 | 2.61 | |
| [illegible] | [illegible] | [illegible] | | 1700 | 160 | 1000 | 600 | 3.0 | 0.17 | 0.73 | 0.71 | 21.9 | 2.28 | |
| 4-10 | 15.3 | 20° | 10.4 | 1510 | 150 | 1000 | 300 | 3.7 | 0.15 | 0.70 | 0.35 | 20.9 | 2.23 | 1300 |
| 4-11 | 15.2 | 20° | 9.3 | 1330 | 450 | 1400 | 150 | 5.0 | 0.43 | 0.89 | 0.16 | 20.0 | 0.7 | 1300 |
| 5-1 | 17.1 | 20° | 0.9 | 1800 | 420 | 1250 | 2200 | 3.2 | 0.94 | 1.87 | 5.30 | 45.4 | 9.3 | |
| 5-2 | 17.3 | 20° | 0.9 | 2000 | 350 | 1300 | 2200 | 3.0 | 0.86 | 2.14 | 5.96 | 50.0 | 9.9 | 1350 |
| 5-3 | 16.7 | 20° | 0.9 | 1800 | 290 | 1350 | 1200 | 4.0 | 0.62 | 1.95 | 2.86 | 43.8 | 8.52 | |
| 5-4 | 17.8 | 20° | 8.7 | 1800 | 170 | 1100 | 400 | 4.2 | 0.25 | 1.10 | 0.66 | 30.4 | 3.75 | |
| 5-5 | 19.3 | 20° | 5.9 | 1800 | 220 | 1250 | 250 | 5.3 | 0.39 | 1.47 | 0.49 | 35.8 | 3.74 | |
| 5-6 | 20.0 | 20° | 2.7 | 1800 | 550 | 1750 | 250 | 6.0 | 1.14 | 2.43 | 0.57 | 42.2 | 3.75 | 1380 |
| 5-7 | 16.4 | 20° | 9.9 | 1800 | 120 | 1150 | 180 | 3.2 | 0.16 | 1.06 | 0.27 | 28.0 | 3.75 | |
| 5-8 | 15.1 | 20° | 12.0 | 1800 | 170 | 1300 | 660 | 2.0 | 0.20 | 1.04 | 0.87 | 24.2 | 3.75 | |
| 5-9 | 12.4 | 20° | 13.6 | 1800 | 880 | 3500 | 1200 | 0.4 | 0.95 | 25.2 | 1.42 | 21.8 | 3.75 | 1350 |
| 6-1 | 16.2 | 20° | 9.8 | ~1800 | 260 | 1150 | 710 | 4.0 | 0.36 | 1.07 | 1.10 | 28.2 | 3.63 | 1320 |
| 6-2 | 16.1 | 10° | 9.0 | 1700 | 120 | 700 | 420 | 3.8 | 0.17 | 0.65 | 0.64 | 28.0 | 2.28 | 1420 |
| 6-3 | 15.6 | 10° | 10.1 | 1800 | 140 | 1000 | 950 | 2.0 | 0.19 | 0.93 | 1.44 | 28.0 | 3.63 | 1440 |
| 6-4 | 15.6 | 20° | 10.1 | 1800 | 280 | 1550 | 1850 | 2.0 | 0.38 | 1.44 | 2.80 | 28.0 | 5.5 | 1350 |
| 6-5 | 16.4 | 20° | 8.25 | 1800 | 250 | 1250 | 1750 | 2.8 | 0.37 | 1.24 | 2.86 | 30.2 | 6.23 | |
| 6-6 | 15.1 | 20° | 9.45 | 1800 | 380 | 2300 | 2250 | 1.3 | 0.53 | 2.20 | 3.50 | 28.8 | 6.23 | |
| 6-7 | 18.1 | 20° | 6.20 | 1800 | 190 | 1130 | 800 | 4.2 | 0.32 | 1.29 | 1.50 | 34.6 | 6.23 | 1360 |
| 6-8 | 18.4 | 10° | 6.30 | 1800 | 110 | 750 | 280 | 4.2 | 0.19 | 0.87 | 0.52 | 34.5 | 2.96 | 1460 |
| 6-9 | 13.4 | 10° | 8.6 | 1800 | 550 | 17000 | 1250 | 0.4 | 0.81 | 16.8 | 2.04 | 30.0 | 6.02 | |
| 6-10 | 14.4 | 10° | 7.8 | 1800 | 260 | 6000 | 1600 | 0.6 | 0.40 | 6.23 | 2.70 | 31.5 | 6.23 | |
| 6-11 | 15.7 | 10° | 6.5 | 1800 | 150 | 1250 | 1450 | 1.7 | 0.25 | 1.42 | 2.70 | 34.4 | 6.23 | |
| 7-1 | 15.0 | 30° | 13.1 | 1800 | 700 | 1400 | 2750 | 2.2 | 0.79 | 1.07 | 3.44 | 23.0 | 3.86 | 1250 |
| 8-1 | 14.8 | 30° | 13.2 | 1800 | 640 | 1425 | 2600 | 2.1 | 0.72 | 1.08 | 3.24 | 23.0 | 3.86 | 1250 |
| 8-2 | 15.6 | 30° | 8.7 | 1800 | 590 | 1275 | 3400 | 2.2 | 0.86 | 1.25 | 5.50 | 29.7 | 6.85 | 1270 |
| 8-3 | 15.6 | 20° | 3.0 | 1800 | 520 | 1750 | 3600 | 1.8 | 1.05 | 2.40 | 8.10 | 41.4 | 10.80 | 1340 |
| 9-1 | 16.6 | 20° | 10.2 | 1800 | 350 | 1175 | 1300 | 3.5 | 0.49 | 1.10 | 2.00 | 28.4 | 4.10 | 1300 |
| 9-2 | 17.7 | 20° | 10.1 | 1800 | 250 | 1100 | 475 | 4.0 | 0.34 | 1.02 | 0.72 | 28.0 | 3.96 | 1300 |
| 9-3 | 17.5 | 20° | 7.9 | 1800 | 250 | 1130 | 1130 | 3.5 | 0.40 | 1.21 | 1.98 | 32.4 | 5.6 | 1310 |
| 9-4 | 16.8 | 20° | 0.9 | 1800 | 270 | 1140 | 2350 | 3.5 | 0.59 | 1.69 | 5.72 | 44.8 | 10.6 | 1310 |
| 10-1 | 14.1 | 30° | 11.85 | 1800 | 790 | 1370 | 3250 | 2.4 | 0.95 | 1.10 | 4.30 | 24.4 | 4.55 | 1240 |
| 10-2 | 13.8 | 30° | 14.1 | 1800 | 740 | 1525 | 2340 | 2.0 | 0.73 | 1.00 | 2.54 | 20.0 | 3.45 | 1240 |
| 10-3 | 13.8 | 30° | 14.1 | 1800 | 705 | 1525 | 2375 | 1.8 | 0.69 | 1.00 | 2.56 | 20.0 | 3.37 | 1240 |
| 10-4 | 14.6 | 20° | 0.85 | 1800 | 600 | 2450 | 3810 | 1.5 | 1.29 | 3.55 | 9.10 | 43.9 | 12.5 | 1370 |
| 11-1 | 15.5 | 10° | 6.4 | 1800 | 140 | 1000 | 800 | 3.4 | 0.23 | 1.13 | 1.48 | 34.0 | 4.86 | 1400 |
| 12-1 | 17.1 | 20° | 7.5 | 1800 | 270 | 1500 | 920 | 4.2 | 0.42 | 1.58 | 1.60 | 31.9 | 5.00? | 1300 |
| 12-2 | 18.0 | 20° | 6.2 | 1800 | 185 | 1100 | 395 | 5.1 | 0.31 | 1.25 | 0.74 | 34.3 | 4.45? | 1310 |
| 12-3 | 16.8 | 20° | 0.95 | 1800 | 230 | 1450 | 1970 | 4.2 | 0.50 | 2.12 | 4.73 | 44.2 | 9.75 | 1320 |
| 13-1 | - | | 10.2 | 2100 | 470 | 1400 | 2000 | 1.7 | 0.72 | 1.44 | 3.40 | 31.2 | 4.28 | 1400 |
| 13-2 | - | 20° | 6.0 | 1500 | 580 | 2000 | 2100 | 1.4 | 0.74 | 1.60 | 2.96 | 26.0 | 4.93 | 1340 |
| 13-3 | - | 20° | 8.5 | 1800 | 450 | 1320 | 1850 | 2.2 | 0.64 | 1.27 | 2.94 | 29.2 | 4.0 | 1350 |

BLANK PAGE

## TABLE 9.4

## EFFECT OF AIR-FUEL RATIOS ON POLLUTANT MASS RATE

| Test Nos. | Air-Fuel | Oxygen Exhaust in (Percent) | Pollutant Mass Rates (grams/min) HC | CO | $NO_x$ (as $NO_2$) |
|---|---|---|---|---|---|
| A. 10.5 hp; 1800 rpm; 20° BTDC | | | | | |
| 5-9 | 12.4 | 0.4 | 0.95 | 2.52 | 1.42 |
| 5-8 | 15.1 | 2.0 | 0.20 | 1.04 | 0.87 |
| *5-7 | 16.4 | 3.2 | 0.16 | 1.06 | 0.27 |
| 5-4 | 17.8 | 4.2 | 0.25 | 1.10 | 0.66 |
| 5-5 | 19.3 | 5.3 | 0.39 | 1.47 | 0.49 |
| 5-6 | 20.0 | 6.0 | 1.14 | 2.43 | 0.57 |
| B. 15 hp; 1800 rpm; 20° BTDC | | | | | |
| 6-6 | 15.1 | 1.3 | 0.53 | 2.20 | 3.50 |
| 6-5 | 16.4 | 2.8 | 0.37 | 1.24 | 2.86 |
| *6-7 | 18.1 | 4.2 | 0.32 | 1.29 | 1.50 |
| C. 15 hp; 1800 rpm; 10° BTDC | | | | | |
| 6-9 | 13.4 | 0.4 | 0.81 | 16.80 | 2.04 |
| 6-10 | 14.4 | 0.6 | 0.40 | 6.23 | 2.70 |
| *6-11 | 15.7 | 1.7 | 0.25 | 1.42 | 2.70 |

---

*Best runs (tests resulting in lowest pollutant mass rates under the range of utilized conditions).

air-fuel ratio (on either side of the optimum value) can cause severe changes in the HC and $NO_x$ mass rates.

Table 9.5 data demonstrate the effect of spark timing on pollutant mass rates. Spark retard substantially reduces the hydrocarbon levels in the exhaust at all power settings and for all air-fuel ratios. Its effect on $NO_x$ is a function of air-fuel ratio and the engine manifold pressure.

If the power output of the engine is held constant by spark retardation and manifold pressure changes (part A), NO control at constant air-fuel ratio is effective. If power is controlled by increasing the mixture ratio (richer mixture) at constant manifold pressure, then spark retardation is also effective in NO control.

A significant effect of spark retard is the increase in exhaust gas temperature with retardation. For the tests reported here, the temperature increased an average of 100°F per 10° of retard. Systems employing catalytic converters where the conversion efficiency is severely temperature dependent will probably require some retardation to maintain converter temperature.

Table 9.6 shows the dependence of emission mass rates on power output. For the range of power settings investigated, $NO_x$ is most sensitive to power output, increasing more rapidly with power than would be expected on the basis of air flow rates. There appears to be a small increase in HC flow with power; however, these variations may be caused by air-fuel ratio effects which cannot be separated from the data. CO is very insensitive to power level.

### 9.2.4 Conclusions

The test program demonstrated the magnitude of the "cold start problem" of a spark ignition engine. For a conventionally carbureted and choked engine, the CO and HC mass levels during the initial phases of engine operation greatly exceed the 1975 standards. On the other hand, mixture ratio control and spark timing can reduce or eliminate the problem if there is no requirement of engine driveability, i.e., the engine can be effectively uncoupled from the wheels during the warm-up period.

## TABLE 9.5

## EFFECT OF SPARK TIMING ON POLLUTANT MASS RATE AND EXHAUST TEMPERATURE

| Test Nos. | Air-Fuel | Spark Degrees BTDC | Pollutant Mass Rates (grams/min) HC | CO | $NO_x$* | Exhaust Temperature |
|---|---|---|---|---|---|---|
| A. 15 hp; 1800 rpm; approx. constant air-fuel at 15.8 | | | | | | |
| ** | 15.9 | 30 | 0.73 | 1.25 | 4.54 | 1260°F |
| (6-5) (16.4)<br>(6-6) (15.1) | 15.8 | 20 | (0.37)<br>(0.53) 0.45 | (1.24)<br>(2.20) 1.72 | (2.86)<br>(3.50) 3.18 | 1350°F |
| 6-11 | 15.7 | 10 | 0.25 | 1.42 | 2.70 | 1460°F |
| B. 12 hp; 1800 rpm; approx. constant manifold pressure | | | | | | |
| 3-5 | 18 | 30 | 0.52 | 1.21 | 1.00 | 1300°F |
| 3-8 | 16.9 | 20 | 0.34 | 1.11 | 1.08 | 1320°F |
| 11-1 | 15.5 | 10 | 0.23 | 1.13 | 1.48 | 1400°F |
| C. 9 hp; 1800 rpm; approx. constant manifold pressure | | | | | | |
| 3-6 | 19.4 | 30 | 1.80 | 1.72 | 0.25 | 1250°F |
| 4-2 | 14.9 | 20 | 0.26 | 0.85 | 1.05 | 1320°F |
| 4-6 | 13.3 | 10 | 0.21 | 2.20 | 0.95 | 1430°F |

---

*as $NO_2$

**average of tests 3-4 and 8-2

## TABLE 9.6

## EFFECT OF POWER ON POLLUTANT MASS RATES

A. 1800 rpm; approx. 16.5 air-fuel; 20° BTDC

| Test Nos. | Power hp | Air-Fuel | Throttle Air Flow scfm | Pollutant Mass Rates (grams/min) | | |
|---|---|---|---|---|---|---|
| | | | | HC | CO | $NO_x$* |
| 5-7 | 10.5 | 16.4 | 28 | 0.16 | 1.06 | 0.27 |
| 6-5 | 15 | 16.4 | 30.2 | 0.37 | 1.24 | 2.86 |
| 9-4 | 23 | 16.8 | 44.8 | 0.59 | 1.69 | 5.72 |

B. 1800 rpm; approx. 17.0 air-fuel; 20° BTDC

| | | | | | | |
|---|---|---|---|---|---|---|
| 9-1 | 11 | 16.6 | 28.4 | 0.49 | 1.10 | 2.00 |
| 9-3 | 14 | 17.5 | 32.4 | 0.40 | 1.21 | 1.98 |
| 5-1 | 20.5 | 17.1 | 44.8 | 0.94 | 1.87 | 5.30 |

---

*as $NO_2$

Both cold start and hot engine pollutant mass rates are extremely sensitive to air-fuel ratio:

- Rapid fuel mixture leaning to above stoichiometric air-fuel ratios during cold start and reduce hydrocarbon and $NO_x$ levels by more than 50%.
- Hot engine operation should be confined to lean fuel mixtures. The optimum air-fuel ratio increases with power level settings. With the spark at 30° BTDC and an engine speed of 1800 rpm, the optimum air-fuel ratio lies between 16 and 17.5, depending on the power setting.

Timing is important to emission control. During the cold period:

- Spark retard hinters smooth engine start-up and causes an increase in the hydrocarbon emissions at any given power setting. It substantially reduces the $NO_x$ emissions during this period.
- Spark retard initiated approximately 30 seconds after engine ignition appears to be the best timing schedule as it eliminates difficulties associated with engine start-up, yet introduces $NO_x$ control early and increases the exhaust gas temperature more rapidly.

During hot engine operation:

- Spark retard at constant speed and power reduces the hydrocarbon mass rate in the exhaust at all air-fuel ratios. $NO_x$ mass rate is reduced by spark retard at constant power and air-fuel ratio. CO is relatively unaffected by spark retard.
- Spark retard at constant speed, air-fuel ratio, and manifold pressure substantially reduces HC and $NO_x$ exhaust concentrations; however, engine power is reduced by approximately 33% per 10° of retard.

Emissions are affected by engine power levels in the following: Increased engine power causes an increase in the emission mass rates. The increase in exhaust $NO_x$ is disproportionately large with power increase. Hydrocarbon emissions during the cold period are relatively insensitive to power level.

Figure 9.7 summarizes the results of this study in terms of predicted HC emission performance on a 1972 DHEW cycle. It is assumed that the engine would be started cold and its choke, power and timing schedule would be controlled during the cold period (three minutes) to produce signatures as determined by the VW test results. For the remainder of

EFFECT OF COLD START (3 MINUTES) HYDROCARBON EMISSIONS ON TOTAL HYDROCARBONS EMITTED DURING 22 MINUTES (APPROX. 7 MILES) OF CONSTANT POWER OPERATION OF A 1600 VW ENGINE

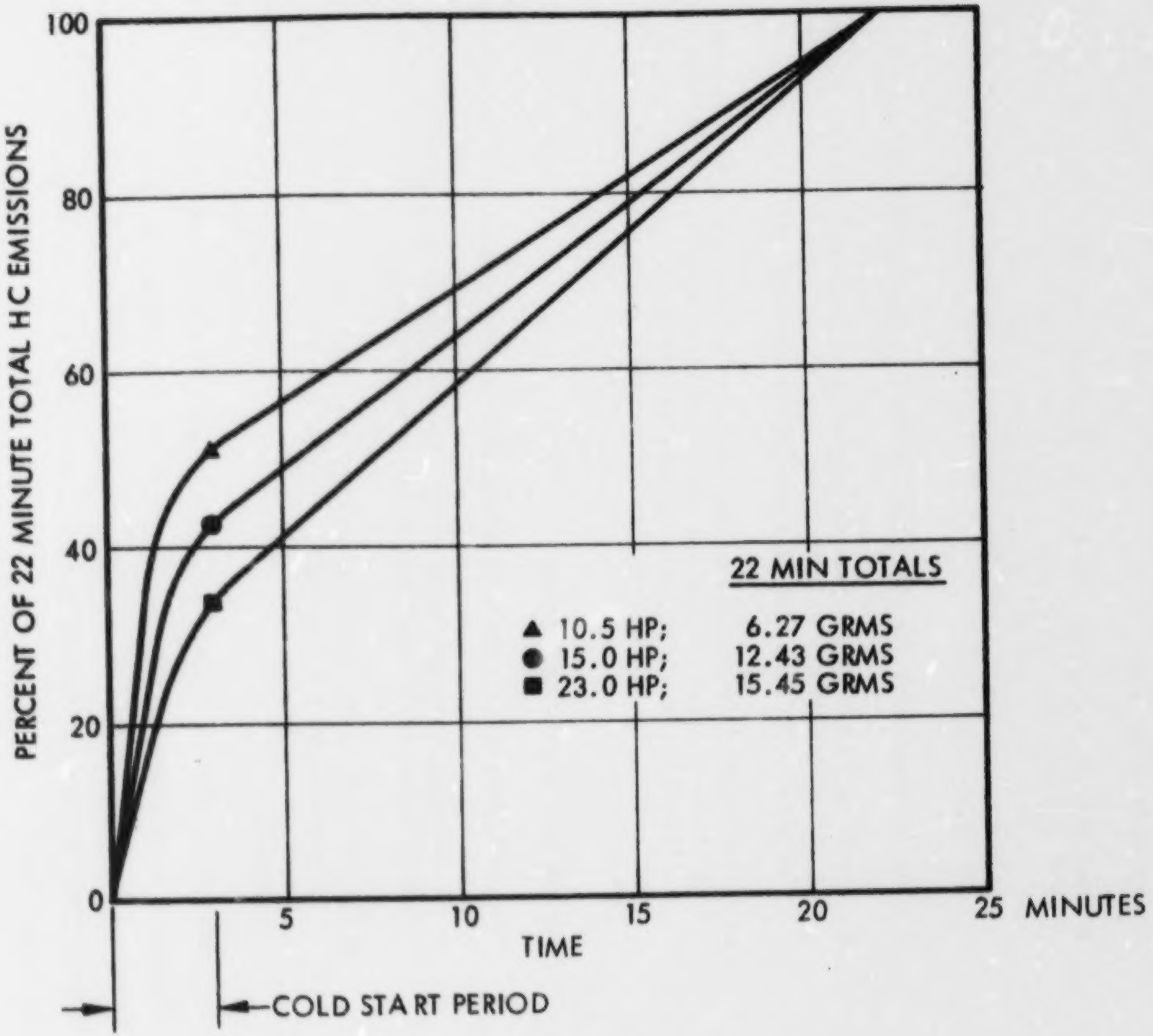

FIGURE 9.7

the cycle the engine would be held at power settings as shown in the figure.

The total hydrocarbon emissions fail to meet the Federal standards due to the cold start. Approximately 50% of the total emissions are released by the end of the third minute of operation. However, during the same period, a conventional engine would have emitted nearly twice as much hydrocarbons and anywhere from three to ten times more CO.

Exhaust emissions can be minimized in the absence of exhaust control devices by adopting the following procedures:

- Start the engine with a fully advanced spark at throttle positions corresponding to 10-15 hp when the engine is hot.
- Retard the spark after 30 seconds.
- Relieve the engine choke rapidly during the first minute of operation while simultaneously increasing the throttle to the desired final power.
- When the engine is hot, use a lean air-fuel ratio (16-17.5) or a ratio closer to stoichiometry (∿15.5) but with a spark retarded 10° or more from the normal operating point.

## 9.3 Effectiveness of a Three-Component Catalyst on Exhaust Emissions

A three-component catalyst system was tested to determine its effectiveness on a constant throttle, constant power engine. The three component catalyst chosen was one of several produced by Universal Oil Products (UOP) of Des Plaines, Illinois. The catalyst is reported to contain only non-noble metals and for a narrow range of air-fuel ratios near stoichiometry is claimed to have CO, HC and NO conversion efficiencies in excess of 90%.

TRW Systems personnel traveled to UOP to coordinate the testing. A late model VW 1600 equipped with fuel injection and a UOP catalytic converter/muffler was tested on a chassis dynamometer. Four hot runs were made.

### 9.3.1 Hot Test Results

Table 9.7 summarizes the four tests. The first two runs were made at very low power settings. The air-fuel ratio was apparently too lean for the catalytic converter to reduce the $NO_x$; i.e., there was insufficient HC and CO in the exhaust stream. The low values of HC and CO are primarily a result of lean engine operation and any catalytic conversion which took place.

In runs 3 and 4, the throttle was opened to a level more consistent with EMT operation. At this setting, the car ran in second gear (automatic transmission) between 26 and 28 mph and the chassis dynamometer load was set at 6.2 to 6.4 hp. In run 3, the mixture ratio was again too lean and the $NO_x$ is not controlled. A change in the air-fuel ratio of about 6% to a richer mixture brought the system to a desirable state of run 4. Contrasting the data of run 4 with hot test 5-6 of Table 9.4 indicates the gain achievable with a catalytic device; a 25% reduction in HC, a 20% reduction in CO and a 37% reduction in $NO_x$.

## 9.4 Prediction of Emission Signature of an EMT System with a Three-Component Catalytic Device

Table 9.8 presents predicted emission levels of an ICE-powered EMT hybrid using a three-component catalytic converter of the UOP type. Predictions are based on combining the cold start test data, C-10, and run 4 of Table 9.7. The system fails to meet the 1975 standards for HC and $NO_x$. The primary source appears to be the three minute contributions of HC and

## TABLE 9.7

## HOT TEST RESULTS OF UOP THREE-COMPONENT CATALYST ON VW 1600 ENGINE

| | Engine RPM | Manifold Pressure "Hg | Exhaust Emissions grams/min HC | CO | $NO_x$ |
|---|---|---|---|---|---|
| Run No. 1 | 1800 | 12.3 | 0.085 | ∿0 | 0.70 |
| 2 | 1800 | 11.8 | 0.084 | ∿0 | 0.65 |
| 3 | 1800 | 8.25 | 0.09 | 0.08 | 0.98 |
| 4 | 1800 | 8.5 | 0.123 | 0.08 | 0.073 |

## TABLE 9.8

## PREDICTED EMISSION PERFORMANCE OF AN EMT HYBRID ON A 1385 SECOND DHEW CYCLE*
(VW 1600 + UOP Catalyst)

| | HC grams/mile | CO grams/mile | $NO_x$ (as $NO_2$) grams/mile |
|---|---|---|---|
| Total Cycle | 0.720 | 4.09 | 0.510 |
| Percent Due to Cold Start | 58 | 95.5 | 66.5 |

---

*engine operating at 14 shaft horsepower

$NO_x$. In terms of the rapid rise in exhaust gas temperature and the delay of $NO_x$ appearance, it is probable that there would be some significant catalytic conversion of $NO_x$ during the three-minute cold period if the catalytic device had been installed on the EMT equipment.

## REFERENCES

1. Gelb, Richardson, Wang, and Berman, "An Electromechanical Transmission for Hybrid Vehicle Power Trains--Design and Dynamometer Testing", Society of Automotive Engineers Paper No. 710235, January 1971.

2. Richardson, Gelb, Wang, and Licari, "System Design Implications of Electric and Hybrid Vehicles", Intersociety Energy Conversion and Engineering Conference, Denver, Colorado, August 1968.

3. Foote and Hough, "An Experimental Battery Powered Ford Cortina Estate Car", Soceity of Automotive Engineers International Automotive Engineering Congress and Exposition, Detroit, Michigan, January 1970.

4. Gelb, Richardson, Wang, and DeWolf, "Design and Performance Characteristics of a Hybrid Vehicle Power Train", Society of Automotive Engineers, Paper No. 690169, January 1969.

5. Byrne and Lacy, "Compatible Controller--Motor System for Battery Electric Vehicles", Proceedings of the IEE, Vol. 117, No. 2, February 1970.

6. Kawai and Miyake, "Pulsating Current Traction Motors for the Electric Multiple-Unit Coaches for the New Tokaido Line, Hitachi Review, Special Issue on the New Tokaido Line, Tokyo, Japan, June 1964.

Further reading on chopper circuits for control of DC traction systems (Section 5.1) can be found in:

Berman, "Battery Powered Regenerative SCR Drive", IEEE 1970 IGA Conference Record, Chicago, Illinois.

Silicon Controlled Rectifier Designer's Handbook, R. Murray, editor, Westinghouse Electric Corporation, April 1964.

SCR Manual, 4th Edition, F. Gutzwiler, editor, General Electric Corporation, 1967.

Koch, "The Electric Car: A Design Challenge", Electro-Technology, May 1968.

Morgan, "Time Ratio Control with Combined SCR and SR Commutation, IEEE Transactions on Communications and Electronics, July 1964.

Heumann, "Pulse Control of DC and AC Motors with SCRs", Proceedings of INTERMAG Conference, Paper No. 63-1011, April 1965.

# APPENDIX A-1

## COMPARISON OF BOOST-BUCK AND BOOST PCUs FOR REGENERATION

### Boost-Buck PCU

Figure 2.15 showed the simple circuit configuration for boost-buck PCU. The power output of the generator per cycle must equal the power delivered to the battery per cycle. Thus,

$$\int V_g \, I_1 \, t_{on} \, dt = \int V_B \, I_2 \, t_{off} \, dt \qquad (1)$$

where:

$V_g$ = generator voltage

$I_1$ = generator current

$V_B$ = battery voltage

$I_2$ = battery current

$t_{on}$ = time $S_1$ is closed

$t_{off}$ = time $S_1$ is open

$T = t_{on} + t_{off}$ = chopper period

The current flows through the inductor continuously, whether or not $S_1$ is open. In addition, if the inductor L is very large so there is a very small ripple component, then

$$I_1 = I_2 = \text{constant} \qquad (2)$$

and $V_g \, I_1 \, t_{on} = V_B \, I_1 \, t_{off}$

or

$$\frac{t_{off}}{t_{on}} = \frac{V_g}{V_B} \qquad (3)$$

The generator average current, $I_{g\ ave}$, is related to the time dependent currents as follows:

$$I_{g\ ave} = I_1 \frac{t_{on}}{T} \tag{4}$$

but, $T = t_{on} \left(1 + \frac{V_g}{V_B}\right)$

hence,

$$I_1 = \left(1 + \frac{V_g}{V_B}\right) I_{g\ ave} \tag{5}$$

The peak current will be larger than the average by $\left(1 + \frac{V_g}{V_B}\right)$. The rms current in the generator can be shown to be $I_{g\ rms} = I_1\sqrt{\frac{t_{on}}{T}}$ thus

$$I_{g\ rms} = I_{g\ ave} \sqrt{1 + \frac{V_g}{V_B}} \tag{6}$$

Assuming the generator speed varies over a 10 to 1 range (as in the case for the Speeder, slightly higher for the Torquer acting as a generator), $V_g$ can go from $V_o$, the generator voltage at lowest speed, to 10 $V_o$. In addition, it is reasonable that in a boost-buck system the battery voltage would be half the maximum generator voltage so that

$$V_B = 1/2\ 10\ V_o$$

Using equation (6)

At 10% mas rpm $I_{g\ rms} = I_{g\ ave}\sqrt{1 + 0.2} = 1.09\ I_{g\ ave}$

At 50% max rpm $I_{g\ rms} = I_{g\ ave}\sqrt{1 + 1} = 1.414\ I_{g\ ave}$

At 100% max rpm $I_{g\ rms} = I_{g\ ave}\sqrt{1 + 2} = 1.732\ I_{g\ ave}$

Since the ohmic losses in the generator are roughly proportional to the square of $I_{g\ rms}$, the copper dissipation in the machine at top speed will be three times larger than that due to the average current.

The inductor conducts current $I_1$ at all times. From equation (5), it can be seen that at top speed the inductor carries

$$I_1 = I_{g\ ave} \left(1 + \frac{V_g}{V_B}\right) = 3\ I_{g\ ave},$$

and the inductor will have to be designed for three times the rated machine current to prevent saturation.

The power delivered by the generator to the battery per cycle is

$$P_B = V_B\ I_1\ \frac{t_{off}}{T} = \frac{t_{on}}{T}\ V_g\ I_1 \qquad (7)$$

or

$$P_B = \frac{I_1\ V_g}{\left(1 + \frac{V_g}{V_B}\right)} \qquad (8)$$

substituting from equation (5)

$$P_B = I_{g\ ave}\ V_g \qquad (9)$$

The average current in the battery is:

$$I_{B\ ave} = I_1\ \frac{t_{off}}{T} = I_1\ \frac{t_{on}}{T}\ \frac{V_g}{V_B} = I_{g\ ave}\ \frac{V_g}{V_B} \qquad (10)$$

The rms current in the battery is:

$$I_{B\ rms} = I_1 \sqrt{\frac{t_{on}}{T}\ \frac{V_g}{V_B}} = I_{g\ ave} \sqrt{\frac{V_g}{V_B}\left(1 + \frac{V_g}{V_B}\right)} \qquad (11)$$

or $I_{B\ rms} = I_{g\ rms} \sqrt{\frac{V_g}{V_B}}$

thus

$$\frac{I_{B\ rms}}{I_{g\ rms}} = \sqrt{\frac{V_g}{V_B}} \qquad (12)$$

## Boost PCU

Using the assumptions and nomenclature of the previous section

$$V_g I_1 = V_B I_1 \frac{t_{off}}{T}$$

or

$$\frac{V_g}{V_B} = \frac{t_{off}}{T} \tag{1}$$

$$I_{g\ ave} = I_1 \tag{2}$$

$$I_{g\ rms} = I_{g\ ave} \tag{3}$$

Since the inductor always carrier current, the inductor will be alway rated for the same average current as the generator.

The average battery current is simply

$$I_{B\ ave} = I_1 \frac{t_{off}}{T} = I_{g\ ave} \frac{V_g}{V_B} \tag{4}$$

and the rms battery current

$$I_{B\ rms} = I_{g\ ave}\sqrt{\frac{V_g}{V_B}} \quad .$$

## APPENDIX A-2

## MATHEMATICAL MODEL OF TORQUER SYSTEM

To facilitate analysis, it is convenient to divide the total chopper period, T, into several subintervals. The current flow in each time interval is determined as follows:

(1) When the power $SCR_1$ is closed and the commutating capacitor is fully charged ($t \geq 0$), the only circuit which contains electric current is shown in Figure A-2.1. Therefore,

$$L_a \frac{di_1}{dt} + R_a i_1 = V_b - E_g \tag{1}$$

where $R_a = R_B + R_M$ is total resistance of the series circuit, $R_B$ the resistance of the battery, and $R_M$ the resistance of the series motor. During the time interval of interest, assuming the machine is saturated, and the machine speed is constant, then $E_g \simeq$ constant, the solution of the equation becomes

$$i_{1(t)} = \frac{V - E_g}{R_a} + I_{M_1} e^{-\frac{R_a}{L_a} t} \tag{2}$$

In most cases $I_{M_1}$ is negative and its value is determined by the boundary conditions to be discussed later.

(2) At $t = t_1$, the commutating $SCR_c$ is turned on and $C_c$ discharges through the linear inductor $L_c$. $S_x$, the saturable inductor is blocking (high impedance) at this instant because it has been driven out of saturation. The circuit diagram is shown in Figure A-2.2.

When $t \geq t_1$, the current $i_{1(t)}$ continues to flow in the battery-armature circuit and an additional current $i_c$ will be started in the commutating circuit. This current is determined by the equation:

$$L_c \frac{di_c}{dt} + R_c i_c + \frac{1}{C_c} \int_{t_1}^{t} i_c \, dt - V_b = 0 \tag{3}$$

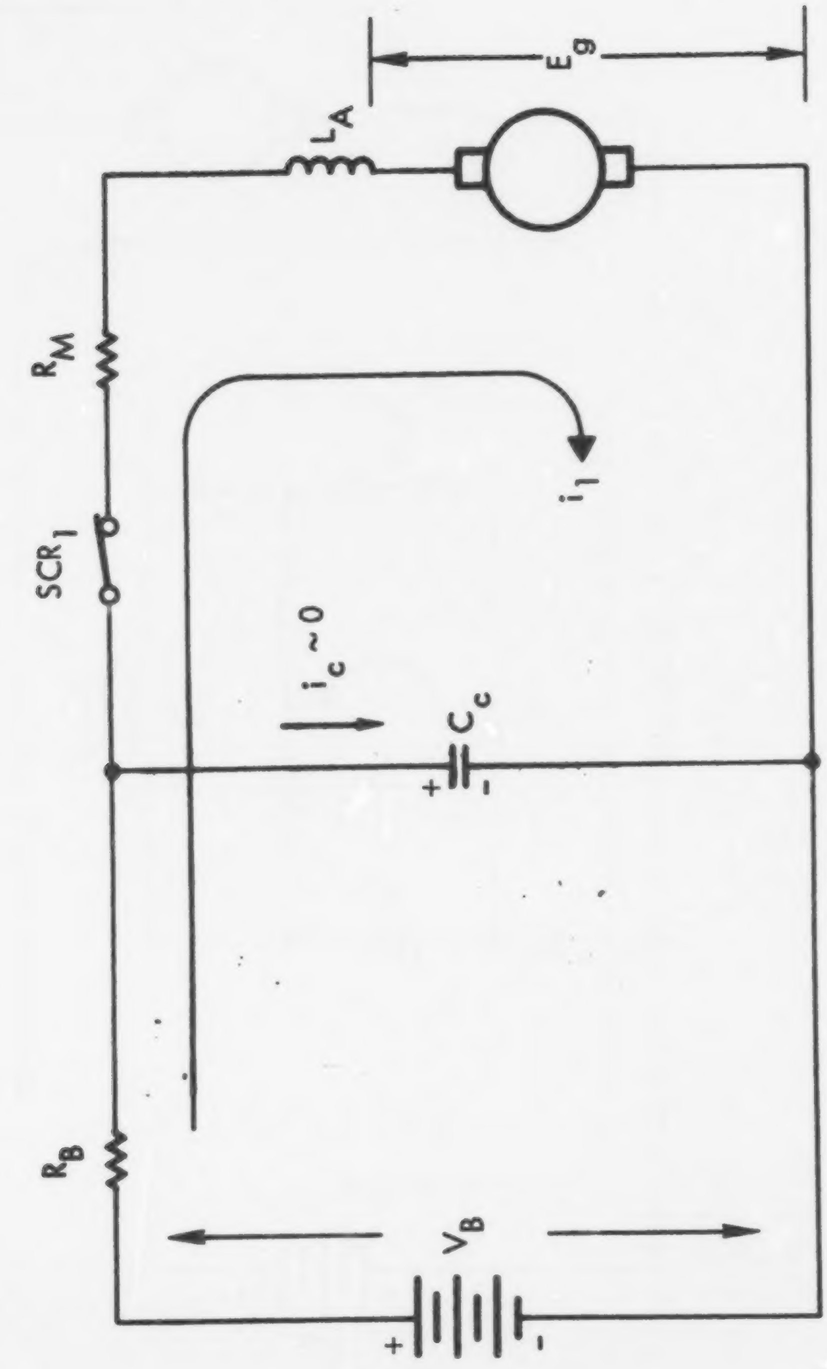
R_B
V_B
+
-
C_c
+
-
i_c ~ 0
SCR_1
R_M
i_1
L_A
E_g

FIGURE A-2.1

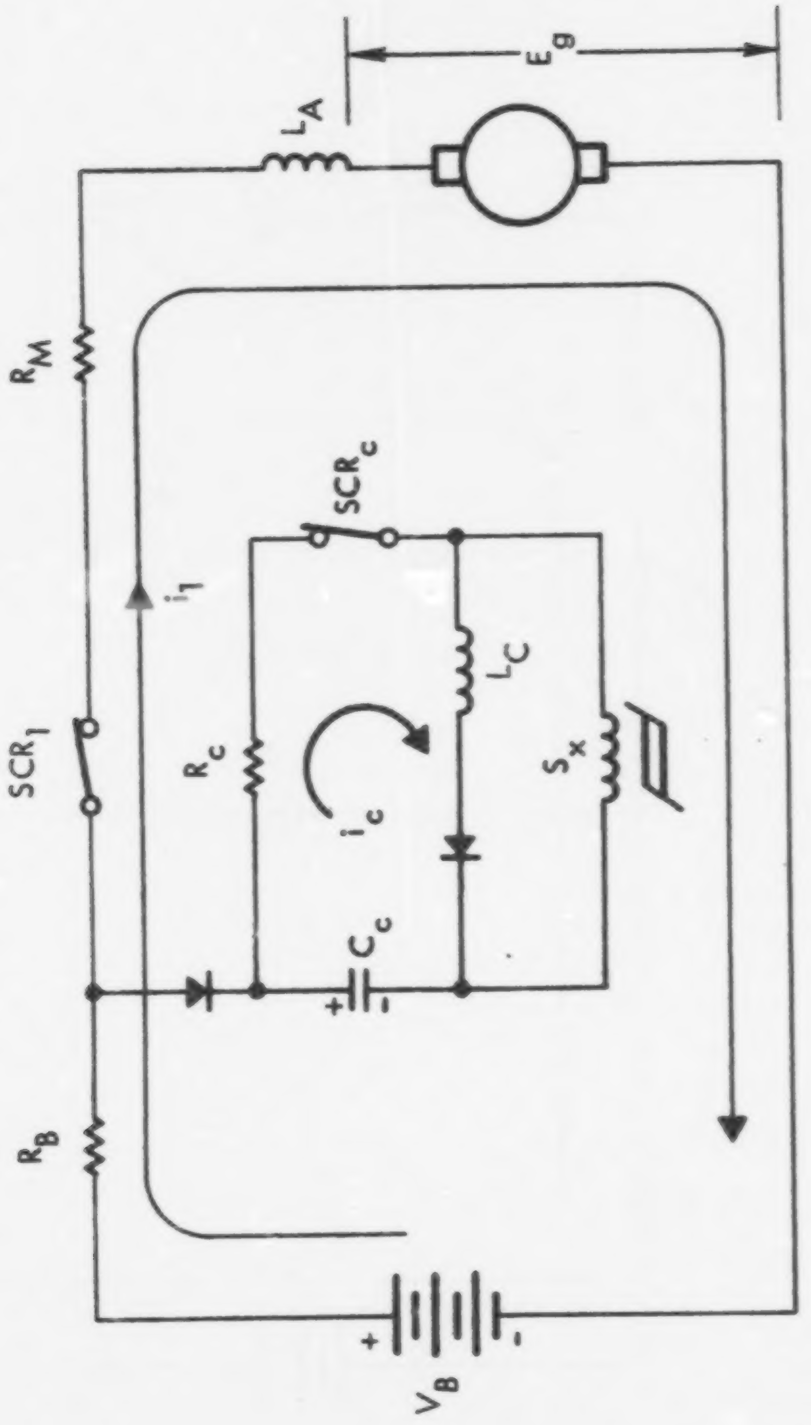
R_B
SCR_1
R_M
L_A
E_g
i_T
SCR_c
R_c
i_c
L_C
S_x
C_c
+
-
V_B
+
-

FIGURE A-2.2

Where $V_b$ is the initial voltage across the capacitor at $t = t_1$. By a change of variable $t' = t - t_1$ the initial conditions are:

$$\left.\begin{aligned} &\text{i) } i_c = 0 && \text{when } t' = 0 \\ &\text{ii) } L_c \frac{di_c}{dt'} + 0 + 0 - V_b = 0 && \text{when } t' = 0 \end{aligned}\right\} \qquad (4)$$

$$\left.\frac{di_c}{dt'}\right|_{t'=0} = \frac{V_b}{L_c} \qquad (5)$$

Differentiating equation (3)

$$L_c \frac{d^2 i_c}{dt'} + R_c \frac{di_c}{dt} + \frac{1}{c} i_c = 0 \qquad (6)$$

therefore

$$i_c = I_1 e^{m_1 t'} + I_2 e^{m_2 t'} \qquad (7)$$

where

$$m_{1,2} = \frac{-R_c \pm \sqrt{R_c{}^2 - 4L_c/C_c}}{2L_c} = \alpha_1 \pm jw_1$$

Substituting (4) and (5) into (7), we have

$$i_c = \frac{V_B}{w_1 L_c} e^{\alpha_1 t'} \sin w_1 t' \qquad (8)$$

(note: $\alpha_1$ is negative in equation (8) )

Because of the diode in the commutating circuit, $i_c$ cannot be negative. The current $i_c$ stops flowing at $t_2=\pi/w_1 \simeq \pi\sqrt{L_c C_c}$, if $R_c$ is small. At the moment current stops commutating $SCR_c$ is turned off. A reversed voltage $V_c$ (the voltage across the capacitor) is applied to the power $SCR_1$ to commutate it off, and the circuit goes into a third mode of operation.

The voltage across the commutating capacitor $C_c$ during the commutation period is

$$e_c = \frac{1}{C_c} \int_0^t i_{c(t)}\, dt - V_b$$

$$= \frac{V_b}{w_1 L_c C_c} \left\{ \frac{1}{\alpha_1^2 + w_1^2} \left[ e^{\alpha_1 t} (\alpha_1 \sin w_1 t - w_1 \cos w_1 t) t w_1 \quad -V_b \right] \right\} \quad (9)$$

when $t' = 0$, i.e., $t=t_1$, $e_c=-V_b$; when $t' = t_2$, i.e., $t=t_1 + t_2$;

$$e_c = \frac{V_b}{w_1 L_c C_c} \left\{ \frac{1}{\alpha_1^2 + w_1^2} \left[ e^{\alpha_1 \pi / w_1} (+w) + w_1 \right] \right\} -V_b \qquad (10)$$

Furthermore if

$$\alpha_1 << w_1$$

$$e_{c(t'=t_c)} = \frac{V_b}{\frac{1}{\sqrt{L_c C_c}} L_c C_c} \left\{ \frac{1}{\frac{1}{L_c C_c}} (2w_1) \right\} -V_b=V_b$$

The power loss in the commutating circuit is

$$P_c = \frac{1}{t_2} \int_0^{t_2} \left[ \frac{r_c V_b^2}{w_1^2 L_c^2} e^{2\alpha_1 t'} \sin^2 wt' \right] dt'$$

$$= \frac{R_c V_b^2}{\frac{\pi}{w_1} w_1^2 L_c^2} \int_0^{\pi/w_1} e^{2\alpha_1 t'} (1- \cos 2w_1 t')\, dt' \qquad (11)$$

The integration of the second term is approximately zero because $2w_1(\pi/w_1) = 2\pi$ is a complete cycle for the cosine function. Therefore,

$$P_c \simeq \frac{R_c V_b^2}{2\pi w_1 L_c^2} \frac{1}{2\alpha_1} \left\{ e^{2\alpha_1 t} -1 \right\}$$

$$= \frac{V_b^2}{2\pi} \sqrt{\frac{C_c}{L_c}} \left\{ 1 - e^{-\pi R_c \sqrt{\frac{C_c}{L_c}}} \right\} \qquad (12)$$

If

$$\pi R_c \sqrt{\frac{C_c}{L_c}} << 1$$

$$P_c \simeq \frac{V_6{}^2}{2\pi} \sqrt{\frac{C_c}{L_c}} \left\{ 1-1 + \pi R_c \sqrt{\frac{C_c}{L_c}} \right\} = \frac{V_b{}^2}{2} R_c \left( \frac{C_c}{L_c} \right) \qquad (13)$$

If

$$\pi R_c \sqrt{\frac{C_c}{L_c}} >> 1$$

$$P_c \simeq \frac{V_b{}^2}{2\pi} \sqrt{\frac{C_c}{L_c}} \qquad (14)$$

The current in the armature circuit at $t = t_1 + t_2$ is

$$i_{1(t_1+t_2)} = \frac{V_b-E_g}{R_a} + I_{m_1} e^{-\frac{R_a}{L_a}(t_1+t_2)} \qquad (15)$$

(3) When $t \geq (t_1+t_2)$, both $SCR_c$ and $SCR_1$ are turned off, the power circuit becomes that shown in Figure A-2.3. The saturable reactor $S_x$ at this time is driven into saturation and its impedance becomes approximately zero. The capacitor continues to discharge through the motor. Therefore,

$$V_b-E_g = R_a\, i_2 + L_a \frac{di_2}{dt} + \frac{1}{C_c} \int_{t_1+t_2}^{t} i_2\, dt - V_o \qquad (16)$$

Where $V_o$ is the initial voltage across the commutating capacitor at $t=t_2+t_1$. By a change of variable $t'' = t\ (t_2+t_1)$, and differentiating equation (16), we have

$$L_a \frac{d^2\, i_2}{dt''} + R_a \frac{di_2}{dt''} + \frac{1}{C_c}\, i_2 = 0 \qquad (17)$$

The initial constants are as follows:

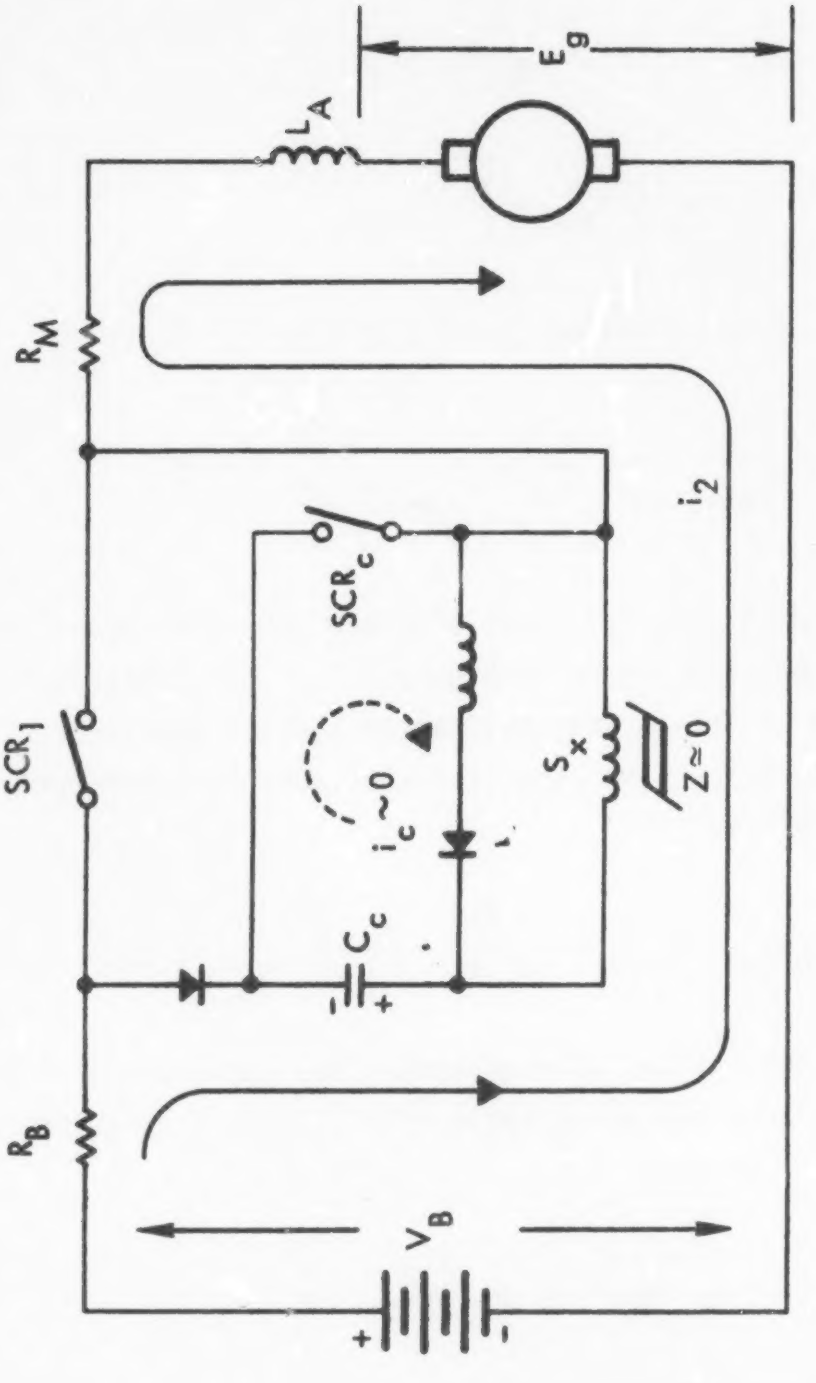
V_B
+
-
R_B
SCR_1
C_c
-
+
i_c~0
S_x
Z≈0
SCR_c
i_2
R_M
L_A
E_g

FIGURE A-2.3

i) $i_{2(t''=0)} = I_o$ which is the value given in equation (15)

ii) $L_a \left.\frac{di_2}{dt''}\right|_{t''=0} = V_b + V_o - E_g - R_a I_o$ assuming $V_o \simeq V_b$ and

$R_a I_o << 2V_b - E_g$

$$\left.\frac{di_2}{dt''}\right|_{t''=0} \simeq \frac{1}{l_a} (2V_b - E_g)$$

The solution of (17) is

$$i_{2(t'')} = I_3 e^{n_1 t''} + I_4 e^{n_2 t''} \tag{18}$$

where

$$n_{1,2} = \frac{-R_a \pm \sqrt{R_a^{\ 2} - \frac{4L_a}{C_c}}}{2L_a} = \alpha_2 \pm j\, w_2$$

Substituting the initial conditions into equation (18) we have

$$i_{2(t)} = I_o e^{+\alpha_2 t''} \left(- \frac{\alpha_2}{w_2} \sin w_2 t'' + \cos w_2 t''\right) + \frac{2V_b - E_g}{w_2\, L_a}\ e^{+\alpha_2 t''} \sin w_2 t'' \tag{19}$$

or

$$i_{2(t'')} = e^{\alpha_2 t''} \left\{ I_o \cos w_2 t'' + \left(- \frac{\alpha_2}{w_2} I_o + \frac{2V_b - E_g}{w_2\, L_a}\right) \sin w_2 t'' \right\} \tag{20}$$

If during the time interval of interest

$$e^{\alpha_2 t} << 1, \text{ and } \frac{\alpha_2}{w_2} I_o << \frac{2V_b - E_g}{w_2 L_a}$$

$$i_{2(t'')} \simeq I_o \cos w_2 t'' + \frac{2V_b - E_g}{w_2 L_a} \sin w_2 t'' \qquad (21)$$

(4) The free wheeling diode will start to conduct when

$$L_a \frac{di_2}{dt''} + E_g \leq -1 \text{ volt} \simeq 0 \qquad (22)$$

Using the approximate expression of $i_2$ given in equation (21), equation (22) becomes:

$$(2V_b - E_g) \cos w_2 t'' - w_2 L_a I_o \sin w_2 t'' = - E_g \qquad (23)$$

Solving equation (23) for $t'' - t_3$, the new circuit becomes that shown in Figure A-2.4.

The current which continues to flow in the armature circuit when the diode conducts is determined by the equation

$$E_g + L_a \frac{di_3}{dt} + R_M i_3 = 0 \qquad (24)$$

and its solution is

$$i_{3(t)} = - \frac{E_g}{r_M} + I_{M_3} e^{-\frac{R_M}{L_a} t''} \qquad (25)$$

where

$$(t_1 + t_2 + t_3) \leq t'' \leq T$$

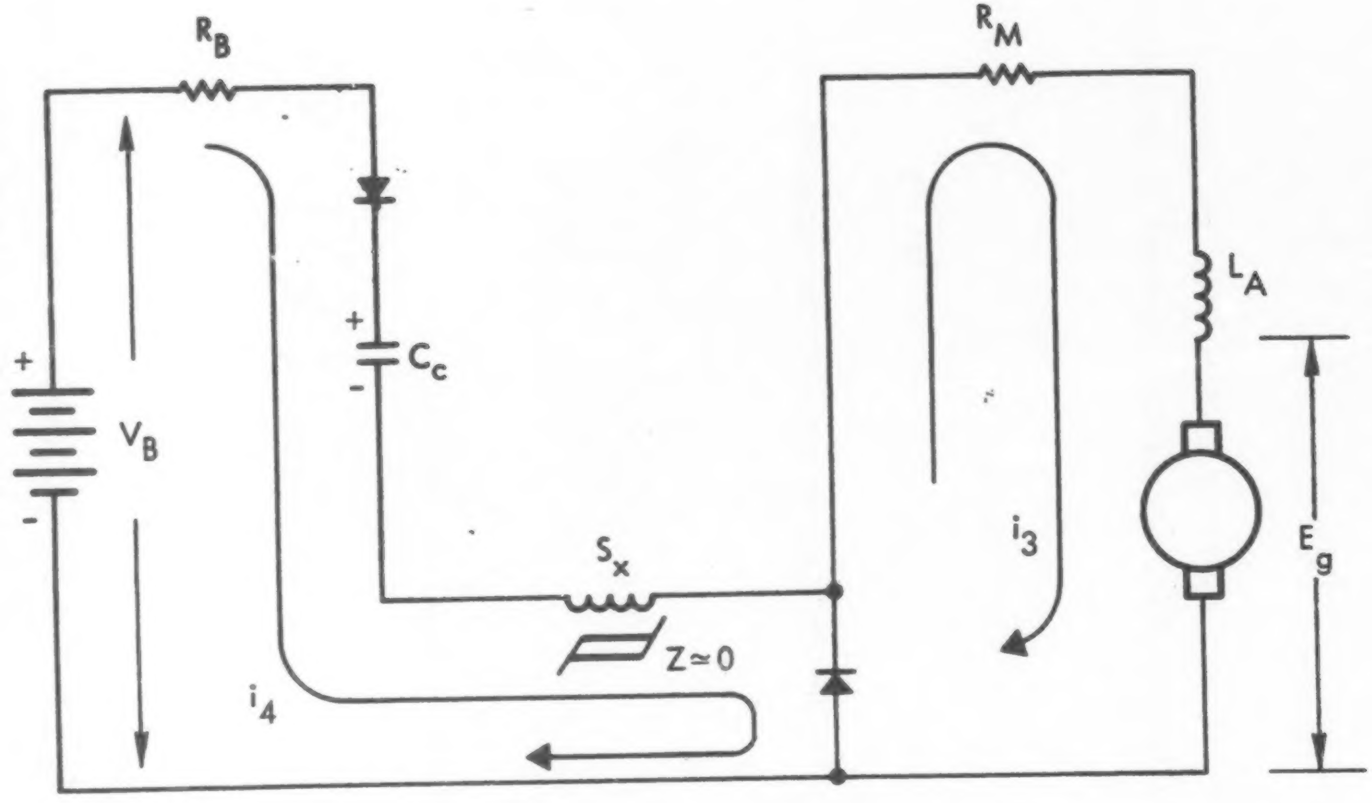
$R_B$
$R_M$
$V_B$
$C_c$
$L_A$
$S_x$
$Z \simeq 0$
$i_3$
$i_4$
$E_g$
+
-
+
-

FIGURE A-2.4

The constants $I_{M_3}$ in equation (25) and $I_{M_1}$ in equation (2) are determined by the following conditions:

i) $i_{2(t=t_1+t_2+t_3)} = i_{3(t=t_1+t_2+t_3)}$

ii) $i_{1(t=0)} = i_{3(t=T)}$

Current will continue to flow from the battery until the capacitor $C_c$ is fully charged. The battery current is determined by the equation

$$V_b = R_B i_4 + \frac{1}{C_c} \int_{t_1+t_2+t_3}^{t} i_4 \, dt + V_c \tag{26}$$

where $V_c$ is the initial voltage of the capacitor when $t = t_1+t_2+t_3$ i.e.,

$$V_{c(t_1+t_2+t_3)} = \frac{1}{C_c} \int_{t_1+t_2}^{t_1+t_2+t_3} i_2 \, dt - V_b \tag{27}$$

The solution of equation (26) is

$$i_{4(t)} = \left(\frac{V_b - V_c}{R_B}\right) e^{-\frac{t}{R_B C_c}} \tag{28}$$

where

$$(t_1+t_2+t_3) \leq t < T$$

Since $R_B C_c \simeq 0$ this current decreases to zero very rapidly. The overall current waveforms are shown in Figure A-2.5.

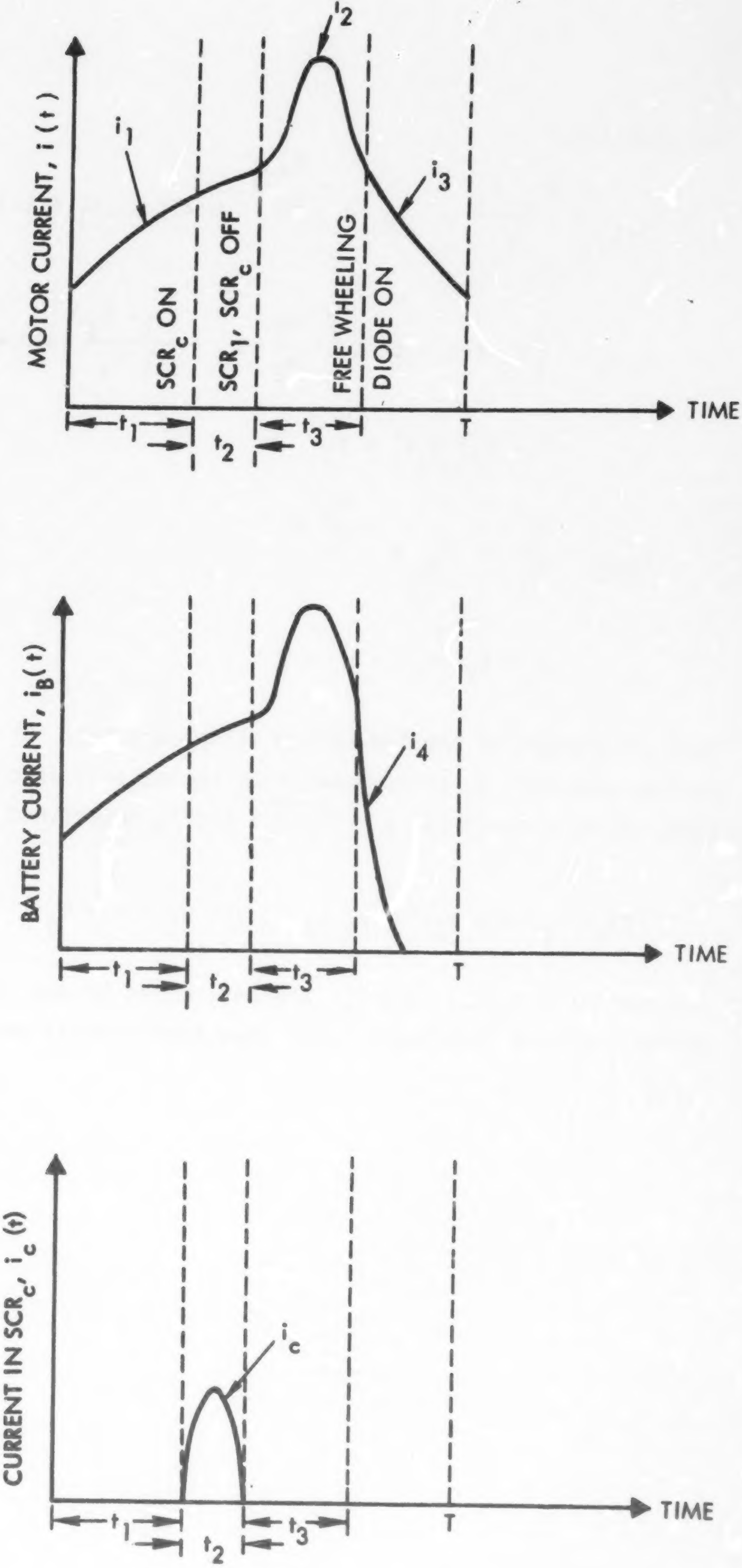
i2
MOTOR CURRENT, i(t)
i1
i3
SCRc ON
SCR1, SCRc OFF
FREE WHEELING DIODE ON
t1
t2
t3
T
TIME
BATTERY CURRENT, iB(t)
i4
t1
t2
t3
T
TIME
CURRENT IN SCRc, ic(t)
ic
t1
t2
t3
T
TIME

FIGURE A-2.5

The equations

$$i_{1(t)} = \frac{V_b - E_g}{R_a} + I_{M_1} e^{-\frac{R_a}{L_a} t} \quad 0 < t < (t_1 + t_2) \tag{2}$$

$$i_{2(t)} = \left\{ I_o \cos w_2 t'' \; t \left( - \frac{\alpha_2}{w_2} I_o + \frac{2V_b - E_g}{w_2 L_a} \right) \sin w_2 t'' \right\} e^{\alpha_2 t''}$$

$$(t_1 + t_2) \leq t'' < t_3 \tag{20}$$

$$i_{3(t)} = \frac{E_g}{R_M} + I_{M_3} e^{-\frac{R_M}{L_a} t''} \tag{25}$$

$$(t_1 + t_2 + t_3) < t'' < T$$

were programmed on the TRW-UCSB on-line computer. $t_1$ is preselected by the operator, $t_2$ is computed from the natural frequency of the commutating circuit ($t_2 \simeq \pi \sqrt{L_c C_c}$) and $t_3$ determined from the equation:

$$(2V_b - E_g) \cos w_2 t'' - w_2 L_a I_o \sin w_2 t'' = - E_g \tag{23}$$

The constants $I_{M_1}$, $I_o$ and $I_{M_3}$ are determined by the conditions that the current must be continuous in an inductive circuit and that $i_{1(0)} = i_{3(t)}$.